

Prosthesis Embodiment:

Sensory-Motor Integration of Prosthetic Devices into the Amputee's Body Image

DISSERTATION

Submitted in partial fulfillment of the requirements for the degree of

Doktor der technischen Wissenschaften

by

Andrei Ninu

Registration Number 0925210

to the Faculty of Informatics
at the Vienna University of Technology

Advisor: Prof. Frank Rattay, Prof. Dario Farina

The dissertation has been reviewed by:

(Prof. Dario Farina)

(Prof. Frank Rattay)

Vienna, 16.09.2013

(Andrei Ninu)

Erklärung zur Verfassung der Arbeit

Andrei Ninu

Vorgartenstraße 112, 1020 Wien

Hiermit erkläre ich, dass ich diese Arbeit selbständig verfasst habe, dass ich die verwendeten Quellen und Hilfsmittel vollständig angegeben habe und dass ich die Stellen der Arbeit - einschließlich Tabellen, Karten und Abbildungen -, die anderen Werken oder dem Internet im Wortlaut oder dem Sinn nach entnommen sind, auf jeden Fall unter Angabe der Quelle als Entlehnung kenntlich gemacht habe.

Wien, 16.09.2013

(Andrei Ninu)

ABSTRACT

Overview: A prosthesis is intended to restore the loss after amputation, this means it should be used not only like a tool, but should also be perceived as part of the body (Prosthesis Embodiment). The development of a prosthesis which will look, move and feel like a natural limb is a task that is broad in scope as well as challenging, with necessary focal points on the prosthesis' cosmetics, kinematics, dynamics and on the interface of the prosthesis with the central nervous system. The latter is the focus of this study, and the problem is addressed as a set of four areas of research. The first area looks at approaches to converting the amputee's sensed EMGs into prosthesis movements. The second area is concerned with providing tactile feedback that is both comfortable and effective. The third area provides for the harmonization of control and feedback pathways. The fourth area, probably the most challenging and important, is the objective assessment of the provided haptic feedback, prosthesis control and the system as a whole.

Methods: Good prosthesis embodiment requires that the prosthesis performs harmoniously with the movements of the body. Therefore, the measurement used to describe the level of embodiment was the degree of synchrony between the body and prosthesis movement. Real prostheses have constructive limitations and control of a complex prosthesis with many degrees of freedom is more demanding, with a lower chance of occurring in harmony with the body. With this in mind, the system complexity was minimized and the task simplified. An immersive 3D virtual environment was created, in which the subjects, controlling a one DOF virtual hand prosthesis (grasp function only), collected spheres spread within the virtual space. The spheres were used because of their simple geometry; they can be directly grasped with a one DOF hand prosthesis without additional movements of the wrist or shoulder. The prosthesis, real or virtual, was classically controlled by two bipolar EMG electrodes placed on the antagonistic muscles of the forearm. The virtual prosthesis had an ideal behavior or, for comparison, simulated the behavior of the real prosthesis by including the real prosthesis in the control-loop of the virtual one. To close the prosthesis control-loop, a self-made stimulator was developed – the Haptic Brace, which is able to generate complex patterns of multimodal stimulation.

Results: The major goal of this study was to analyse the mechanisms allowing for prosthesis embodiment. In order to facilitate embodiment, the system complexity was minimized and the task simplified. It was found that synchrony between movement of the body and prosthesis, a measure of the level of embodiment, is, even under extremely simplified conditions, almost impossible to achieve. In order to increase intuitiveness of prosthesis control, haptic feedback was provided to the subjects and the prosthesis was controlled in close-loop. The measurements have shown, however, that feedback can substitute for or augment vision (as it transmits force feedback which is invisible), but cannot compensate for the inconsistency of the prosthesis reactions while trying to follow the amputee's movement intent. Due to this inconsistency, the amputees have to continuously supervise the prosthesis performance, minimizing the influence of haptic feedback. The lack of

consistency and precision, as well as the slow reaction of the EMG prosthesis control was identified to be the major limitation in harmoniously synchronizing the body and prosthesis movements. Three prosthesis control strategies were implemented and directly compared - derivative, voltage and proportional. It was found that the voltage mode, currently implemented by the commercial devices, might be responsible for this outcome. Voltage mode is robust and allows for good performance in the absence of explicit feedback about grasp force, therefore an optimal compromise for daily-life application; but it is slow, which was identified as a crucial drawback for prosthesis embodiment. The proportional mode was definitively faster, which is very promising, but it is more sensitive to EMG noise or motion artefacts and requires feedback regarding grip force in order to be effective for daily-life applications.

Conclusion: The main contribution of this work is considered to be the development of a novel haptic device – the Haptic Brace, which, in comparison with SOA technologies, allows for a more physiological haptic stimulation of the skin and of the muscles beneath the stimulator. Equipped with such technology, a prosthesis would better reproduce the interaction of the natural limb with the environment, and would consequently allow the amputee to better feel the prosthesis as part of his/her body. Nevertheless, in order to achieve the main goal of this research – Prosthesis Embodiment feedback should be attended by a more intuitive control of the prosthesis. The latter was identified as the main limiting factor in allowing prosthesis embodiment; therefore, future work has to be dedicated to the improvement of the dynamic, precision and consistency of the prosthesis. As during natural behavior, performance is tightly conditioned by fast and precise feed-forward limb control (open-loop), and feedback is mainly involved in learning new skills and allowing adaptation to unpredictable conditions. Feedback facilitates the development of fast motor programs, but the upper bound for prosthesis performance is set by the ability to control the prosthesis in open loop.

EMG prosthesis control was not the focus of the current work as there's plenty of research in the field of EMG signal processing. Evaluating the advantages and disadvantages of these methodologies was, however, a serious challenge as there is a lack of available methodology to objectively assess the prosthesis' controllability in all its complexity. Therefore, special attention was dedicated to developing such a methodology, which should be objective and have a general character. This has a crucial importance for future research in the prosthetics field, as, without such an objective measure, it will be hard if not impossible to identify strengths and weaknesses of various approaches, allowing for systematic and real improvements of the prosthesis' performance.

KURZFASSUNG

Überblick: Eine Prothese soll nach einer Amputation die Funktion der fehlenden Gliedmaßen hinreichend ersetzen. Eine Prothese sollte aber nicht nur als Werkzeug angesehen werden, wünschenswert ist es, dass sie von den Amputierten als Teil des Körpers empfunden werden kann. Die Entwicklung einer Prothese, die im Aussehen einer natürlichen Gliedmaße ähnelt, ist komplex und multi-disziplinär, und stellt eine große Herausforderung dar. In dieser Dissertation befasste ich mich im speziellen mit der Schnittstelle zwischen Mensch und Prothese, welche in vier Themenbereiche aufgegliedert wurde: Ansätze um die EMG Signale, erzeugt von den Amputierten, in Prothesenbewegungen umzuwandeln; Möglichkeiten um sensorische Information, gemessen von der Prothese, haptisch zu den Amputierten zu übertragen; die Harmonisierung der Prothesensteuerung und Feedback; und der letzte, und vielleicht der wichtigste Punkt, die objektive Evaluierung verschiedener Stimulationsansätze und der Prothesensteuerbarkeit.

Methoden: Damit die Prothese als Teil des Körpers empfunden werden kann, ist es erforderlich, dass sie sich harmonisch an die natürlichen Körperbewegungen anpasst. Als Maßstab für diese harmonische Anpassung (Embodiment) wurde daher der Grad der Synchronie zwischen Körper und Prothesenbewegung genommen. Je komplexer eine Prothese ist, desto grösser ist die Herausforderung für die Amputierten, die Prothese zu steuern. Die Komplexität einer Prothese könnte das Embodiment beeinträchtigen, aus diesem Grund, wurde das System auf ein Minimum reduziert: eine Handprothese nur mit Greiffunktion. Da die realen Prothesen aufgrund technologischer Grenzen keine Flexibilität anbieten können, um verschiedene Steuerstrategien auszuprobieren, wurde die Handprothese in einer immersiven virtuellen Realität simuliert. Für Vergleichszwecke, wurde die virtuelle Prothese so implementiert, dass sie auch das Verhalten einer realen Prothese nachahmen kann. Die Probanden haben die virtuelle Prothese am Unterarm angebracht, als wäre es eine reale Prothese, und haben damit virtuelle Objekte (Bälle) in dem virtuellen Raum gesammelt. Bälle wurden auf Grund ihrer Geometrie ausgewählt, da sie mit einer 1DOF Handprothese gegriffen werden können, ohne zusätzliche Bewegungen von Handgelenk oder Schulter. Die Prothese wurde mit Hilfe von zwei EMG Elektroden gesteuert, medial und lateral am Unterarm platziert. Um die Regelschleife der Prothese schließen zu können und um die Prothesensteuerbarkeit intuitiver zu gestalten, wurden verschiedene Prothesenparameter zu den Probanden haptisch übertragen. Für die Stimulation des Unterarms wurde ein haptisches Feedbackelement entwickelt – Haptic Brace, welches die Erzeugung von komplexen und unterscheidbaren Stimulationsmustern ermöglicht.

Ergebnisse: Das Hauptziel der Studie war die Untersuchung verschiedener Ansätze und Methoden, welche zu einem besseren Embodiment der Prothesen führen können. Für diese Untersuchungen, wurden die Komplexität der Prothese und die auszuführenden Aufgaben auf ein Minimum reduziert. Die Ergebnisse haben gezeigt, dass trotz der extrem vereinfachten Bedingungen, synchrone Bewegungen zwischen Prothese und der tragenden Gliedmaße, kaum zu erreichen sind. Um die Prothesensteuerbarkeit intuitiver zu gestalten, wurde der Regelkreis der Prothese geschlossen: das Verhalten der Prothese wurde haptisch (vibrotaktiler Feedback)

zu den Probanden übertragen. Vergleiche mit Untersuchungen im offenen Regelkreis (visuelles Feedback) haben gezeigt, dass die vibrotaktile Stimulation als Ersatz für das visuelle Feedback dienen kann. Das haptische Feedback kann jedoch die Inkonsistenz und Ungenauigkeiten der Prothesensteuerung nicht kompensieren und somit kann die Leistung des geschlossenen Prothesen Regelkreises dem offenen Regelkreis nicht überlegen sein. Der Mangel an Genauigkeit und Reproduzierbarkeit, als auch die langsame Reaktion der EMG Steuerung, wurden als Hauptlimitationsfaktoren in der Harmonisierung der Prothesenbewegung mit dem Körper identifiziert. Mehrere Prothesensteuerungen wurden implementiert und untereinander verglichen – die derivative, hybride und proportionale Steuerung. Der Vergleich hat gezeigt, dass die hybride Steuerung verantwortlich für dieses Verhalten sein könnte. Die hybride Steuerung ist robust und zeigt gute Performance auch ohne direktes Feedback über die Griffkraft; darüber hinaus einen optimalen Kompromiss für Integration in Alltagprothesen darstellt. Die hybride Steuerung ist jedoch langsam, und kann deshalb nicht harmonisch mit den Körperbewegungen synchronisiert werden. Die proportionale Steuerung ist im Vergleich deutlich schneller und intuitiver, allerdings viel empfindlicher auf die Stabilität und Qualität der EMG; darüber hinaus benötigt sie Information über die ausgeübte Griffkraft um als Prothese im täglichen Leben einsetzbar zu sein.

Schlussfolgerung: Ein wichtiges Ergebnis dieser Arbeit ist die Entwicklung neuer Stimulationstechnologien (Haptic Brace), welche im Vergleich mit den herkömmlichen, eine möglichst physiologische haptische Stimulation ermöglichen. Mit Hilfe dieser Technologie könnte eine Prothese die natürliche Interaktion Mensch-Umgebung besser reproduzieren, und es den Amputierten erlauben, die Prothese mehr als Teil des Körpers zu empfinden. In dieser Studie konnte jedoch gezeigt werden, dass für ein optimales Prothesenembodiment, Feedback alleine nicht ausreichend ist, da die Prothesensteuerbarkeit einen limitierenden Faktor der Systemperformance darstellt. Um das Ziel, Prothesenembodiment, zu erreichen ist daher die Erhöhung der Dynamik, der Genauigkeit und der Konsistenz der Prothesensteuerung erforderlich. Die Prothesenbewegung soll das Ergebnis einer Kombination von Feed-forward und Feedback Kontrollparadigmen sein, ähnlich, wie das bei physiologischen Bewegungen von Gliedmaßen der Fall ist. Feedback ist vor allem im Erlernen neuer Fähigkeiten involviert und hilft bei der Anpassung an unvorhersehbare Verhältnisse. Die Performance der Prothese ist jedoch in der Genauigkeit und Konsistenz der Prothesensteuerung im offenen Regelkreis begrenzt.

Die Prothesensteuerbarkeit wurde in dieser Studie bewusst in einem geringeren Ausmaß behandelt, da es derzeit sehr viel Forschungstätigkeit in dem Bereich EMG Signalverarbeitung gibt. Als Schwierigkeit hat sich jedoch herauskristallisiert, dass es keine Ansätze, bzw. Methoden gibt, um die verschiedenen Prothesensteuerungen untereinander objektiv auf ihre Vor- und Nachteile zu evaluieren. Ohne diese Möglichkeit eines Vergleiches, wird es schwer, bis zu unmöglich sein, die Steuerbarkeit von Prothesen intuitiver zu gestalten. Aus diesem Grund befasst sich ein großer Teil dieser Arbeit mit der Entwicklung einer Methodik, die Prothesensteuerbarkeit objektiv zu evaluieren, sowie auch mit der Evaluierung der Fähigkeit von Stimulationstechnologien, haptische Information zu den Amputierten zu übertragen. Die weitere Entwicklung und Validierung dieser Methoden sollte Gegenstand von fortführenden Untersuchungen sein, um die Forschung im Prothetikbereich effektiv weiterführen zu können.

Acknowledgments

I would like to express my gratitude to Dr. Hans Dietl, who supervised, encouraged and sustained this project over the four years I required to finish this work. Without his support this research would not have been possible.

I want to give my thanks to Prof. Dr. Frank Rattay for academic supervision and for helping me in understanding the neural mechanisms behind sensory perception and movement control which have a crucial importance when developing human-prosthetics interfaces.

My sincere appreciation to Prof. Dr. Dario Farina for his guidance and support, as well as for his contagious enthusiasm for scientific research and work.

Many thanks to my Otto Bock colleagues, Andreas Schramel, Arpad Ujvary and Teriss Yakimovic for the technical support they provided in designing experimental setups.

I would like to express my gratitude to Mag. Dr. Hannes Kaufmann, who graciously made available the infrastructure of his virtual-reality laboratories at the TU Vienna for the development of the immersive rehabilitation environment, to Michael Bresler and his major contribution in the software implementation of the VR scenarios, as well as to Cosima Prahm who supervised many of the clinical studies.

Special thanks to my kids Tobias, Maya and Stephan who were my major motivation to finalize this work, and my dearly beloved Mirjam for her support, both vocational and social, and for helping me out with and beyond those lines.

There are a great many people I've been lucky enough to have had around me, who always deserve my gratitude. I would like to thank to all of you who encourage me to think, to question and to wonder: a most heart-felt thanks.

TABLE OF CONTENTS

| | |
|--|----|
| Abstract | v |
| 1. Introduction | 1 |
| 1.1. Problem Statement | 1 |
| 1.2. Thesis Goal | 7 |
| 1.3. Thesis Outline..... | 11 |
| 2. Aspects of Sensory-Motor Integration..... | 13 |
| 2.1. Movement..... | 13 |
| 2.1.1. Movement Generation..... | 13 |
| 2.1.2. Grasping | 16 |
| 2.1.3. Psychophysics of Reach-to-Grasp Movement..... | 18 |
| 2.2. EMG Prosthesis Control | 20 |
| 2.2.1. Muscle Contraction and EMG | 20 |
| 2.2.2. EMG Recording Technologies..... | 21 |
| 2.2.3. EMG Controlled Prosthetics | 22 |
| 2.3. Tactile Sensation & Perception | 23 |
| 2.3.1. Sensation..... | 23 |
| 2.3.2. Wearable Haptic Technologies..... | 27 |
| 2.3.3. Psychophysics..... | 32 |
| 3. Feedback Devices and Haptic Stimulation | 37 |
| 3.1. Single-Element Vibration Motor | 38 |
| 3.2. Arrays of Vibration Motors | 41 |
| 3.2.1. Coplanar Array | 41 |
| 3.2.2. Linear Array | 43 |
| 3.3. Single-Element Electro-Stimulation | 45 |
| 3.4. Electro-Stimulation Array..... | 46 |
| 3.5. A Novel Wearable Haptic Technology..... | 48 |
| 3.5.1. Principle of Functioning..... | 48 |

| | | |
|--------|---|-----|
| 3.5.2. | Characterization of Physical Properties | 52 |
| 3.5.3. | Conclusions | 54 |
| 3.6. | Comparison with Eccentric Weight-Based Vibration-Motor..... | 56 |
| 3.7. | Psychophysical Assessment | 59 |
| 3.7.1. | Tracking the Stimulation | 59 |
| 3.7.2. | Psychophysics of the Vibro-Vactile Stimulation | 60 |
| 3.8. | The Haptic Brace | 73 |
| 4. | Pattern Generation Strategies | 74 |
| 4.1. | Staircase Patterns | 74 |
| 4.2. | Continuous Patterns | 75 |
| 4.3. | Multimodal Stimulation Patterns..... | 81 |
| 4.4. | Pattern Generation Mechanisms | 82 |
| 4.5. | Comfort, Intuitiveness, Acceptance | 84 |
| 5. | EMG Driven Prosthetics Devices | 87 |
| 5.1. | Pattern Recognition Strategies | 87 |
| 5.2. | Low-Level Prosthesis Control | 88 |
| 6. | Open vs. Closed Loop Prosthesis Control..... | 90 |
| 6.1. | Experimental Setup | 91 |
| 6.2. | Experimental Task | 93 |
| 6.2.1. | Full Visual Feedback | 93 |
| 6.2.2. | Full Haptic Feedback | 94 |
| 6.2.3. | Subjects | 95 |
| 6.3. | Experimental Protocol | 95 |
| 6.4. | Approaches to Data Analysis..... | 97 |
| 6.5. | Results..... | 97 |
| 6.6. | Discussion..... | 102 |
| 7. | An Immersive Virtual Reality Environment | 106 |
| 7.1. | Markers | 107 |
| 7.2. | Infrared Camera | 108 |

| | | |
|--------|---|-------------------------------------|
| 7.3. | Video Tracking System | 108 |
| 7.4. | The Virtual Reality Environment | 109 |
| 7.4.1. | Prosthesis | 110 |
| 7.4.2. | Objects | 111 |
| 7.5. | The Head-Mounted Display (HMD)..... | 112 |
| 7.6. | Control Brace | 113 |
| 8. | Assessment of EMG Prosthesis Control | Error! Bookmark not defined. |
| 8.1. | Problem Statement | 115 |
| 8.2. | The Proposed Assessment Approach..... | 119 |
| 8.3. | VR Scenarios..... | 123 |
| 8.3.1. | Body Functions | 123 |
| 8.3.2. | Activity..... | 127 |
| 8.3.3. | Performance..... | 128 |
| 8.4. | Control Strategies | 129 |
| 8.4.1. | Glove Prosthesis Control | 129 |
| 8.4.2. | Prosthesis in the control Loop..... | 130 |
| 8.4.3. | VR Prosthesis Control..... | 131 |
| 8.5. | Assessment and Comparison of Prosthesis Control Strategies..... | 132 |
| 8.5.1. | Conditions | 132 |
| 8.5.2. | Glove Prosthesis Control | 133 |
| 8.5.3. | Hybrid Prosthesis Control..... | 135 |
| 8.5.4. | Comparison of Prosthesis Control Strategies..... | 137 |
| 8.6. | Prosthesis-Limb Coordination | 139 |
| 8.6.1. | Glove Prosthesis Control | 139 |
| 8.6.2. | Hybrid Prosthesis Control..... | 141 |
| 9. | Discussion..... | 144 |
| 10. | Final Conclusions and Future Work | 152 |
| | Bibliography | 155 |
| | Appendix | 162 |

| | |
|---|-----|
| Menu - Virtual Reality Environment..... | 162 |
| Mappings..... | 162 |
| Prosthesis Editor | 163 |
| Control Panel..... | 164 |
| Objects Editor..... | 165 |
| Bluetooth Connection (BT)..... | 169 |
| Fitting Settings | 169 |
| Network Connection (TCP/IP) | 170 |
| Scope..... | 171 |

ABBREVIATIONS

- AF** – Amplitude/Frequency
- AFC** – Alternative Force Choice
- AP** – Action Potential
- BUS** – Binary Unit System
- BLDC** – Brushless Direct Current
- CNS** – Central Nervous System
- CPM** – Control Point Matrix
- DC** – Direct Current
- DOF** – Degrees of Freedom
- EMG** – Electromyography
- ICF** – International Classification of Functioning
- IFC** – Interval Force Choice
- JND** – Just Noticeable Difference
- PR** – Pattern Recognition
- RHI** – Rubber Hand Illusion
- SD** – Standard Deviation
- SE** – Standard Error
- SIAM** – Single Interval Adjustment Matrix
- SOA** – State Of the Art
- TC** – Time to Complete
- TMR** - Targeted Muscle Reinnervation
- TSR** - Targeted Sensory Reinnervation
- ULPOM** – Upper-Limb Prosthetic Outcome Measures
- VR** – Virtual Reality
- WF** – Weber Fraction
- WHO** – World Health Organisation

1. INTRODUCTION

1.1. Problem Statement

Technology is improving rapidly and prosthetic devices are much more complex than before, with sophisticated kinematics, higher performance and much improved wearing comfort, all bringing the modern prosthesis closer to the performance of a natural limb. However, a major difference remains; only a natural limb is integrated directly into the nervous system and provides direct feedback to the brain, which controls motion. The integration of the prosthesis into the amputee's body image implies that prosthetics and the amputee's body have to merge harmoniously; biological structures have to interface with engineering entities, and they have to understand each other to restore, in an effective way, the loss due to amputation (Saradjian et al. 2008). Technology and biology should merge to achieve a harmonious and effective "bionic reconstruction" of the lost limb. This task involves a deep understanding of the neural processes behind the control of the natural limbs, which is the subject of various research directions.

A prosthetic device has the goal of compensating the loss suffered due to amputation. On one hand, it has to reproduce the kinematics and dynamics of the amputated limb; on the other hand, it has to be interfaced with the interrupted neural terminations. Technological forecasting, advances in materials, design methodologies, and actuators all anticipate the development of prostheses with improved dynamics and kinematics. But a major limitation in obtaining multifunctional artificial limbs, with all pre-amputation functions recovered, remains the neural interface with the prosthesis (Riso 1999). The interfacing process demands a very close bond between prosthesis and amputee, and has a great importance, much more importance than the prosthesis itself, critically influencing prosthesis acceptance by amputees. Well-interfaced, yet less complex prostheses are better accepted than highly complex, yet poorly-interfaced ones.

A myo-prosthesis can provide an alternative for the lost limb. Controlled by the remaining healthy and disaffected muscles of the stump, the prosthesis will follow, to some extent, the expressed movement intent by amputees. Surface electromyography (EMG) electrodes will measure the electrical signals generated by the muscles beneath the skin, which, after processing, will be converted into commands for prosthesis control. There are many signal processing strategies to convert measured EMGs into prosthesis commands (Oskoei & Hu 2007); however, most of these strategies allow joint-by-joint prosthesis movement only, one movement being the consequence of a muscle or group of muscle contractions.

In order to recover the loss due to amputation, most approaches attempt to detect the amputee's movement intention by surface EMG and to control the prosthesis correspondingly, to measure the interaction with the environment and to transmit it back to the amputee as haptic feedback (Munih & Ichie 2001). This strategy is addressed in order to reconstruct the movement mechanisms of the natural limb in a physiological manner. Nevertheless, practical implementations of this approach have shown that currently available technologies are

not able to cope with the complexity of the neural transition mechanisms. From the huge amount of neural information coming from the higher levels of the CNS, but still available at the amputation level as AP propagated along neural pathways, the current state-of-the-art prosthesis is able to detect just a narrow amount (Zhou & Rymer 2004). Mostly, this information is used to control only a degree of freedom (e.g. open/close) of a hand prosthesis. If the prosthesis has many degrees of freedom, the co-contraction, a simultaneous contraction of agonist muscles, switches the control sites to the next joint, e.g. wrist with pronation/supination or elbow with flexion/extension.

In an attempt to get more control signals, a new surgery technique called “Targeted Muscle Reinnervation” was developed by Dr. Kuiken in Chicago (Kuiken et al. 2009). The methodology consists in denervating one or more spare muscle of the stump, then reinnervating them with the interrupted nerves which controlled the pre-amputated arm. Directly extracting the neural information from nerves is technologically very challenging; nevertheless, reinnervated into the stump’s muscles, this information will be made available by EMG. These muscles act like amplifiers to the information passing the efferent nerves, and their contraction is correlated with the intent of the amputee to move the natural limb. The amputee will try to move the limb, now amputated, and the prosthesis will move instead, which allows for more intuitive prosthesis control.

Targeted Sensory Reinnervation (TSR) is similar to TMR, but addresses the afferent neural pathways, reconstructing, to some extent, the tactile/proprioceptive sensibility of the lost limb. The sensory nerves, interrupted after amputation, will be innervated into the skin of the stump, establishing a neural connection with the natural receptors responsible for sensation. Touching the stump, the amputees will feel their amputated limbs (Marasco et al. 2009).

TMR has the immense benefit of increasing the dimension and intuitiveness of the human-prosthesis interface, allowing a “prosthesis thought control.” The intent to control the limb, expressed similarly to before amputation, is conveyed into prosthesis movement and, due to TSR, the reinnervated skin of the stump is prepared to feel, as the natural limb did. Together, TMR and TSR allow a better preparation of biological structures to be interfaced with technological entities.

TMR allows for the creation of new control sites, which can be used for more direct and intuitive prosthesis control; however, propagated to the surface of the skin, due to filtering effects introduced by tissue and bones, the surface EMG will just roughly describe the neural mechanism generating the muscle contraction. Increasing the dimension of the control interface beneath the skin with TMR will not have the targeted effect, as the measured signals at the surface of the skin are less consistent and have a narrow resolution. Sensed by surface electrodes, the detected EMG will also be noisy, being strongly influenced by motion artifacts, socket technology, skin condition and many other factors. Therefore, there is a compromise to be made between the dimension of the human-prosthesis interface and its quality (Kamavuako et al. 2013).

In order to overcome these limitations, more ambitious approaches try to capture the expressed movement intention of the amputee using implantable technologies (Kamavuako et al. 2009; Farina et al. 2008). Using

electrodes placed around or inside the muscle of interest, the myoelectrical activity during contractions is sensed as a series of APs which propagate along the muscle fibers. Being implanted into the stump, these electrodes capture in more detail the myoelectrical activity during muscle contraction, though only locally, while the force developed by a muscle during contraction results from the individual contraction of various types of muscle fibers non-uniformly distributed within the muscle.

Very intensive research efforts are being conducted, aiming to decode the neural information at the amputation level. Still, the complexity of biological structures is very challenging, including for the latest implantable technologies. Decoding the neural information in its utmost intimacy is currently almost impossible with the available technologies and compromises have to be made in order to extract high-resolution, consistent signals for prosthesis control while accurately reproducing the amputee's movement intent (Farina et al. 2004).

Coordinating the complex movements of the natural limbs requires the individual control of all participating muscles in a dynamic fashion, allowing continuous adjustment of muscle contractions based on the visual, tactile or proprioceptive feedback. However, the neural mechanism of limb control is not just a closed control loop with set point generation, movement execution and feedback. There is a hierarchical organization which has the goal of distributing the complexity of the movement tasks from high cognitive centers to lower control mechanisms specialized for execution. The basic commands for the successful performance of motor tasks originate in higher neural centers such as the motor cortex, but the actual muscle activation takes place on lower levels of movement execution – the spinal cord. The mechanism of limb movement has a top-down organization and is characterized as being conscious and cognitive (Kandel et al. 2000).

In contrast to the limb control, the sensory perception mechanism has bottom-up architecture (Barsalou 1999). In natural perception, interaction with the environment in all its large diversity and complexity is broken down by specialized receptors into specific features. Different receptors differently encode physical interaction into trains of APs, which are sent to higher levels of the CNS through parallel sensory pathways (Dargahi & Najarian 2004). According to past experience, context or knowledge, the sensed information is bound into new representations. The same mechanical deformation of the tactile receptors or proprioceptors may generate the same neural codes, but the perception will interpret them differently, depending on various factors, such as vision and attention (Longo & Sadibolova 2013; Zopf et al. 2011).

The perceived stimuli are very diverse; yet this diversity does not result from the capacity of individual receptors to discriminate between the huge varieties of stimuli. Instead, embedded in the skin, bones or muscles, the receptors are specialized to sense particular properties of the stimuli, e.g. high- or low-frequency vibration, steady pressure or dynamic deformation of the skin. Stimulation of these receptors determines the generation of signals transmitted to higher centers in the brain in sequential steps. At each processing stage the information coming from individual channels is integrated into more complex information. This mechanism

allows high discriminability between the large variability of physical stimuli resulting from the interaction with the environment (Caldwell et al. 1996).

The amputation is an interruption of these efferent (top-down) and afferent (bottom-up) hierarchies. Numerous neural terminations dedicated to the execution of complex tasks of the hand, for example, are barred from carrying out their physiological functions. The motor nerves send movement commands in vain and the sensorial terminations are marked by futility. As a result, the correspondence between action and reaction is lost.

Upper-limb prosthetics aim to reconstruct this interruption. Controlled by EMG, the prosthesis will move and interact with the environment, but its performance will be followed mainly visually. The visual feedback provides an overview of the entire visible scene and, for this reason, it is said that visual feedback acts on higher levels of perception. Being global, but also slow, due to the huge amount of information processed, the visual feedback is only used in natural behavior to generate movement targets in body space. The target is set mainly by vision, but the execution of the movements is performed on lower cognitive levels, by motor programs specialized in performing specific tasks, and is therefore fast. Visual feedback roughly corrects the trajectory, but tactile and proprioceptive feedback close the high-speed control loop of movement execution (Land 2006).

The bodily experience during natural limb control is the result of successfully integrating multiple sensory inputs in a bottom-up fashion, and controlling the movements in a top-down fashion. On one hand, the CNS structures and processes all available sensory information to affect conscious and subconscious motions; on the other hand, based on sensory experience, the CNS generates commands in the form of movement programs (Ayres et al. 2005).

The joints of the prosthesis are individually controlled by amputees, and the prosthesis performance is followed by amputees mainly visually. As a result, the prosthesis control is slow, and a large cognitive effort is required for the amputee working with high levels of perception (vision) and conscious low levels of actuation (joint by joint).

In contrast with the prosthetics, the control of natural limbs is faster and more intuitive, working with low levels of perception and conscious high levels of control - the targets are specified in body coordinates, while the low levels of actuation remain subconscious and the movement of the limb itself and its interaction with the environment are sensed by tactile perception and proprioception.

Future prosthetic devices need to function more like natural limbs, which is no trivial undertaking. The movements have to be more task-oriented, e.g. grasping a glass or using utensils, and should not be focused on the movement itself. On the other hand, in order to restore the natural movement mechanisms, well-structured sensory information is required, informing the amputees about performance and interaction

between the prosthesis and its environment. This sensory information should not only be perceived, but also intuitive and comfortable allowing a natural assimilation of prosthetics by amputees.

In order to be accepted by amputees, the prosthesis has to be highly integrated into the body's control mechanism. At rest and during functional activity, the prosthesis must work reliably, have proper kinematics and dynamics in order to respond in harmony with the prosthesis wearer, and close the control loop interrupted by amputation by providing tactile and proprioceptive sensation. In targeting an improvement in the acceptance of prosthetic devices by amputees, special attention has to be paid to intuitiveness of prosthesis control.

An amputation does not only mean the loss of the limb; there are also structures in the brain affected by it. The phantom limb phenomenon is well known; it is the sensation that the amputated limb is still attached to the body and it is reported by 60 to 80% of amputees (Lotze et al. 2001). Sometimes amputees report the phantom limb being controllable in accordance with their intention to move, sometimes "reduced mobility" is reported, and sometimes it is only perceived as being attached to the body. The patients will sometimes feel as if they are gesturing with the phantom limb, feel itches, twitch, or even try to pick things up. However, most patients associate phantom limb sensation with pain (Giummarra & Moseley 2011).

Until recently, it had been thought that the phantom limb phenomenon was determined by "neuromas" – tumors of the cut nerves that develop after amputation. The idea was that neuromas would send confusing signals to the brain which would react to the nonsense by generating pain sensations. Recent research (Ergenzinger & Pons 2001) reveals that the somatosensory cortex undergoes substantial reorganization after amputation. Research published by Flor et al. (1995) demonstrated that phantom limb pain is more closely correlated with this cortical reorganization than other phantom sensations.

There is also evidence that the brain has an internal representation of the body. In amputees, the limb is missing but not its representation in the brain, which is currently thought to be responsible for the phantom limb phenomenon. Sustaining this theory, McGeoch & Ramachandran (2011) reported the case of a woman born with a congenital deformation of the right hand, consisting in three fingers and a rudimentary thumb. After a car crash, the hand was amputated, which gave rise to phantom hand sensations. The phantom hand was experienced, however, as having all five fingers. The visual, tactile and proprioceptive feedback of the physical hand overruled the image in the brain, but after amputation, and in the absence of the disruptive feedback, the five-fingered hand, deeply embedded in the brain, reappeared as a phantom limb. Other experiments carried out by Moseley & Brugger (2009) indicated that the natural limbs are somehow like a glove covering the brain's representation of the limb. In these experiments, the amputees were encouraged to contort their phantom limbs into impossible configurations, and four of seven subjects succeeded. The natural limb covers its brain representation like a glove, and the movement of the natural limb is restricted by physical limitation of the joints but, after amputation, the glove is removed and the brain's representation of the limb is

freed from these physical restrictions, reverting to a more fundamental representation, making it more flexible in its movement intentions.

These new findings led to the idea that the phantom limb is not necessarily something which should be *treated*, but something which offers potential in merging human and prosthesis in a physiological and very intuitive way. However, in order to *wear* the phantom limb with a real prosthesis, the phantom limb should be alive and fully under the amputee's control.

Loss of control over the phantom limb is indicated by many studies as being an important factor in determining the elevation of pain. This is also in accordance with the experience that stress, anxiety and weather strongly influence the appearance of pain. Most approaches to treating the phantom pain, analgesics or antidepressants, vibro- or electro-stimulation of the stump, spinal cord stimulation and so on, have all been shown, in a large survey conducted by Flor et al. (2006), to be ineffective. But one approach, which gained a great deal of public attention, is the mirror box developed by Ramachandran et al. (1995). By providing the amputees with visual feedback that is congruent with their intention to move the limb, it becomes possible for the patient to gain control over the phantom limb and to unclench it from painful positions. Repeated training has led in a few cases to long-term improvement, though the pain alleviated by the therapy very often reappears shortly after the training session. Recently, graded motor imagery and sensory discrimination training have emerged as promising therapeutic tools for dealing with phantom limb pain (Moseley 2006).

1.2. Thesis Goal

There is strong evidence that phantom pain emerges from a simple lack of control over the phantom limb, and it seems likely that control over the phantom limb can be gained when the amputee's expressed movement intent is acknowledged by any kind of feedback, including visual. Thus, the "mirror therapy" could turn out to be one of the most successful methodologies in alleviating phantom pain (Weeks et al. 2010). By imagining that they move both arms simultaneously, while actually moving only one arm, and having the mirrored visual feedback of both arms moving simultaneously, amputees subconsciously establish the correspondence between movement intent and performance, which is thought to be determinant in alleviating phantom pain. Within the mirror box, the brain receives the feedback it expects after sending movement commands; however, outside the box the feedback disappears and the pain very often reappears, in some cases with more violent manifestations than before therapy.

The current work was mainly inspired by the opportunity gained from the phantom limb phenomenon to better integrate prosthetic devices into the amputee's body image. Providing haptic feedback, congruent with movement intent, is expected to produce results similar to mirror therapy. If haptic feedback is present and integrated into the socket at all times, rather than only during therapy sessions, it will allow for conditions more conducive to long-term alleviation of phantom pain. It is not likely, however, that results will be gained by providing just any kind of feedback; intuitiveness and harmony of prosthesis control, intuitiveness and comfort of feedback, smooth training procedures and objective assessment are all factors that must contribute to success.

The mechanisms determining phantom pain are very complex, and the available knowledge about the physiology of it does little to explain the mechanisms generating it. The framework of this study does not directly address the neurological basis of the phantom limb phenomenon, but it does aim to make strides in better integrating the prosthesis into the amputee's body image, which is hypothesized to have an important contribution to the alleviation of the phantom limb pain. The focus of this work is, therefore, the optimization and harmonious integration of amputee and prosthesis through careful examination of both the efferent and afferent interfaces between them, and for this the following aspects were addressed:

Increasing intuitiveness of prosthesis control

The amputees express their intent to move by contracting a group of residual stump muscles, and signal processing algorithms convey this information, sensed by EMG, into movement references for prosthesis control. Good rehabilitation may require the reconstruction of most degrees of freedom (DOF) lost in amputation, and this is the long term goal. However, if the prosthesis is not well controlled, the amputees will have no benefit from it. Moreover, such a sophisticated prosthesis may generate frustration and even rejection by amputees. Therefore, during this study the complexity was reduced to minimum, one single degree of freedom (the open-close function of a prosthetic hand), while the focus was set in analyzing various factors

improving controllability. Controllability, as used here, means more than just moving the prosthesis, but moving quickly and precisely, in harmony with the body and in synchrony with the natural limb movement.

This goal is addressed in the following chapters: Chapter 2, which briefly describes the neural mechanisms behind the control of the natural limbs; Chapter 5, which tried to eliminate ambiguity with regard to the terminology used to describe the control mechanisms and strategies used during this thesis; Chapter 6, in which the closed-loop parameters and variables with influence on increasing intuitiveness of prosthesis control were systematically analyzed; Chapter 8, which emphasized the advantages and disadvantages of different control strategies.

Optimal wearable technology for providing haptic feedback

Increasing prosthesis controllability it is not just a matter of improving the interpretation of the sensed EMG to more accurately reproduce the natural movements; there are also various studies indicating that providing the amputees with haptic feedback regarding prosthesis performance will help to increase intuitiveness by augmenting one of its necessary conditions: less demanding, more comfortable control. By better replicating control of natural limbs, which move in accordance with body dynamics and are able to feel, prosthetic devices will be better integrated into the body image of the amputee.

A prosthesis moves and interacts with the environment, and one important goal of this work is to close the prosthesis control-loop by providing haptic feedback to the amputee. Current state-of-the-art technology provides various wearable stimulation devices which are designed to be sensation-inducing for the person wearing them, most popularly based on vibro-mechanical and electro-stimulation. The former, most commonly adopted by the industry, is efficient and robust but provides a narrow range of sensations; the frequency and amplitude of stimulation are tightly correlated, being a function of applied voltage to the motor. On the other hand, the latter, electro-stimulation, is capable of modulating amplitude and frequency independently and is consequently capable of generating a large amount of differentiable stimulation. Nevertheless, electro-stimulation does not provide consistent stimulation, at least applied at the surface of the skin, and is also not practicable for daily life use due to the required self-adhesive electrodes. In an attempt to combine the advantages of both technologies, a haptic device was developed which is able to generate complex vibro-tactile stimulation patterns by independently modulating frequency and amplitude of stimulation. In order to increase the amount of stimuli, besides the frequency and amplitude, a new degree of freedom has been introduced; the same device is also able to induce pressure sensation by lightly and concentrically squeezing the stump by way of a belt mounted in the socket.

In order to identify the requirements, a haptic device must first accomplish in order to optimally stimulate the skin, Chapter 2 reviewed the physiological mechanisms of tactile perception in humans, and also tried to catch the technological SOA in wearable haptic devices, to avoid putting efforts in wrong directions. In Chapter 3, the advantages and disadvantages of various stimulation systems were discussed and a new wearable stimulation

technology was proposed – the Haptic Brace, targeting the combination of the advantages of different stimulation technologies while minimizing their drawbacks.

Psychophysical assessment of stimulation

Stimulation can be characterized by physical parameters measured with e.g. an accelerometer, a dynamometer or an oscilloscope. However, from the provided physical stimulation, the human body will be able to perceive a narrow range of stimuli. Therefore, a series of psychophysical measurements were done with the goal to evaluate the maximum number of discriminable stimulation (vibels) and of building a model of the stimulation. This model allows a direct comparison between many technologies and recommends the optimal solution for implementation of closed-loop prosthesis control.

A brief overview of the methodologies available to psychophysically describe the tactile stimulation was given in Chapter 2. They were mostly developed for the characterization of audio/visual perception, and also recommended for tactile perception, but they do not entirely fit our requirements; therefore an adaptation of a classical methodology (SIAM) was proposed and described in Chapter 3.

Generating intuitive, comfortable and effective feedback patterns

The model of the stimulation, resulted after performing series of psychophysical measurements, delivers essential information for the creation of stimulation patterns as it allows for the generation of continuous stimulation trajectories by interconnecting discriminable stimulation points (vibels). But not all perceived feedback will be intuitive, effective or comfortable, which are necessary conditions for the integration of feedback into the prosthesis control loop. Therefore, a study on the phenomenology of feedback acceptance was also done. For this purpose, the potential offered by the Rubber Hand Illusion (RHI) (Botvinick & Cohen 1998) was exploited.

Approaches to combining stimulation primitives into patterns and to evaluate their degree of intuitiveness were proposed and described in Chapter 4.

Intuitively mapping feedback patterns with sensory information

Parameters delineating the movement of the limbs, such as joint position or speed, and interactions with objects within the environment, such as force, all measured by the attached prosthesis' sensory system, have to be conveyed in patterns of discriminable haptic information, which, when perceived by the amputees, will close the prosthesis control-loop. However, complex information, haptically transmitted to the amputees, will decrease the discriminability of perceived stimulation, and the right compromises between dimensionality and efficiency have to be identified. Moreover, in order to be intuitive, the haptic feedback should be correspondingly mapped with the sensory-information measured by the prosthesis. Every sensory signal has to be properly encoded by haptic feedback patterns in order to be intuitively interpreted by amputees.

This goal was addressed in Chapter 6, in which as an example, first contact, velocity and grip force were encoded by different discriminable vibrotactile patterns.

Assessment of prosthesis controllability

Developing new strategies for more intuitive prosthesis control, in open as well as in close-loop control, is very important. But an objective assessment of the prosthetics controllability is crucial. Without such an objective measure, it will not be possible to identify the strengths and weaknesses of various approaches, making systematic improvements to the system hard, if not impossible. In order to have a general character, the assessment of prosthetics control must be made within a standardized environment. This is a vital requirement, as the outcomes should be compared between subjects who are geographically separated, and it will allow for the quantification of performance over a larger timespan. Replicating real environments and assessment scenarios in different places, or at different instants in time, is quite a challenge, explaining to some extent the lack of widely accepted solutions for the assessment of prosthetics performance.

Therefore, a 3D immersive virtual reality (VR) system was introduced in Chapter 7 of this study. In Chapter 8, an assessment methodology was proposed, inspired by an internationally recognized standard, the “International Classification of Functioning, Disability and Health” - ICF.

1.3. Thesis Outline

This thesis consists of ten main chapters. Chapter 1 – “Introduction” familiarizes the reader with the field of prosthetics as well as with the current challenges in making upper-limb transradial prosthetic devices a better replacement for the loss due to amputation. The motivation of this work is presented and the specific goals of the study are pointed out. Chapter 2 – “Aspects of Sensory-Motor Integration” gives background information about the physiology of natural movement, tactile perception and the mechanisms allowing for harmonious integration of feedback into goal-driven tasks common in the natural behaviour. The prosthetic devices are a replacement for an amputated limb; therefore the same chapter also briefly describes the SOA in upper limb prosthetics and their EMG control, from the physiology of muscle contraction, recording technologies, to strategies for converting the sensed EMG into prosthesis movements. Providing feedback to the amputees and closing the prosthesis control loop is an important topic of the study, so an overview of the most widely-used wearable stimulation devices is given to understand what is currently technologically possible. Chapter 3 – “Vibrotactile Stimulation,” discusses the implementation and gives a partial evaluation of some of the most popular wearable stimulators. The strengths and weaknesses of all implemented technologies are discussed and a novel technology is introduced, which is presumably able to combine the advantages of different technologies while minimizing their drawbacks. This stimulation technology, able to generate vibrotactile stimulation patterns by independently modulating amplitude and frequency, is physically as well as psychophysically evaluated by measuring the stimulation parameters with an accelerometer and by performing a series of psychometric measurements in order to quantify the amount of discriminable stimuli perceived by humans. In order to emphasise its advantage over the stimulation generated by a classical vibration motor with eccentric weight, a direct comparison is made. To prepare the integration of vibrotactile feedback into the control loop of prosthetic devices, the stimulation has to be mapped with sensory information measured by the prosthesis. Therefore, discriminable and continuous stimulation patterns have to be generated, which are able to intuitively convey the sensory information measured by the prosthesis to the amputee. This topic is addressed in Chapter 4 – “Pattern Generation Strategies.” Chapter 5 – “EMG-Driven Prosthetics Devices” briefly describes the common low-level EMG pattern recognition strategies implemented in the commercial prosthetic devices: *First Wins*, *Difference* and *Largest Wins*. The low-level prosthesis control modes, known as *Speed* or *Force* which partially describe the real prosthesis behaviour, are redefined with *Proportional*, *Derivative*, or *Voltage (Hybrid)* in order to intuitively describe the behaviour of the prosthesis with regard to the movement intent by the amputee, expressed as EMG. Chapter 6 – “Open vs. Closed Loop Prosthesis Control” is a study about feedback modality and variables used to close the control loop of prosthetic devices. The performance in controlling grasp strength with a hand prosthesis was evaluated when different types of feedback (vibrotactile or visual) are provided to the user. The following chapter, Chapter 7 – “An Immersive Virtual Reality Environment,” describes the architecture and the components of a VR system implemented to be used as a training environment for the EMG prosthesis control or as a prototyping tool which, due to its remarkable flexibility, allows for the evaluation of various kinematics or dynamics of hand prosthetic devices. But its most important advantage was considered its capability to provide standardized scenarios and

conditions which allow for an objective and systematic assessment of prosthesis controllability/embodiment between different subjects geographically separated, or for monitoring the learning curve and performance, controlling prosthetic devices over a larger time span. The assessment procedure was inspired from an internationally recognized standard for describing health and health-related states, the International Classification of Functioning, Disability and Health, known as ICF and described in Chapter 8 – “Assessment of EMG Prosthesis Control.” The ICF belongs to the family of international classifications developed by the World Health Organisation (WHO) for application to various aspects of health, including rehabilitation. The chapter, Chapter 9 – “Discussion” is an overall recapitulation of the topics and experiments treated in this thesis. The final chapter, Chapter 10 – “Final Conclusions and Future Work,” enumerate the contribution of the thesis with respect to the initial goals and give future perspective on the development of a new generation of prosthetic devices which have to function in better harmony with the body dynamics in order to be better perceived as part of the amputee’s own body.

2. ASPECTS OF SENSORY-MOTOR INTEGRATION

2.1. Movement

2.1.1. MOVEMENT GENERATION

The mechanisms responsible for movement generation have a hierarchical organization (Newell & Vaillancourt 2001). Higher processing centers in the brain plan, coordinate, and execute complex movements of the body. The commands generating movement are the result of processing sensory information provided by various modalities, e.g. vision, proprioception, and of a highly complex process of tacking decisions. The mechanism for generating voluntary movements requires high cognitive effort, and is therefore slow. In contrast, the reflexes are basically motor programs activated by various sensory inputs and are much faster. In natural movement, voluntary and reflexive movements are well-integrated, allowing the generation of adaptive movements. The motor system generates three types of movements: reflexive, rhythmic and voluntary (Kandel et al. 2000).

Reflexive Movements are sequences of pre-programed movements consisting of successive contraction/relaxation of muscles or groups of muscles initiated by sensory stimuli. These programs are hard-coded into the CNS, but it is possible to slightly change the correspondence between triggering stimuli and performed movements under certain conditions. Reflexes are performed subconsciously, have relatively simple circuitry, and so react quickly. They are incorporated into more complex volitional movements initiated by the central commands (Kandel et al. 2000).

Rhythmic Movements are repetitions of the same movements in a cyclical manner, such as locomotion or chewing. The rhythmic movements are initiated at the spinal cord level without assistance from the sensory system. The commands generated by the spinal cord give only the basic rhythm for movement, e.g. during locomotion, the spinal cord generates bursts of activity in the flexor and extensor motor neurons. The final movement of the limb is regulated by sensory inputs from various modalities, e.g. proprioception, vision, or from the vestibular apparatus controlling balance (Kandel et al. 2000).

Voluntary Movements are the most complex of the three types. They are consciously performed, task oriented, and generated by CNS after the integration of the information from the various sensory modalities. In contrast to reflexes, voluntary movement is the result of a cognitive process, meaning that processing of the same stimuli can result in different movement sequences. While the behavior of the reflexes is pre-programmed, the voluntary movements can be greatly improved with experience and training. With experience, an optimization process will eliminate the redundant sensory-motor connections and automatism will develop; the movements will become faster, more precise, and require less cognitive effort (Kandel et al. 2000).

Voluntary movements improve when subjects learn to predict the sources of noise which could potentially perturb the preprogrammed trajectories. If they succeed in anticipating and effortlessly correcting these

environmental perturbations, body movements gain in fluency and become more precise (Schmidt & Lee 2005). The movement mechanisms employed by the CNS use two strategies to correct these perturbations. The sensory signals are continuously evaluated, and future movements are planned. This step-by-step movement strategy is called feedback [Figure 1A]. The feedback strategy is robust in eliminating environmental perturbations, but is also slow. The second strategy is called feed-forward control [Figure 1B].

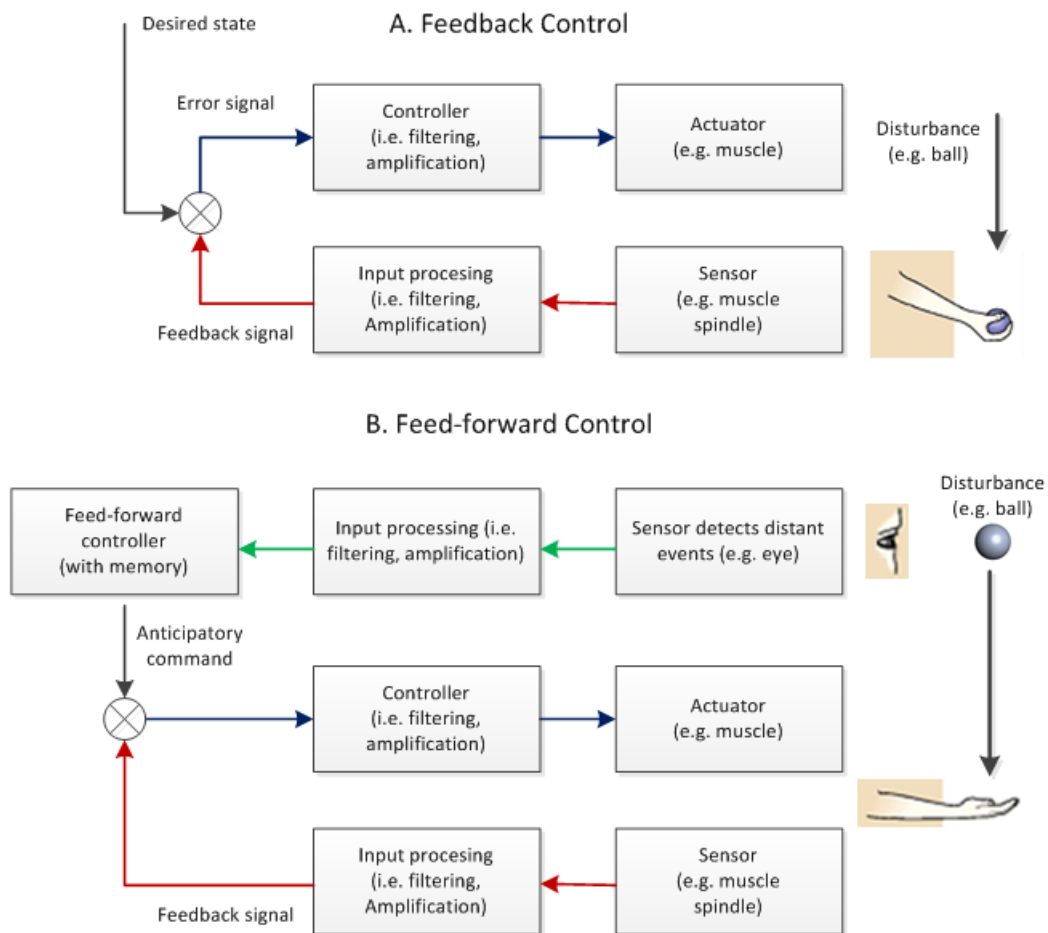


Figure 1: Feed-forward vs. feedback control circuits. The feedback control paradigm continuously compares the desired with the real posture of the body and their difference is used to adjust the motor output. In comparison the feed-forward control estimates the perturbations, based on previous experience, and generates motor programs able to compensate them (Kandel et al. 2000, p.655).

During feed-forward control, perturbations are estimated and movement programs are generated based on previous experience, in order to optimally reach the target. The feedback control strategy continuously compares the desired body posture with signals provided by the sensory system, and the difference is used to adjust the motor output, thereby canceling the difference.

The feed-forward control is aimed at canceling potential perturbations in advance in order to generate faster motor programs; the movement is performed before the sensory system is able to provide any information. Feed-forward control is mainly based on experience and the human capacity to predict and compensate for environmental perturbations. This control strategy may derive from the feedback strategy. If the responses during feedback-based movements are close to the expectations, optimization mechanisms will increase the sampling rate of this moment-to-moment control strategy, with the consequence of movement being more efficient. Ideally, interactions with the environment are predictable, and no feedback is required. However, in reality, there is interplay between the feedback and feed-forward paradigms.

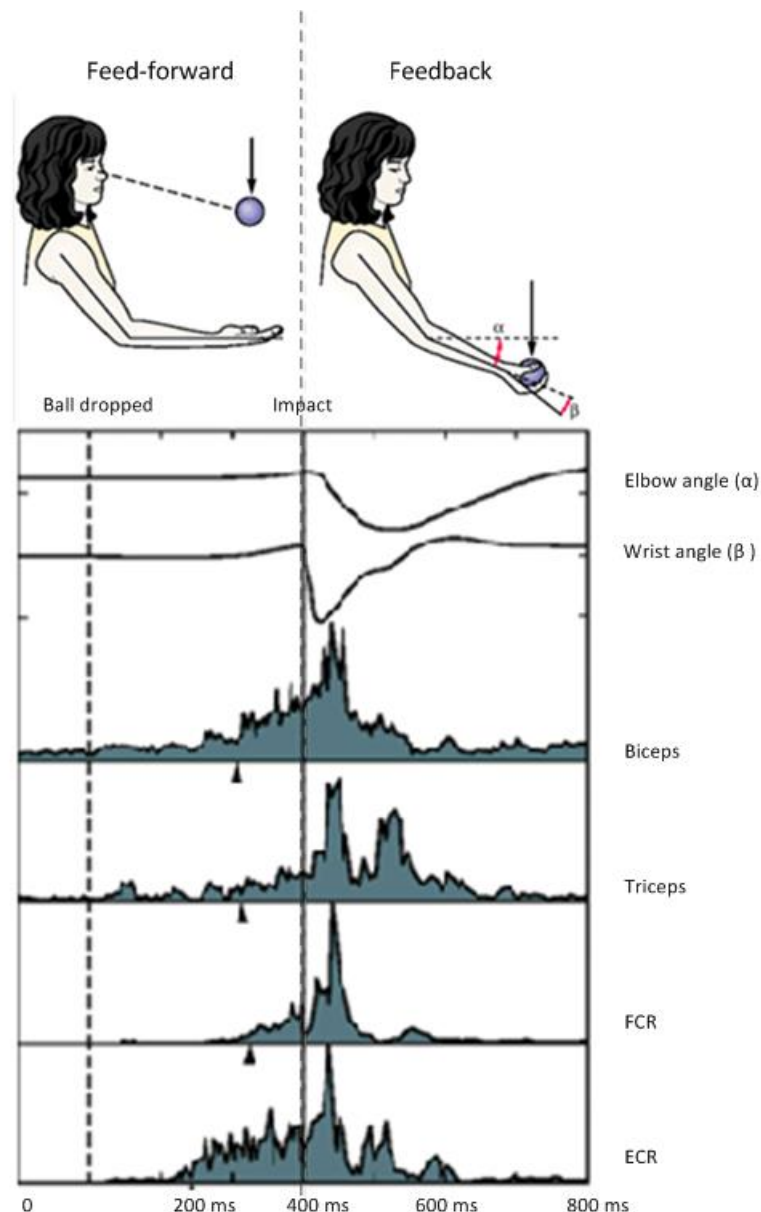


Figure 2: Catching a ball requires feed-forward and feedback coordination. When the ball approaches, co-activation of biceps and triceps is increasing the stiffness of the arm, preparing it to catch the ball. After catching the ball, further contraction of biceps and triceps are rejecting the unexpected “noise” minimizing the deflection of elbow and wrist (Kandel et al. 2000, p.656).

Catching a ball is an example of feedback and feed-forward coordination [Figure 2]. A ball was dropped from a height of 0.8 m. When the ball approaches the hand, co-activation of the biceps and triceps prepares for interaction with the ball. After catching the ball, further co-activation of flexors and extensors rejects the unexpected 'noise', minimizing the deflection of elbow and wrist. In this example of catching a ball, the feed-forward mechanism was initiated by vision. The anticipatory muscle contractions were activated sooner or later, depending on the velocity of the ball approaching the hand; experience is determinant for feed-forward control. The feedback mechanisms take control over the limbs only when the ball hits the hand and proprioception and tactile perception are activated (Kandel et al. 2000).

This interplay between feedback and feed-forward control is a matter of motor learning. In the incipient phase, when learning a new motor skill, the movements are slow and poorly coordinated; the movements rely mainly on feedback. While performing in a novel environment, the visual information is evaluated intensively, concentration is at a maximum, and subconscious processes work to integrate perceived sensory information with the motor commands. The more consistent the feedback while producing motor commands in previously experienced environments, the faster the movement will be. Otherwise, unexpected events will determine a slow-down of the movement, and new movement strategies will be tried. This is the phase in which movement intentions, expressed in body coordinates, are converted into individual joint movements – the programming phase (Yousif & Diedrichsen 2012).

The learning process is facilitated by the rate of success; as a result, the sequencing and timing of movement becomes automated, shifting from direct visual control to a more internalized form of control. The learned movements become faster, smoother and better-coordinated, requiring less attention. The goal can be achieved without conscious intervention due to the coexistence of feed-forward and feedback control (Schmidt & Wrisberg 2000).

2.1.2. GRASPING

Grasping requires coordination of the forces measured by the hand and fingers in order to hold an object in a stable position. Researchers have studied the mechanisms for grasping extensively (Johansson et al. 2001) (Westling & Johansson 1984) (Johansson & Westling 1987), and one focus of these studies was to evaluate the role of the cutaneous mechanoreceptors in the coordination of fingertip forces. They found that when an object is grasped with two fingers (thumb and index), from a supporting surface, the normal and tangential forces increase at the same ratio (Johansson & Westling 1988). When the grasp forces become constant (the static phase), the minimum force needed to prevent the object from slipping is called *slip force*, and has been found to be in most cases proportional to the weight of the object. It is obvious, the slip force will also depend on the friction between hand and object; a lower friction coefficient will require higher slip force to stably grasp an object, and smaller slip force when the friction is higher. The stability of the grasp is maintained by increasing/decreasing the grip force in parallel with the load force. When slippage is detected, the natural hand is able to react within 70 ms to form a more stable grasp (Johansson & Westling 1987). The reaction time of

this mechanism is twice as fast as a voluntary change of grip force elicited by a tactile stimulation. Microneurographic recordings indicate that the slip is detected by the cutaneous mechanoreceptors, even though they are usually not perceived (Johansson & Westling 1987).

These mechanisms for avoiding the slippage of grasped objects are reactions to unexpected events. If the weight and slipperiness are able to be estimated, then feed-forward motor commands are generated to compensate for them, without assistance from sensory information, though both feedback and feed-forward controls are used when lifting an object [Figure 3].

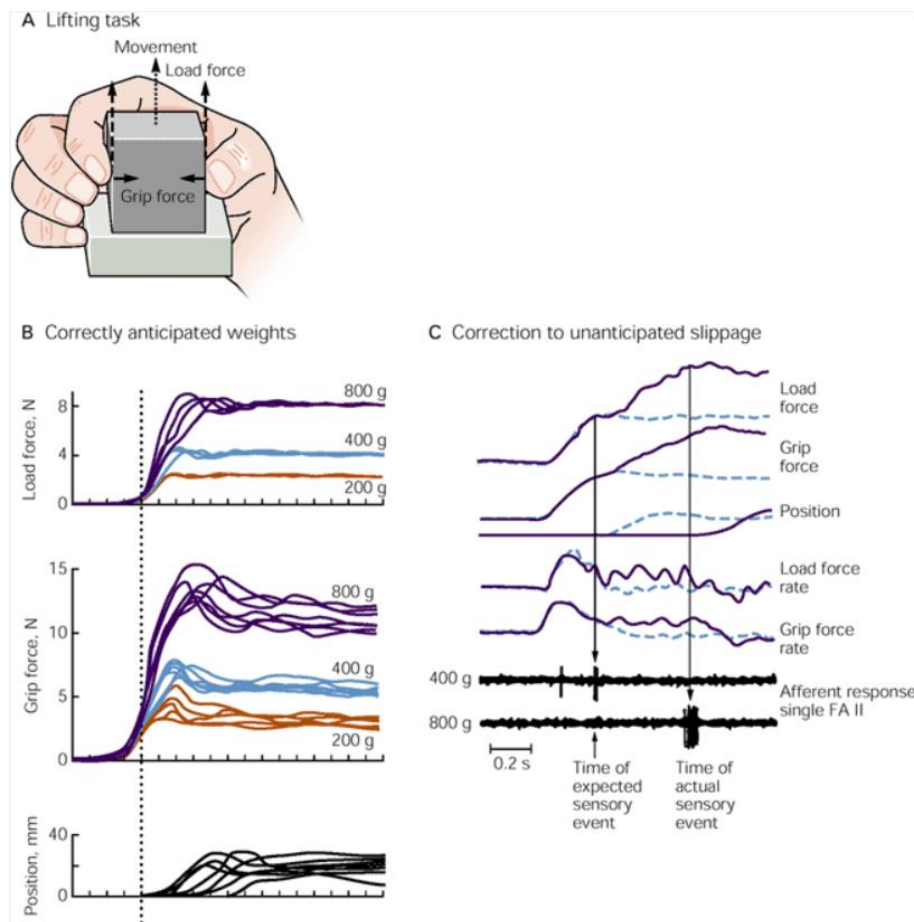


Figure 3: Both feedback and feed-forward controls are used when lifting a slippery object. A-The subjects lift an object from a supporting surface. B-When the weight of the objects is known from previous trials, the force required for lifting an object was applied as result of one single, firm contraction. C-The weight was unknown for the subject, therefore the feedback control was activated to compensate the target weight misestimation, and to compensate for undesired slippage (Kandel et al. 2000, p.660).

The subject lifts an object from a supporting surface in Figure 3A. When the weight of the targeted object was known to the subjects from previous grasps, the applied force resulted from only one fast contraction (feed-

forward), which was sufficient for lifting the object. This was repeated for three different loads with 200g, 400g and 800g respectively, and Figure 3B shows the correspondences between load force, grip force and position. When the weight was larger than expected, the feedback control was activated to respond to slippage. In Figure 3C one particular case is presented, in which, after some trials lifting a 400g weight (dashed lines), the subject was given an 800g weight having the same geometry and appearance (solid lines).

2.1.3. PSYCHOPHYSICS OF REACH-TO-GRASP MOVEMENT

The psychophysics of movement allows for an objective assessment of the performed movement with regard to the movement intent. Especially important for the topic of this thesis is the example of psychophysics during reach-to-grasp movement. During reach-to-grasp movement, the hand aperture and posture changes in conformity with the dimensions and orientation of the target object. The main feature investigated during the psychophysical evaluation of reach-to-grasp movement, would be the correlation between the hand aperture, object size and the distance to the object. A reach-to-grasp movement comprises three distinct phases: first, the hand approaches the target – the reaching phase; second, the hand adjusts its configuration to prepare for an optimal grasp – the grasp phase; last is the phase in which the object is grasped and manipulated – the manipulation phase (Armbrüster & Spijkers 2006).

Ideally, while the hand is approaching the target, it follows a relatively straight path, regardless of its starting or final position. As the target is approached, the speed of the hand at first increases, and then declines to zero. The brain generates a representation of the movement before its execution, but, while approaching the target, vision, in cooperation with other senses, continuously updates the trajectory in order to optimally stop the movement once the target is reached (Jeannerod 1992).

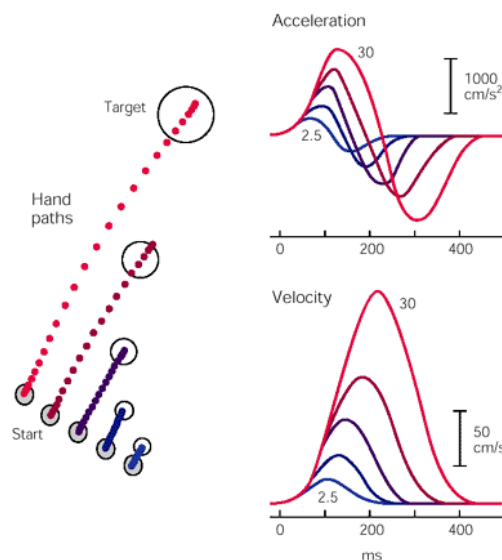


Figure 4: Acceleration and velocity of the hand scale with the movement extent indicating that a known movement is executed as a preprogrammed automatism (feed-forward) with little influence of feedback (Kandel et al. 2000, p.659).

Examples of such reach-to-grasp movements, with the target located 2.5, 5, 10, 20 and 30 cm from the starting position, are shown in Figure 4. While executing one of the five reach-to-grasp movements, chosen at random, the subjects were blindfolded. Different colors indicate the velocity and acceleration profiles for all five distances, and dots are hand positions at 20 ms intervals. The average acceleration and velocity were linearly scaled with the distance to the target. The acceleration/deceleration profiles, with their smoothness, indicate that the movement is preprogrammed before the execution is initiated; accelerated at the beginning of the movement and decelerated when the target is approached (Kandel et al. 2000).

While Figure 4 shows only the hand trajectory approaching the target, Figure 5 depicts the correlation between the movement of the hand toward the target and the hand aperture. The targets were placed at three different distances from the observer, 250, 320 and 400 mm, but the velocity profile was always a bell-profile, synchronized with the movement duration.

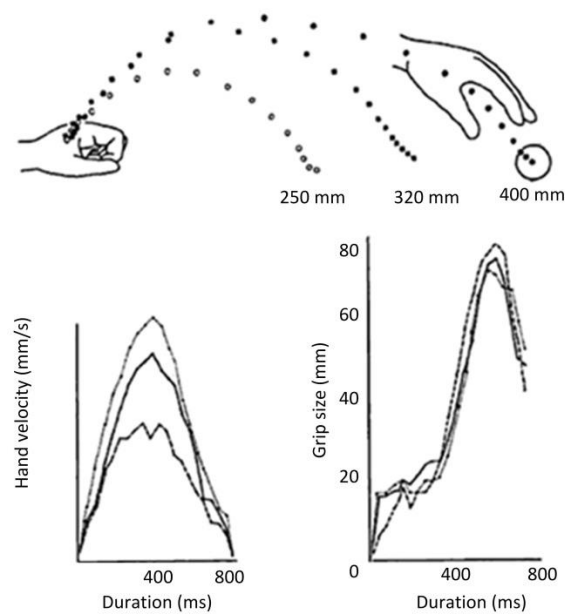


Figure 5: During a reach-to-grasp movement the grip size synchronizes with the velocity of the hand toward the target. When grasping the same object placed at three different distances, the reach-to-grasp movement requires the same amount of time, but the movement is executed at three different velocities. (Gentilucci et al. 1991).

During a reach-to-grasp movement, the hand is shaped in accordance with the geometry of the target object, preparing the grasp. While approaching the target, the hand first opens, then closes, generating a bell-profile for velocity. The most common feature used to characterize the grasp is the amplitude of the maximum grip aperture, which is correlated with the object's size and the distance from the hand to the target (Gentilucci et

al. 1991). Since three different distances to the target were used in the trials, three bell profiles for hand velocity with three distinct amplitudes resulted. Nevertheless, the grip size for all three measurements was almost the same.

2.2. EMG Prosthesis Control

2.2.1. MUSCLE CONTRACTION AND EMG

Movement is the result of contractions of muscles or groups of muscles. The muscles are actuators which convey the neural information provided by the CNS into movement or force. They are made of fibers, with a thickness about that of a human hair (50 μ m) organized in groups known as motor units (Zajac 1988). All fibers in a motor unit are innervated by a single motoneuron, so when a command is relayed from the CNS, the entire unit contracts simultaneously [Figure 6].

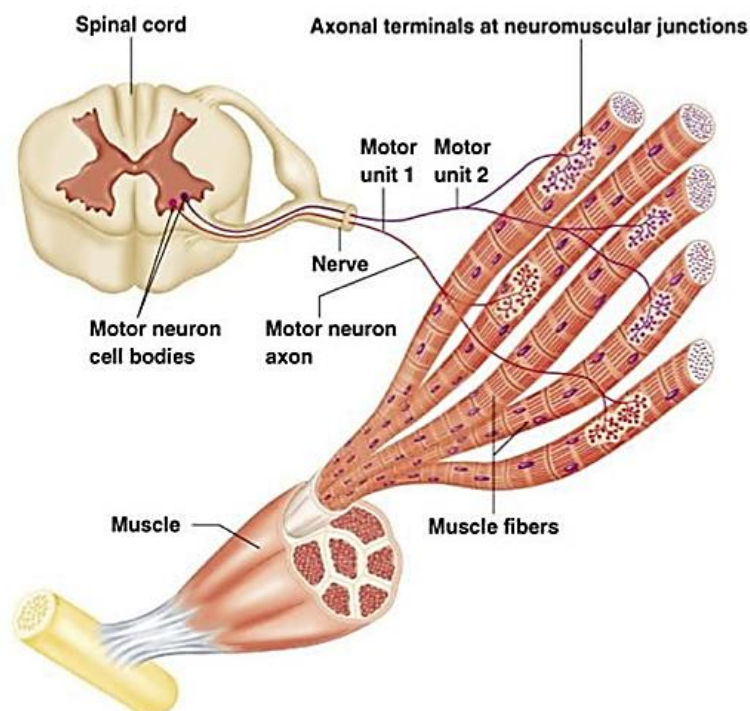


Figure 6: The muscle fibers of a motor unit are innervated by a single motoneuron, and the CNS controls the muscle contraction by turning motor units on and off. An AP traveling along one nerve triggers an electrical discharge in each of the muscle fibers that it innervates determining a muscle contraction (www.studyblue.com).

The commands coming from the CNS are encoded by electrical impulses, called action potentials (AP), and propagated along the motoneuron axon. Every AP will determine the fibers to twitch, and when impulses come at a fast rate (15/s) the twitches fuse producing steady force. The nervous system controls the force of a

muscular contraction by turning motor units on and off and by modulating their discharge rates. A muscle's motor unit is always recruited from smallest to largest. During a sustained contraction, the frequency of the AP controlling the muscles ranges from ten to twenty-five discharges per second. The intervals between the AP of a particular motor unit are not perfectly regular, but vary slightly, by several milliseconds (Merletti et al. 2008).

An AP traveling along one nerve triggers an electrical discharge in each of the muscle fibers that it innervates. The APs originate at the point of innervation and then spread along the muscle fibers in two waves outward from the innervation point toward the fiber's ends. When a motor unit discharges, APs generated by all the muscle fibers in the unit are summed together to produce a motor unit AP (MUAP) (Farina et al. 2004).

The EMG signal is the summation of the discharges of all the motor units within the pick-up range of the electrode. During a sustained weak contraction, the sequence of APs propagated along two muscle fibers might be recorded with a needle electrode and the recorded EMG signal will consist of two distinct trains of APs. However, when the APs propagating along the fibers simultaneously pass the recording volume, the electrode senses their summation. The resultant waveform can be either larger or smaller than the individual APs, depending on whether the overlap results in constructive or destructive interference (Farina et al. 2013). During a stronger contraction, the EMG signal contains AP trains from many motor units. Due to the large number of superpositions, the individual MUAPs are difficult to distinguish. If the muscle contraction is stronger, the superposition contains a large number of individual APs, so that even high-pass filtering isn't helpful in extracting individual MUAP trains (Farina et al. 2010). Furthermore, decoding the neural information available as EMG is very challenging because it is dependent on a large variety of factors. The EMG content varies with the strength of contraction, length of the muscle, fatigue, and the dynamic of the muscle contraction (Stashuk 2001; Farina 2006).

2.2.2. EMG RECORDING TECHNOLOGIES

In order to record the EMG signals generated during muscle contraction, many categories of electrodes may be used: the needle electrodes, fine-wire electrodes, and surface electrodes. Needle/fine-wire electrodes have the advantage of being able to record detailed characteristics of the generated EMG. They are inserted into the muscle close to the motor units, allowing a less noisy signal acquisition. These electrodes have a good selectivity, but for reasons of practicality, they cannot be used in commercial prosthetic devices dedicated for daily activities. The main advantage of the surface electrodes is that they are completely non-invasive and therefore easy and comfortable to use in the prosthetics context. Nevertheless, they are only able to measure EMGs at the skin's surface, which is noisier and less consistent. The surface electrodes are far away from the muscle fibers, and therefore the amplitude of the recorded APs is very small and unstable (Farina & Enoka 2011). A way to solve, to some extent, the uncertainties introduced by the noisy interface between muscle and electrodes is the use of electrode arrays which have shown good performance to obtain decomposable signals (Holobar et al. 2010), (Farina et al. 2002).

The voltage generated during a muscle contraction is a relatively low 0-10 mV peak-to-peak (-5 to +5mV), or 0-15mV RMS. In order to make these signals useful for prosthetics control, they have to be conveyed from biological to electrical voltages, amplified and processed. For this purpose, EMG electrodes are used, which receive signals generated by muscle fibers and propagated over voltage fields within the volume surrounding the muscles. The changing potential gradients will produce electrical currents in the electrode leads. These weak electrical currents will then be amplified by the amplifier's input stages of the EMG electrode, converting them into large output voltages (Merletti & Parker 2004).

There are many types of EMG electrodes - monopolar, bipolar, tripolar, multipolar, barrier or patch, and belly tendon electrodes. A monopolar electrode measures the potential between one active contact and the ground, and this voltage is further amplified by a monopolar amplifier. A bipolar electrode has two active contacts, one connected with the positive input and the other one with the negative input of one differential amplifier. Due to its configuration, the bipolar electrode measures the slope of the voltage traveling beneath the electrode's contacts, which is insensitive to the ground potential of the skin, providing good stability. However, it will only work optimally if the distance between the electrodes is properly chosen. If the electrodes are placed too far apart, it will work like a double monopolar electrode. Placing them too close together will cause the voltage difference to be too low, resulting in a weak, unusable signal. An additional reference electrode is still needed for the amplifier circuit. A tripolar electrode has three active electrodes placed at equal intervals along a straight line. In actuality, there are two bipolar electrodes; from the four inputs, two of them are connected with each other, resulting in three inputs. The outputs of the two bipolar preamplifiers are further inputs into a cascaded bipolar preamplifier. The ground contacts of all three amplifiers will be connected together to one additional ground electrode. The tripolar electrode has the advantage of being less sensitive to distant noise sources but is still sensitive to the electrical activity of the tissue to which the electrode contact is attached. A multipolar electrode consists of rows of bipolar electrodes and is mainly used to record the propagation information along the muscle fiber. As with all the other types, the multipolar electrode requires a reference electrode (Merletti & Parker 2004).

2.2.3. EMG CONTROLLED PROSTHETICS

EMGs are widely used in controlling upper-limb prosthetic devices. Commercial prostheses mostly use bipolar electrodes for sensing EMG activity, e.g. with antagonist placement on the stump for the case of trans-humeral or trans-radial amputations. The contraction of a group of muscles is recorded by the electrodes, rectified, and filtered, resulting in a continuous electrical signal used as movement reference for the prosthetic device. This type of control is known as *Direct Control* and is widely used in commercial systems, being simple, stable and robust. However, the direct correspondence between EMG hot-spots and joint movement greatly simplifies the dimensionality of the interface with the prosthesis. Often, the fitted prosthesis has many more degrees of freedom than available EMG hot-spots. A common solution is the use of switching mechanisms; one pair of muscles, agonist/antagonist contracting simultaneously, will sequentially control many prosthesis joints, one at a time. This approach is very simple, and is an acceptable solution for many amputees. However, this co-

contraction approach is demanding and non-physiological. In an attempt to extract more control signals, many more complex signal processing algorithms have been tried: analysis of the EMG in frequency domain and in time domain, the use of electrode arrays, or EMG decomposition (Merletti et al. 2010; Farina et al. 2010). They have proven to faithfully distinguish the movement intent from the surface electromyography, but these approaches often result in an increased processing time, or are too sensitive to various biasing factors common during daily life, e.g. motion artifacts.

2.3. Tactile Sensation & Perception

Understanding the strengths and weaknesses of various haptic stimulation technologies, or even designing new technologies, requires a clear understanding of the mechanisms by which humans perceive tactile physical stimuli. The users of such devices will be successful in retrieving and interpreting information haptically only when the generated stimulation fully fits the addressed modalities of touch and proprioception. The somatic modalities of touch and proprioception are mediated by neurons with encapsulated terminals – tactile receptors. The tactile receptors are able to sense the mechanical interaction with the environment, the intensity of the contact as well as the position that is touched, to discriminate the amplitude and frequency of vibrating objects, and to recognize shapes and textures (Bolanowski et al. 1988).

2.3.1. SENSATION

Sensation is an awareness of sensory stimuli in brain. The interaction of the body with the environment is sensed by specialized receptors distributed throughout the body and has four major modalities: discriminative touch, proprioception, nociception and temperature sensitivity (Johnson 2001). In order to serve the current research, only the first two modalities need to be discussed further. Discriminative touch is the perception of pressure, vibration and texture; proprioception is the sense of relative position and movement of neighboring parts of the body as well as the required effort in joints. Each of these modalities is mediated by a distinct system of receptors and is conveyed to the brain along specific neural pathways – sensory neurons. Sensory neurons have two branches: one is sensitive to external stimuli and responsible for stimulus transduction, in which external stimuli are converted into a body-internal representation; the second projects to the central nervous system with a transmission function (Sotnikov 2006).

Each sensory neuron is specialized in the detection of specific properties of the interaction determined by the type of the peripheral terminals of the axon, which can be free or encapsulated nerve endings. The free nerve endings mediate painful, thermal and some secondary tactile sensations, while the encapsulated nerve endings (mechanoreceptors) mediate the somatic modalities of touch and proprioception. The sensitive branch transduces the specific types of stimuli energy by creating graded potentials or action potentials which are then conveyed to the central nervous system by afferent sensory neurons. The sensed information is coded in a series of action potentials which are sent along different specific pathways simultaneously to different targets

in the brain. The perceived sensation is the result of the brain's processing of different patterns of electrical signals (Olshausen & Field 2004).

Physical interaction with the environment causes mechanical alteration or deformation of the skin which is detected by corresponding mechanoreceptors. The mechanoreceptors are specialized end organs surrounding the nerve terminal. Having a specialized structure the mechanoreceptors must be deformed in particular ways in order to excite the sensory nerve. To respond to different types of mechanical stimulation, the receptors are specialized in coding different submodalities of touch or proprioception (Gardner 1988).

The conversion of physical stimuli into sensations is ensured by three or four principle classes of tactile sensory nerves [Figure 7], falling into two broad groups. One group, called slowly adapting (SA) receptors and afferent fibers, is responsive to static mechanical displacement of skin tissue and is made up of two classes, the type I (SAI) fibers that innervate Merkel receptors and the type II (SAII) fibers that innervate Ruffini endings. The second broad group displays a pure dynamic sensitivity to tactile stimuli and also falls into two principle classes, the rapidly adapting (RA) tactile fibers that are associated with Meissner corpuscle receptors and the Pacinian corpuscle (PC)-associated class of tactile afferent fibers (Bolanowski et al. 1988). These classes of functional nerves appear in glabrous skin regions as well in the hairy skin of the arms, legs and trunk. Receptors in close association with the long bones of the limbs include groups of Pacinian corpuscles distributed along the interosseous membranes. These are highly sensitive to dynamic forms of mechanical stimuli - vibrotactile disturbances in particular (Kandel et al. 2000).

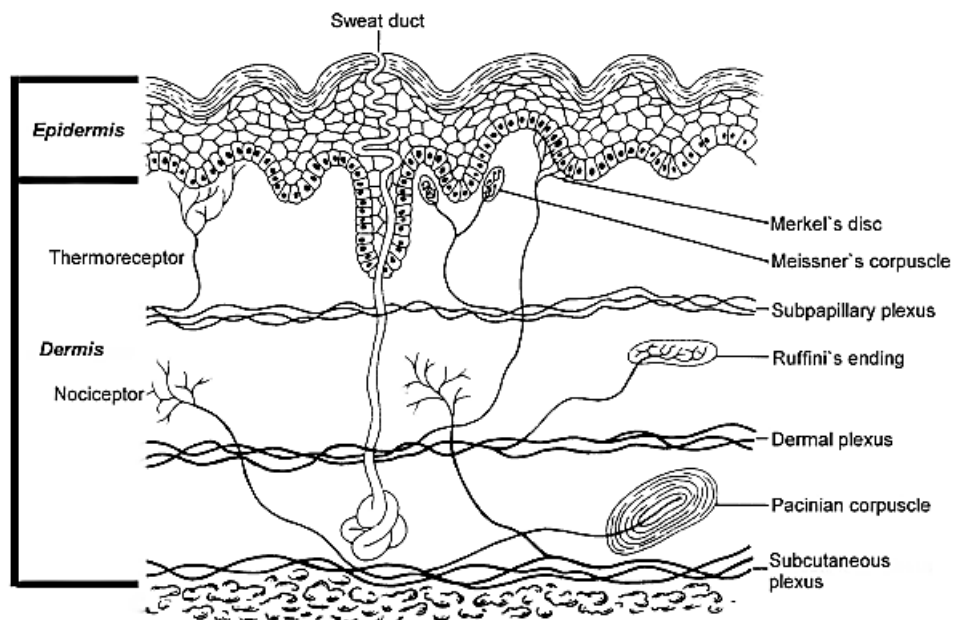


Figure 7: Cross-section of the skin showing the dermis and epidermis. Four groups of mechanoreceptors, embedded in the skin, are responsible with the detection of physical interaction with the environment: the Merkel disks, the Ruffini endings, the Pacinian and Meissner corpuscle (Bolanowski et al. 1988).

Meissner's Corpuscle is a small fluid filled structure in which the sensory nerve terminal lies between the various layers of the corpuscle. The receptors are located at the surface of the skin, mechanically coupled with the edge of the papillary ridge, so that the corpuscle's receptive fields are sharply defined. The nerve sensitive endings are located in a fluid. Due to this condition a sustained stimulus is sensed only at the first contact with the skin when the nerve membrane is stressed by the propagated mechanical wave. Mechanically controlled ion channels in the nerve membrane will open, generating action potentials. Shortly after the first perturbation, the nerve endings come to rest, the vibration being damped by the fluid surrounding it. A large intensity of the stimulus is coded into a high-frequency trains of action potentials and, correspondingly, mechanical stimuli with smaller intensity, into a low-frequency trains of action potentials (Jadhav et al. 2009).

The Pacinian corpuscle is the largest sensory end organ in the body (approx. 0.5 mm wide and 1mm long). It is the most deeply embedded in the skin and consists of approximately 70 layers assembled in an onion-like fashion on the end of a peripheral nerve fiber separated by a gelatinous material. The large capsule of this receptor is flexibly attached to the skin in the deep dermal layers as well as in skeletal joints. In the center of the corpuscle is the inner bulb, a fluid-filled cavity with a single afferent un-myelinated nerve ending. Due to this condition, a sustained stimulus is sensed only at the contact with the skin when the nerve membrane is briefly stressed by the generated mechanical wave. Mechanically controlled ion channels in the nerve membrane will open generating action potentials. After the first contact perturbation is gone, the membrane of the sensitive nerve endings comes back to rest. A large intensity of the stimulus is coded into high-frequency of action potentials and vice-versa. Because the corpuscles are situated deep in the dermal layer, the receptive field is diffuse (Kandel et al. 2000).

Merkel's Disc is a small cell that surrounds the nerve terminal, consisting of a semi rigid structure. Tactile disks connected to the Merkel cells transmit pressure from the skin to the sensory nerve ending. Being situated close to the surface of the skin, the corpuscle receptive fields are sharply defined. Having a semi rigid connection, the nerve endings are continuously deformed as long as the stimulus persists. The sustained pressure is signaled by a continuous train of action potentials. The intensity of the stimulus is coded into frequency of action potentials. The receptors have a sustained reaction and are believed to respond to pressure applied perpendicularly to the skin at frequencies below 5 Hz (Kandel et al. 2000).

Ruffini endings are located in the deep layers of the skin, and are specialized in sensing the stretch of the skin, or mechanical deformation within joints. They exist only in the glabrous dermis and subcutaneous tissue of humans. This receptor is shaped like a spindle and contributes to the kinesthetic sense and control of finger position and movement. It is specialized in detecting slippage of objects along the surface of the skin, allowing modulation of grip on an object. Having a semi rigid connection, the nerve endings are continuously deformed as long as the stimulus persists. The sustained pressure is signaled by a continuous train of action potentials. The intensity of the stimulus is coded into frequency of action potentials (Kandel et al. 2000).

Hair follicle receptors and field receptors respond to hair displacement. Field receptors are located primarily over the joints of the fingers, wrist and elbow. They sense skin stretch when the joint is flexed or when the skin is rubbed (Kandel et al. 2000).

Proprioception is mediated by mechanoreceptors embedded in the muscles and has two submodalities; one characterizes the stationary position of the limbs, and the second the limb movement in space. Three types of mechanoreceptors mediate proprioception: spindle receptors located within the fleshy part of the muscle and specialized muscle stretch receptors, Golgi tendon organs that sense contractile force or effort exerted by a group of muscle fibers and receptors located in joint capsules that sense flexion or extension of the joint. In addition, stretch-sensitive receptors in the skin (Ruffini endings, Merkel cells in hairy skin, and field receptors) also signal postural information (Kandel et al. 2000).

Joint receptors are mechanoreceptors (e.g. Pacinian corpuscle) located in and around joints that gather information about limb position and joint movement. Muscle spindles are small encapsulated sensory receptors that have a spindle-like or fusiform shape. When the muscle fibers are stretched, the sensory endings are also stretched and increase their firing rate. Because muscle spindles are arranged in parallel with the extrafusal muscle fibers that make up the main body of the muscle, the intrafusal fibers change in length as the whole muscle changes. Thus, when a muscle is stretched, the activity in the sensory endings of the muscle spindles is increased. When a muscle shortens, the spindle is unloaded and the activity decreases. When a muscle is stretched, there are two phases of the change in length: a dynamic phase, the period during which length is changing, and a static or steady-state phase, when the muscle has stabilized at a new length. Structural specializations within each component of the muscle spindles allow spindle afferents to signal aspects of each phase separately (Kandel et al. 2000).

Golgi tendon organs are sensory receptors located at the junction between muscle fiber and tendon; they are therefore connected in series to a group of skeletal muscle fibers. Each tendon organ is innervated by a single (group Ib) axon that loses its myelination after it enters the capsule and branches into many fine endings, each of which intertwines with the braided collagen fascicles. Stretching of the tendon organ straightens the collagen fibers, thus compressing the nerve endings and causing them to fire. Because the free nerve endings are intertwined with the collagen fiber bundles, even very small stretches of the tendon organs can deform the nerve endings. Whereas muscle spindles are most sensitive to changes in length of a muscle, tendon organs are most sensitive to changes in muscle tension. A particularly potent stimulus for activating a tendon organ is a contraction of the muscle fibers connected to the collagen fiber bundle containing the receptor. The tendon organs are thus readily activated during normal movements (Kandel et al. 2000).

The properties of the body's interaction with the environment are sensed by a population of mechanoreceptors [Figure 8]. Specific tactile sensations occur when distinct types of receptors are activated. Selective activation of Merkel cells and Ruffini endings produces a sensation of steady pressure on the skin

above the receptor. When the same patterns of firing occur only in Meissner's and Pacinian corpuscles, the tingling sensation of vibration is perceived (Watanabe et al. 2007).

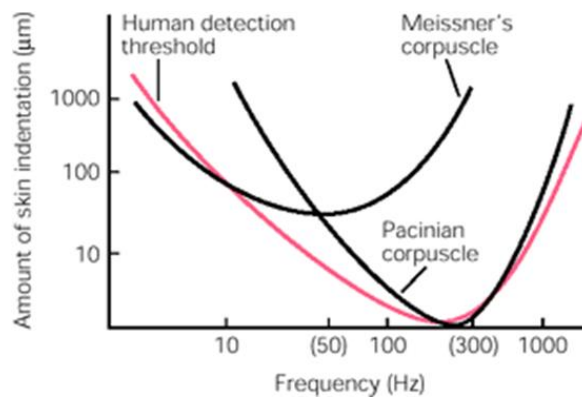


Figure 8: The threshold for detecting vibration corresponds to the tuning threshold of the mechanoreceptor. From all mechanoreceptors, Pacinian corpuscles are most sensitive having the lowest detection threshold at around 250 Hz (Kandel et al. 2000).

Pacinian corpuscles also sense the displacement of the skin when the hand moves across an object, it provide also information for texture identification. The Meissner's corpuscle is particularly sensitive to abrupt changes in the shape of objects that occur at the edges or corners and to small irregularities on the surface sensed during palpation by the hand. Meissner's corpuscles are used to detect and localize small bumps or ridges on an otherwise smooth surface. More salient bumps or edges are required to activate the slowly adapting Merkel disk receptors. However, once stimulated, the Merkel receptors provide a clearer image of contours by changes in the frequency of firing. If the surface is flat, these receptors fire continuously at relatively low rates. Convexities that indent the skin increase firing rates whereas concavities silence these receptors. Responses are proportional to the surface curvature; large-diameter, gently curved objects evoke weaker responses than small-diameter objects. The strongest responses occur when sharp edges or punctate probes, such as a pencil point, contact the receptive field (Kandel et al. 2000).

2.3.2. WEARABLE HAPTIC TECHNOLOGIES

The tactile interaction of the human body with the environment is sensed by specialized receptors embedded in the skin, each of them dedicated to sensing high/low-frequency vibrations or steady pressure. Consequently, the tactile human interaction with the environment is expressed in terms of vibrations and/or steady state pressure.

Vibration is an important component of haptically-transmitted information. In order to be effective, though, the applied vibration should physiologically fit the task in which the human subject is involved. Vibration may be perceived as comfortable or relaxing, but may also cause annoyance and discomfort. By providing vibration feedback, it is possible to improve performance during e.g. a handling task, but may also disturb the subject,

reducing the system performance. To optimally convey information haptically there should be established correspondences between the type of tasks the subjects are involved in, between the physical information desired to be conveyed and the stimulation parameters of amplitude and frequency. "Human Vibrations" is multidisciplinary and in order to be able to harmonize the applied vibratory feedback with the complex structures of human perception, knowledge is required from diverse disciplines, such as engineering, ergonomics, mathematics, medicine, physics, physiology and statistics (Griffin 2007). The current work intends to use available knowledge from all these fields to physiologically close the control loop of assistive devices and to improve the human performance aspect of various daily living tasks. How to provide effective vibro-tactile feedback is only one part of a more elaborate research project which deals with providing haptic feedback to persons with physical disabilities who rely on using devices like prostheses or orthoses. These devices are, nowadays, mainly controlled in open loop; the patients, volitionally activate one or more functions of the device, and the performance of e.g. hand or knee prosthesis is observed mainly visually. Based on the gathered information, the patients plan their next movements. Vision is global and able to process a huge amount of information, but is slow and has to be shared between different activities. As a consequence, it is thought that the performance of the artificial limb or supportive device might be limited by the slow processing speed of vision (Blank et al. 2010). Therefore the next generations of e.g. prosthetic devices have to embed sensorial systems capable of emulating the main features of lost bio-receptors due to amputation. It is no trivial task to transmit them to the amputees by means of invasive or non-invasive methods. Invasive methods directly stimulate nerve fibers to transmit sensations to the brain. Non-invasive methods are more widespread in their implementations and will also be a subject of the current work. Transcutaneous (surface-mounted) electrical and mechanical stimulation are the most widespread methods of transmitting information to the body and are also in use in the context of prosthetics.

Because of its global property, vision is used in the natural solution to identifying targets in the visual space. Being slower than the dynamic requested by the movement of the natural limb, vision is not able to follow limb performance at high resolution. It only supports the movement correction mechanisms, sampling the limb trajectory by a rate in accordance with the speed of the executed movement and with other psychological factors, e.g. attention. In the natural limb behavior, the execution of the movement is assisted by haptics and proprioception which are specialized senses, able to convey movement into information that the CNS can process quickly (Kuchenbecker et al. 2007). In contrast with higher hierarchical levels of motion where cognitive processes are involved between sensation and action, the movement execution is subconsciously controlled by sensation. Action is not the result of a high cognitive process; but is a preprogrammed automatism, a predefined reaction to specific stimuli which is a skill acquired during a learning process (Schmidt & Wrisberg 2000).

This more intuitive, high-dynamic control loop for prosthetic or orthotic devices doesn't yet exist and the amputees rely mainly on vision, making the control slow and demanding due to the high cognitive effort. It is thought that, by providing haptic or proprioceptive feedback to the subjects, the control of prosthetic devices

can be improved, and the effort required for their control, reduced. It has been supposed that this result can also improve amputees' prosthesis acceptance (Dhillon & Horch 2005). However, before the integration of the feedback into the control loop of prosthetic devices, we face the challenge of finding the proper stimulation technology. For this purpose, a literature review has been conducted to bring together insights from state-of-the-art haptic technologies as well from psychophysical measurement methodologies, which will be necessary for evaluation.

The widely used haptic technologies can be divided in three major categories: thermal stimulation, electro- and mechanical stimulation (Shimoga 1993; Van Veen & Van Erp 2001).

Thermal stimulation could be an interesting approach in a trial to integrate the prosthesis into the body schemata, to make the prosthesis a part of self (Jones & Berris 2002). However, the inertia which characterizes the thermal displays and the large power consumption do not recommend the use of this technology in the prosthetic field.

Electro-stimulation provides sensation of touch through electro-tactile excitation. This technology mostly uses self-adhesive electrodes to produced localized tactile sensations by passing impulses of small electrical currents through the skin (Kaczmarek et al. 1991). The applied electrical currents generate electrical fields which stimulate the nerve fibers responsible for the transport of the sensory information from the receptors to the CNS. The elicited sensations can be described as tingle, pressure, vibration, or pain, depending on the electrode and waveform properties (Benali-khoudja et al. 2004). Because this technology doesn't require moving parts or mechanical mechanisms, it can be embedded in small geometries. For the same reasons, the reliability of electro-stimulation is higher in comparison to mechanical tactors. Some examples of tactile arrays that utilize electrodes made from conductive rubber for electro-stimulation are shown in Figure 9.



Figure 9: Examples of rubber array electrodes used for electro-stimulation (McGrath et al. 2008)

Vibro-mechanical stimulation provides the sensation of touch by directly activating specialized mechanoreceptors in the skin (Kaczmarek et al. 1991). The methodology is much more complex, requiring different types of actuators and additional mechanical systems in order to deform the skin and generate the expected sensations (Argall & Billard 2010). Despite all these disadvantages, the mechanical stimulation is preferred due to its consistency. Some of the most widespread mechanical stimulators are briefly presented here.

ROTARY CENTRIFUGAL ELECTRO-MECHANICAL TACTORS



Figure 10: Optec-2890w11 pager motor (McGrath et al. 2008)

The rotary centrifugal electro-mechanical tactor consists of a flat DC motor spinning an eccentric mass around its rotational axis. The motor is embedded in a housing which vibrates when the motor is rotating, stimulating the skin. This technology is reliable and accessible, therefore widely adopted by various consumer electronics, e.g. game controllers, cell phones. The OPTEC-2890W11 is a commonly used motor for tactile stimulation and is pictured in Figure 10. The rpm of the motor defines the tactile frequency stimulus and is typically in the range of 4000 – 9000 (i.e., 70 – 150Hz). These “pager-motor” tactors are increasingly made in-house by the laboratories undertaking research work. For example, TNO (The Netherlands) and FOI (Sweden) have produced custom rotary centrifugal tactors for specific tactile applications (e.g., presenting navigation, targeting, or orientation information), and include custom housings and custom drive electronics [Figure 11]. The size, cost, robustness, and low power consumption, characteristics of the “pager-motor” tactor, make it a popular choice for many applications (McGrath et al. 2008).



Figure 11: TNO custom rotary-inertial tactor (left). TNO tactor array housed in vest (right) (Mcgrath et al. 2008)

LINEAR ELECTRO-MECHANICAL TACTORS



Figure 12: C2 tactor (McGrath et al. 2008)

Linear actuator tactors are miniature, coil-based actuators incorporating a moving “contactor” that is lightly preloaded against the skin or can be embedded in a closed housing. When an electrical signal is applied, the “contactor,” or housing, oscillates perpendicularly to the skin. In case of a moving contactor, the surrounding skin area can be “shielded” with a passive housing. This provides a strong, point-like sensation that is easily felt and localized. Linear, coil-based actuators have good frequency and amplitude control in the range around their resonance frequency (McGrath et al. 2008).

PNEUMATIC TACTORS

Pneumatic tactors are linear actuators consisting of a membrane covering the opening of a reservoir. Changing the pressure of the air within the reservoir causes the elastic membrane to generate force against the skin which is perceived as vibration. These tactors are robust and produce a high-intensity tactile sensation. Pneumatic tactors have been integrated into the Tactile Situation Awareness System (TSAS) (Rupert 2000), a tactile display for presenting spatial orientation information to pilots. The tactors are integrated into a flight cooling vest and are “powered” by the existing pressurization systems for G-suit inflation (Van Veen & Van Erp 2001).

OTHER TACTORS

Pin-based tactile displays have a dense array of metallic pins embedded in a surface. Correspondingly activated, the heads of the pins press or vibrate against the skin transmitting textual or graphical information to the person. A prominent example of this type of display is the Optacon (Heller et al. 1990), a vibrotactile display originally developed for displaying text characters onto the fingertips of blind users. Text materials are scanned into the Optacon system, and the pins in the array vibrate against the skin using spatial patterns consistent with the shapes of the characters. Vibrotactile fingertip displays are generally efficient, low-powered systems, as the fingertip is among the most sensitive parts of the body. However, not all pin-based arrays use vibration. For example, ABTIM’s VideoTIM operates in a manner similar to that of the Optacon, but it is based on feeling the differential displacement of the pins in the array (McGrath et al. 2008).

The hydraulic tactor has the same principle of functioning with the pneumatic tactor, but uses fluid instead of air as a medium. An example is a system developed by QinetiQ for use in the Diver Reconnaissance System (DRS). It uses an electric motor (24V dc, 400mA) to drive a piston which forces fluid into the DRS handles that expand and contract to provide the tactile / haptic stimulus to the driver's hands. The typical frequency range is 1 – 5Hz with large amplitude displacements of up to 25 mm (McGrath et al. 2008).

The piezoelectric device is a linear actuator which generates a mechanical displacement when an electrical voltage is applied. The high cost, low force and displacement coupled with high voltage requirements have prevented widespread use (McGrath et al. 2008).

Electroactive polymers (EAP) are a category of smart materials that are polymer-based, and react in the presence of an electric current. Typically these materials contract, expand or bend to a limited extent when an electric current or voltage is applied to them. New EAP materials contract by 20% (McGrath et al. 2008).

2.3.3. PSYCHOPHYSICS

SENSATION THRESHOLD

The basic function of a psychophysical measurement is to detect energy or changes of energy in the environment. In this case of our application, psychophysical measurement is performed in order to detect the capacity of different haptic technologies to induce sensations. If the goal is to determine the minimal amount of energy which lifts the observer sensation over the threshold of consciousness, then the result is called an absolute threshold. Otherwise, if the result refers to the minimum intensity to produce a noticeable perceptual difference, then the detected level is called a difference threshold. The goal targeted by all psychophysical procedures is to determine the correlation between physical applied stimuli and sensation (Leek 2001).

As proposed by E.H. Weber, this correspondence can be described by the equation which is called Weber's Law after the name of its discoverer: $\Delta\theta = c * \theta$ (Murray 2010). Weber's Law states that the ratio between the just noticeable difference and the magnitude of the stimulus is a constant, c , and is called Weber's Fraction. For experimental data, Weber's Law doesn't hold in all situations: Weber's Fraction is not constant for perception at very low or very high intensities [Figure 13].

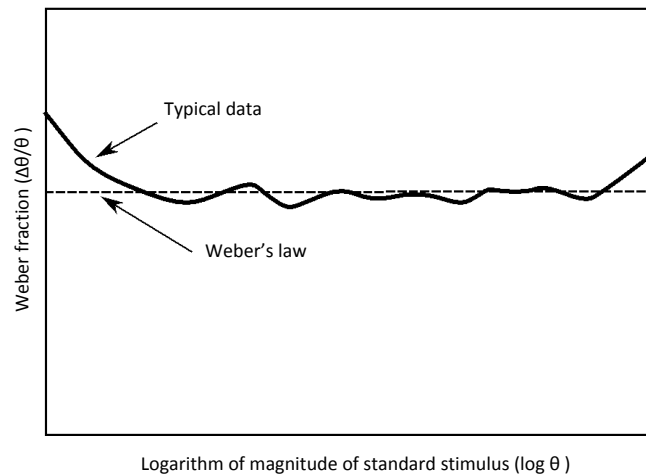


Figure 13: The weber's Law doesn't hold over the whole stimulation range. The weber fraction is not constant for perception at very low or very high intensities

It is supposed that this behavior is determined by an internal noise which is a supposition of various stochastic processes (Ewert & Dau 2004). For this reason the original Weber's Law was modified by introducing a constant, n , which takes into account the internal noise: $\Delta\theta = c * (\theta + n)$ (Marks 1974). The n represents the internal noise and the spontaneous activity of the nerve fibers, respectively. If θ increases, the influence of n is not important, but if θ decreases it becomes more important.

Theoretically, a sensation threshold is the level by which a stimulus is perceived (e.g. Level 3 - Figure 14 left). However, the biological systems are variable in reaction to fixed stimuli; there is a large variety of intrinsic and extrinsic parameters influencing it. Therefore, in psychophysics the sensation threshold is defined as the level at which the stimulus is detected with a predefined probability (e.g. 50% - Figure 14 right). The same notion for sensation threshold is used for detection as well for discrimination thresholds.

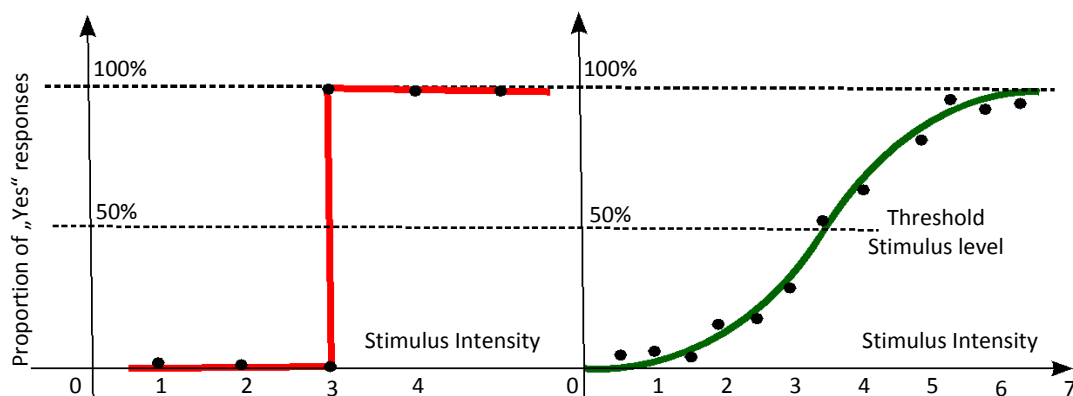


Figure 14: Theoretical vs. Real sensation threshold. Theoretically the stimulation threshold is the level by which a stimulus is perceived. The real stimulation threshold however, is not the result of a deterministic process, but of a stochastic one, and the sensation threshold is defined as the level at which the stimulus is detected with a predefined probability.

PSYCHOMETRIC FUNCTION

A psychometric function characterizes not only the sensation threshold for a predefined probability, as previously discussed, but the correspondence between the probabilities to detect stimulus as a function of stimulus magnitude, so, for the estimation of such a function, the repeated application of stimuli with different magnitudes is required. The resulting collection of “yes - perceived” answers then fit a cumulative shape of the normal distribution (integral of the Gauss distribution) curve, which is called psychometric function. The psychometric function describes the sensitivity to a stimulus by two parameters: the level at which the stimulus is perceived with a certain probability, and the slope of the psychometric function at this point (Gescheider 1997). As detection is not a deterministic but a probabilistic process, evaluation requires a lot of redundant trials at appropriate signal levels to give a good estimate of the threshold. The appropriate signal levels are not known at the beginning of the test, and so adaptive procedures are used to adjust the signal level. The signal level will thus oscillate around its target value.

PSYCHOPHYSICAL EVALUATION METHODS

For the purpose of characterizing psychometric performance as a function of changes in stimulus strength, several methodologies have been developed. In the following, based on a review performed by Treutwein (Treutwein 1995), the most popular psychophysical procedures used in sensory research are briefly described.

In the *method of adjustment* the subjects are allowed to adjust the intensity of the stimulus until it becomes just noticeable, (to measure absolute thresholds), or appear to be just noticeably different from, or to just match, some other standard stimulus (to measure a difference threshold). The estimated threshold is the average of the turn points after performing successive series in which the signal strength is increased and decreased.

In the *method of limits* a single stimulus is changed in intensity in successive discrete steps and the observer's response to each presentation is recorded. The initial presentation will be too weak to be perceived and the answer will be “not seen”; intensity will then increase in steps until the stimulus becomes visible, or vice versa starting with a high level of stimulation “seen”, and decreasing the stimulus intensity until the stimulus is not detected at all. The average of the intensity of “last seen” and the first “not seen” is the estimation of the absolute threshold. The method is also applicable for threshold difference detection.

The *method of constant stimuli* is based on applying a set of stimuli with strengths spanning the sensation's range of interest. Each member of the stimulus set is presented to an observer many times, at random, and an observation response is requested after each presentation. The data are then plotted with stimulus intensity along the abscissa and percentage of perceived stimuli along the ordinate. The resulting graph represents the psychometric function.

The psychometric function may be sampled by evaluating the percentage of presentations of each member of the stimulus set that's detected, making the measurement of this single point on the function very expensive in terms of time.

In order to address this major problem, adaptive psychometric procedures have been developed. The common characteristic of currently used adaptive methods is a systematic manipulation of the stimulus level along the experimental dimension of interest. Each method results in a series of stimulus levels presented over the course of the experiment, along with the associated subject responses. Experimental variables that may impact the results of the methodology include the amount of difference between stimulus values presented (the step size), the initial starting value of the stimulus, the process that guides the sequence of presentation levels on each trial (the tracking algorithm), and the decision for ending the process (the stopping rule). The general goal of each procedure is to measure characteristics of the subject's performance over the shortest amount of time, without sacrificing accuracy.

The adaptive methodologies may be placed in three general categories, defined by their systems for placing trials along a stimulus array and by the manner in which each estimates a final outcome: parameter estimation by sequential testing (PEST), maximum-likelihood and staircase procedures.

PEST is characterized by an algorithm for threshold searching that changes both step size and direction (i.e., increasing and decreasing level) across a set of trials. The PEST algorithm is designed to place trials at the most efficient locations along the stimulus axis in order to increase measurement precision, while minimizing the number of trials required for threshold estimation. In the original PEST procedure the threshold estimate was simply the final value of the track.

The initial threshold level and the step size are selected to begin a track. After each presentation at a fixed level, a statistical test is applied to indicate whether performance at that level is better or poorer than the targeted performance level (e.g., 75% correct detections). Once that determination is made, the level may change by the current step size, and a series of presentations occurs at the new level, again testing after each presentation whether the level should be changed.

Maximum Likelihood adaptive procedures use an estimated psychometric function for the best placement of the stimulus on each trial, driven by consulting the current best estimate of the entire underlying psychometric function after every stimulus-response trial. As the adaptive track grows in length, the estimated function becomes better defined by the collection of data points generated from previous trials. After each trial, the set of stimulus levels and the proportion of correct responses associated with each level are combined to form a psychometric function. The individual points are fitted with an ogival function of some kind and a current estimated threshold level is extracted. A new psychometric function is generated after each trial or set of trials, and subsequent trials are placed at a targeted performance level on the most up-to-date function.

Staircase Procedures, in comparison with the two above-mentioned procedures, are more simple and flexible. In contrast with maximum-likelihood methods, the staircase doesn't need any assumption about the form of the psychometric function. In contrast with PEST, the trial placement, step size, and stopping decisions are all relatively simple and straightforward. These methods generally use the previous one or more responses within

an adaptive track to select the next trial placement, then provide a threshold estimate in a variety of ways, most commonly by averaging the levels at the direction reversals in the adaptive track.

Although the transformed up–down methods are widely used, one restriction that has been noted is that only a small number of target levels can be estimated. Kaernbach (1990), introduced a simple up–down procedure that could be used to estimate performance at many more target levels than allowed by the transformed methods by varying the step sizes used in the two different staircase directions. The value of Kaernbach’s procedure, as he described it, was in the simplicity of the algorithm, relative to the sometimes quite elaborate rules necessary for the transformed procedures, and its ability to target any performance level, not just those that could be estimated with a specific sequence of up and down trials. In Kaernbach’s simple up–down weighting procedure, a performance level is analyzed according to the desired ratio of up - to - down steps, and the stimulus level is changed after every trial. Kaernbach described an example of targeting 75% correct performance with a ratio of up - to - down step sizes of $(1-p)/p$ or, in this case, $.25/.75$, or $1/3$. In order to target that point on the psychometric function, the stimulus level should be changed upward after an incorrect response and downward after a correct response, and the size of the upward step should be three times the size of the downward step.

The value of this type of the staircase adaptive procedure is in the very few assumptions necessary for its implementation. In contrast to the maximum-likelihood methods, no form of the psychometric function need be assumed, and there is no need for complicated computation and fitting procedures between trials. Furthermore, in contrast to PEST, the trial placement, step size, and stopping decisions are all relatively simple and straightforward. The only necessary assumption for use of these methods is a monotonic relationship between stimulus levels and performance levels.

All the psychophysical methods discussed so far rely on the observer’s subjective report of what was perceived. In the yes-no psychometric task, the observer gives one of those two responses indicating whether the stimulus was perceived or not. These methods may be termed *subjective*, because the experimenter cannot control whether the observer’s report is correct or not. In such subjective experiments, results may depend on the criterion that the observer uses for judging whether or not a stimulus was perceived. The forced-choice method provides a more objective approach. In this method, the observer is required to make a positive response on every trial, regardless of whether the stimulus was perceived or not. In a forced-choice paradigm, two or more stimulus alternatives are presented on each trial and the subject is forced to pick the alternative that is the target. The alternatives can be presented successively (temporal forced choice) or in different positions in the visual field (spatial forced choice). Forced-choice methods, especially two-alternative forced-choice (2AFC) are widely used as an alternative to the yes/no paradigm.

3. FEEDBACK DEVICES AND HAPTIC STIMULATION

To reach the goal of a closed-loop system, the prosthesis has to be instrumented with sensors and the measured sensorial information has to be translated into discriminable haptic stimulation patterns. This is not a trivial task as the haptic technology should be able to transmit a large amount of information, while at the same time being practical and convenient for integration into the prosthesis, and also intuitive and non-disturbing. In order to transmit the information measured by the prosthesis, the skin may be stimulated electrically or mechanically (Kaczmarek et al. 1991). Electrical stimulation is based on the delivery of low-level current pulses stimulating superficial cutaneous afferents and thereby activating the tactile sense. This method does not utilize moving mechanical parts, can be embedded in small geometries and is also very energy-efficient. However, its applicability in prosthetics for daily use is limited because it requires self-adhesive electrodes for inducing good haptic sensations. Dry electrodes, which are convenient for practical application, can easily produce discomfort and pain, and this could decrease the acceptance among the users. Mechanical stimulation can be delivered using several methods: piezoelectric devices, shape memory alloy actuators, pneumatic and hydraulic actuators, or linear or rotary electromagnetic motors (Jones & Sarter 2008; Choi & Kuchenbecker 2012; McGrath et al. 2008). Electromagnetic actuators are more commonly used, compared to the alternative technologies, many of which are still in the research phase. Linear motors employ the electromagnetic field generated by the energized coils to move a ferromagnetic core (solenoid) or permanent magnet (voice coil) back and forth, generating vibrations perpendicular to the skin. The most common approach to generate vibro-mechanical stimulation is still the rotary electromagnetic actuator in the form of a DC motor spinning an eccentric mass around its rotating axis. This technology is widely accessible, low cost, simple, practical, and energy efficient, and is therefore routinely embedded in pagers and mobile phones. However, its main disadvantage is that it provides a small range of discriminable stimulations. The amplitude and frequency of the stimulation are tightly correlated, both being a function of the motor velocity and, consequently, motor voltage (Ninu et al. 2013).

A new methodology has been proposed in Cipriani et al. (2012) to overcome these drawbacks and generate more diverse vibro-stimulation patterns. The stimulation system is constructed by rigidly connecting several standard vibration motors within a single casing. The motors within the stimulation array can have different geometries and can be individually controlled. The individual stimulations generated by the motors superpose, resulting in a variety of complex vibration patterns. However, the patterns are stable and consistent with the control signals only when the angular movement of the individual motors within the array is perfectly synchronized. When using regular vibration motors, this synchronisation cannot be achieved, and additional sensors and control mechanisms are required. This will increase the system complexity, but it will still not allow a fully independent modulation of the amplitude and frequency. Piezo-electric based devices were also used to induce frequency- and amplitude-modulated tactile vibro-sensations. However, the high costs, low forces and

displacement coupled with high voltage requirements have prevented their widespread use (McGrath et al. 2008).

Currently, the only commercially available wearable devices that can simultaneously modulate both the frequency and amplitude of mechanical vibrations are the aforementioned coil-based linear actuators, such as C2-tactor from EAI (Engineering Acoustic Incorporated). A moving contactor is elastically preloaded against the skin and controlled by a magnetic field generated by the coils embedded in the closed housing. When an electrical signal is applied, the “contactor” oscillates perpendicular to the skin and, since the surrounding area is shielded by a passive housing, this elicits a localized, point-like sensation. These actuators have good frequency and amplitude control, but in a very limited range around their resonance frequency.

With the goal of finding the proper stimulation technology for closing the control-loop of prosthetic devices by providing haptic feedback to the amputees, some of the most popular technologies were implemented and evaluated.

3.1. Single-Element Vibration Motor

The most common approach to generating vibro-mechanical stimulation is the rotary electromagnetic actuator in the form of a DC motor spinning an eccentric mass around its rotating axis [Figure 15]. The core of the vibration motor is a normal brushed DC, whose speed is controlled by varying the voltage supply. The resulting vibration is generated by an eccentric weight, rigidly coupled with the rotational part of the motor and rotated with a speed dependent on the applied voltage. Vibration is generated by the centrifugal force which is directly proportional to the mass of the eccentric weight, the distance from the rotational axis to the center point of the weight and to twice the rotational speed $-m \Omega^2 r$. Therefore, when the applied voltage is small, the eccentric weight will slowly rotate, resulting in vibrations with low amplitude and frequency. When rotating the weight with higher speed, the vibration magnitude as well as the frequency will be higher.

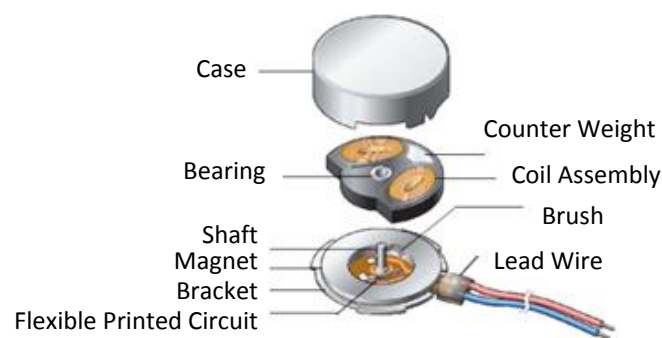


Figure 15: The structure of an eccentric weight based vibration motor. A DC motor is spinning an unbalanced mass around its rotational axis, and the resulting centrifugal force is perceived as vibration.

This technology, because it is widely accessible, low-cost, simple, practical, and energy efficient, is routinely embedded in pagers and mobile phones. However, its main disadvantage is that it provides a low range of discriminable stimulation. The amplitude and frequency of the stimulation are dependent on each other, both being a function of the motor velocity and, consequently, of motor voltage.

In the incipient phase of this research, closed-loop prosthesis control was implemented using this technology; the motor voltage generating the vibration was proportionally controlled by the force sensors instrumenting the hand prosthesis (SensorHand™, Otto Bock). This system was then evaluated by an amputee during laboratory trials. From the vibration provided to the skin, the subject was able to identify the grasp force developed by the prosthesis. This scenario reproduced previous work done by Pylatiuk et al. (2006). The message propagated by these studies was also confirmed by our measurements: grasping is more ergonomic in closed-loop control, as the force required for grasping the same object was slightly lower compared with open-loop control.

However, the time required for grasping increased, confirming the outcomes from other studies (Stepp & Matsuoka 2010). This is an indication that grasping is more demanding during the closed-loop condition, which contradicts what was initially assumed. The aim of the closed loop is to make prosthesis control less demanding. Haptic stimulation should allow the amputee to feel the prosthesis and to develop movement automatisms, subconsciously performed, while vision should allow high-level control mechanisms, as is the case during natural behavior in identifying targets and roughly correcting movement trajectories.

The increased time-to-complete of a grasp may be explained by the lack of experience of the amputee with this new condition. Therefore, long-term fittings were planned with the closed-loop prosthetic system. The assumption was that a longer accommodation period with this system would help the amputees to better understand the perceived feedback and then to perform faster. The subject reported that the stimulation was annoying and rejected the idea of having such a system for daily use.

One explanation for this rejection might be the discomfort generated by continuous vibration during grasping. Secondly, the stimulation itself was reported by the subject as being non-intuitive and very disturbing, leading to the idea that the stimulation parameters used to encode force did not physiologically match the tactile receptors embedded in the skin. The frequency and amplitude of the vibration do not cover the range allowing comfortable and intuitive perception of the stimulation.

Since the continuous stimulation during grasping was perceived by the amputee as annoying and uncomfortable, during the next trials, instead of force, its derivative was encoded with vibrations. During steady-state grasp, the derivative of force is zero and so no vibrations were generated, but the vibrations were encoding changes of the grasp force - the magnitude of the delivered vibration bursts was proportional with the magnitude of the force derivative. This is a much more physiological mapping between the measured force and vibrotactile feedback, better reproducing the natural interaction. Grasping with the natural hand

determines a kind of vibration at contact with an object or when dynamically grasping. This encoding is closer to how humans perceive interaction with the environment, but can be implemented only by technologies able to react quickly and deliver stimulation with higher resolution. The classical vibration motor is slow and the resolution and diversity of the stimulation low - characteristics which do not recommend it for this kind of application.

The stimulation provided by an eccentric-weight vibration motor has a sinusoidal profile, whose frequency is proportional to the applied voltage and to the amplitude which is, in turn, proportional to the centrifugal force generated by spinning the eccentric mass around its rotational axis. Increasing the motor voltage results in a change of motor velocity and, consequently, the frequency and the amplitude of the stimulation will increase. When the motor voltage is increased, the slope of the sinusoidal profile also increases, but these small changes are not highly discriminable due to accommodation effects.

A different approach to controlling the same vibration motor, proposed by Cipriani et al. (2012), proved to be more efficient. Typically, the vibration motor is controlled by a PWM (pulse-width modulation) signal. The PWM signal is a discrete signal that has two states, but the pulse width and frequency are adjustable. This discrete signal is applied to the motor coils, and the motor inductivity filters it, resulting in a quasi-constant voltage. The higher the PWM frequency, the more constant the resulting voltage will be. The average of the voltage supplying the motor's coils is proportional to the duty cycle of the PWM signal.

For common application, the duty cycle is continuously changed in order to vary the armature voltage, while the PWM signal has high frequency in order to guarantee a low-ripple voltage signal. Contrary to this, the approach proposed in (Cipriani et al. 2012), controls the motor with very low PWM frequencies. The PWM signal has two states: HIGH (maximal voltage) and LOW (null voltage). When the PWM is HIGH, the motor has the strongest vibration, and it will stop vibrating when the PWM is LOW. The stimulation generated by HIGH/LOW sequences results from changing the PWM frequency rather than changing the duty cycle. Theoretically, the stimulation can be adjusted by changing both the PWM frequency and the duty cycle. Practically, they are not completely independent. Compared with the classical voltage control, this strategy has been proven to be able to generate stimulation with higher resolution.

Despite all these proposed strategies to control the classical vibration motor, single-element vibration motors are embedded in various consumer electronic products, but the role they play is mostly to alert the user to discrete events. There is also a demand to haptically encode continuous signals, such as displacements, velocities or forces, e.g. in video-games. However, due to the low resolution and apparently uncomfortable and non-intuitive stimulation, the vibration motors were not adopted for such applications.

3.2. Arrays of Vibration Motors

In single-element configuration, vibration motors are not able to generate large amounts of discriminable stimulation. Therefore, a new approach was implemented and evaluated, in which single vibration motors were combined into arrays. Two arrays were tested: one in which seven vibration motors are rigidly connected in a single casing, and another in which eight motors are equidistant and elastic, embedded in a belt to be placed around the arm.

3.2.1. COPLANAR ARRAY

This stimulation system is constructed by rigidly connecting several standard vibration motors within a single casing. The motors within the stimulation array can have different geometries and can be individually controlled by different voltages. The individual stimulations generated by the motors superpose, resulting in a variety of complex vibration patterns. This approach was designed by Cipriani et al. (2012). Coin motors with different geometries were placed on top of each other, and a psychophysical measurement revealed that the device was able to generate differentiable vibro-patterns. This placement of the motors is, however, not very advantageous. The coin motors stimulate in the plane in which the individual centrifugal force is generated and, when placed on top of each other, the individual centrifugal forces cause the device to tilt, generating a 3D stimulation. This stimulation may be more complex, but it is almost impossible to consistently control it.

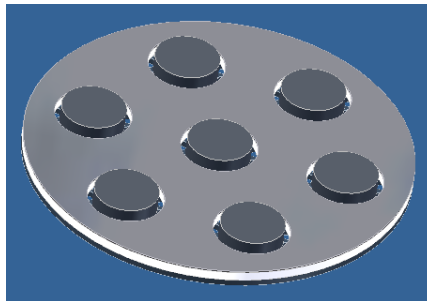


Figure 16: An approach to superimpose individual stimulation waves into vibration patterns. Seven pancake vibration motors were rigidly connected within the same casing. When individual motors will vibrate with different phase, frequency and amplitude, the generated vibration will have a complex pattern, result of the supposition of individual stimulation waves.

Therefore the complexity was reduced by rigidly connecting the seven coin motors within the same stimulation plane [Figure 16]. For control of this device a PC-SW interface was created [Figure 17], and various patterns were tested. This interface allowed for the generation of static patterns by adjusting the voltage of the individual motors. Moreover, the interface allowed for the combination of static patterns into timed patterns. In the program “Monika,” for example, there are 12 stimulation patterns. The presentation time of every static pattern, as well as the frequency of the transition from one pattern to the next, was also adjustable.

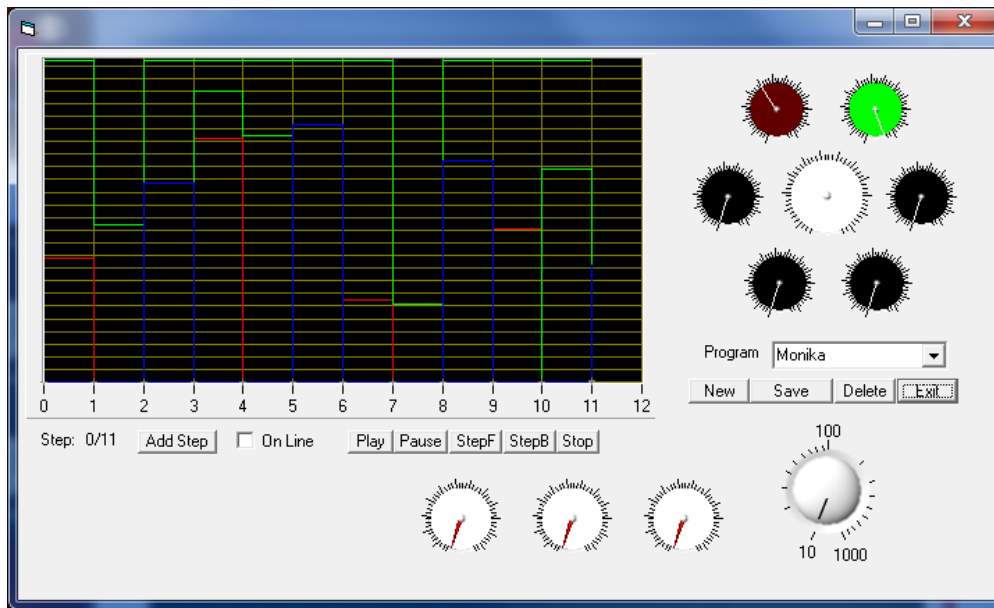


Figure 17: The software interface implemented for designing various stimulation patterns. The colored staircases displayed in the scope represent the voltage patterns which supply individual vibration motors.

The static vibro-tactile patterns were initially evaluated in the laboratory with able-bodied subjects, but outcomes did not meet expectations. The haptic sensations generated by co-activating several motors were different; however, the generated patterns were not consistent with the applied voltages. Noisy, uncontrollable oscillations were perceived as being confusing; this made the discriminability of the perceived stimuli low and very slow.

In order to eliminate the noisy oscillations and gain control over the stimulation patterns, the angular movement of the individual motors within the array should be perfectly synchronized. When using regular vibration motors, this synchronization cannot be achieved, and additional sensors and control mechanisms are required. This would increase the system complexity, but the stimulation would cover only a narrow range within the amplitude and frequency representation, which is not a good compromise. Complexity would rapidly increase without an equal boost in performance.

It was observed that timely, switched patterns could make for a better alternative. This would induce the sensation of spatiality, and the stimulation could be associated with hand aperture, force or other slow-changing sensory information. Initially, the seven motors were rigidly coupled, but for the next trials they were elastically connected in order to stimulate the skin locally; essential for this trial was that the punctual stimulation of every motor be easily differentiated.

The configuration was the same as in the previous measurements – six motors were placed at the edges of a hexagon and the seventh one in the middle. This configuration allows flexibility in generating various trajectories, there being many ways to interconnect the motors. Various trajectories in interconnecting the vibration motors should induce various discriminable stimulation patterns. The psychophysical evaluation showed that some trajectories were highly discriminable but their recognition was still demanding and slow.

3.2.2. LINEAR ARRAY

It is obvious that the goal is to have many more discriminable stimulation trajectories, but only if they are also intuitive and easy to recognize. Increased effort to identify the individual stimulation patterns diminishes the efficiency of the system. Therefore, during the next steps, the motors were embedded into a brace, placed around the forearm, and two patterns were used: one in which the motors were activated in a clockwise fashion, and the second pattern was counterclockwise. This simple configuration allows for prediction of the stimulation and proved to be the most efficient from all those tested. The distance between the motors was increased in order to make the stimulation more identifiable. Initially, it was thought that this stimulation approach could be useful in encoding slow-changing parameters of a prosthesis, position or grip force, e.g. the first motor activated would indicate when the prosthesis is closed and the last motor in the array would indicate when the prosthesis is open. But this turned out to be somehow disturbing to the subject (discrete bursts of vibrations) and the absolute prosthesis aperture was less discriminable.

A comfortable stimulation should be perceived not as punctual and intermittent, but as a fluid rotational motion. The condition necessary to achieve this was to correlate the distance between the motors with the switching frequency. This stimulation induced a rotating sensation, recommended for encoding prosthesis velocity or the force derivative.

The scenario described below was to be one of the most efficient: while the prosthesis slowly closes, the stimulation induces slow movement in the counterclockwise direction, and is reversed when the prosthesis slowly opens. However, this was intuitive and physiological only when the right hand was stimulated. For the left hand, the direction of the patterns had to be reversed. The general rule would be: closing is induced by stimulation moving in the pronation direction while opening is induced by patterns moving in the supination direction. When the velocity is further increased, the patterns move faster. The discriminability of various velocities may be emphasized by also encoding velocity in the stimulation of the individual motors. While the prosthesis slowly closes, the motors vibrate more lightly, and the vibration is stronger when the velocity of the movement is higher.



Figure 18: A linear array comprising eight vibration motors. The motors were activated in sequences aiming to induce sensation of movement in the subjects' forearm, correspondent with the prosthesis movement, or were simultaneously activated in static patterns to transmit grasp force.

When an object was grasped, the applied vibro-patterns were static: while the grasp force increased, the number of activated motors increased (opposite 2, 4 and 8 motors). The transitions between the three states were made by increasing or decreasing the motor voltage. It was thought that this encoding would also allow the detection of compliant grasp. Prosthesis movement was encoded with moving patterns, grasping with pattern change. When an object was grasped very lightly, two motors were activated at once. If grasping a soft object, the prosthesis moved and grasped, with the consequence that the two-motor pattern further rotated around the forearm. When grasp force was increased, the movement was slower; therefore, the four-motor pattern was activated but with a lower rotation velocity.

This strategy to implement full closed-loop control with affordable and reliable vibration-motors has a nice theoretical concept behind it. It may work for quasi-slow processes, but it is not suitable for upper-limb prosthetics. Natural grasp is a very dynamic process; a moderate grasp requires about 300 ms. Nevertheless, the activation of individual vibration motors requires about 100 ms or more when driven by lower voltages. Consequently, the discrimination of the stimulation patterns generated by using the coin vibration motors are much lower than that afforded by the application of closed-loop control of prosthetic devices.

3.3. Single-Element Electro-Stimulation

In order to transmit the information measured by the prosthesis, another approach would be to stimulate the skin electrically. Electrical stimulation is based on the delivery of low level pulses of electrical current to stimulate superficial cutaneous afferents, thereby activating the tactile sense. Compared with the previous technology, this should have the advantage of generating much more complex stimulation patterns by independently adjusting the frequency and the amplitude of the stimulation.

Aiming to evaluate the performance of electrical stimulation of the skin, a custom-made stimulation device was used. It comprises a stimulation logic unit which generates a PWM signal and a power stage which amplifies the control logic signals (0-5V) to a freely-adjustable voltage (0-32V). This sequence of electrical spikes are applied to the skin through a pair of self-adhesive electrodes, one active (+) and one passive, the ground (-) [Figure 19].

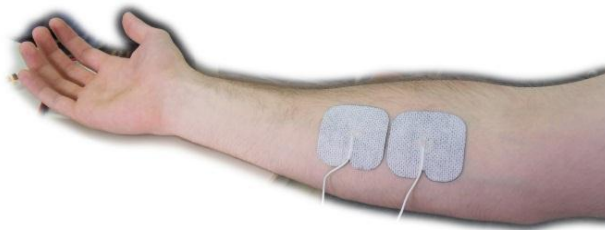


Figure 19: Single element electro-stimulation; sequences of electrical spikes applied on the skin through a pair of self-adhesive electrodes are inducing haptic sensation in the forearm.

Monopolar electro-stimulation was considered in the current application, so the signal parameters influencing the stimulation were duty cycle and frequency of the electrical spikes. This setup allows stimulation with frequencies between 12-500Hz, and a duty cycle between 0 – 100%. Monopolar stimulation is considered to have some side-effects, including redness of the skin and even burns, and is therefore not optimal for such an application. However, these side-effects emerge only when the stimulation lasts for a long time and the intensity of the stimulation is high. Bipolar stimulation in constant current mode is more appropriate for this kind of application, but its implementation is also more demanding. Considered to provide the right compromise between stimulation efficiency and complexity, the evaluation was performed with the monopolar stimulation. The stimulation control logic generates a PWM signal, which is applied to the surface of the skin after amplification.

Aiming to obtain more complex stimulation patterns by independently modulating the amplitude and frequency of the stimulation, the monopolar stimulation was evaluated in laboratory conditions. The outcomes of these trials were, however, lower than the expectations. The perceived sensations, when the amplitude or frequency was changed, were not very clearly discriminable; instead, the perceived sensation was diffuse.

A possible explanation for this behavior comes from analyzing the process of stimuli generation with electro-stimulation. The electrical signal applied on the surface of the skin generates a potential field which propagates between the electrodes, through the arm. At the intersection of the potential field lines with the afferent neural pathways a potential will be induced, depolarizing the membrane of the sensorial nerves. If the depolarization exceeds the neural activation threshold, a series of APs will be generated and propagated to higher levels of perception, generating tactile sensations. The stimulation doesn't address individual types of receptors, but is volumetric; not only one nerve ending, but all sensory nerve endings within the induced potential field will be activated. Bursts of stimulation were easily identifiable, but not the fine tuning of amplitude or frequency. During mechanical stimulation, changes in frequency or amplitude determine a weighted activation of different types of mechano-receptors. Instead, changing the amplitude and frequency of the electro-stimulation results in different geometries of the activated volume. In this volume, the sensory terminations are mixed and electro-stimulation doesn't target specific types of receptors; it is, rather, global. This results in more diffuse perceived stimuli as compared with mechanical stimulation. The two degrees of freedom of the stimulation - amplitude and frequency - are not independent from each another, but their combinations result in much more diversity of stimulation compared with the eccentric-weight vibration motors.

3.4. Electro-Stimulation Array

In order to increase the ability of this technology to encode information, the electrodes were grouped into arrays. The stimulation electrodes were placed around the forearm, and the velocity/grasp force of the prosthesis was encoded with rotating/static patterns. The procedure was similar to the previous case of vibrotactile stimulation.

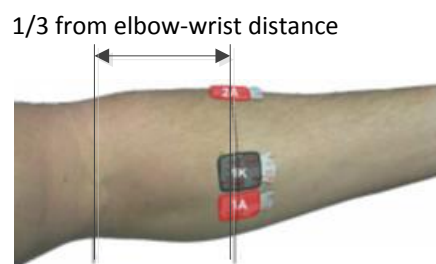


Figure 20: Electro-stimulation electrodes as a linear array placed around the forearm. Activated in sequences or simultaneously, the pairs of electrodes are able to induce static or dynamic haptic sensations in the forearm (Schahinger, 2011).

Prosthesis velocity and grasp force were able to be encoded with this strategy, but the stimulation seemed to be less discriminable as well as slower when directly compared with the mechanical stimulation. Mechanical stimulation was much more consistent, being equally perceived at all stimulation points. In contrast with these outcomes, the electro-stimulation was very variable; the stimulation provided by the electrodes placed on the glabrous side of the forearm induced strong sensations, while the stimulation provided by the electrodes placed on the hairy side was hardly perceivable.

Another drawback of this technology was identified to be the high sensitivity to motion artefacts. A setup was prepared to simulate the case of a real prosthesis: the stimulation electrodes were placed around the forearm of an able-bodied subject, and then covered by a socket. While stimulating the forearm, the socket was fixed and the subject tried to pronate/supinate; this simulated what may happen during real fittings. The outcome of this trivial experiment was that the same stimulation patterns applied to the forearm, resulting in strong variability of the perceived sensation, or even painful stimulation. Another source of strong variability was identified to be the pressure exerted from the exterior; this may be the case when an amputee is e.g. supporting the forearm (the socket) on a table, during a common task, like writing.

This variability in the perception of stimuli is obvious if the mechanism of electro-stimulation is analysed in more detail. The stimulation electrodes were placed at the surface of the skin with the intention of stimulating as superficially as possible. Electro-stimulation does not address the mechano-receptors responsible for tactile perception, as is the case during mechanical stimulation, but only the sensory-nerves innervating them. Therefore, in order to be perceived, the stimulation should reach deeper layers beneath the skin, and not only the very superficial layers. When pressure is exerted from outside, the skin layers will be squeezed together, and the stimulation will reach deeper nerves, possibly generating painful sensations, or non-volitionally activating motor-nerves. Otherwise, if the pressure is uniformly distributed, but the subject is pronating/supinating the forearm while the socket is coerced into a fixed position, the skin will slide over the forearm muscles, and the stimulation will reach nerves which were not initially targeted. During this movement the stimulation is not consistent, which could result in pleasant or painful stimulation.

Besides the non-practicality of the electro-stimulation, due to the required self-adhesive electrodes, the strong variability of the stimulation and the random potentially painful sensations are very demotivating, raising a very serious question with regard with the applicability of surface electro-stimulation: how to provide haptic feedback to the amputees and close the prosthesis control-loop. This experience with surface-electro-stimulation doesn't disqualify the applicability of electro-stimulation in implants. Implantable devices may stimulate more precisely to reach targeted specific neural terminations, and the advantages of this technology are better highlighted. Electro-stimulation has no mechanical parts, thus may be embedded into very small geometries; electro-stimulation also makes it possible to generate a series of APs replicating the original neural

coding, allows low energy consumption, and so on. However, in order to be widely adopted, this technology should still wait for technological advances in other disciplines like medicine or engineering.

3.5. A Novel Wearable Haptic Technology

During previous trials, mechanical as well as electro-stimulation were implemented. But these technologies demonstrated weaknesses which do not recommend them for integration into prostheses for daily use. On one hand, the mechanical stimulation is very consistent and practical, but the amount of differentiable stimuli generated by the eccentric-weight vibration motors is poor and, as the subjects reported, annoying. On the other hand, the electro-stimulation allows the generation of much more complex patterns by independently modulating the amplitude as well as the frequency of the stimulation, but it is not practical for implementation into prosthetics for daily life. In order to be well-perceived, the electro-stimulation requires self-adhesive electrodes, which is a serious impediment for daily use.

Trying to combine the consistency allowed by mechanical stimulation with the complexity of the stimulation patterns allowed by the electro-stimulation, a novel vibro-tactile stimulation methodology was developed. This allows generation of complex vibro-patterns by independently modulating the amplitude and frequency of vibrations over a range which physiologically fits the tactile receptors embedded in the skin. In order to assess its capabilities, the correspondence between commands and vibration was identified by generating and measuring vibrations of different frequencies and amplitudes, covering the whole working range of the device. Then, the psychophysical properties were tested in order to evaluate how well the subjects could perceive and discriminate the features of the generated vibrations.

3.5.1. PRINCIPLE OF FUNCTIONING

In an attempt to come a step closer to the requirements of an ideal haptic device, a novel inertial vibro-mechanical technology was proposed. It functions based on the principle of Newton's third law of motion which states that for every action there is always an equal and opposite reaction. In our case the "action" is generated by the rotor of a rotational electro-mechanical machine. The rotor is accelerated by the electrical torque developed by the motor coils, and the resulting inertial force ("reaction") drives the stator. The stator is the stimulating part of the device, preloaded against the skin and embedded into a socket or case by using bearings with small coefficient of friction. The inertial force transmitted by the stator is then perceived as mechanical stimulation - vibration.

By applying an alternating voltage or current wave to the motor coils, an alternating electrical torque will be generated and the motor operates in what is known as *voltage* or *current* mode. The developed electrical torque will drive the rotor at a predefined moment of inertia. The product of the rotor's moment of inertia and its angular acceleration further generate an inertial force which coerces the stator to move in the opposite direction. The stator is preloaded against the skin and the alternating inertial forces transmitted by it are perceived as vibration. The vibration is characterized by two parameters: frequency and amplitude. The

frequency is tightly correlated with the frequency of the signal wave applied to the motor's coils, and the vibration amplitude will be a function of the electrical torque developed by the motor coils, the rotor and the stator's moment of inertia. Since the moment of inertia for the rotor and stator are constant, as defined by the system design, the only dimension influencing the vibration amplitude is the electrical torque.

The electrical torque developed by the motor coils is the product of magnetic flux and armature current, so the amplitude of the vibration can be set by adjusting the current passing through the motor coils – the motor has to be driven in *current* mode. After comparing the motor's *current* vs. *voltage* operation modes, it was decided that the *current* mode would be the more suitable for this application because it allows for direct control of the inertial forces which generate the vibration. However, the implementation of high speed, closed-loop current controllers and the additional sensorial system required for this implementation, introduce a level of complexity which strongly affects the cost-effectiveness of the device.

In *voltage* mode, the applied alternating voltage doesn't control the inertial forces directly, the current passing the motor coils being a function of applied voltage, motor inductivity and the rotor's angular speed. However, for this application, in which the motor continuously vibrates, the rotor's angular speed is limited by the frequency of vibration; the frequency also influences the transient response of the motor's current by applying an alternating armature voltage.

There is no consistent behavior between the applied voltage and motor current; however, for this particular application these nonlinearities are considered to be well defined by the motor parameters, the wave form and the frequency of applied alternating voltage. Under these assumptions, the *voltage* mode, which is a cost-effective solution, was considered for the current evaluation, providing valuable results.

The references for vibration amplitude and frequency are converted by the *Logic Control* block into a square wave signal corresponding to the motor voltage. The *Electrical Commutation* unit, based on this voltage reference, generates three sinusoidal PWM voltages, 120 degrees apart, supplying the three motor coils correspondingly. The sinus commutation guarantees a ripple-free electrical torque which smoothly accelerates the rotor without additional noisy vibrations introduced by the commutation itself. The stator, mounted on bearings, will be driven by inertial forces developed by accelerating the rotor back and forth, always in the opposite direction, generating vibrations. The stator is constrained to move circularly around the rotational axis of the rotor and consequently stimulates the skin by stretching it tangentially, which has been demonstrated to be more efficient than normal indentation of the skin (Biggs & Srinivasan 2002).

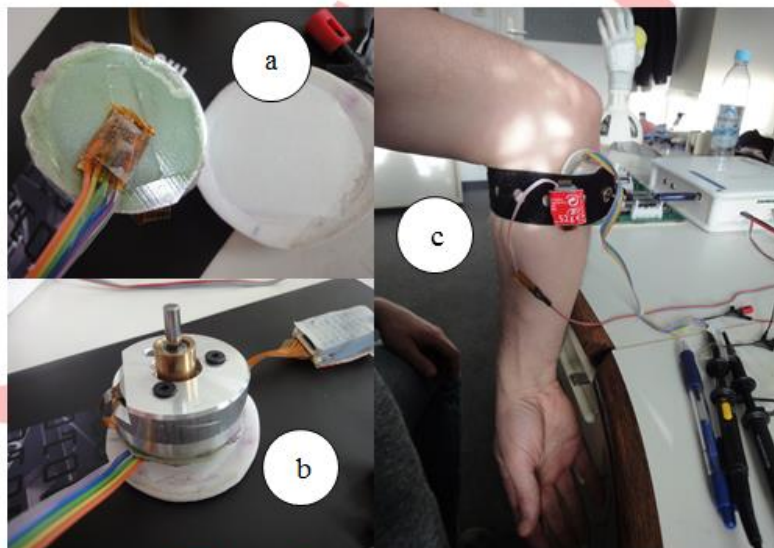


Figure 21: The stimulation device and its placement on the forearm: a) the placement of the accelerometer on the stimulator; b) the stimulation device – BLDC motor embedded into an aluminum case; c) the placement of the device on the subjects forearm.

To maximize reliability, a brushless DC (BLDC) motor (MAXON EC32), which used electronic rather than mechanical commutation, was used as an actuator for the stimulator. This required additional development effort: the Logic Control Unit converting the references for vibration amplitude and frequency into sequences of PWM logic signals, as well as the Power Stage converting the PWM logic signals into the voltages to be applied to the motor coils, were custom made. However, these efforts were rewarded by a system which guarantees long motor life in dynamic applications such as this one, in which the motor must continuously accelerate and decelerate to generate vibrations. The motor has Hall sensors and a flat construction (Maxon Motors - EC32). With a thickness of 8 mm and a diameter of 32 mm, supplied with 12.6 V to achieve 6 W of electrical power, the motor provides a good compromise between efficiency and geometry. The motor was embedded in an aluminum case [Figure 21b] and strapped to the subject by a band placed around the forearm near the elbow joint [Figure 21c]. The stator was rigidly connected to the casing, and the generated vibrations were measured with a three axis accelerometer (Sander Electronic, MMA7368L) placed on the casing, since this is the stimulating part of the device [Figure 21a].

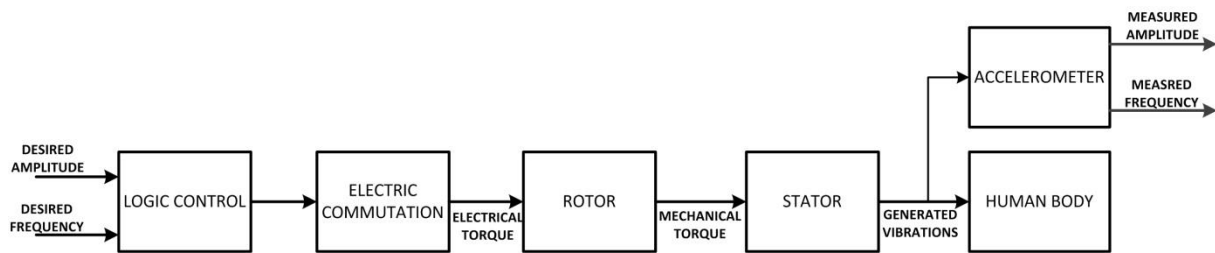


Figure 22: The mechanism of vibration generation. The rotor is driven into back and forth oscillations by an alternating voltage signal and reaction forces produce vibrations of the “floating” stator. The amplitude and frequency of the generated vibrations are determined by the corresponding parameters of the input voltage waveform.

The operational principle is schematically described in Figure 22. The inputs into the stimulator are the reference values for the desired vibration amplitude and frequency. Those are converted by the Logic Control block into three square wave signals, 120 degrees apart – the logic PWMs which shape the voltages to be applied to the motor coils. However, before being applied to the motor coils, the logic control signals are amplified by the power stage, which is part of the Electric Commutation unit, supplying the three corresponding motor coils.

The frequency of the generated vibrations is identical to the frequency of the electrical torque generated by the currents passing through the motor coils, and the vibration amplitude is a function of the magnitude of the electrical torque. The electrical torque developed by the motor coils is the product of the magnetic flux and the armature current, so the vibration amplitude can be set by adjusting the current that passes through the motor coils. This can be done if the motor is driven in the *current* mode. In the *voltage* mode, the vibration parameters are set by adjusting the voltage supplying the motor coils. For this phase of the project, the voltage mode was selected as a simpler solution that still provides a good performance (see Results). The frequency of the stimulation spans the range from 10 to 250 Hz in order to optimally activate the skin’s vibration-sensitive mechano-receptors: the Merkel disks sensitive to low frequencies (5-15Hz), Meissner’s corpuscles sensitive to midrange stimuli (20-50 Hz) and Pacinian corpuscles sensitive to high frequency vibrations (60- 400Hz), the lowest detection threshold being at 250Hz (Kandel et al. 2000).

3.5.2. CHARACTERIZATION OF PHYSICAL PROPERTIES

Physical measurements were performed by attaching the device, as previously described, to the forearm of a healthy subject (male, age 39). This allowed the estimation of the effects introduced by damping and elasticity of the human skin interface. While the subject completely relaxed the forearm muscles, the skin was preloaded with a force of approximately 2N (measured normal to the skin). The subject was comfortably seated in a chair with the arm relaxed and placed on the table in front of him.

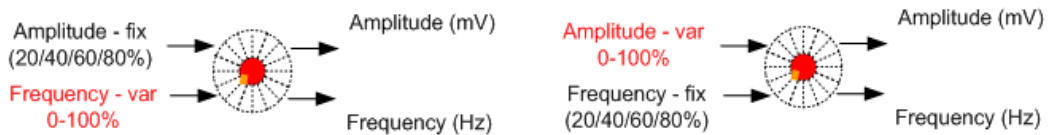


Figure 23: The stimulation device has two inputs (desired frequency and amplitude) and two outputs (the generated/measured frequency and amplitude)

The stimulator can be regarded as a 2 input – 2 output system [Figure 23]. The reference values for the desired amplitude and frequency are the inputs, while the outputs are the measured acceleration and frequency of the generated vibrations. In order to identify the transfer function of this multi-input, multi-output system, the system performance was evaluated using a set of control points distributed to cover the whole amplitude-by-frequency range [Figure 24].

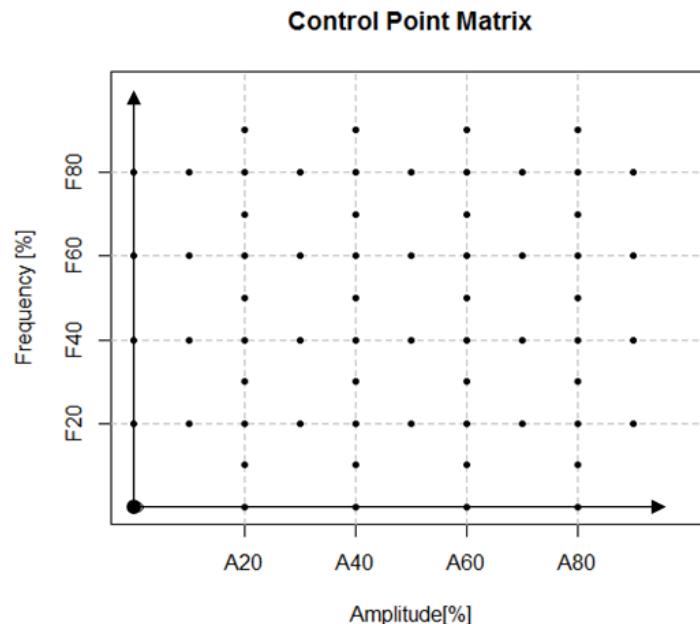


Figure 24: Control point matrix consisting of 80 points uniformly distributed across the stimulation range. The frequency and amplitude which characterize the individual control points were input parameters for the system, and the measured frequency and amplitude of the vibration were characterizing the system response.

The control points were adopted using the following procedure: one reference control input was set to be constant at 20/40/60/80% of its maximum, while the other reference control input was driven in 10 equidistant steps throughout the whole working range of the motor. This resulted in 4 x 10 points for both the constant amplitude and the constant frequency conditions. For each control point the vibrations were generated for 5s and measured by the accelerometer placed onto the casing with a 2 kHz sampling rate. The magnitude of the acceleration was determined as the RMS (root mean square) of the AC RMS accelerations measured on every axis, where AC RMS is the RMS value of the waveform minus the mean value of the signal – equivalent to a ripple measurement.

The results from the recordings are summarized in Figure 25. The amplitude and frequency of the generated vibrations for the constant amplitude and constant frequency conditions are given in Figure 25(a, b) and Figure 25(c, d), respectively. The representation Input Frequency – Output Frequency [Figure 25] shows a behavior very close to linear and the plots for all four constant amplitude conditions entirely overlap. This indicates that the frequency of vibration followed the reference, independently of the vibration amplitude. The representation Input Frequency – Output Amplitude [Figure 25a], reveals that the vibration amplitude was strongly influenced by resonance effects determined by the elasticity of the skin-device interface. The amplitude of the generated vibrations changed as the reference input frequency was modulated from 10% to 100% with an amplitude peak around F40 and, as expected, this effect was more pronounced for the higher amplitudes (A60 and 80). The cross measurement Input Amplitude – Output Frequency [Figure 25d], confirmed the previous observations - the vibration frequency was independent from the changing stimulation amplitude; the measured frequency was very stable while the amplitude was changed from 10% to 100%. The last representation, Input Amplitude – Output Amplitude [Figure 25c] showed a linear correspondence between reference and generated vibration amplitude for all four conditions, and once more revealed the resonance around 40% of the frequency range. The F20/40/60/80 plots were not sequentially ordered, as was also the case for A20/40/60/80. Due to the resonance effect, the F40 plot showed a response which overtook all other F20/60/80 plots. For the same change of the amplitude reference, between 10% and 100%, the response covered a wider range of vibration amplitudes with respect to the other three conditions. The F60 condition followed next, covering the amplitude range that was approximately half that of F40. Finally, the plots for the F80 and F20 conditions behaved nearly identically.

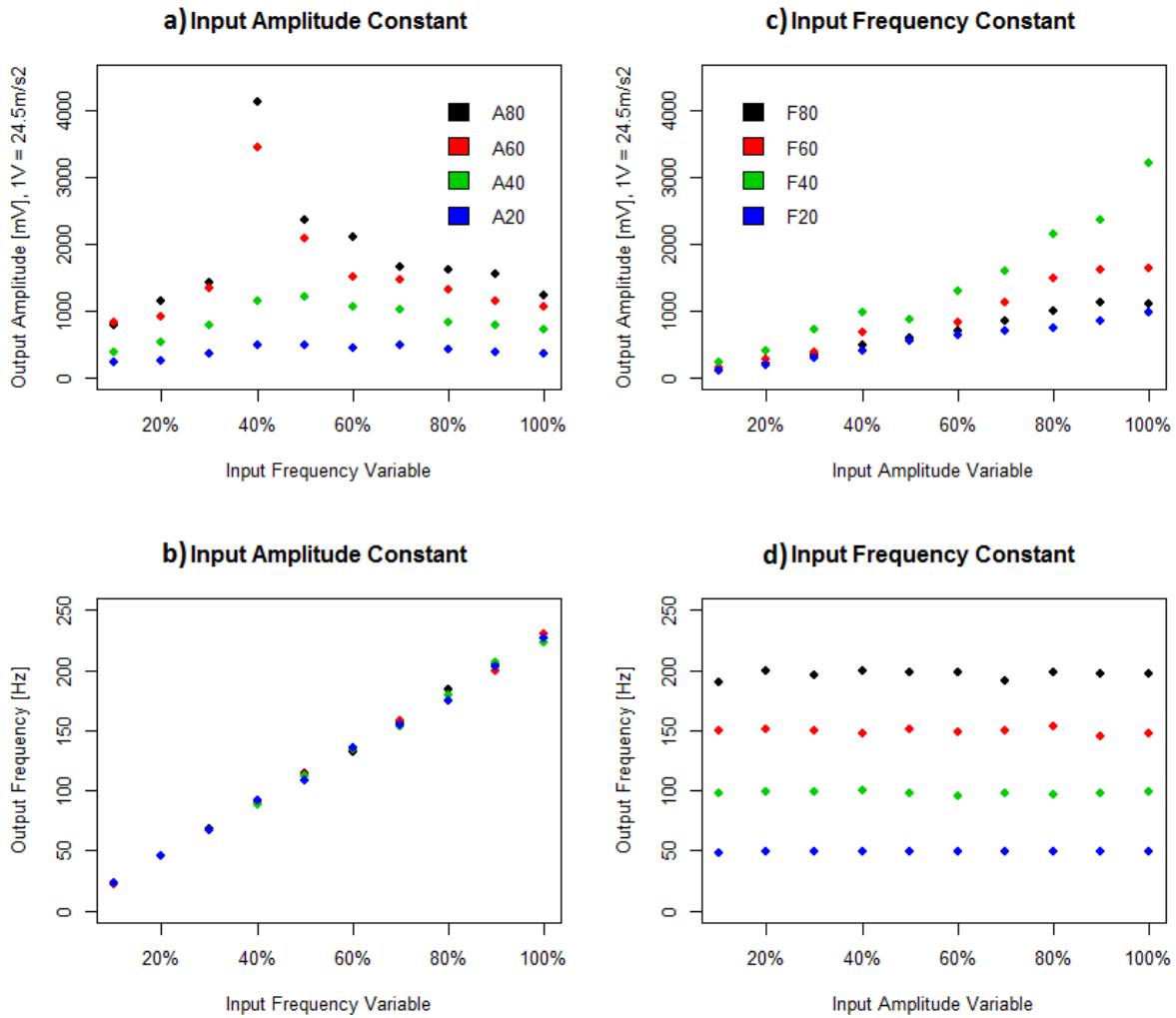


Figure 25: The system response to the system inputs from the control point matrix (the desired amplitude/frequency of the stimulation). The bullets are amplitudes/frequencies pairs characterizing the measured vibration under standardized conditions: the device was placed on the forearm and preloaded with a force of approximately 2N measured normal to the skin.

3.5.3. CONCLUSIONS

After performing physical measurements, it was shown that the introduced technology is able to generate complex AF modulated vibro-stimulation. The results illustrate that the novel method for generating vibro-tactile stimulation can provide a wide range of haptic stimulation patterns, as demonstrated by generating vibrations over a discrete grid of points in the amplitude by frequency range (physical assessment). The two stimulation parameters can be independently and simultaneously modulated through a large range along each degree of freedom. The generated frequency matches the reference very well and this is almost independent from the reference amplitude. However, the generated amplitude depends also on the reference frequency, and this coupling reflects the resonant properties of the stimulator-skin interface. Nevertheless, as shown in

Figure 25a, the constant amplitude profiles indeed change during the modulation of the frequency, but still remain separated from each other, which is important for their psychophysical discrimination.

An important advantage of the proposed stimulation method is that it can be implemented very simply, using a standard electric motor placed within a casing and strapped to the forearm. The methodology is inherently flexible, since different motors will have different geometries (skin contact) and stimulation parameter ranges. It has to be emphasized that the current implementation is not ideal; the chosen BLDC motor was not driven in the optimal working range, as it was initially designed for other applications, and so the vibration generation is not energetically optimal. However, the described methodology proved its capacity to generate vibrations with amplitude and frequency independently controlled. Furthermore, due to practical considerations, the voltage mode was used to drive the motor. As explained earlier, better control could be achieved in the current-driven mode.

Improving the system efficiency will be addressed in future developments. A significant gain in the flexibility of this novel stimulation method with respect to conventional approaches (e.g., miniature vibration motors) comes at the expense of a larger geometry and energy expenditure. The choice of the motor will critically influence the performance, and it will be necessary in the future to evaluate different motor types or to modify them to increase their efficiency for use in this specific application. Furthermore, both the power requirements and desired performance can be improved upon by the introduction of passive elements to the design. The stator/rotor/motor casing could be connected by torsional springs which would allow manipulation of the resonant characteristics of the motor-spring system, either to obtain very strong vibrations in a narrow range or, conversely, to smooth out the resonance peak and achieve even better decoupling of the two degrees of freedom. This is an important step for future developments.

3.6. Comparison with Eccentric Weight-Based Vibration-Motor

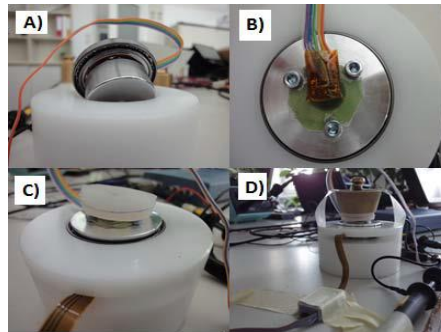


Figure 26: Experimental setup for the measurement of stimulation parameters (frequency/amplitude) – inertial vibration motor. The stator of the motor, the stimulation part of the device, was mounted on bearings (A) and preloaded with a 200 g mass (D) through a silicon layer (C) which simulated the properties of the natural skin. The properties of the vibration were measured with an accelerometer mounted on the stator (B).

In order to better emphasize the capacity of the novel stimulation device to generate vibro-stimuli, a direct comparison with a regular vibration motor was made. A set of tests was done using an artificial setup, emulating, to some extent, realistic conditions. The stator - the stimulation part of the device - was preloaded with a 200 g mass through a silicon layer to simulate natural skin [Figure 26]. The stimulation device is a two-input, two-output system, having as inputs the references for Vibration Amplitude (IVA) and Frequency (IVF), and for outputs the measured frequency and amplitude of the vibration. In the first group of measurements, the IVA was kept constant at 20, 40, 60 and 80% of its maximum, and for each of these levels the IVF was changed from 0 to 100% in 26 equidistant steps. In the second group, the IVF was kept constant at 20, 40, 60, and 80% while IVA was changed from 0 to 100% in 26 equidistant steps. The generated vibrations were measured by using a three-axis accelerometer (MMA7368L). The sensor was placed on the stator with the two sensitive axes in the horizontal plane. The signals were acquired at 2 kHz. Ten measurements were performed for each condition. The vibration amplitude was assessed using a peak-to-peak value of the measured acceleration.

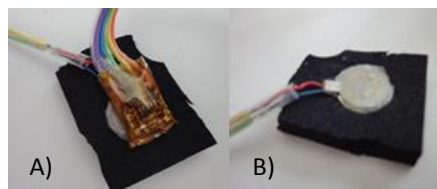


Figure 27: Experimental setup for the measurement of the stimulation parameters (frequency/amplitude) - centrifugal vibration motor. The casing of the motor was embedded in foam like material, and the properties of the vibration were measured with an accelerometer (A) mounted on the casing (B)

In order to emphasize the differences between the novel and classical methods of generating vibrations, the same test was conducted using a conventional coin-type 12mm vibration motor with an eccentric mass [Figure 27]. The motor voltage, which is the only degree of freedom, was changed in 26 equidistant steps, and the vibration frequency and amplitude were recorded.

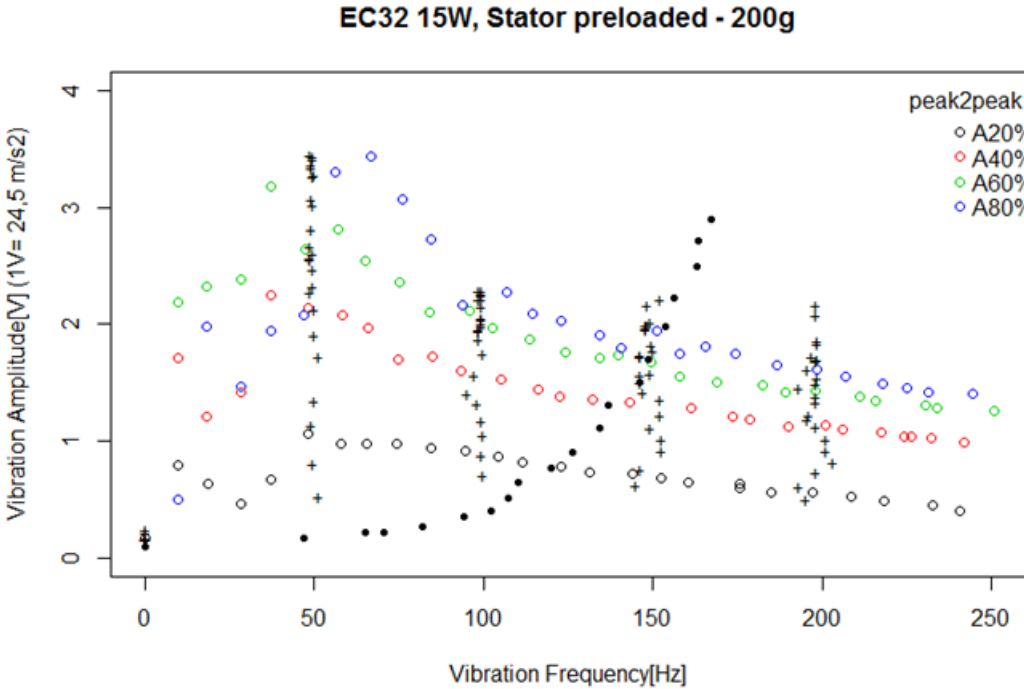


Figure 28: Direct comparison between the centrifugal and inertial vibro-tactile stimulation: summary results. The colored circles are BLDC system responses when the frequency of the desired stimulation was varied in 26 equidistant steps, and the amplitude was kept constant at 20, 40, 60 and 80% of the maximum. The black crosses are BLDC system responses when the amplitude of the desired stimulation was varied in 26 equidistant steps, and the frequency was kept constant at 20, 40, 60 and 80% of the maximum. The black bullets are the response of the pancake vibration motor when the input voltage was varied in 26 steps between 0-100% (0-3V).

Figure 28 depicts the summary results (average values, standard deviation less than 5%). The colored circles are recordings from the constant amplitude, and the black crosses are from the constant frequency measurements. The profiles described by the colored circles show the nonlinear correspondence between the IVA, which was kept constant, and the actual measured vibration amplitude over the entire frequency range (10-250Hz). This behavior is due to a resonant effect caused by the elasticity of the silicon layer simulating the natural skin.

As is visible from these plots, the natural frequency of the silicon layer is approximately 60Hz: the amplitude increases with frequency up to this point and afterward it decreases. The measured vibration was not linearly related to the IVA: the shift between values at lower vibration amplitudes was higher than the shift at higher amplitudes. Moreover, the shift at higher frequencies was smaller than that at lower frequencies. In the second

group of measurements, the measured frequency followed the IVF when the IVA was changed in 26 equidistant steps. Finally, in the case of a coin-type motor, the vibration frequency varied linearly with the applied voltage, while the vibration amplitude was a quadratic function of it. It is well known that the centripetal force which generates vibrations is proportional to the square of the motor's angular velocity which is proportional to the applied motor voltage.

The outcomes of these measurements reveal that the amplitude and the frequency of the stimulation are independently controllable. This resulted in a collection of points strewn within the amplitude/frequency representation of the stimulation map - the small circles in Figure 28. These points are not stimulation points; they describe the response of the system when the inputs were changed within the maximum range.

In comparison, the stimulation generated by the coin-type vibration motor is able to generate stimuli spread only along a quadratic curve (black bullets) because the frequency of the stimulation is tightly correlated with the amplitude. Nevertheless, there is a compromise which has to be made with regard to the device's volume and energy consumption. The vibration motor with the eccentric mass is the most efficient, therefore occupies also a small volume. The proposed methodology could also be implemented using very small motors, but this would limit the stimulation range. In actual applications, there is a tradeoff between the geometry and the stimulation range; the larger the motor, the larger the stimulation range. However, the potential of this methodology is not entirely exploited by the current implementation. The reduction of the stimulation range observed when increasing IVA and IVF is caused by the current approach to motor voltage control. By controlling the motor in *current mode*, the stimulation range can be extended and made more regular, although this would also increase the system complexity.

3.7. Psychophysical Assessment

The outcomes discussed above describe the transfer function of the system - the way the electrical energy fed into the motor is converted into vibration. However, in order to determine the stimulation map, psychophysical measurements had to be made. The psychophysical measurements aim to describe the correlation between the provided stimulation and perceived stimuli.

3.7.1. TRACKING THE STIMULATION

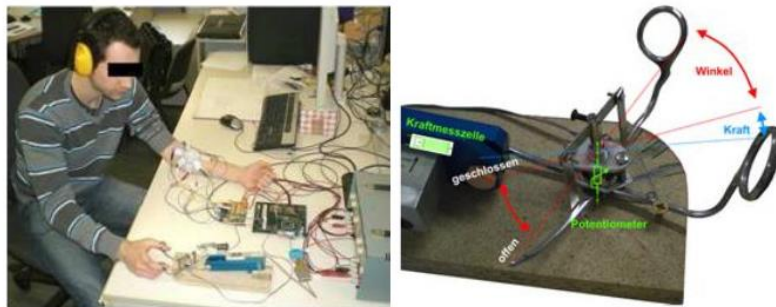


Figure 29: The experimental setup for the psychophysical evaluation of the stimulation using the tracking approach. Patterns of stimulation were applied on the forearm of the left hand, while the subjects tried to reproduce the perceived stimuli by proportionally controlling the aperture of scissors with the right hand (Schahinger, 2011).

With this goal, an experimental setup was devised, consisting of the stimulation device and scissors. The stimulation device provided haptic feedback to the subjects, simulating the prosthesis movement and grasp. Various scenarios were executed, and the subjects were instructed to reproduce the perceived stimuli by moving the scissors with the other hand.

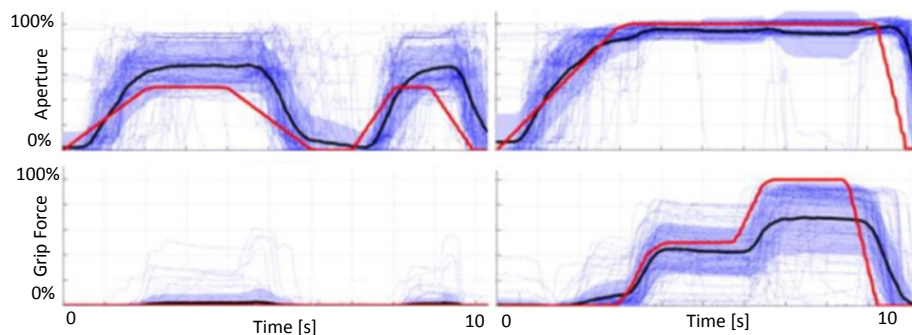


Figure 30: Outcomes of the tracking psychophysical measurements. The red profile represents the reference which was induced haptically to the subjects, the thin-blue profiles are individual responses measured with the scissors, and the dark-blue profile the average of the individual measurements (Schahinger, 2011).

The red line in Figure 30 represents the trajectory induced with haptic feedback, and the thin blue profiles are the signals measured by the scissors. The dark-blue line is the average of the measured data and the blue shadow, the standard deviation.

Analysing the outcome illustrated in Figure 30, it is obvious that the trend of the measured prosthesis aperture follows to some extent the red reference. However, the individual answers, the thin blue profiles, and the large standard deviation indicate the very low precision in following the reference. The poor precision was determined to some extent by the poor perception of applied stimuli. The bias introduced by the psychophysical methodology was a dominant cause. The subjects perceived increase/decrease of the stimulation or pattern change, but they were not able to precisely quantify the absolute values of grasp or aperture. They tried to follow the stimulation which was continuously changing, but their answer was very relative. For the same stimulation patterns, answers varied widely from subject to subject. This approach to assessing the perceived stimulation turned out not to be the proper choice for this application, being unable to describe it objectively and consistently.

3.7.2. PSYCHOPHYSICS OF THE VIBRO-VACTILE STIMULATION

Psychophysical measurements are common when assessing a stimulation technology; however the methodology used is often unable to entirely characterize the quality of informational transfer between haptic devices and humans. Acknowledging the perception of few stimulation points within the stimulation range (Pylatiuk et al. 2006) is not sufficient. Moreover, the identified stimulation points should be equally perceived in order to allow for a uniform mapping between sensory information and stimulation. If the stimulation points are perceived by humans with different recognition rates, combining them into a pattern will result in a non-uniform stimulation. For example, continuously increasing the grasp force will be perceived by subjects as a series of ups and downs, which is not effective and might also be annoying. Therefore the stimulation points should all be perceived with the same recognition rate, in order to get a uniform and continuous stimulation when, e.g., force changes.

Another aspect of stimulation which has to be taken into consideration is the perception probability. If the probability is 1 (100% recognition rate), the stimulation space accommodates an undefined number of stimulation points. There might be ten stimulation points or eight or five, all 100% perceived. But the main goal of a psychophysical evaluation is to identify the maximum number of distinct stimulation points. A 100% recognition rate will result in an undefined number of stimulation points. Therefore, the recognition rate must always be lower than 100% in order to have a well-defined number of stimulation points. Let's assume that there are twenty stimulation points with 75% recognition rate. Increasing the recognition rate would result in a lower number of stimulation points. Conversely, decreasing the recognition rate would increase the number of stimulation points. Every recognition rate will result in a specific maximum number of stimulation points. In this study, a methodology was introduced to allow for the complete description of the capability of the proposed device to induce vibro-tactile sensations in humans.

SUBJECTS

Four healthy, able-bodied volunteers (two female and two male, between 20 and 40 years of age) participated in the psychophysical tests. The study was approved by the local ethics committee and the subjects signed an informed consent form. The subjects were instructed about the tasks to be performed and then practice tests were run to get them familiar with the task and setup. Only when the subject felt comfortably prepared were the experiments started. The preparation time varied among individuals and lasted between 10 and 30 min.

EXPERIMENTAL SETUP

The experimental setup for the psychophysical evaluation is depicted in Figure 31. The control unit (CU) is a microcontroller-based system which implements the psychophysical experimental protocol and communicates with the periphery. The stimulator was strapped to the subject [Figure 21c], and connected to the CU by a proprietary Otto Bock communication link (AxonBus, Otto Bock, AT). The CU operated the stimulator by sending control commands that were selected depending on user input during the experiment. A standard desktop PC computer ran a user-friendly software interface for the control and supervision of the experiment. The PC was connected to the CU using serial communication.

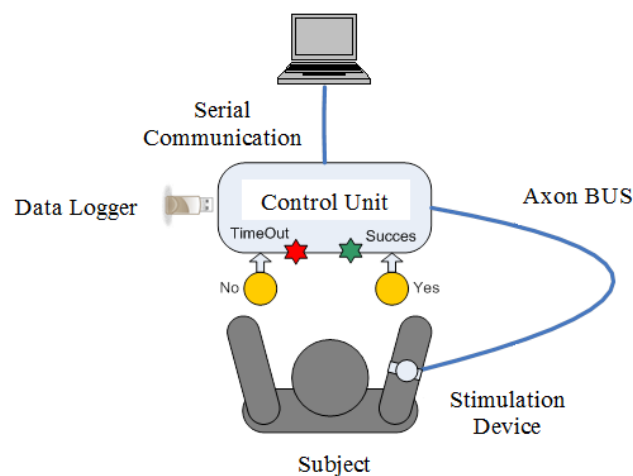


Figure 31: Experimental setup for the psychophysical evaluation of vibro-tactile stimulation which comprises: 1) a microcontroller based unit with two levers for user input and LED diodes for visual feedback, 2) standard PC for monitoring and supervision. 3) data logger to capture the results, and 4) stimulation device mounted on the subject's forearm.

A data logger was plugged into a USB port of the CU in order to record the experimental data. The user interacted with the system using two levers to provide either a "YES" or a "NO" answer during the psychometric testing. Visual feedback to the user was conveyed using green and red LEDs. The subjects were comfortably seated in a chair, facing the setup and letting their arms rest on the table so that they were able to pull the levers while avoiding contact between the stimulator and the table, which could induce unwanted confounding vibrations.

PSYCHOPHYSICAL PROCEDURE

The goal of the psychophysical measurement was to identify the maximum available number of distinct stimulation points (*vibels*) within the stimulation range, characterizing the quality of perceived stimulation with regard to a specific position on the body (i.e., below elbow). The notion of *vibel* was introduced in (Cipriani et al. 2012), as being a hardware part of a vibro-stimulation device. However, the *vibel* is used in the current paper as the elementary entity of the vibro-stimulation space. This was inspired by an analogy with a digital image. A digital image is described by a collection of pixels; consequently the vibro-stimulation space is here characterized by a collection of *vibels* – vibration elements or vibration pixels. The *vibel* not only describes the capacity of the haptic device to generate vibrations, but also the human tactile capacity to perceive vibro-stimuli. Thus, it provides information for characterizing the efficiency of information transfer between the haptic device and humans.

Perception is not a deterministic, but a stochastic process and the subject's answers can be biased by different physical and psychological factors. Therefore the psychophysical methodology used to describe the perceived stimulation must consider a large amount of data, and has to be done with respect to a specific *response criterion* (Gescheider 1997). For this purpose, a method was devised which provides a complete psychophysical description of a two degree of freedom haptic stimulator in the form of a matrix of *vibels* covering the whole frequency/amplitude stimulation domain.

The first *vibels* on each axis are placed on the detection threshold (DT) which corresponds to the minimum intensity of the stimuli that can be sensed by the subjects. From DT, the *vibels* are distributed along the frequency and amplitude axis, spaced by a "just-noticeable difference" (JND). A JND refers to the minimal change of the stimulus magnitude (frequency or amplitude), with respect to a baseline stimulus, that is needed to produce a difference in the human sensory experience. Therefore, a complete psychophysical characterization of a stimulation method would need to include determining a full sequence of JND steps, starting from the DT and going up to the maximum stimulation by applying the following rule: the current baseline stimulus equals the previous baseline stimulus + JND. This would, however, require a very large number of tests, especially when the stimulation method has a larger number of degrees of freedom. We therefore implemented an approach to estimate this detailed psychophysical characterization by using a significantly reduced number of measurements. The method comprises the following steps [Figure 32]:

1. The control space of the device was sampled by a matrix of 2x4x10 control points (CPs) distributed to cover the whole amplitude-by-frequency stimulation domain. The CPs were identical to the ones used for the physical characterization of the device: 2 conditions (constant frequency and constant amplitude) x 4 values of the constant input (20%, 40%, 60% and 80%) x 10 values of the test reference input (10%, 20% ... 100%). The resolution of the CP grid was determined after preliminary measurements which indicated that this sampling is dense enough to provide detailed information, while significantly reducing the duration of the experiment.

2. For the control points of the constant frequency / constant amplitude condition, the corresponding vibels (i.e., DTs and JNDs for amplitude) were determined. For each point, the vibels were measured in the increasing direction: from the baseline stimulation value, as defined by the control point, towards the maximum value (100%) of the tested input. In total, 2x4 DTs and 2x4x9 JNDs were determined per subject (80 values in total, 40 for constant frequency and 40 for constant amplitude). A modified version of a classical SIAM method (see below) was used to estimate a JND.
3. Webber fractions (WFs), i.e., a JND normalized to the value of the baseline stimulus, were computed for the JNDs calculated in the previous step.
4. A least square linear model was fitted through all the calculated amplitude WFs and the same was done for the frequency WFs to obtain a continuous representation of WF along both amplitude and frequency.
5. Finally, the entire stimulation range was covered by vibels starting from the amplitude (frequency) DT and going along the amplitude (frequency) axis using a recursive formula. From the resulting grid along the two axes, the vibels were expanded to cover the whole amplitude-by-frequency plane.

To determine a JND, a modified version of a psychophysical procedure proposed by Kaernbach, called the Single-Interval Adjustment-Matrix (SIAM) (Kaernbach 1990), was used. This procedure has been described as being unbiased and adaptive, requiring half as many trials to achieve the same precision as the classical two-interval forced-choice method. Importantly, the standard SIAM method was modified in order to make it more suitable for this context. In the standard approach, a single stimulus is presented and the subject is asked to guess if the stimulus belongs to the baseline or the signal (i.e., baseline + JND) without any time constraints. The signal or baseline presentations are always followed by a no-stimulation phase, which precludes the possibility of a direct comparison between the baseline and signal levels. The larger the time window between the presentations, the more biased will be the resulting JND. Vibro-feedback patterns for the closed-loop operation of a prosthetic device are obtained by connecting neighboring stimulation points (vibels), and an optimal feedback trajectory (i.e. feedback information to stimulation mapping) should connect the smallest stimulation parameter changes that can be perceived (i.e., JNDs). In this context, the user has to detect a change in the signal value rather than the presence or absence of the signal itself. Therefore, the standard SIAM procedure was modified to accommodate the discrimination of transitions between the baseline and signal.

Determination of a JND for a single control point requires several staircase sequences (as explained in the next section) and each sequence comprises several detection/discrimination trials. The general structure of a detection/discrimination trial is shown in the diagram in Figure 33.

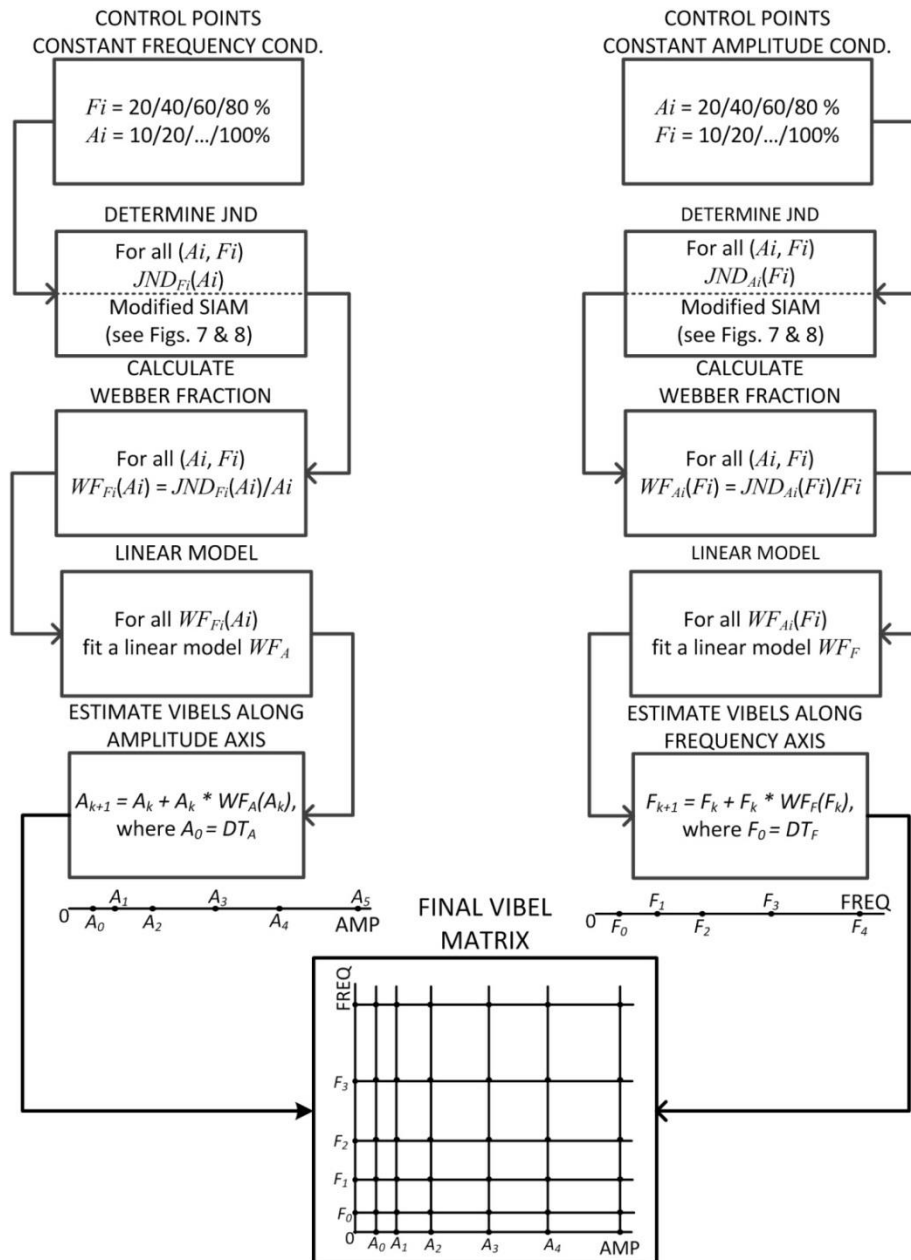


Figure 32: Method overview: from control points to the vibel matrix. JNDs for amplitude and frequency were determined in the control points for the constant frequency (left) and constant amplitude (right) conditions, respectively, using modified SIAM method.

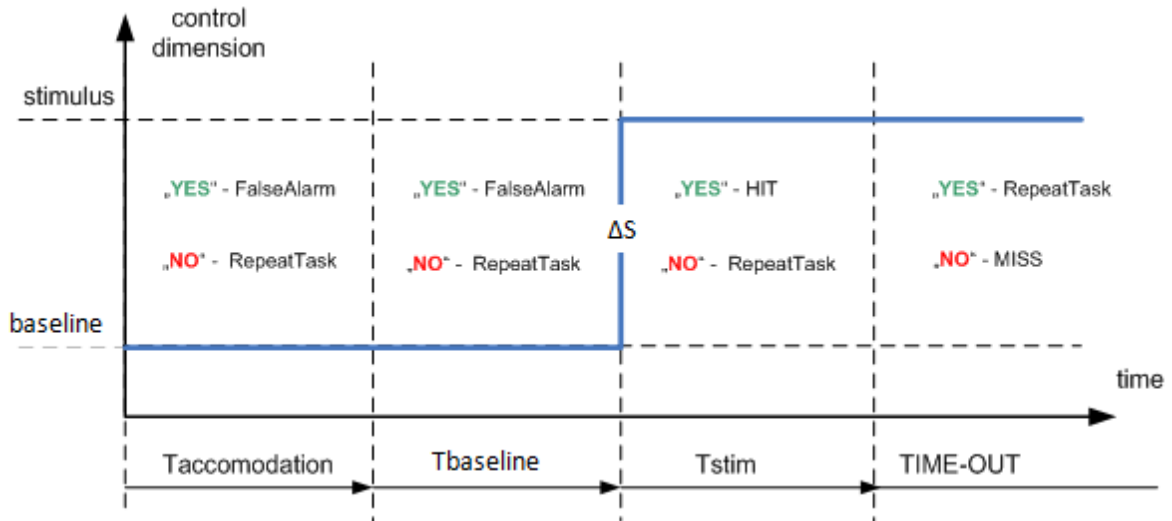


Figure 33: A psychophysical trial consists of four states: two during baseline and two during signal presentation (baseline + ΔS). Subjects use the “YES” and “NO” levers to indicate the detection of the transition from the baseline to the signal. Depending on the time interval, the subject’s response triggers different signal detection events.

The trial was initiated by the subject pulling on the “YES” lever. When the lever was pulled, the baseline stimulus, defined as the stimulation with the parameters corresponding to the current control point, was delivered. When the subject released the lever, the trial sequence started. The subject was instructed to focus on the stimulation and to try to detect if and when there was a change in the stimulation level, i.e., a transition from the baseline to the signal. He/she signaled the presence or absence of transition using the levers “YES” and “NO”, respectively. The sequence comprised three phases with durations Tacc, Tbase, and Tstim. Tacc and Tstim lasted for 400 ms, while Tbase was randomly selected within the interval 0 – 1000 ms; these values were chosen following the recommendations from (Kingdom & Prins 2009). During the interval Tacc + Tbase, the baseline stimulation was delivered. After that, the signal stimulus, defined as the transition from the baseline to the baseline + ΔS , was presented. The value of the ΔS (i.e., transition amplitude) in the current detection trial was adjusted by the staircase sequence, as explained below. Note that the instant in which the transition from the baseline to the signal occurred was unpredictable to the subject due to the randomness of the Tbase. A “YES” and “NO” during the interval Tacc + Tbase (baseline stimulation) were interpreted in accordance with the framework of the signal detection theory as a “FALSE ALARM” and “CORRECT REJECTION” event, respectively. In the case of the “CORRECT REJECTION”, the trial was repeated. After the signal stimulus was presented, in the time instant Tacc + Tbase, there was a time window of Tstim milliseconds for the subject to acknowledge the presence of the signal by answering “YES”. If the subject acknowledged the transition, a green light was turned on to communicate to the subject a successful recognition (“HIT” event). Otherwise, a red light flashed signaling a TIMEOUT event. If the subject judged that the signal was missed due to a lack of attention, slow reaction or other subjective factors, there was a

possibility to repeat the trial by pulling the “YES” lever. By pulling the “NO” lever, the subject reported a confident non-perception of the stimuli and a MISS event was correspondingly registered.

A staircase track is a collection of trials. In every trial the transition ΔS was adjusted adaptively, based on the event that was registered in the previous trial: HIT reduced the current ΔS for ΔM , while MISS and FALSE ALARM increased the current ΔS for ΔM and $2 \Delta M$, respectively, where ΔM was the tuning step size [Figure 34]. The track was deemed completed after the occurrence of a predefined number of reversals in signal presentation, where a reversal is defined as the switch in the sign of the signal magnitude change (e.g., HIT event followed by a MISS event). The maximum number of reversals as well as the adjustments of the ΔM along the track were prescribed by a so-called reversal array which, in our case, was adopted as {0, 1, 0, 0, 0, 1, 0, 0, 0, 0, 0, 1, 0, 0, 0, 0, 0, 0, 0}. The track therefore comprised 19 reversals, and a new step size was calculated after the 2nd, 6th and 12th reversal by dividing the current ΔM by 2. Decreasing the step size allows convergence and therefore precise identification of the JND. Initial conditions necessary to start the staircase track are the initial values for the baseline stimulation (defined by the current control point), and an initial estimation for the transition magnitude ΔS and tuning step size ΔM . In order to achieve a good convergence of the algorithm, three tracks were used to determine a single JND. In the first track the initial values for the ΔS were set to 10% and ΔM to 5% of the stimulation range, respectively. In the second track the initial ΔS was set as the average of the trials from the previous track and the initial ΔM as the standard deviation of the same data set. The same initialization was performed for the third track. This iterative strategy guarantees a strong convergence of the algorithm and a high precision in determining the JND.

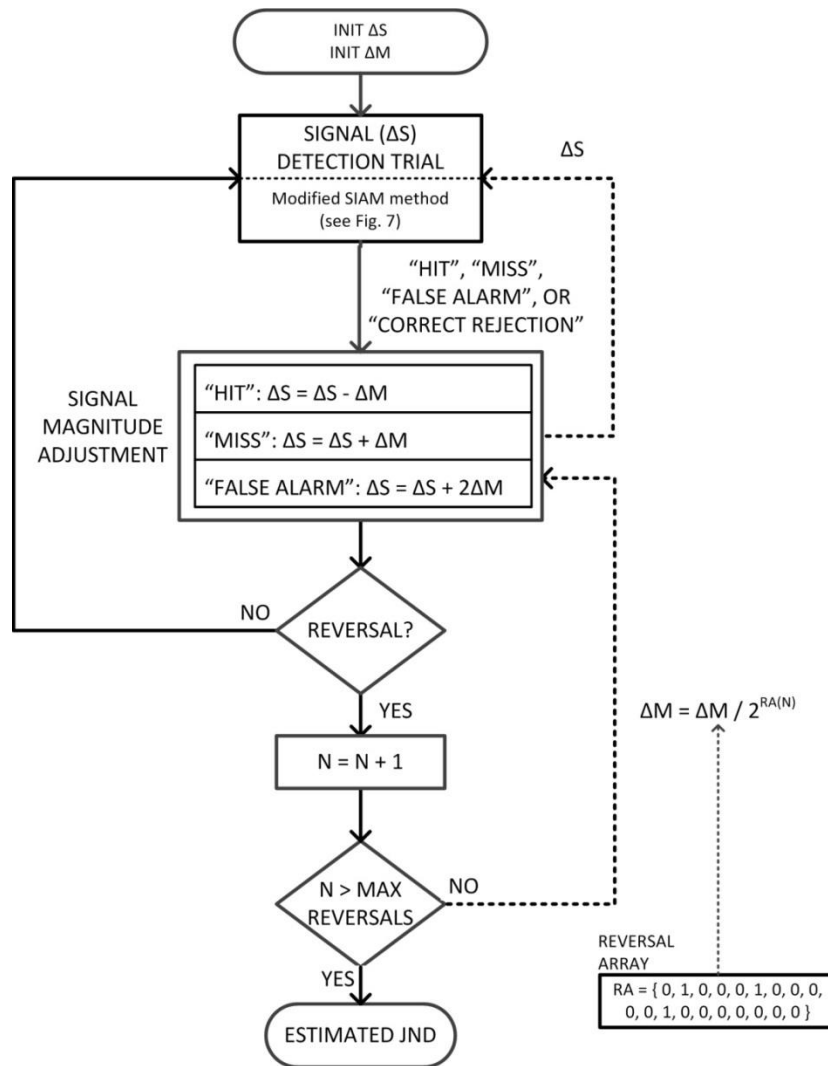


Figure 34: Determining a JND with a staircase sequence. JND is determined through an adaptive sequence of signal detection trials. The outcome of every trial is used to increase/decrease the magnitude of the transition (ΔS) between the baseline and the signal. The amount of signal change is regulated by the tuning step size (ΔM). If the reversal in the sign of the signal change occurred, the tuning step size is also adapted as defined by the reversal array RA. After the predefined number of reversal, the sequence is deemed finished, and the JND is adapted as the current value of ΔS .

For each JND in amplitude $JNDF_i(A_i)$ and frequency $JNDA_i(F_i)$, the corresponding Weber fractions $WFF_i(A_i)$ and $WFA_i(F_i)$ were calculated. For reasons explained in the Results section below, all four $WFF_i(A_i)$ were approximated by a constant value – KF, and all four $WFA_i(F_i)$ by KA. Then, starting from the DT for amplitude (A_0) and using the calculated KF, all JNDs along the amplitude axis were determined by using the following iteration: $A_{k+1} = A_k + JNDF_k(A_k) = A_k + A_k * KF$. Similarly, starting from the DT for frequency (F_0) and using KA, all JNDs along the frequency axis were determined. Orthogonally interconnecting all JNDs, on amplitude and frequency axes, results in a matrix of vibels covering the whole stimulation domain.

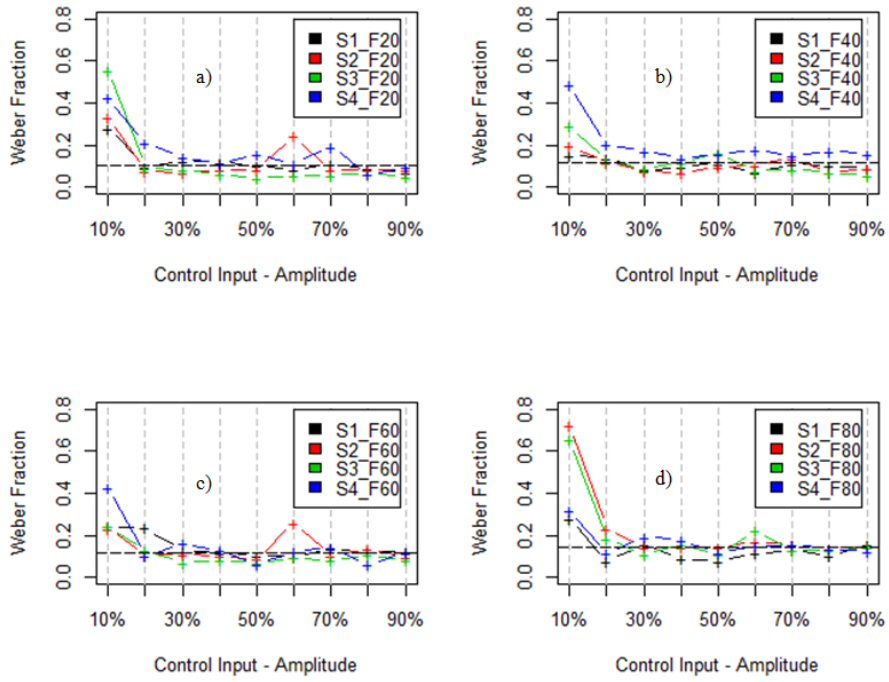


Figure 35: The WFs determined during constant frequency condition. Note the within- and cross-subject variability. Except for the first WF, the average trend is delineated by an overall mean (black dashed line).

Notation: S1 to S4 denote subjects, and F20 to F80 refer to the constant value of the frequency.

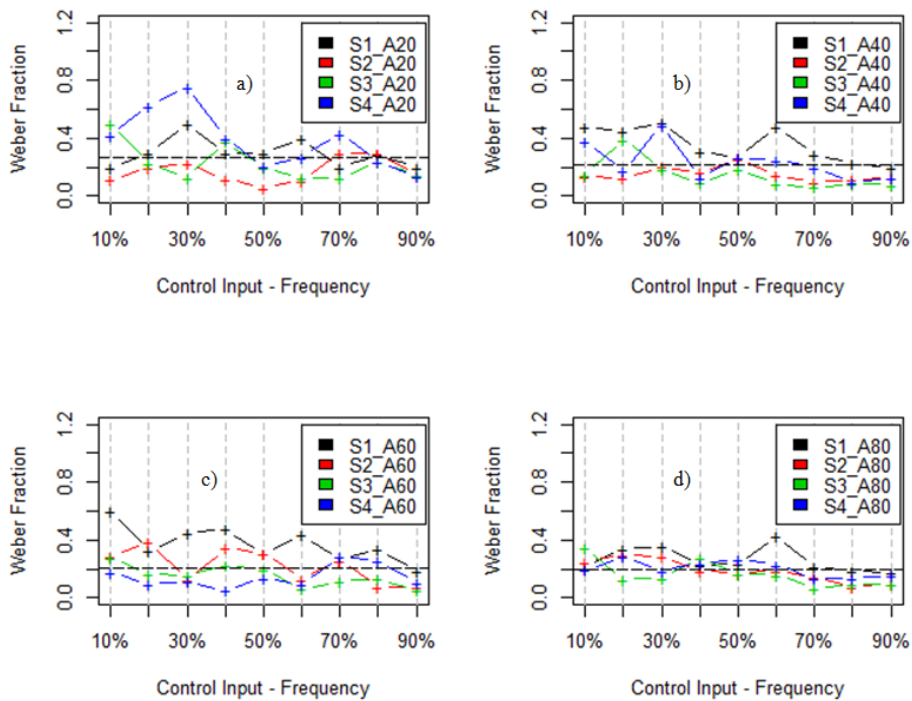


Figure 36: The WFs determined during constant amplitude condition. Note the inter- and intra-subject variability. The average trend is delineated by the least-square linear fitted model (black dashed line). Notation: S1 to S4 denote subjects, and A20 to A80 refer to the constant value of the amplitude.

The calculated WFs for the constant frequency and constant amplitude conditions are plotted in Figure 35 and Figure 36, respectively. The amplitude WFs for all subjects within one constant frequency condition (e.g. F20) were pooled together (4 subjects x 9 WFs) and averaged to obtain a continuous representation (the black dot-line in Figure 35a. The same was done for the conditions F40 (Figure 35b), F60 (Figure 35c) and F80 (Figure 35d), as well as for the amplitude-constant conditions A20 (Figure 36a), A40 (Figure 36b), A60 (Figure 36c) and A80 (Figure 36d). For each frequency- and amplitude-constant condition, the four values obtained in the previous step (F20/40/60/80 and A20/40/60/80) were averaged with KF and KA, summarized in Figure 37.

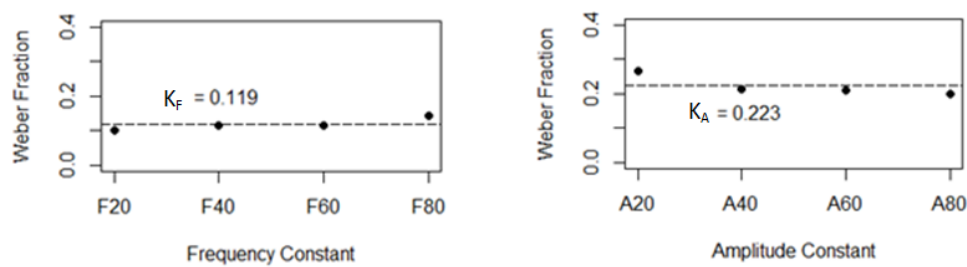


Figure 37: The least-square linear fitted WFs during constant frequency (left) and constant amplitude (right) conditions. The black dashed line represents an overall mean. The overall means are adopted as the two, overall WFs for amplitude and frequency.

There was a certain degree of variability both within subjects and across subjects. A single profile, representing the WFs in one subject for a specific value of the constant reference input, zigzags. The variability was particularly pronounced in the constant amplitude condition, while there was a decrease in variability of frequency WFs with increasing magnitude of the changing input (i.e., along the abscissa).

There was no clear increasing or decreasing trend in WFs for different steps of the tested input while it was changing from 10% to 90%. This was confirmed by a statistical analysis. There were no statistically significant differences between the WFs obtained in four subjects for different frequency steps in the constant amplitude condition. In the constant frequency condition, there was a significant difference only between the first step (10%) and all the other steps. However, this curvature of the WF at low magnitude of the stimulation is common when WF is evaluated from data acquired experimentally (Gescheider 1997). This non-linearity was not considered when fitting a linear model to determine the WF, and the model was fit by considering only the rest of the data (20% - 90%).

For the constant frequency condition, there was a slightly increasing tendency of the WF when the frequency increased from F20 to F80. For the constant amplitude, the trend was opposite, but the differences were minimal and they did not reach statistical significance. Therefore, a single constant value of WF for amplitude (KF) was adopted to describe the constant frequency condition, and the same was done for the frequency (KA) in the constant amplitude condition.

Finally, the vibel matrix was determined, its resolution outlining the quantity of the perceived vibro-stimulation with respect to the part of the body on which the stimulation was applied [Figure 38] The vibel matrix was obtained after applying a recursive equation to generate the JNDs along the stimulation parameter axes: $A_{k+1} = A_k * (1 + KF)$ and $F_{k+1} = F_k * (1 + KA)$. This resulted in 15 JND levels along the frequency axis and 27 JNDs along the amplitude axis, with JNDs increasing with the increase in the stimulation parameter value (i.e., from left to right along abscissa, and from bottom up along the ordinate).

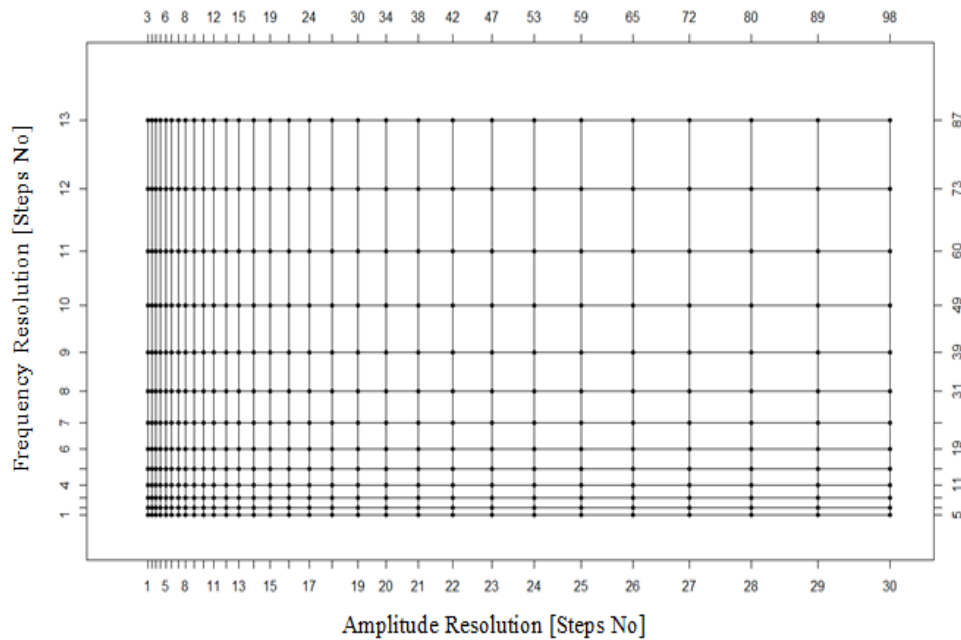


Figure 38: Matrix of vibels describing the space of the perceived stimulation. The structure is regular and represents the averaged psychophysical performance for the tested group of subjects.

CONCLUSIONS

After performing physical and psychophysical measurements, it was shown that the introduced technology is able to generate complex patterns of vibro-stimulation. Firstly, physical measurements were performed in order to identify the device's capacity to generate vibrations. However, the human tactile sense does not have the ability to entirely perceive the provided stimulation and so, in order to completely characterize the novel method, a psychophysical assessment was performed.

The psychometric tests have demonstrated that a human subject is able to perceive the generated vibrations and discriminate their parameters. The outcome of the psychophysical assessment is represented by a matrix of vibels with a resolution of 15 x 27 in the frequency-amplitude domain and this demonstrates that the

proposed method is able to induce a large amount of differentiable stimuli ($405 = 15 \times 27$). The perception of vibro-tactile stimuli is inherently subjective and is typically characterized by a large variability (Gescheider 1997). This was confirmed by our psychophysical measurements and reflected in the results shown in Figure 35 through Figure 37. To obtain the parameters that would capture the mean response of the subjects being tested, a number of measurements were conducted for each subject and the results averaged across subjects and conditions. However, instead of testing JNDs sequentially, starting from the detection threshold and proceeding until the end of the stimulation range for each condition, the amplitude by frequency plane was sampled using a limited number of points (80). This limited sampling was then exploited to reconstruct the full set of sequential JND steps along both degrees of freedom, resulting in a matrix with 405 points.

The matrix obtained has great practical relevance. It can be used to guide the delivery of haptic feedback. Using this information, vibro-patterns can be generated by changing the amplitude and/or frequency by following the steps in the vibel matrix. This increases the likelihood that a subject will detect the change, since the matrix comprises the JNDs characterizing the average perception of a group of subjects. Mapping the sensorial information from prosthesis into haptic patterns by using a vibel matrix will allow for a much more efficient informational transfer between the prosthetic device and the human body.

In the model, the vibels are distributed in a very regular pattern, along the lines parallel to the frequency and amplitude axes. This representation should not be viewed as absolute, however. As discussed earlier, the regular structure presented in Figure 38 captures the average psychometric performance of a group of subjects. Importantly, the same set of data collected in the experiment can be used to determine a “personalized” vibel matrix for each subject. This can be done if the results are not averaged, and the subject-specific WFs are used to reconstruct the vibel matrix. In this case, the vibel matrix would lose the aforementioned uniformity, but perhaps better represent the instantaneous structure of the perceived stimulation in a single subject. Tactile perception is a variable process and tactile acuity changes continuously with various factors, both external and internal - temperature, skin condition, body posture, attention, mood and motion artifacts are all factors influencing tactile perception. The vibel matrix can be imagined as having a dynamically changing structure, sensitive to all the factors mentioned above (and perhaps more). However, the intended real-life application of this system does not allow a continuous monitoring of these changes, and therefore the model that was created averaged this variability in a convenient way.

Moreover, tactile sensitivity varies greatly between different individuals. Hence, we performed the measurements with four persons and to some extent we registered this inter-subject variability in Figure 35 and Figure 36. For both constant amplitude and frequency conditions, there was no clear trend between individual outcomes; however the general trend expressed by the mean over the entire data set was obvious. This knowledge allows for a strong simplification of the methodology; measurements should not necessarily be performed for all 20/40/60/80 constant amplitude or frequency conditions, but only for a few relevant control points. Importantly, these simplifications of the procedure will allow the recruitment of a larger population, and the results will gain a more general character.

Psychophysical measurements are common when the perception of haptic stimuli must be evaluated, but very often they do not entirely characterize the stimulation, being restricted to determination of only a few stimulation levels; this determination is often performed without a specific subject response criterion. In the current work, the psychophysical evaluation received special attention. The target was to build a complete model of the perceived stimulation consisting of the maximum number of perceptible vibro-tactile stimuli accommodated within the stimulation range, rather than merely receiving acknowledgment from the subjects that vibration was perceived on some values of frequency and amplitude. Determining a model of the stimulation is challenging and very time-consuming, but this effort is rewarded by the possibility of optimally mapping the sensor signals to the stimulation. This allows an efficient transfer of information between sensors and humans, exploiting the full capability of the stimulation device to transmit information haptically to amputees.

A practical and efficient procedure to construct a model of the stimulation has a great importance not only for the mapping as mentioned above, but also for comparing various stimulation technologies which employ different modalities. The physical stimulation parameters allow the evaluation of a stimulation technology and can also be used to compare haptic devices using the same modality. Should there be a need to choose between the technologies stimulating in different modalities, or to evaluate a multi-modal stimulation (e.g. vibro-stimulation and electro-stimulation), a direct comparison of stimulation parameters is not possible. The vibel matrix can characterize the resolution of a multi-degree-of-freedom haptic device (e.g., multi-modal stimulation) and can thus be used for an objective comparison. Psychophysical measurements are direct outcomes of the conscious human tactile perception and provide a unified result irrespective of the stimulation technology. Therefore the identification of a stimulation model consisting of a collection of vibels may be a very efficient approach to comparing the quality of stimulation provided by different technologies stimulating simultaneously or separately.

This study presents a methodology to build up the stimulation model; however, in the current form it has a major limitation. The model was constructed based on JNDs determined for every control point in the control matrix, but only in an increasing direction of stimulation, i.e., towards 100% on the amplitude and frequency axes. Currently, a vibel is characterized by its center - the control point and two DTs on the amplitude and frequency axes in an increasing direction. However, to efficiently integrate the haptic stimulation into the control loop of the prosthesis, the vibel should also contain the JNDs determined in a decreasing direction. It is expected that a JND in a decreasing direction will be larger than in an increasing direction of the stimulation, due to the "masking" effects which will reduce the stimulation discrimination.

3.8. The Haptic Brace

In order to augment the vibrotactile stimulation generated by the haptic device, previously described, the same motor used for the generation of AF modulated vibration was integrated into a novel haptic device, the so called Haptic Brace. Wrapped around the forearm, the Haptic Brace has the ability to generate a sensation of pressure and squeeze the forearm while simultaneously vibrating. Additionally, the Haptic Brace is also able to lightly and cyclically squeeze/release the forearm generating a kind of vibration there.

Consequently the stimulation generated by the Haptic Brace is the result of combining five distinct stimulation primitives: the amplitude and frequency generated by the inertial forces developed during the motor acceleration/deceleration, the amplitude and frequency of the vibration generated by cyclically squeezing-releasing the forearm, and the steady pressure developed by pulling the brace together.

The capability of the Haptic Device for generating stimulation patterns was not evaluated, but is planned in future research. However, due to its capability for multi-modal stimulation of the skin and muscles beneath the brace, it is believed that the device will allow for a more physiological stimulation, simultaneously addressing different types of receptors in skin, muscle and bones, and better reproducing the natural interaction with the environment.

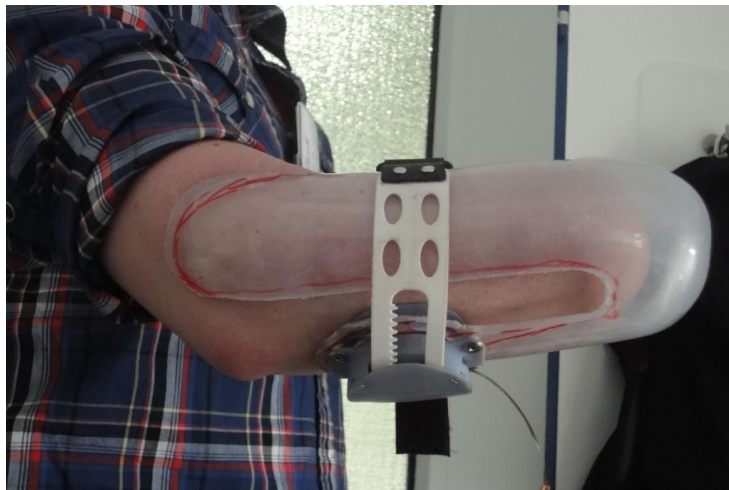


Figure 39: The Haptic Brace integrated in the socket of an amputee is able to generate multimodal stimulation by simultaneously vibrating and generating sensation of pressure and squeeze the stump.

4. PATTERN GENERATION STRATEGIES

4.1. Staircase Patterns

The matrix of vibels, previously determined, describes the capability of a stimulation technology to induce vibro-tactile stimuli by evaluating its dimensionality. The more discriminable vibels available within the stimulation matrix, the more vibro-tactile stimuli can be induced in humans. A matrix of vibels may be used to compare different stimulation methodologies with respect to a predefined position on the body, or to evaluate the sensitivity of various sites on the body by comparing their reactions to a single stimulation technology. The largest benefit of the vibel matrix is that it allows the generation of uniform feedback patterns. Interconnecting singular vibels, it is possible to design stimulation profiles with various resolutions (length), which has great importance when mapping with the sensory signals measured by a prosthesis. A stimulation profile consists of a sequence of vibels. The larger the number of vibels, the more accurate the sensory signals haptically transmitted to the amputees, because they have higher resolution.

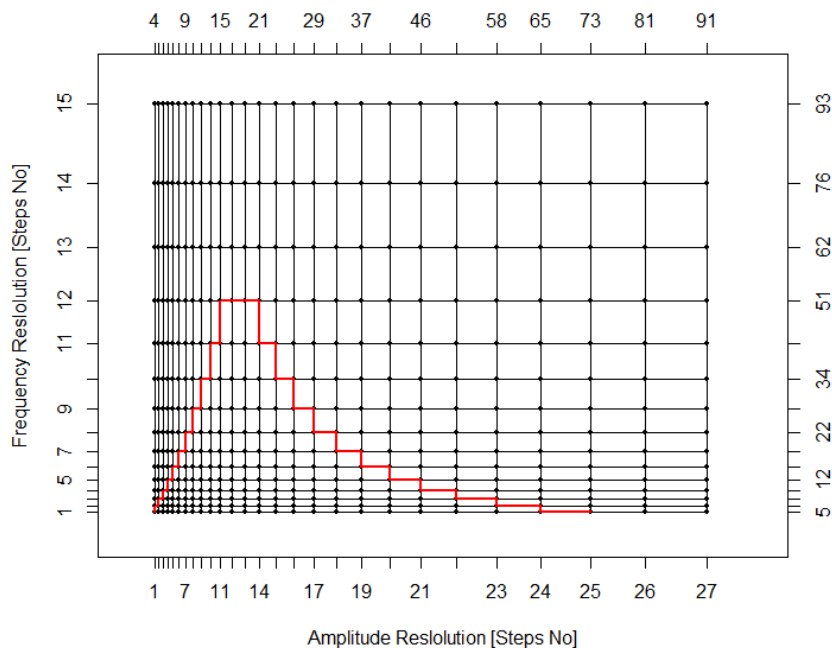


Figure 40: An example of a vibrotactile stimulation pattern – the red profile, obtained interconnecting individual vibels in a continuous trajectory.

One potential profile is depicted in Figure 40 as a red line, connecting the vibels. In principle, one could deliver the sensor information haptically by, for example, selecting a constant frequency and modulating the amplitude. In this case, the profile would be a horizontal line along the vibel matrix, and according to the

matrix resolution, there would be 27 different levels available for the information coding. Similarly, if one selected to modulate the frequency, only 15 levels could be used. On the other hand, by following the indicated profile which implies the simultaneous modulation of amplitude and frequency, the number of levels increases to 44. Importantly, the vibel matrix map is very flexible, and many different profiles can be constructed. However, the design and evaluation of different profiles is important future work.

4.2. Continuous Patterns

The vibel matrix, previously presented, consists of vibels interspaced by JNDs, identified by simply changing either the amplitude or the frequency of the stimulation. Thus, the resulting stimulation has a staircase profile. However, taking into account the theory of multisensory integration, also known as multimodal perception, it is expected that the discrimination thresholds, when simultaneously changing the amplitude and the frequency of the stimulation, will be different compared with the case when only the amplitude or the frequency is changed. One principle of multisensory integration, namely the principle of inverse effectiveness, states that it is more likely or stronger when the constituent unisensory stimuli evoke relatively weak responses when presented in isolation. The CNS is able to integrate information from different senses, such as sight, sound, touch, smell, self-motion and taste (Lewkowicz & Ghazanfar 2009).

Following the same pattern of reasoning, it was also hypothesized that, by simultaneously changing the amplitude and frequency of the vibration, the same outcomes may be targeted. Tactile perception is gained by many types of mechanoreceptors embedded in the skin, each specialized to detect a particular type of stimulation. When, for example, high-frequency vibration is applied to the skin, Pacinian corpuscles are activated, sending trains of action potentials to the CNS. When steady pressure is applied, the Merkel Cells will perceive and forward the stimulation. When vibrating and simultaneously exerting pressure on the skin, Merkel Cells and Pacinian Corpuscles are simultaneously activated, and the mechanical interaction is transmitted on parallel pathways to the CNS. While simultaneously activating, the vibration and pressure receptors will decrease the perception threshold compared with unimodal stimulation.

While the example of pressure and vibration modalities helps to make the physiological mechanisms, which have been thought to facilitate the generation of complex stimulation patterns, easily understandable, the main focus here is on the generation of vibro-tactile stimuli. Vibration is sensed also by many types of receptors; changing the amplitude or frequency of the vibration will determine that e.g. Pacinian or Meissner's corpuscle will differently fire APs. Following the same progress of thoughts as for the case of multimodal stimulation vibration-pressure, it has been hypothesized that the stimulation thresholds, if simultaneously varying amplitude and frequency, will have lower magnitude than independently changing the amplitude or the frequency.

In order to evaluate this hypothesis, the same psychophysical methodology was used as in the preceding study, in which only changes in amplitude or frequency were evaluated. However, the structure of the Control Point

Matrix was changed to allow the evaluation of simultaneously changing frequency and amplitude. The structure of the new CPM is outlined in Figure 41. During the previous measurements in detection tasks, the borders of the stimulation were identified. Therefore, for the diagonal case, these measurements were not repeated, and the control points were placed within the previously defined stimulation range.

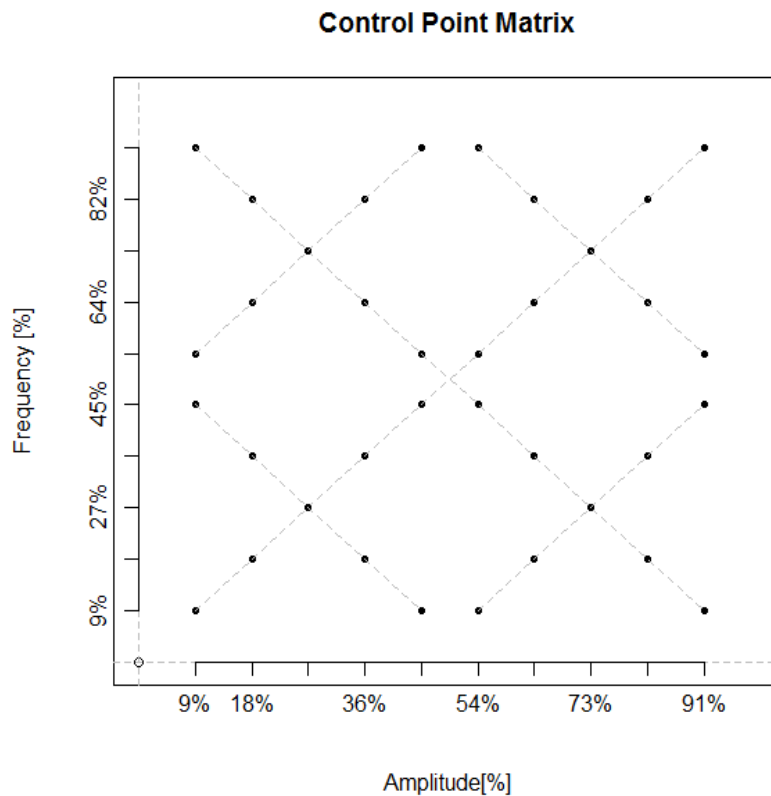


Figure 41: Control point matrix consisting of 40 points, diagonally and uniformly distributed over the stimulation range. For the control points along the first diagonal (45°), the JNDs were determined while the frequency and amplitude of the stimulation simultaneously and equally increased. For the control points along the second diagonal (135°), the JNDs were determined while the frequency of the stimulation increased and the amplitude simultaneously and equally decreased.

For this study, only changes in the direction of increasing amplitude were evaluated, while the frequency was both increased and decreased. This resulted in two directions to be followed within the stimulation space, that of the first diagonal, with a slope of 45 degrees, and the second diagonal, with a slope of 315 degrees. Similar to the frequency and amplitude constant conditions, the points within the CPM are bases for which corresponding JNDs will be determined.

As in the previous study, the method included the following steps:

1. The control space of the device was sampled by a matrix of diagonally distributed control points, to cover the whole amplitude-by-frequency stimulation domain. Starting from low amplitude, and increasing, following the direction of the main diagonal (45 degrees), the control points were placed

on one long and two short equidistant diagonals. The points were similarly distributed along the 135-degree diagonal.

2. For all control points in the matrix, the corresponding JNDs were determined. For each point, the JNDs were measured in the direction of increasing amplitude and frequency, as well in the amplitude increasing/frequency decreasing direction.
3. Weber fractions (WFs), i.e. a JNDs normalized to the values of the baseline stimuli, were computed for the JNDs calculated in the previous step.
4. A least square linear model was fitted through all the calculated WFs for the 45-degree diagonal as well as for the 135-degree diagonal.
5. Based on individually determined WFs, interpolated with a spline function, a continuous representation for the Weber fractions was computed, which was called the Weber Function.

Four healthy, able-bodied volunteers (two females and two males, between 20 and 40 years of age) participated in the psychophysical tests. The study was approved by the local ethics committee and the subjects signed an informed consent form. The subjects were instructed about the tasks to be performed and then performed test runs to become familiar with the task and setup. Only when the subject felt comfortably prepared were the experiments started. The preparation time varied among individuals and lasted between 10 and 30 min.

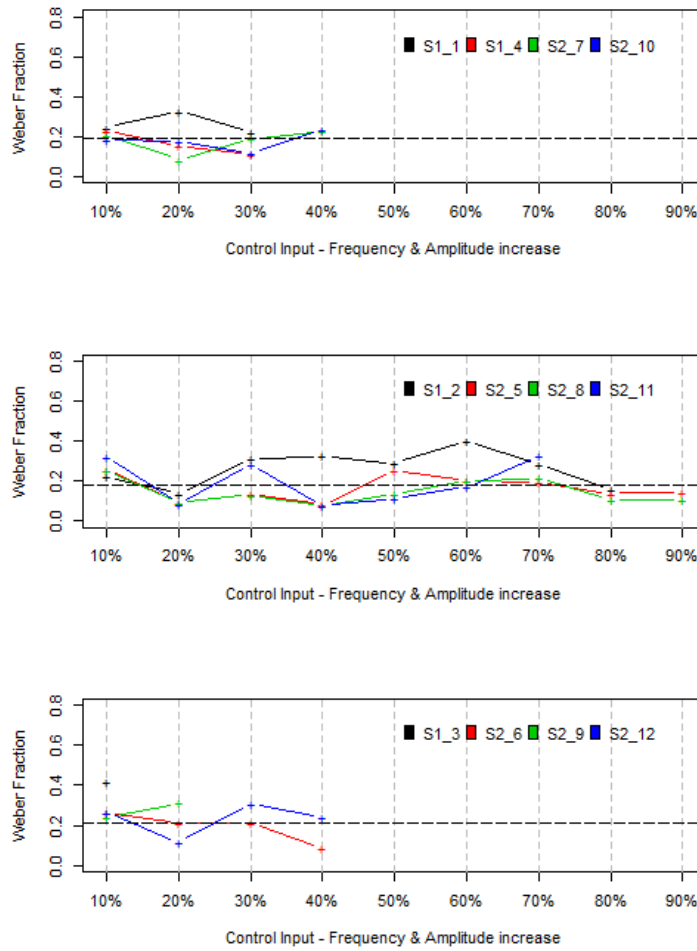


Figure 42: The WFs determined during the 45 degrees diagonal condition. The average trend is delineated by the least-square linear fitted model (black dashed line). Notation: S1 to S4 denote subjects.

The obtained data, the collection of WFs for all control points in the matrix, was separately analyzed for all six diagonals. Preliminary analysis revealed that there were trend similarities within every group, the three 45-degree and 315-degree datasets, however, showed clear differences when compared with each other. In order to facilitate better transparency of individual trends, every diagonal, performed by all four subjects, were represented in one subplot. Figure 42 shows the 45-degree case and Figure 43 the 315-degree.

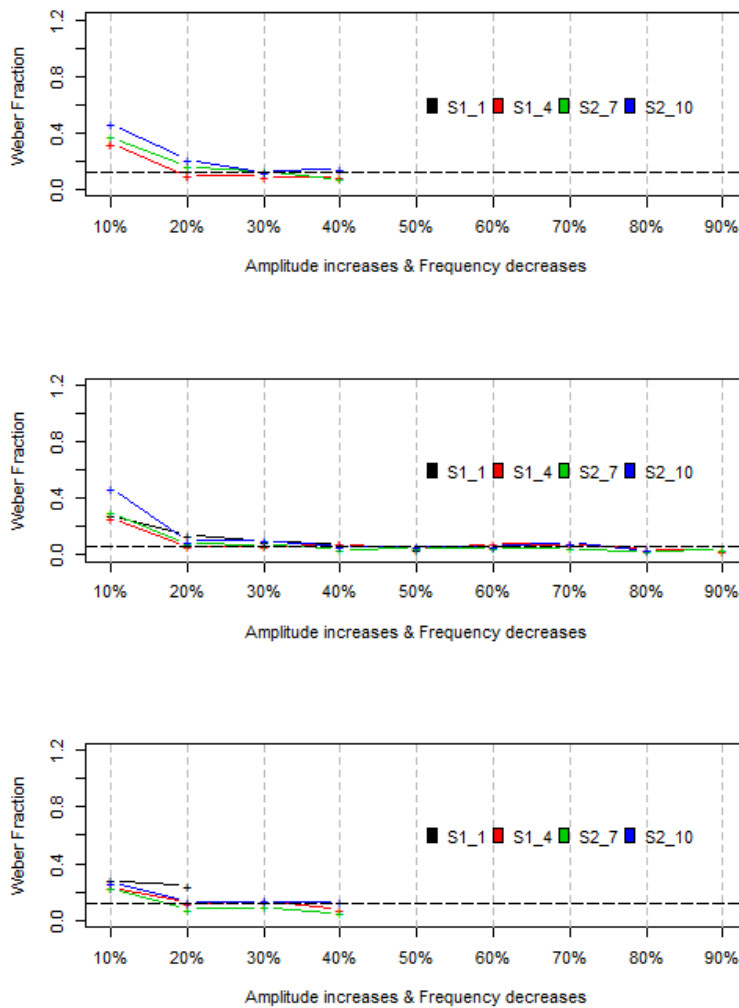


Figure 43: The WFs determined during the 135 degrees diagonal condition. The average trend is delineated by the least-square linear fitted model (black dashed line). Notation: S1 to S4 denote subjects.

The data collected from all diagonals, was then fitted by a line, and these results, the averaged WF for all diagonals, were summarized, shown in Figure 44.

Having defined the borders of the stimulation space, and the WF for the 45- and 315-degree diagonals, would allow for the building of a new diagonal vibel matrix by using the recursive equations from the preceding study. However, this could result in confusion. It may also be useful to have vibel matrices defined by 10 or 20 degrees, or any other pairs within 0-360 degrees. This would result in an unmanageable number of vibel matrixes, of no use when vibro-tactile patterns have to be generated.

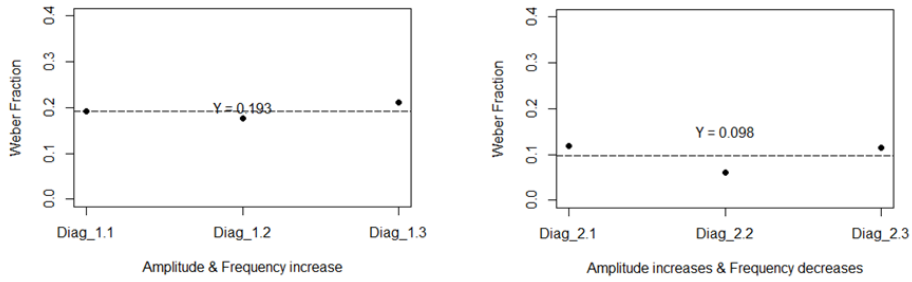


Figure 44: The least-square linear fitted WFs during 45 degrees (left) and 135 degrees (right) conditions. The black dashed line represents an overall mean.

In light of this, the strategy for building vibro-stimulation patterns was modified. The individual WFs for all slopes were not directly used to generate the vibels, but considered as a dataset spread over the range of 0-360 degrees. This slope represents the results when simultaneously changing the amplitude and the frequency. When only the amplitude is changed, the slope will be zero; when only the frequency is changed, the slope will be 90 degrees. Equally increasing the amplitude and the frequency will result in a slope of 45 degrees, and equally increasing the amplitude, while decreasing the frequency will result in a slope of 315 degrees. The set of four WFs were fit into a polar diagram Figure 45, and represented by the black vectors. The length of the vector is the WF and the slope, the ratio between frequency and amplitude.



Figure 45: The fitted Weber Function was obtained interpolating pairs of measured WFs (black/gray arrows) by a spline (the red profile).

Instead of eight measurements to describe the WFs along the axes with the slopes 0, 45, 90, 135, 180, 225, 270, 315 degrees, we performed only four. The used psychophysical procedure was simplified but it is still demanding in terms of execution time. In order to be able to perform the measurements along all eight axes, and to recruit for measurements a larger number of subjects (not only four) and give the measurements a more general character, the time required by the psychophysical procedure has to be further reduced. This is not a trivial task as this simplification has to be done without sacrificing precision in estimating the individual WF.

However, for now, the four estimated WFs were mirrored and included in the diagram as grey vectors [Figure 45]. The grey vectors outline the case of decreasing the amplitude (slope 180 degrees), decreasing the frequency (slope 270 degrees), decreasing the amplitude, but increasing the frequency (slope 135 degrees), and decreasing the amplitude and frequency (slope 225 degrees). In order to fully illustrate the approach intended to be used for pattern generation, all eight vectors measured and mirrored were fitted by a spline curve. It is obvious that in reality the complement vectors will have completely different length, and the fitting function will not be symmetrical as presented in Figure 45. Having determined such a function, the next step would be to generate vibels by using recursive formulas, and interconnecting them with vibro-tactile patterns.

4.3. Multimodal Stimulation Patterns

Patterns may be generated not only by changing the amplitude or frequency of the vibro-stimulation, but also simultaneously changing, for example, the pressure applied to the skin, or by stretching the skin in various directions. Actually, there are many possible ways to combine unimodal stimulations into multimodal stimulations by simultaneously stimulating the skin with many technologies. These technologies will address specific tactile receptors embedded in the skin and, as stated by the multimodal integration, it is expected that the perception thresholds during multimodal stimulation will be much lower than during unimodal stimulation.

In order to implement this kind of multimodal stimulation, the system described in Figure 46 was implemented. A master unit communicates wirelessly with the prosthesis and gets sensory information from it. After preprocessing, the sensory information is segmented into stimulation primitives. For example, the amplitude and/frequency of the BLDC vibration can be simultaneously changed with the frequency and amplitude of electrostimulation; all are distinct parameters delivered by the Feedback Axon Master as a data string along the AxonBUS. Connected to the BUS, as AxonNodes, the stimulation devices will interpret the received data and convert it into physical stimulation.

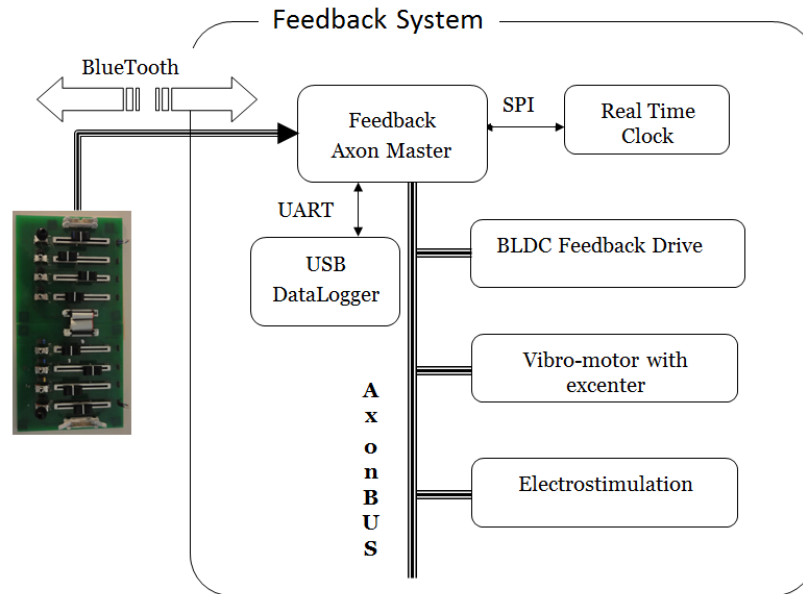


Figure 46: The block diagram of the experimental setup prepared for the study of multimodal stimulation. The positions of the sliders, or sensory information from the prosthesis, are coded in a data stream, and serial transmitted to the Feedback Axon Master (wired or wireless). The Axon Master has the function to decode this information, to generate stimulation patterns, and to encode it into a set of stimulation primitives, transmitted along the AxonBUS to the correspondent attached stimulation devices.

In addition to the wireless communication, the device may be manually controlled by changing the position of the sliders attached. The feedback master can work in two distinct modes: in the first, every slider controls one primitive of the stimulation, and in the second mode, every slider controls a stimulation pattern, as the sensory signal controls it.

4.4. Pattern Generation Mechanisms

The mechanism of generating stimulation patterns should allow diversity in combining stimulation primitives, while being both flexible and easily adjustable. Many approaches were tested and the one most closely fitting the requirements is illustrated in Figure 47. Sensory information measured by the prosthesis and values adjusted by sliders are fed into a pattern generation block, which has one input and a number of outputs corresponding with the number of stimulation primitives constituting the stimulation. When the prosthesis or slider board delivers more than one signal, the pattern generation blocks will be correspondingly replicated.

In Figure 47, the four sensory-inputs were fed into the four pattern generation blocks. This corresponds with a system in which the sensory information comes from the OB Michelangelo Hand prosthesis, and haptically stimulates using e.g. the Haptic Brace. The hand prosthesis measures the aperture and force, and in order to redundantly transmit the same information haptically with multimodal stimulation, shown to be more efficient than unimodal stimulation, the derivative of position and force are determined, expanding the sensory input

number from two to four. As a result, the feedback generation system will have four inputs and sixteen outputs.

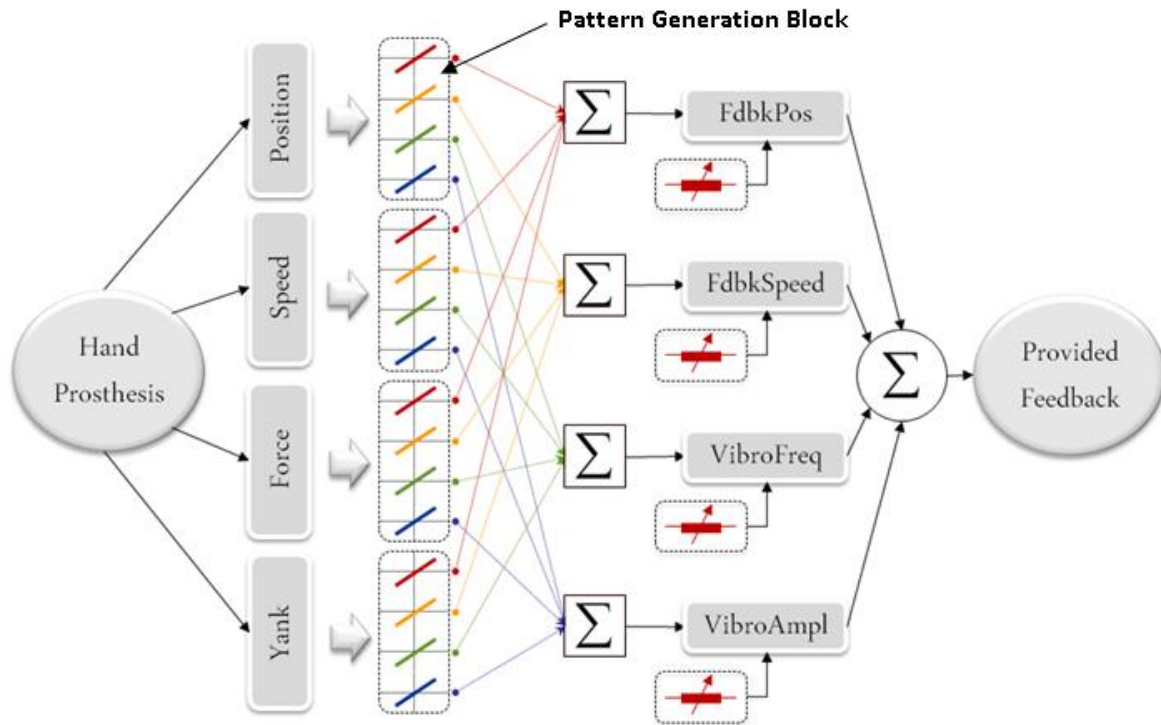


Figure 47: The strategy to combine stimulation primitives into stimulation patterns. The stimulation primitives, e.g. amplitude or frequency of the vibrotactile stimulation, are determined as linear combinations of sensory information measured by prosthesis or simulated by sliders. Different stimulation patterns can be defined by different sets of coefficients of the linear regression defined by changing the slope and intercept of the colored lines.

In the current implementation, the conversion between one input and every output is linear, this transformation being schematically represented in Figure 47 by colored lines of red, orange, green and blue. If the line is horizontal, intercepting the axis through origin, the output will always be zero, independent of the input values. If the line is horizontal, but intercepting the vertical axis through a positive value, the output will always be the intercept with the vertical axis. By changing the slope and the intercept of this linear transformation, various combinations may be achieved. For example, a 45-degree slope and zero-intercept will simply forward the input to the output, or a 135-degree slope will determine that the output will be mirrored, inversely proportional to the input.

As previously mentioned one linear function has its own output and is a sub-block within the Pattern Generation Block. Consequently, in this example, the Pattern Generation Block has four outputs, each directly

influencing one stimulation primitive. However, the stimulation primitive is not exclusively controlled by only one input, but, as depicted in Figure 47, by the weighted sum of the outputs from the Pattern Generation Block.

While this simplified version may be a very strong tool, allowing physiological mappings between prosthesis and feedback, this strategy of pattern generation doesn't fully exploit the capabilities of the stimulation technology, as there is no way to define custom patterns by non-linearly combining the stimulation primitives. In order to achieve this level, the inclusion of intermediate processing layers between the pattern generation block and the stimulation primitives is required, and/or the Feedback Generation block has to include more complex functions.

4.5. Comfort, Intuitiveness, Acceptance

The psychophysical analysis will recommend the technology or the combination of technologies to transmit haptic information to the body. Then, stimulation patterns have to be generated, which, mapped with measured sensory-information, will close the prosthesis control-loop. Generating stimulation patterns which are readily perceived by amputees, but also comfortable and intuitive, is very challenging. During this study, various patterns of haptic feedback were generated, but how well these patterns can be correlated by amputees with the prosthesis behavior, and the scope and nature of the rules that would allow for intuitive mapping of the feedback with the prosthesis, are vital questions which are still not answered by state-of-the-art technologies currently available.

For this purpose, the potential offered by the Rubber Hand Illusion (RHI) was exploited during this study (Prahm et al. 2011). The RHI convinces people that a rubber hand is their own by putting it on a table in front of them, while stimulating it in the same way and in synchronicity with their real hand. This illusion opens new perspectives in understanding how sight, touch and proprioception combine to create a convincing feeling of body ownership, revealing how the brain represents the body, which is a problem of multisensory-integration. In the case of prosthetics, understanding these mechanisms may be of great value; understanding how to combine natural vision with artificial stimulation will create a basis for allowing better integration of the prosthetic device into the amputee's body image.



Figure 48: Experimental setup used to induce robber-hand illusion (Botwinick, 1998). The RHI is induced by simultaneously stimulating a rubber hand and the subject's natural hand with a brush, while the rubber hand is visible and the natural hand is hidden.

RHI is induced by simultaneously stimulating a rubber hand and the subject's natural hand while the rubber hand is visible and the natural hand is hidden, and they have congruent positions - Figure 48. In the classical experiment, fine brushes are used for stimulation. The brush stimulation is very complex, activating diverse haptic receptors, so that the RHI illusion is easily induced. If the complexity of the stimulation is reduced from brush stimulation to simple strokes, the illusion is harder to induce. A lower complexity of stimulation comes closer to the stimulation generated by state-of-the-art haptic technologies, which were also tested. The first stimulation tested to induce RHI was punctual vibration, generated by regular vibration motors. But using this stimulation approach it was not possible to induce the RHI into subjects. However, by placing many vibration motors along a finger or forearm, and sequentially activating them, one by one, from e.g. fingertip to wrist, the sensation of a movement was simulated. In this way another type of illusion was created, the cutaneous rabbit illusion. This illusion may be created by delivering a rapid sequence of punctual taps on two or more places e.g. longitudinally on the forearm, generating the sensation that there are some hopping taps going from the wrist to the elbow, although no physical stimulus was applied between the two actual stimulus locations.

Synchronous with this induced sensation of movement, the rubber hand was stimulated by simply touching it, and moving along the artificial finger. As reported by the involved subjects, the RHI illusion reappeared; not as strongly as during the brush stimulation, but at least there was a sign that RHI can be induced with artificial stimulation.

The results of these incipient measurements showed that reducing the complexity of the stimulation during natural interaction causes the intensity of RHI to be strongly reduced. It follows that the RHI will be stronger in correlation with the complexity of stimulation using haptic devices as well. This points to RHI as a methodology to intuitively correlate the visual feedback, or mental processes, with the haptically-provided feedback, and to identify the degree of intuitiveness of perceived stimulation patterns which are mapped with the prosthesis behavior. Therefore, the future intentions are to induce RHI in an immersive virtual environment. The subjects

will have a virtual prosthesis attached to the arm and they will control and visually supervise it. Then various haptic feedback patterns will be applied to the subjects, haptically describing the behavior of prosthesis, in synchronicity with the prosthesis performance. For example, the prosthesis aperture may be encoded by various haptic patterns, and the degree of induced RHI may recommend the most intuitive mapping between feedback and prosthesis.

The discussed strategy to evaluate intuitiveness of haptic feedback may be claimed to be very subjective, not being supported by an objective measure. Indeed, the above discussion is based solely on personal experience. Objectively evaluating the RHI is still quite challenging. Typically, the proprioceptive drift or change of the body's temperature/conductivity is used for this purpose. However, when tested during initial experiments, these measures were not very consistent with what has been subjectively perceived. This still remains a challenge, which needs to be analyzed in more depth by future research. A possible approach to addressing this issue may be proprioceptive drift; not in a real environment, but in an immersive virtual one. The advantage of the immersive VR is that it allows far more flexibility than the real environment. Within the virtual reality, the posture and limb position and orientation of the subjects may be precisely monitored, as well as the position and orientation of the virtual prosthesis, allowing the description of proprioceptive drift in a much more consistent manner.

5. EMG DRIVEN PROSTHETICS DEVICES

Single or multi-DOF prosthetic devices, controlled by simple bipolar electrodes or by complex arrays, EMG driven prosthetic devices have the architecture described in Figure 49. From the sensed EMGs, specific features are extracted which, processed by pattern recognition algorithms, are further conveyed into movement references for prosthetics. The number of simultaneously activated movement references will determine the number of prosthetic joints moving simultaneously.

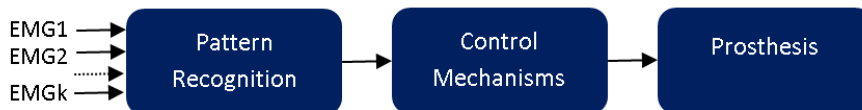


Figure 49: EMG controlled prosthetic devices - control signal flow. The recorded EMGs are input in the Pattern Recognition block, which, after processing, delivers movement references for prosthesis. Depending on the control strategies, implemented in the prosthesis, e.g. position or velocity, the movement references are converted into voltages which will drive the prosthesis' motors correspondingly.

Expressing their intention to move prosthetic devices, the amputees contract groups of muscles. The movement intention by amputees is then sensed by either a single EMG electrode or an array of them, which, converted into electrical signals, amplified and further processed by signal processing algorithms, are further conveyed into movement references for prosthetics. Further, the control blocks implementing various control strategies transform the movement references, e.g. velocity or force in movement commands for the prosthesis, e.g. voltage.

5.1. Pattern Recognition Strategies

The pattern recognition module has, at input, an amount of EMGs which, processed by signal processing algorithms, are further transformed into movement references for the prosthesis, e.g. position or force. In order to better extract the information coded by EMG and to map it with prosthesis movements, extensive work has been done. Complex pattern recognition algorithms have been developed to more efficiently extract the movement intent by amputees from the sensed EMG (Jiang et al. 2010). However, in most cases there is a compromise to be made between the quality of the EMG prosthesis control and the dimensionality. The more degrees of freedom there are to be controlled, the less controllable will be the individual joints. Dimensionality is, for this study, not primary, therefore a hand prosthesis, with open-close function was used. Classically, every movement is driven by two different EMGs, but prostheses can perform only one movement at a time. Therefore, also for the trivial case of single DOF, pattern recognition mechanisms have to be implemented to map specific input configurations with prosthesis movements. Next, the most trivial pattern recognition

mechanisms most implemented in commercial prostheses are presented: the *First Wins*, *Difference*, and *Largest Wins*.

The *First Wins* is maybe one of the oldest PR techniques: the first of two available EMGs to cross the activation threshold will gain control over a prosthesis movement while the second EMG is completely ignored. Changing the prosthesis movement first requires that both EMGs are under the activation threshold, then that one EMG becomes activated. This method has the advantage of being very robust when the EMGs are hardly discriminable, and the disadvantage of introducing a kind of dead lock when the movement changes, i.e. from open to close or vice-versa. The methodology requires a complete relaxation of both EMGs before changing the movement, this being a drawback when the amputees try to dynamically control the prosthesis requiring fast switching between movements.

The *Difference* method has much more simple rules – it is namely the difference between the two EMGs. Having no “dead lock” mechanisms, this strategy allows for a more dynamic control when switching between movements, but it is less effective when the EMGs are not highly discriminable. The control EMGs have similar magnitude and their difference will result in a very weak signal which is not optimal for the prosthesis control.

In the *Largest Wins* strategy, the largest between the two EMGs will gain control over the prosthesis. This method overcomes the disadvantages of *First Wins* and *Difference* PR strategies; it has no dead-lock and when the EMGs are close together, the resulting movement reference, after signal processing, will have a magnitude which allows for good prosthesis control. Nevertheless, when the EMGs are not highly differentiable, the fast response time of the *Largest Wins* might be a drawback. By introducing additional switching logic, e.g. filtering, the right compromises between robustness and the dynamics of response can be individually tuned.

5.2. Low-Level Prosthesis Control

The most common low-level control mode implemented by the state-of-the-art upper-limb prosthetics is the *voltage mode*. The voltage supplied to the motor driving the prosthesis will be proportional with the prosthesis control signal (EMG). Consequently, constant EMG magnitude determines the prosthesis to move with constant velocity and after contact with the target object, to grasp with constant force. The term *voltage mode* is a fitting description of the behaviour of the prosthetic devices, but its meaning is not self-explanatory. Therefore, it is very common to characterize the prosthesis performance in terms of speed, position or force. During movement, the prosthesis runs in speed mode, and during grasp in force mode. Because the speed and force are proportional with the control EMG, this behaviour is called *proportional*. Grasp force describes a static situation, while speed is a measure of change, and using the term proportional control for both, speed and force may be very confusing.

When moving their limbs, humans express their movement intent in the Cartesian space as position or grasp. Therefore, it has been considered that the term *proportional control* better characterizes the prosthesis

behaviour when the amputees directly control the position or grasp; *proportional control* expresses a direct correspondence between movement intent and prosthesis reaction, position or force. Velocity is the derivative of position, and making an analogy, it might be said that velocity describes the derivative of the movement intent by amputees. The amputees controlling a prosthesis in velocity mode contract the muscles and wait until the prosthesis is accomplishing the task. The prosthesis reaction is not directly correspondent with the movement intent expressed by amputees.

Therefore, the terms proportional and derivative were redefined for the rest of this study: proportional describes the position and force control, while derivative describes the speed and yank (force derivative) control modes. In proportional mode, the amputees have to continuously change the control signal to determine a change of the prosthesis state, while, in derivative mode, the amputees have to constantly keep the control EMG at a consistent value and wait until the task is accomplished – the control signal magnitude will set the prosthesis velocity. The proportional mode is most intuitive and physiological, but requires stable and high-resolution control signals which are hard to obtain from EMGs. In contrast, with the derivative mode, good prosthesis performance can be achieved, even when the input signals have a narrow quality. In derivative mode, when EMG is used, the amputees have only to keep the muscle contraction constant to move the prosthesis. This mode is more demanding, requiring the amputees to continuously follow the prosthesis, but is a good compromise when the quality of the control signals are poor.

6. OPEN VS. CLOSED LOOP PROSTHESIS CONTROL

The idea to close the loop through the use of tactile stimulation is not novel, and a number of studies have been performed to investigate to what extent the sensory information measured by prostheses, haptically transmitted to the amputees, might restore the natural tactile sensation and proprioception (Childress 1980; Saunders & Vijayakumar 2011). Different interfaces for sending information to the user via direct mechanical or electrocutaneous stimulation have been developed and tested. Initial studies aimed at evaluating subjective sensitivity to stimulation and the number of discernible levels that can be recognized with a certain confidence (Pylatiuk & Mounier 2004). In several early studies, the feedback interfaces were actually implemented within simple prosthetic systems leading to the first prototypes with closed-loop control. These early developments were presented as technical reports, describing technical and implementation aspects in detail, whereas the system evaluation was limited to a report of the user's subjective experience about satisfaction and performance while using the closed-loop system (Kyberd et al. 1993; Gruver n.d.). Finally, there are several more recent studies in which the feedback was actually tested in a pool of subjects in an objective, quantitative way (Chatterjee, Chaubey, Martin & N. V. Thakor 2008; Cipriani et al. 2008; Pylatiuk et al. 2006; Saunders & Vijayakumar 2011; Meek et al. 1989; Patterson & Katz 1992). Most experiments demonstrated that the feedback improved the performance in grasping tasks (Pylatiuk et al. 2006), although there were also many reports showing lack of difference with respect to no-feedback condition (Cipriani et al. 2008), or an improvement limited to certain conditions or subjects (Saunders & Vijayakumar 2011; Chatterjee, Chaubey, Martin & N. Thakor 2008).

In one approach (Cipriani et al. 2008) the grasping force feedback was transmitted by modulating the frequency of a single pager-type vibration motor. The experiments demonstrated that the artificial feedback did not improve the performance, although the subjects did consider the feedback as quite important (verbal report). In other approaches (Pylatiuk et al. 2006) the subjects operated a myoelectrically controlled hand to grasp objects of different weights placed in an opaque box. The provision of vibrotactile feedback improved subject ability to regulate the grasping force without the help of vision. Saunders and Vijayakumar (2011) implemented force feedback using a spatial coding via an array of vibrators positioned along the forearm. The feedback showed to be useful only when uncertainty was introduced in the form of random time delays in the response of the hand controller. Patterson and Katz (1992) used a force-matching task with the subjects operating a myoelectrically controlled gripper to compare several feedback modalities: vibrations (motors) and pressure (pressure cuff), with and without vision. Meek et al. (1989) also investigated the application of the modality-matched feedback by using a motor-driven pusher. Providing the feedback improved grasping task performance (i.e., lifting a heavy and brittle test object) but it did not decrease the time needed for the task accomplishment. Chatterjee et al. (2008) developed a haptic simulator comprising a myoelectric prosthesis, C2 tactor for the tactile feedback, and a personal computer for the visual feedback of grasping force. Force matching task with three different force levels (low, medium and high) was used for evaluation. The tactile

feedback improved the performance but only for the medium level of the target force and only in the group of subjects that had previous experience with myoelectric prostheses.

As described above, the utility of the artificial force feedback has been investigated in many previous studies and the conclusions were different. In the current work, we have developed a flexible experimental setup for closed-loop control of a prosthetic device with integrated augmented reality that allowed changes in the extent and type of provided visual and vibrotactile feedback. One goal of the study was to test to what extent the vibro-tactile feedback was able to substitute for visual feedback. The success of this substitution is a necessary condition for more intuitive and less demanding control of prosthetic devices. Then, the vibro-feedback was integrated into the AR setup, and a systematic investigation of the closed-loop control performance was made.

In the previous studies about closed-loop control of grasping force, the feedback was limited to the actual controlled variable: the force was measured using an integrated or externally placed sensor and this signal was transmitted to the subjects visually or through haptic stimulation. Therefore, the feedback was activated only after the hand contacted the object (force > threshold). However, the force generation is only the last step in the process of grasping. To grasp an object, the user has to close the hand, contact the object and establish a firm grip. Therefore, the force generation is ultimately connected to and depends on the flow of the steps preceding it (see below). To take this into account, the end goal of the current experiment was also to control the force, but the subjects had to perform a complete sequence (i.e., from hand fully open to reaching a desired grip strength). In addition, visual or haptic feedback was provided on the force but also on the other important variables characterizing the prosthesis operation (e.g., contact and velocity of closing). As will be shown later, this holistic approach to the control of grasping and force indeed provided some important and novel insights.

6.1. Experimental Setup

The setup contained the following components Figure 50: 1) a Sensor HandTM Speed (Otto Bock Healthcare Products GmbH, Vienna, AT) equipped with a conventional Otto Bock myoelectric interface (Myobock system), 2) a dynamometer with 3 cm distant grip handles, and an output voltage proportional to the applied force, 3) a haptic feedback system comprising a custom-made vibro-tactile stimulation device and a control unit, and 4) an augmented reality system including a digital camcorder (Sony HandyCam CX-150) and a virtual reality headset (EVG920V, VRD-Glasses, DE).



Figure 50: The experimental setup for the study of prosthesis closed loop control: a) sensor hand speed and the dynamometer, b) the myoelectric interface to the prosthesis, and c) the complete setup including the haptic device and the video system.

The Sensor HandTM Speed is a commercially available hand prosthesis with open/close function, controlled by two dry bipolar EMG electrodes (OB 13E200=50, Otto Bock Healthcare Products GmbH, Vienna, AT). The electrodes were placed on antagonistic muscles of the forearm, as depicted in Figure 50b, and used to capture the movement intent of the subjects. The signal provided by the electrode placed on the volar side of the forearm (over flexor muscles) proportionally controlled the speed of the prosthesis during closing and increased the grasping force, while the electrode on the dorsal side of the forearm (over extensor muscles) controlled the prosthesis speed during opening and decreased the grasping force. To minimize the indirect feedback from the prosthesis to the subject (e.g., motor sound, vibrations), the prosthesis and the subjects were “detached”. The prosthesis was mounted on a table, Figure 50a and Figure 50b, while the subject was seated next to it, with the cables being the only physical connection between the two. In addition, a white noise was played through the headset blocking any sound feedback from the prosthesis.

The grip handle was used as the target object for grasping and at the same time as a sensor element measuring the generated grasping force. It was positioned on the table between the thumb and index finger of the prosthesis so that when the prosthesis was closed, it grasped the handle. Importantly, the handle was concealed under a black cover, and thereby made invisible to the subjects.

The haptic feedback system used to induce vibro-tactile stimuli was a custom made device (Ninu 2010), (Ninu et al. 2013) able to generate vibratory patterns more complex than those produced by the common vibration motors with eccentric weight. Namely, it allowed independent modulation of the frequency and amplitude of vibrations by modulating the voltage input into a small brushless DC motor (Maxon 32W). This was used to feed the prosthesis parameters (velocity of opening/closing, contact with the target, grasping force) back to the user by using distinct and discriminable vibro-patterns, as explained below. The mapping between prosthesis state and haptic stimulation was done by the control unit of the haptic device which acquired the sensory data from the prosthesis through an RS232 serial connection and converted it into mechanical vibro-tactile stimulation. The vibro-tactile stimulator was integrated into a brace and tightened around the subject’s forearm just proximal to the elbow (see Figure 50c), so that the device pressed against the skin with a force of approximately 20 N.

The camera was mounted on a tripod, which was placed onto the table so that the camera was looking almost vertically into the prosthesis and the gripper, with the black cover as the background [Figure 50c]. Video stream acquired by the camera was fed into the host PC where it was processed using the Eyes Web Image Processing Library (Camurri et al. 2000). The processed video was sent to the virtual reality glasses worn by the user. This setup allowed for manipulation of the visual feedback provided to the user by masking certain elements of the scene (e.g., the prosthetic hand) and/or by introducing virtual objects into the scene (augmented reality).

6.2. Experimental Task

At the beginning of each trial, the prosthesis was fully open. The task was to cyclically close the prosthesis, grasp the grip handle, generate a grasping force within a predefined force window and then open the hand. In the case of low target force, the target force window was set between 5 and 15 N and from 30 to 40 N for the high force target. The maximum force that the prosthesis could produce was 50 N. In order to provide comparable outcomes, all grasps started from the same position (hand completely open). When the grasps were performed blindly (see Experimental protocol) there was no guarantee that the full open position of the hand was reached. Therefore, the gain for the hand opening was set to a high value, so that very low extensor activation resulted in a fast opening of the hand to the full extent.

In order to emulate the way grasping is performed by the prosthesis users in real life, the subjects were instructed to execute the task in one attempt, i.e., by generating a single continuous contraction: they were supposed to activate the flexor muscles, close the hand, build up the force and then, when they assumed that the desired force level has been reached, activate the extensors and open the hand. In other words, the subjects were instructed to refrain from “servoing” the force using fine control, i.e. oscillating around the target value until the correct level was achieved.

6.2.1. FULL VISUAL FEEDBACK

Figure 51 depicts the execution of the grasping task for the high target force and with the full extent of the visual feedback. The subjects could see the prosthetic hand, the desired force window (red rectangle), the measured grasping force (white bar), and the virtual object (yellow circle) that was the target for grasping. In addition, a counter was informing the subjects in real time about the progress of the task in deci-seconds. The yellow circle had the same diameter as the grip handle which was positioned directly beneath, concealed from the subject by a black cover. The borders of the virtual object coincided with the borders of the grip handle. Therefore, for the subjects, it looked like they were grasping the virtual object, while in fact the hand was closing around the grip handle.

At the beginning of each trial Figure 51a, the prosthesis was completely open, and consequently the grasp force was zero, i.e., the thin white line represents the baseline for the measured force. When the prosthesis closed, and the measured force reached the target (i.e., the white bar was within the red square, [Figure 51b]), the grasped virtual object (yellow circle) disappeared. If the force measured by the grip handle exceeded the

borders of the target force window [Figure 51c], the task was considered unsuccessful, and the presence of the yellow disc indicated this to the subjects. As explained above, if the subject activated the extensor muscles in an attempt to reduce the excessive force in Figure 51c, it would not work since it would trigger a fast hand opening due to the high gain set for the EMG signals from the extensor muscles.

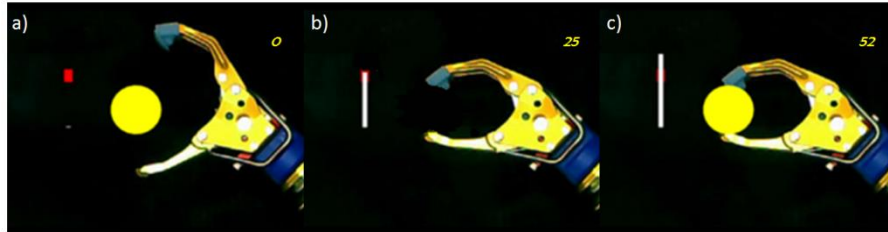


Figure 51: The execution of the grasping task for the high target force with full visual feedback. a) initially, the prosthesis was open and the measured force was zero, b) the prosthesis closed, the exerted force was within the target range, and the yellow target disappeared (successful trial), and c) the prosthesis closed, but the exerted force was outside the desired range, and the yellow target did not disappear (unsuccessful trial).

6.2.2. FULL HAPTIC FEEDBACK

Full extent haptic feedback was provided by delivering discriminable patterns of vibrations encoding the velocity during prosthesis opening/closing, first contact with the target object and current grasping force. To provide feedback on the velocity, the intensity coding was used: the vibration amplitude was proportional to the prosthesis velocity, while the frequency was constant. However, to differentiate between the hand closing and opening, two different frequencies were used (90 Hz and 45 Hz). Grasping force was coded by simultaneously modulating the amplitude and frequency of vibrations proportionally to the amplitude of the measured force. In both cases, the mapping was linear, i.e., the whole range of forces/velocities that could be generated by the hand was linearly mapped to the whole range of amplitudes/frequencies that could be produced by the stimulator. First contact was conveyed to the subject in the form of a tactile icon, i.e., by delivering a short vibro pattern eliciting a sensation of “bumping”. An example of the vibro-tactile pattern generated during a grasping trial is given in Figure 52. The vibrotactile pattern was recorded by a microphone while the stimulator was placed on an elastic membrane which converted the vibration into hearable sound.

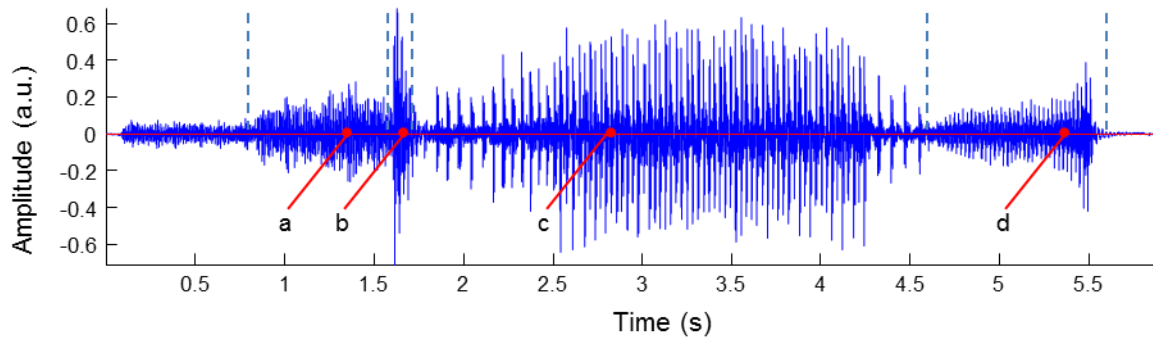


Figure 52: An example of a vibro-tactile pattern. The four segments represent the feedback about: a) hand closing, b) first contact, c) increasing and decreasing grasping force, and d) hand opening.

6.2.3. SUBJECTS

Thirteen subjects volunteered for the experiment (age: 30 ± 7 yrs): four of them were transradial amputees and the rest able-bodied. The subjects had not suffered from any accidents or pathology that could affect sensory sensibility, visual acuity or muscular activity of the forearm. The study was approved by the local ethics committee and the subjects signed an informed consent form before participation.

6.3. Experimental Protocol







During the experimental session, the subject had to perform high- and low-force grasping tasks under several feedback conditions. In each condition, the subject had to grasp the target object repeatedly for 60 s. Seven conditions were tested, in which visual feedback (VIS) was gradually reduced and then replaced by haptic feedback (HAP) (see Table 1). The conditions are listed in the following, with the provided feedback modalities given in parentheses and the code name indicating the type of feedback (VIS and HAP) together with the letters for the active feedback modalities: VIS-FHS (force, hand, success indicator), VIS-HS (hand, success indicator), VIS-S (success indicator), BLIND (no feedback), HAP-VFC (velocity, force, contact), HAP-FC (force, contact), HAP-VC (velocity, contact).

VIS-FHS was the condition with the full visual feedback used as the benchmark for all the other conditions. The second condition (VIS-HS) resembled actual real-life application: since the commercial systems do not provide any direct feedback, the user sees the prosthesis and thereby has the visual feedback about its aperture and velocity, but does not have direct information about the force during grasping. However, he/she is able to estimate if the grasp is successful or not, which was emulated in this condition by the success indicator. In VIS-FHS and VIS-HS the subject could see the hand during the task, and he/she was therefore able to assess the current position (aperture), velocity of closing/opening as well as the contact with the target object. However, since the grip handle was stiff, it was not deformed by the applied force. Therefore, information about the current grasp force was not available. In VIS-S, the hand was also masked out, and the subject could see only the success indicator. Finally in the BLIND condition, a black screen was projected onto the video glasses. This

gradual degradation of the feedback, from VIS-FHS to BLIND, aimed at evaluating the performance when the subjects were deprived of external feedback and were therefore forced to rely more and more on the proprioceptive and kinesthetic feedback arising from their own muscle contractions.

In the subsequent tests, the visual feedback was replaced by the haptic feedback. The extent of feedback was modulated: from a single variable, velocity (HAP-VC) or force (HAP-FC), and contact information to a comprehensive haptic feedback including velocity, contact and force together (HAP-VCF). Simultaneously providing visual and haptic feedback would be closer to a real-life application. However, the two kinds of feedback were provided separately in order to clearly identify the extent to which the haptic stimulation was able to replace the visual feedback. While the visual tasks were performed in a predefined order, from full visual feedback to no feedback, the three conditions involving haptic feedback were performed in a random order. All mentioned conditions are summarized in Table 1.

Table 1: Seven conditions have been tested in which visual feedback was gradually reduced and then progressively replaced by haptic feedback

| | | VIS-FHS | VIS-HS | VIS-S | BLIND | HAP-VC | HAP-VCF | HAP-CF |
|------------------------|---|---|---|---|-------|----------|----------|---------|
| Visual Feedback | F |  | | | | | | |
| | H |  |  | | | | | |
| | S |  |  |  | | | | |
| Haptic Feedback | V | | | | | Velocity | Velocity | |
| | C | | | | | Contact | Contact | Contact |
| | F | | | | | | Force | Force |

Notation: VIS and HAP stand for visual and haptic feedback; the letter H denotes that the hand was visible to the subject and the letters V, C, F and S denote the visual/haptic feedback on the velocity, contact, force and successful accomplishment, respectively.

At the beginning of the experimental session, the subjects practiced the experimental task until they got accustomed to it. The practice time varied among individuals and lasted between 20 and 30 min. In addition, before performing the tests in each condition, the subjects were provided with a short training (10-15 min). In the conditions with the haptic feedback, the training at the beginning included both visual and haptic stimulation so that the subjects could learn to “understand” the vibro-tactile information coding. The total duration of the experimental session was approximately 3 hours.

6.4. Approaches to Data Analysis

To evaluate the performance, three outcome measures were used: the success rate in the task accomplishment, the dispersion (spread) of the generated forces, and the time to accomplish the task. The task was deemed successful if the subject during grasping generated a force within the predefined window (see Experimental task). Success rate is a discrete measure of performance (task succeeded/failed) evaluating the accuracy in generating desired force levels. The dispersion of the generated forces is a continuous variable which assesses the consistency in performing the task over multiple trials (i.e., all trials within a certain feedback condition). The time to accomplish was measured between the instant when the user started closing the prosthesis until the instant in which the user gave the command for the prosthesis to open. Before data processing, we excluded the outliers for each subject (< 5% per subject). The outlier was defined as the value that was higher than $Q75 + 1.5 * (Q75 - Q25)$, where Q75 and Q25 are 75th and 25th percentile for the corresponding performance measure, respectively.

A two-way mixed model ANOVA with the subject group (able bodied, amputees) as a between subjects factor, and force level (high/low) and feedback condition as within subjects factors were applied to compare the performance measures. Statistical significance was set to $p < 0.05$. The Student Newman-Keuls test was used for the post hoc pairwise comparisons. To test if there was a statistically significant difference in the force dispersions among the feedback conditions, we used the Bartlett multiple-sample test followed by the Ansari-Bradley test with Bonferroni correction for multiple comparisons.

6.5. Results

Success rate depended on the interaction between the force level and the feedback condition ($p < 0.001$). Three- and two-way interactions including subject group as one of the factors (group*force level*condition, group*force level and group*condition) as well as the group main effect were not significantly different. Therefore, the data from the two groups were pooled together. The average performance is reported as mean \pm standard deviation.

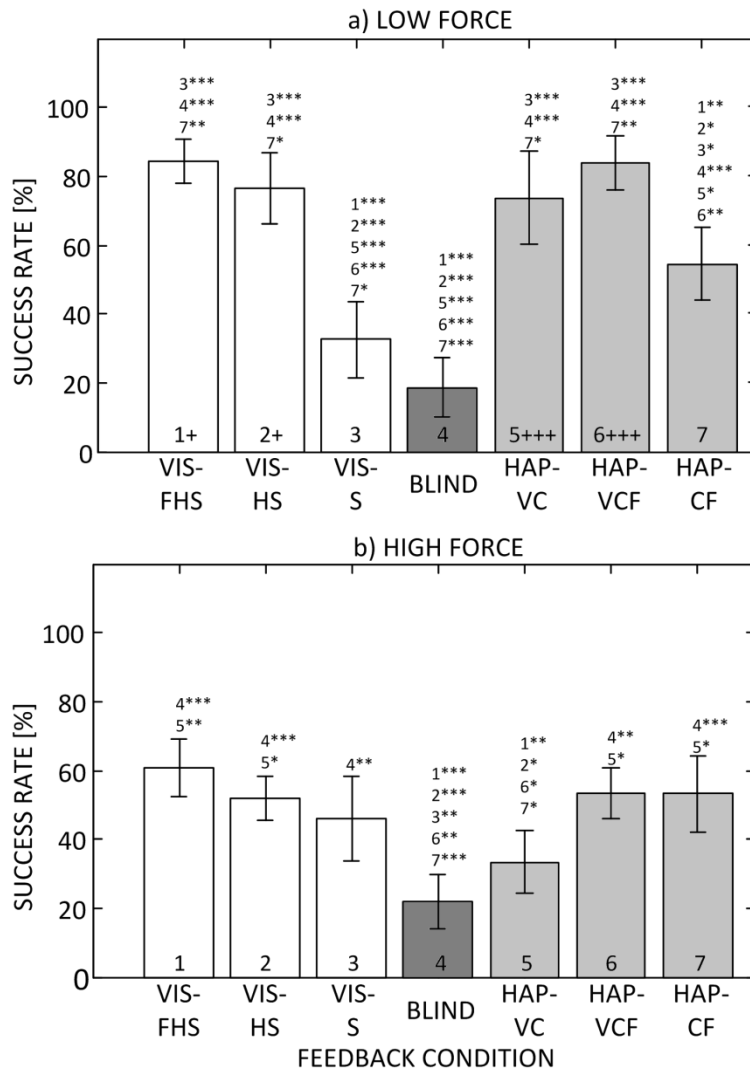


Figure 53: Mean (\pm standard deviation) of the success rate in the task accomplishment for the 7 feedback conditions in the low (a) and high force tasks (b).

Average success rates for the two force levels and seven feedback conditions across subjects ($n=13$) are presented in Figure 53. In general, grasping with the high force was more difficult for the subjects. The success rates for the low versus high force grasping were significantly higher in the two visual (VIS-FHS, $84\pm 13\%$ vs. $60\pm 17\%$ and VIS-HS, $76\pm 20\%$ vs. $51\pm 12\%$) as well as two haptic conditions (HAP-VC, $73\pm 21\%$ vs. $33\pm 18\%$ and HAP-VCF, $84\pm 15\%$ vs. $53\pm 14\%$). The performance between the conditions with the visual feedback exhibited a similar trend for both high and low forces. Namely, there was a drop in the average performance as less and less feedback was provided: from $84\pm 13\%$ to $18\pm 17\%$, and from $60\pm 17\%$ to $21\pm 15\%$ for the VIS-FHS and the BLIND conditions in the low and high force tasks, respectively. Interestingly, there was no significant difference in success rates between the benchmark condition (VIS-FHS) and VIS-HS. Therefore, with or without visual feedback about the grasping force, the subjects achieved similar precision of grasping as long as they could see the hand and the success indicator, indicating that explicit visual feedback about the grasping force was not truly essential for the task accomplishment. This is a surprising result since the actual task at hand was to

control the force. For the low force grasping, seeing the hand was a necessary condition to maintain the success rate comparable to the benchmark (VIS-FHS). When only the success indicator was provided, the performance dropped significantly with respect to the full feedback (i.e., $32\pm 21\%$ for VIS-S vs. $84\pm 13\%$ for VIS-FHS) and was not significantly different from the BLIND condition ($18\pm 17\%$). However, this was not the case for the high force grasping; the success rate in VIS-S ($46\pm 24\%$) was significantly better compared to BLIND ($21\pm 15\%$) and not significantly different from VIS-FHS ($60\pm 17\%$) and VIS-HS ($51\pm 12\%$). Therefore, the sole feedback about the task accomplishment was enough to maintain the performance at a level close to the benchmark (VIS-FHS).

Contrary to visual feedback, the overall pattern of performance for the haptic feedback conditions was different between the low and high force tasks. During the low force grasping, all three conditions recovered the performance with respect to minimal feedback and no feedback; the success rates were significantly better than in VIS-S and BLIND. Full haptic feedback resulted in the highest average success rate, similar to that of the full visual feedback condition ($84\pm 15\%$ for HAP-VCF vs. $84\pm 13\%$ for VIS-FHS). Again surprisingly, the performance with the feedback on velocity was significantly better than the performance with the force feedback ($73\pm 27\%$ in HAP-VC vs. $54\pm 20\%$ HAP-CF). In addition, there were no statistically significant differences between HAP-VC and full visual (VIS-FHS) and haptic feedback (HAP-VCF), while all conditions except VIS-S and BLIND were significantly better than HAP-CF. Therefore, a direct force feedback was less effective than the feedback on velocity in the force control task with the haptic stimulation.

For the high force task, the results were opposite. The velocity feedback resulted in poor performance (HAP-VC, $33\pm 18\%$), not significantly different from no feedback (BLIND, $21\pm 15\%$). The performance in all conditions except VIS-S and BLIND was significantly better than in HAP-VC. Feedback on force, on the other hand, resulted in performance similar to that of the full haptic feedback ($53\pm 22\%$ in HAP-CF vs. $53\pm 14\%$ in HAP-VCF). There were no statistically significant differences between these two haptic conditions (HAP-CF and HAP-VCF) and the three visual feedback conditions with similar success rate (VIS-FHS, VIS-HS, and VIS-S). Therefore, in the case of a high force target, direct force feedback was more effective than the feedback on velocity. In fact, providing the velocity information in addition to the force (HAP-CF vs. HAP-VCF) did not improve the results.

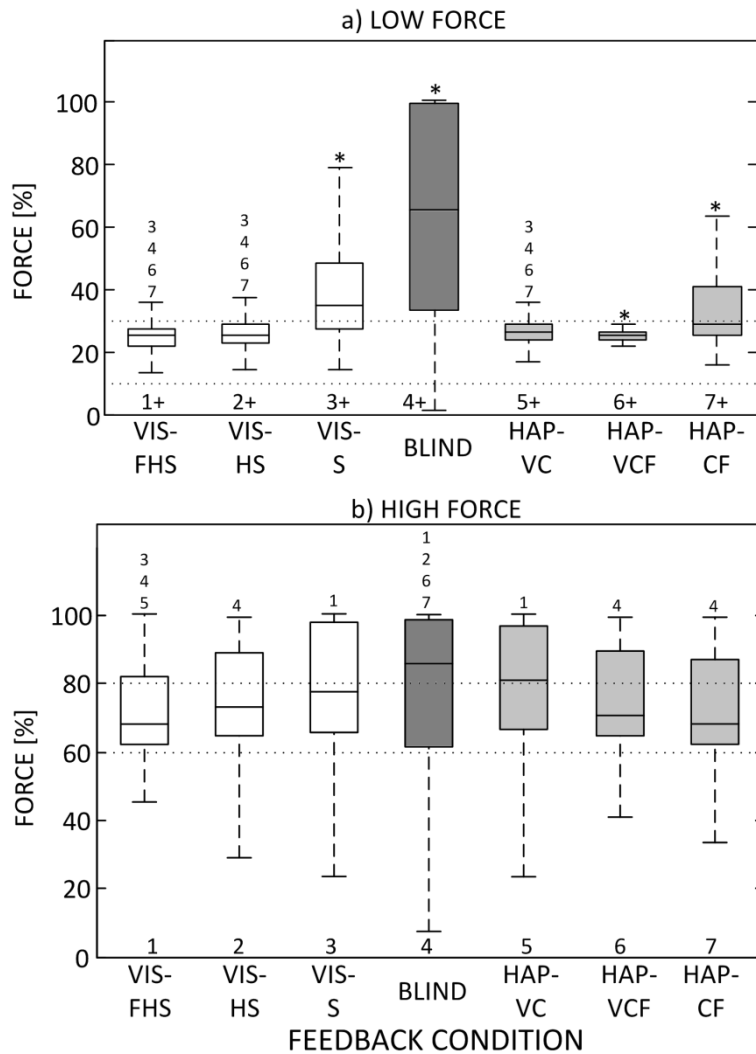


Figure 54: Distribution of the generated forces (normalized with respect to the maximal prosthetic hand force) in the 7 feedback conditions in the low (a) and high force tasks (b).

The second outcome measure (force dispersion) confirmed the main conclusions from the analysis of the success rates. Figure 54 depicts a dispersion of the forces generated in each trial in different feedback conditions. In the text, this outcome measure was reported as the interquartile range IQR, defined as $IQR = Q75 - Q25$, where $Q75$ and $Q25$ are the 75th and 25th percentile of the data set. In every condition apart from the BLIND, the force variability was significantly higher ($p < 0.001$) during the high force grasping, meaning that the subjects were less consistent across the trials when they had to reach a higher level of force.

During the low force grasping, for the visual feedback conditions, the trend was analogous to that observed for the success rate, i.e., the dispersion was similar for the two conditions with feedback on the prosthetic hand (6.0% for both VIS-FHS and VIS-HS) and significantly increased (i.e., performance dropped) when the hand was removed from the scene (21.0% and 66.0% for VIS-S and BLIND). Although there was no significant difference in success rates between VIS-S and BLIND, the force variability was significantly lower in the former. Any form

of feedback resulted in significantly less force variability compared to the BLIND condition. The full haptic feedback (HAP-VCF) was characterized by the most consistent overall performance (2.4%). The force dispersion in the HAP-VC condition (4.8%) was similar to that of VIS-FHS (6.0%) and VIS-HS (6.0%), whereas in HAP-CF it was higher than in the benchmark condition (VIS-FHS) as well as in VIS-HS. HAP-VC resulted in significantly lower force dispersion compared to VIS-S (21.0%), BLIND (66.0%) and HAP-CF (15.6%).

During the high force grasping, the differences between the conditions were not so clearly expressed. Only the conditions VIS-S (24.0%), BLIND (37.2%) and HAP-VC (30.0%) demonstrated a significantly higher dispersion (lower consistency) when compared to the benchmark (19.8% in VIS-FHS), although VIS-S and VIS-FHS were not significantly different with respect to success rates. When comparing HAP-VC to HAP-VCF (24.6%) and HAP-CF (24.1%), the variability in HAP-VC was higher, but the difference was not statistically significant. However, contrary to HAP-VC, the consistency in the HAP-VCF and HAP-CF conditions was similar to that of the benchmark (VIS-FHS). In addition, the force variability in HAP-VCF and HAP-CF was significantly lower than in BLIND, whereas there was no significant difference between HAP-VC and BLIND.

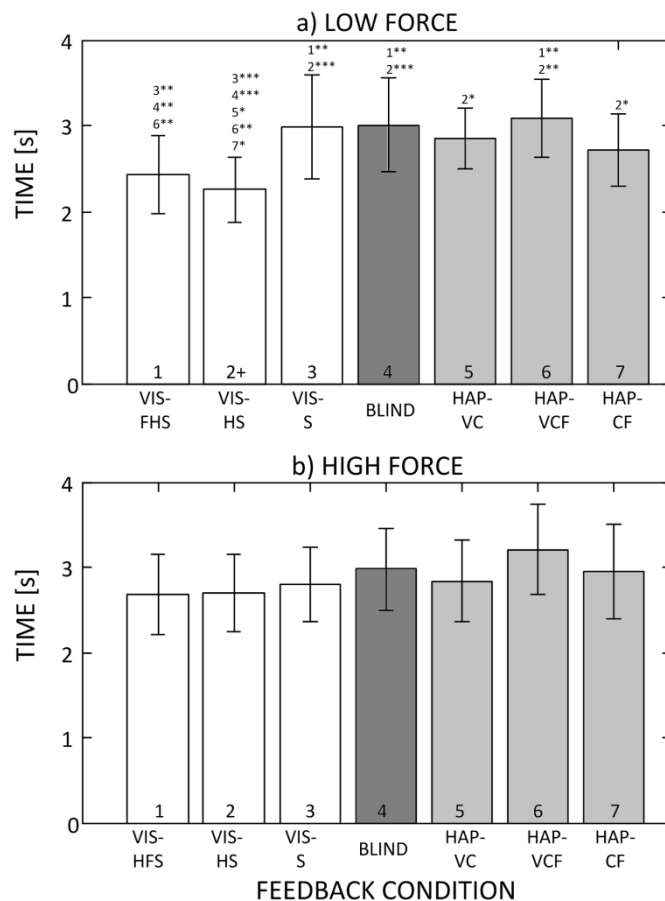


Figure 55: Mean \pm standard deviation for the time to complete the task in the seven different feedback conditions in the low (a) and high (b) force tasks.

For the time to accomplish the task [Figure 55], a two-way interaction between the condition and force level ($p < 0.05$) and a main effect of condition ($p < 0.01$) were statistically significant. The interactions with the group factor and group main effect were non-significant. For the low force grasping, less time was required when visual feedback of the prosthetic hand was provided (2.4 ± 0.9 s in VIS-FHS and 2.3 ± 0.8 s in VIS-HS) compared to full haptic feedback (3.1 ± 0.9 s in HAP-VCF); visual feedback limited to the success indicator (3.0 ± 1.2 s in VIS-S) as well as no feedback (3.0 ± 1.1 s in BLIND) conditions. No statistically significant differences were registered between the conditions during the high force grasping. The time-to-complete was similar for the high (2.9 s) and low (2.8 s) force tasks; VIS-HS was the only condition in which the performance was significantly different between the target force levels (2.3 ± 0.8 s for low vs. 2.7 ± 0.8 s for high).

It is worth noting that the three outcome measures were not significantly different between amputees and normally limbed subjects, indicating that the obtained results apply to the prospective prosthesis users. However, the number of amputee subjects was limited - four, which may have influenced the outcome of the statistical analysis.

6.6. Discussion

During this study the prosthesis control loop of a hand prosthesis was closed by providing feedback to an amputee/able-bodied population. Visual and vibro-tactile feedback was implemented, and their direct comparison indicated to what extent vibro-tactile feedback is able to substitute the visual feedback. In a previous work (Ninu et al. 2013), the capacity of a novel technology to generate vibro-tactile stimuli was evaluated. Implemented by the current set-up, the capacity of this stimulation technology in communicating sensory information measured by prosthesis to the user was also addressed.

However, the major goal of the study was to assess to what extent the users, provided with haptic feedback, are able to improve performance when controlling prosthetics devices. The setup integrated an augmented reality system and a custom made vibro-tactile stimulation device, thereby allowing full control over the extent and type of feedback information provided to the subject. We utilized the setup to experimentally investigate the influence of different feedback conditions on the control of force during grasping. Full visual feedback was presented to the subject and gradually reduced to absence of feedback, and then haptic feedback was introduced as a replacement for the missing visual information.

An important and optimistic outcome is that the subjects performed with the full haptic feedback (HAP-VCF) similarly to the full visual feedback (VIS-FHS) during both low and high force grasping. Moreover, any haptic feedback was significantly better than absence of feedback (BLIND), and in some cases even partial feedback was enough to ensure no difference with respect to the visual condition. This is a strong indication that the implemented methodology to generate vibro-tactile stimuli, different from the conventional ones, is able to faithfully convey the sensory information measured by prosthesis into a sensory experience perceived by humans. The stimulation technology proved its feasibility, allowing the transfer of the cognitive load from the

visual to the cutaneous tactile sense. Consequently it has been supposed that the prosthesis users would be able to distribute the attention and accomplish parallel tasks, facilitating a more intuitive and effective use of the prosthesis.

As various studies indicated (Pylatiuk et al. 2006; Meek et al. 1989) providing the users with force feedback will allow for better regulation of the grip force. In order to reproduce this scenario, the grip force was measured and further transmitted to the subjects as a vibro-tactile pattern (HAP-CF). This study reproduced, to an extent, these outcomes; when the target was high, the vibro-tactile feedback about grip force allowed for performance similar with the VIS-FHS and VIS-HS (visual feedback). Vibro-tactile feedback is able to substitute for vision which is very accurate and might be considered as reference. Nevertheless, the 50% success rate was not satisfactory, which was mainly determined by the poor prosthesis controllability. Controlling a commercially available hand prosthesis using the simplest myoelectric control interface (two channels) was not a trivial task for the subjects. Even when the full visual feedback was provided (hand visible, success indicator, and force bar), there were occasional outliers, i.e., after a few successful trials the subjects would suddenly generate a force very different from the target level (see methods). The average success rate for VIS-FHS was about 85% and 60% in the low and high force tasks respectively, and in the latter the forces became quite variable (i.e., in the range 45 - 100% of the prosthesis maximum force).

This outcome is an indication that providing feedback and closing the prosthesis control loop cannot compensate for poor prosthesis controllability; therefore, the controllability of the prosthesis was considered to have the highest impact allowing for improvement of prosthesis performance.

In comparison with the high force target, the low force condition was even less effective. The success rate in HAP-CF condition was about 50%, much lower than the ~80% obtained in both VIS-FHS and VIS-HS, considered as reference. While during the high target condition, the subjects had enough time to evaluate the perceived feedback to tune the muscle contraction in order to accomplish the goal, during the low force target condition, the feedback came too late, and the subjects were not able to efficiently react to the perceived feedback. Better results were, however, obtained, when feedback about prosthesis velocity was provided to the subjects. Velocity feedback allowed for a more substantial improvement of grasping than force feedback which is a cue that grip force is indirectly estimated from velocity.

Another indication that the subjects controlled the grasp mainly relying on velocity (predictive control) was the drop in performance when the transition VIS-HS (with hand feedback) to VIS-S (without hand feedback) was made. These outcomes were complemented by the verbal feedback from the subject who reported a large increase in the task difficulty. The same conclusion is shown by the similarity between VIS-FHS and VIS-HS; with or without direct feedback about grip force, the outcomes were comparable.

This result may appear counterintuitive, but it can be explained by considering the principle of operation of the commercially available hand prostheses. The considered EMG controlled prosthesis is driven by a regular DC motor and the EMG is directly controlling the voltage of the prosthesis. Motors are electro-mechanical systems

which convert the electrical energy into mechanical energy. If the motor is freely rotating (minimal and constant resistance), the electrical energy is mostly transformed into movement. Otherwise, if the motor stalls, the electrical energy is transformed in mechanical torque. Consequently, during the “free” movement, the same EMG signal sets the prosthesis velocity and, after contact with the object, the grasping force. Effectively, this means that the force may be predicted from the hand velocity just before closing, i.e., the faster the prosthesis closes, the stronger the subsequent grasp. Therefore, although in the VIS-HS condition information on the exerted force was not provided directly, it could be estimated from the prosthesis movement and used for predictive control. Namely, the grasp was prepared by adjusting the proper velocity of closing, and this was “automatically” converted into proper force once the object was grasped. This “automatic” conversion from velocity to grip force holds only under ideal conditions. Real driving systems, motors and gearboxes, are characterized by different and inconsistent static and dynamic friction. This will determine inconsistencies when converting the electrical energy into grasp force. Due to variable friction, the same applied voltage (control EMG) will result in different grasp forces; the supplied electrical energy is also used to overcome the variable friction. This variability will be more emphasized when the forces are large and the prosthesis will have a behavior closer to the ideal one when the forces are low.

Contrary to popular opinion, it seems that the commercially available prosthetic systems do provide indirect information about the grasp strength and that grasping is therefore not completely blind as is usually assumed. This holds if the grasping task is performed at once, using one steady contraction of the muscles, minimizing additional corrections. This corresponds to the way a prosthesis is used in real life by amputees, and so was employed in this study. However, the subjects have no direct information about the strength of the grasp, so they should be able to blindly regulate the grasp force while holding a stiff object, i.e., by relying only on the proprioceptive and kinesthetic information from his/her own muscles. As demonstrated by the BLIND condition, controlling the prosthesis based on the proprioceptive and kinesthetic feedback from the muscle contraction only is almost unattainable. The uncertainty due to the inherently noisy myoelectric interface and prosthesis dynamics was simply too high to be able to consistently control grasp force without any feedback regarding the prosthesis state. The provision of a success indicator was intended to allow for performance improvement; an unsuccessful grasp was an indication that the muscle contraction should be made differently to hit the target. If the prosthesis is faithfully replicating the movement intent of the subjects, the VIS-S condition (only success indicator) should allow for a continuous improvement in performance, as it is a matter of learning. When the subjects feel confident controlling the prosthesis, the VIS-S and the VIS-FHS outcomes should be comparable; after learning a movement, the feed-forward control of the hand is dominant compared with the feedback control. It was, however, not the case, which emphasizes the lack of consistency in following the subjects movement intent by prosthesis as the main limitation of the SOA prosthetic devices and not necessarily the lack of feedback.

Voluntarily moving the natural limbs is the results of a cognitive process. The movement toward a target is performed in sequential steps and, at every step, commands are generated based on the perceived feedback

determined by the precedent movement – feedback control. Performing an unknown movement is time consuming and tedious; however, with experience, an optimization process will eliminate the redundant sensory-motor connections, and automatism will develop. The movements will become faster, more precise, requiring, at the same time, less cognitive effort. Feedback control continuously compares the desired hand position with the sensed position, and the difference adjusts the motor output. On the other hand the feed-forward control aims to cancel all perturbations in advance and generate faster motor programs. The movement is performed before the sensory system is able to provide any information. Feed-forward control is mainly based on experience, and on the human ability to predict and compensate for environmental perturbations.

We aim to reproduce these mechanisms of movement by using EMG controlled prosthetic devices. Therefore the control loop of the prosthesis was closed by providing feedback to the subjects; force feedback was intended to improve force control. The results indicated that force feedback was, to some extent, effective, but only for the high target condition (HAP-CF). For the low target, which actually reproduces the most common grasp scenario during daily tasks, the subjects were not able to be fast enough, to react to the perceived force feedback. Therefore the grasp force mostly exceeded the upper target's borders. For the control of the low level of force, the predictive control proved to be more effective. This is implemented by the SOA hand prosthesis; the grasp force was predicted from the prosthesis velocity just before grasping, which should allow for faster and less demanding prosthesis control. This predictive control strategy compensates for the lack of force feedback when grasping with low forces, but the time-to-complete of a grasp was still large (~2,5 s).

For low, as well as for high force target condition, the time to complete was similar. This indicated that the prosthesis spent most of the time for movement, and minimal time for grasp. A predictive control should allow for a less demanding and more precise grasp. However, due to the slow prosthesis movement, preceding the grasp, the potential of the predictive strategy is not entirely exploited. This emphasizes the importance of the reliable command interface; essentially, the precision and stability of the control pathway places an upper bound on the utility of the feedback and closed-loop control. If the user is not able to grasp objects in a consistent and precise manner even when he/she is assisted by the full visual feedback (high fidelity information), providing haptic stimulation will not compensate for the poor prosthesis controllability, but likely make grasping even more tedious, time consuming and frustrating.

7. AN IMMERSIVE VIRTUAL REALITY ENVIRONMENT

Fitting an amputee with an EMG-controlled prosthesis is not always a straightforward procedure. Between muscle contraction and prosthesis movement, there is a chain of uncertainties generated by the poor interface of biological with technological entities, e.g. EMG recording, socket, and stump condition. The lack of consistency during prosthesis control is a serious challenge, especially for inexperienced amputees, but it is very common during regular fittings. With training, the amputees learn to find ways to contract their muscles and to get a much more consistent reaction from the prosthesis, in accordance with their expressed movement intent. This training, at least in the incipient phase of a fitting, may be very burdensome because of the very high failure risk. The amputees have to grasp and manipulate various objects, but real objects may break or fall. In the presence of observers, an unsuccessful grasp may be even more frustrating. High risk of failure is a serious drawback of the classical training strategies, slowing or even threatening the rehabilitation process.

In order to allow the amputees to fine-tune their abilities in a risk-free environment, isolated from disturbing factors, and to encourage them to follow training sequences with a progressive degree of difficulty, an immersive virtual training environment was created. The developed software package was based on an off-the-shelf game engine Unity3D and used the framework developed at TU Vienna, AT – Interactive Media System Group (Mossel et al. 2012).

A transradial Michelangelo Hand (OttoBock, Austria) was modeled, entirely reproducing the kinematics of the real prosthesis: the prosthesis has one pinch-grip (all fingers closed together) and one lateral-grip (the thumb closes over the side part of the index finger), can pronate and supinate, flex and extend the wrist joint.

Using information provided by a video tracking system, the virtual prosthesis is virtually attached to the amputee's stump. The tracking system consists of a set of markers placed on the subject's forearm and head, a series of infrared video cameras placed at the borders of the tracking system, and a processing unit. The video cameras observe the scene, and the processing unit determines the coordinates of the head and stump in the real space. This information is further used to interface the amputee with elements of the virtual reality. The hand coordinates are used to fit the virtual prosthesis with the real stump, and the head coordinates define the viewpoint from which the amputees will see the virtual scene in the video glasses.

This set-up allows for a natural immersion of the subjects in the virtual reality. The subjects are able to move within the tracking area, to move their arm or head, and the processing unit continually updates all these correspondences. The resulting virtual scene is seen in video glasses by the amputees, who become deeply immersed in the virtual environment.

The virtual prosthesis is controlled similarly to the real one: two antagonist electrodes placed on the stump will sense the muscle contractions of the forearm and the resulting signals, after processing, will control the open/close function of the prosthesis.

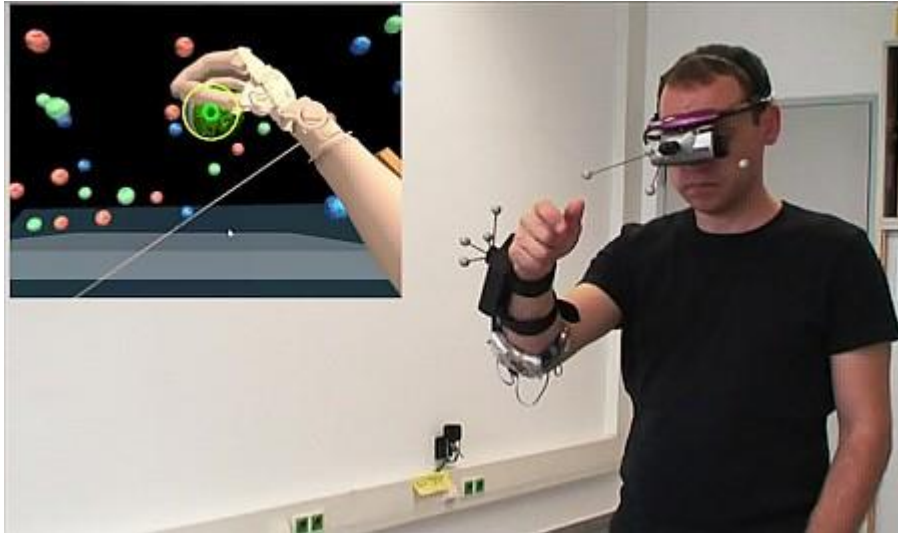


Figure 56: The immersive virtual reality setup consisting of markers attached on the head and forearm of the subjects, video-glasses and control-brace. An example of the virtual scene, visible in the vide glasses, is depicted in the upper-left corner, and comprises virtual target objects and the virtual prosthesis.

An example of the set-up is shown in Figure 56. The virtual prosthesis visible in the left corner of the picture is virtually attached to the subject's forearm. The marker indicating the position and the orientation of the forearm in space is superposed with a coordinate frame, attached to the virtual prosthesis. The result is a perfect synchronization of the arm and the body with the virtual prosthesis and the observed virtual scene.

7.1. Markers

A marker comprises four identical spheres, has a retro-reflecting surface, and is connected to a base by levers of different lengths [Figure 57]. The orientation and the distance of the four spheres, relative to the base, has a unique configuration which makes possible the identification of one particular marker among the many others present in the virtual environment.

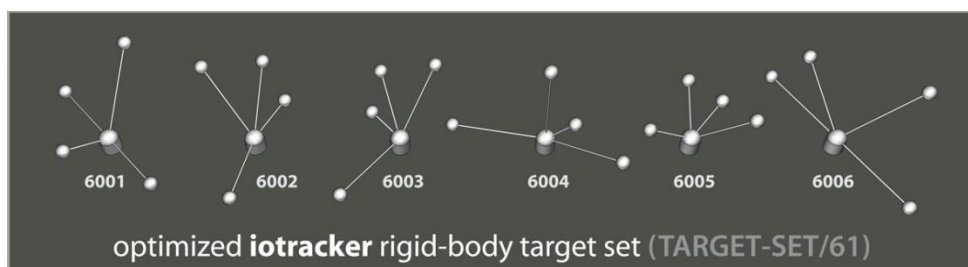


Figure 57: Rigid body target set used within VR environment to identify the position and orientation of the head and forearm (Pintaric & Kaufmann 2008).

One of the four spheres of a marker is somewhat redundant, as three such spheres allow for the full characterization of the marker's coordinates, but necessary in order to deal with uncertainties when the markers overlap or when noisy reflections disturb their detection (Pintaric & Kaufmann 2008).

7.2. Infrared Camera

The sensing element of the system is an infrared camera with an integrated infrared spotlight. This generates synchronized infrared flashes, which are reflected by the markers and appear on the image acquired by the video cameras [Figure 58]. The image acquired by each camera has a black background and is strewn with small white circles which indicate the spheres of the markers. The configuration of every marker is determined during a pre-calibration phase, and the tracking system updates the position of the observed white circles in real time. The images acquired by the cameras contain the spheres of all observed markers from different viewpoints. This information is centralized on a computational unit, placed in a higher level of the processing hierarchy, which identifies the coordinates of all visible markers in the tracking area (T. Pintaric & Kaufmann 2007).

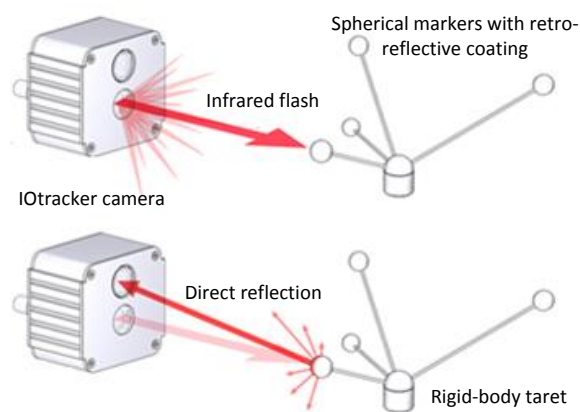


Figure 58: The infrared-optical pose-tracking system. The IOtracker camera is sending an infrared flash, which are reflected by the retro-reflective surface of the markers and sensed by the infrared camera (T. Pintaric & Kaufmann 2007).

7.3. Video Tracking System

The information delivered by one camera should be sufficient to identify the position and orientation of one marker within the virtual reality. However, one camera will not be able to see the markers at all times. During the performance, various objects or even the body of the participant might cover the markers entirely or partially. If this occurs, accurate identification of the marker is impossible. Moreover, the image acquired by cameras might be noisy as well, e.g., because of unexpected reflections, and could consequently reduce the precision of the identification of the marker. So, in order to increase the visibility of the markers and the accuracy of their identification, the system uses four to eight video cameras distributed in every corner of the

tracking space. The information delivered by the system of cameras may be partially redundant, but this way of handling the setup will increase precision under unfavorable environmental conditions [Figure 59].

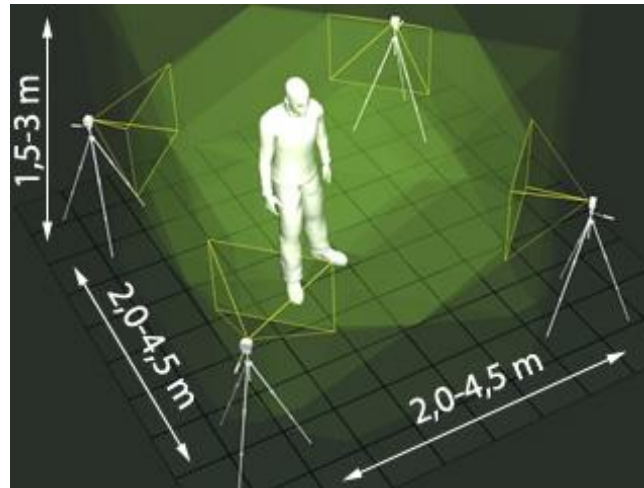


Figure 59: The tracking area has at its corners a system of four or eight infrared video-cameras which allow for the identification of the position and orientation of all markers within the tracking area (T. Pintaric & Kaufmann 2007).

7.4. The Virtual Reality Environment

The tracking system allows for a natural immersion of the subjects into the virtual environment. Within the virtual environment the subjects perform as they would in a real environment; they move their limbs and their bodies, aiming to reach and grasp virtual objects with their prostheses. However, in comparison with the real environment, the virtual one allows flexibility in designing various scenarios and behaviors of the prosthesis, as well as various interactions with the objects. The tasks within the virtual learning environment can be easily changed by modifying the coordinates of the objects within the tracking space, or changing their properties, all simply defined in a configuration file. Within real learning environments, only a predefined set of physical objects may be used, and their placement depends on the available facilities. While real learning environments cannot be easily standardized, the virtual scenarios may be simply defined by standard configuration files, and shared between clinicians spread all over the world.

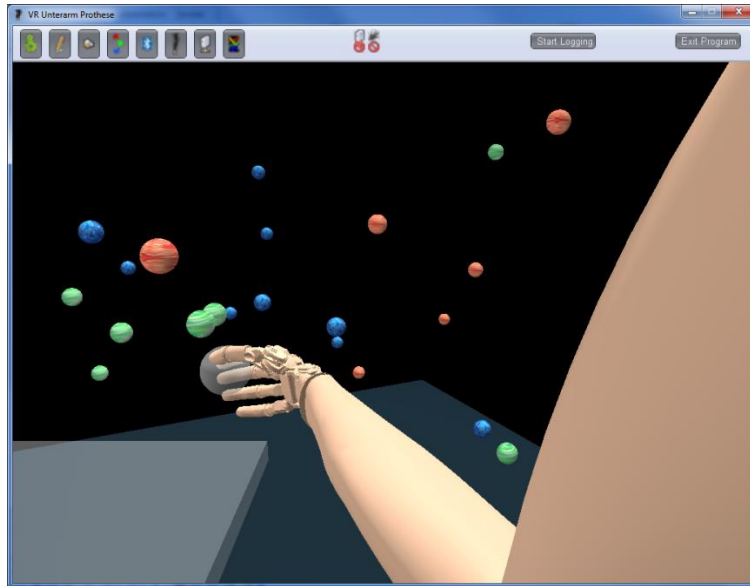


Figure 60: The artificial environment consisting of virtual prosthesis and virtual objects.

The virtual environment was implemented using Unity3D – a 3D game engine (Higgins 2010). The main components of the virtual environment are the prosthesis and a set of virtual objects (spheres). The prosthesis is virtually attached to the subject’s forearm, and the objects float within the virtual space. The task to be completed consists in grasping the available objects with a predefined force, and collecting them in a basket.

7.4.1. PROSTHESIS

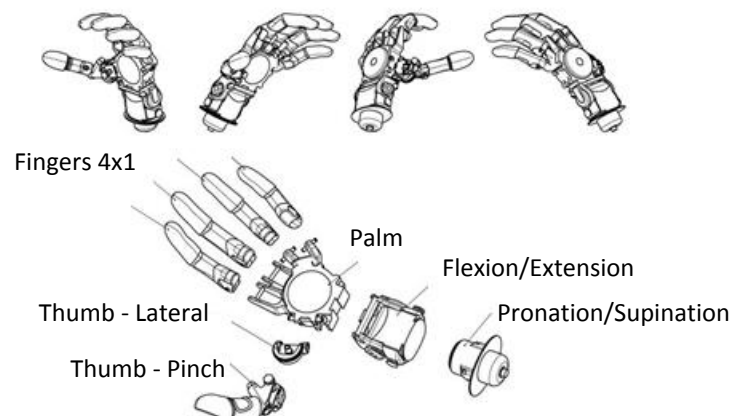


Figure 61: The model of the simulated transradial Michelangelo hand prosthesis. The prosthesis has 8 DOF: 4x1 fingers, 1x2 thumb (pinch and lateral grip), 1x1 wrist (pronation/supination), 1x1 wrist (flexion/extension).

The virtual hand prosthesis entirely reproduces the transradial OB Michelangelo Hand; each of the four fingers is connected to the palm by one rotational joint, whereas the thumb is connected by two rotational joints allowing pinch grip (thumb closes over the finger tips) and lateral grip (thumb closes on the lateral side of the index finger). The virtual prosthesis has the same kinematics as the real one, though there are some differences between them. First, the virtual prosthesis has ideal dynamics, not being restricted by any electro-mechanical physical components and, second, all fingers are individually controllable.

7.4.2. OBJECTS

One of the major goals of implementing the immersive virtual environment was to study and improve the mechanisms of grasping with upper-limb prosthetic devices, and to allow the amputees a smoother transition through different phases of the rehabilitation process. Classically, the training sessions are performed within real environments, with a real prosthesis – the so-called ADL tests (Activities of Daily Living). The objects involved are common in daily life and so have very diverse geometries.

The human hand is highly configurable, enabling it to deal with this diversity while most of the available commercial prostheses have limited kinematics. In trying to accomplish the ADL tasks, the amputees try to compensate for the lack of prosthesis flexibility by making use of additional, non-physiological movements. They are forced to move the shoulder or elbow unnaturally, or to change the posture of the body, to accomplish a simple pick-and-place task.

The current work doesn't directly address the amputees' performance during daily life activities, but focuses on the grasping mechanisms. More specifically, this study aims at identifying the mechanisms allowing the amputees to synchronize the prosthesis movements with the movements of their own bodies. More intuitive grasping will undoubtedly have the consequence of better performance during ADL. Due to the unnatural movements required by grasping complex objects with simple prostheses, there is no chance to synchronize approaching the target and grasping. Therefore, the implemented VR uses spheres only. They might not be representative of the objects in daily life, but the spheres are compatible with the prosthesis implemented within the virtual reality. The spheres can be addressed by amputees from any direction, without additional movements, facilitating a straight reach-to-grasp movement followed by the grasp.

The spheres are characterized by diameter and hardness, parameters which are adjustable at creation. The hardness is defined by a span (offset and width) within the force range. In order to be collected, the prosthesis has to grasp with a force stable within the target's borders.

If the lower/upper limits of force for the target coincide with those of the force range, the objects are not destroyable. However, if the target's upper force limit is lower than the developed grasp force, the object gets broken. Otherwise, if the developed force is lower than the lower force limit of the target, the objects cannot be extracted from their initial position within the virtual reality. By changing the width and the offset of the target, the degree of difficulty in grasping the objects may also be adjusted.

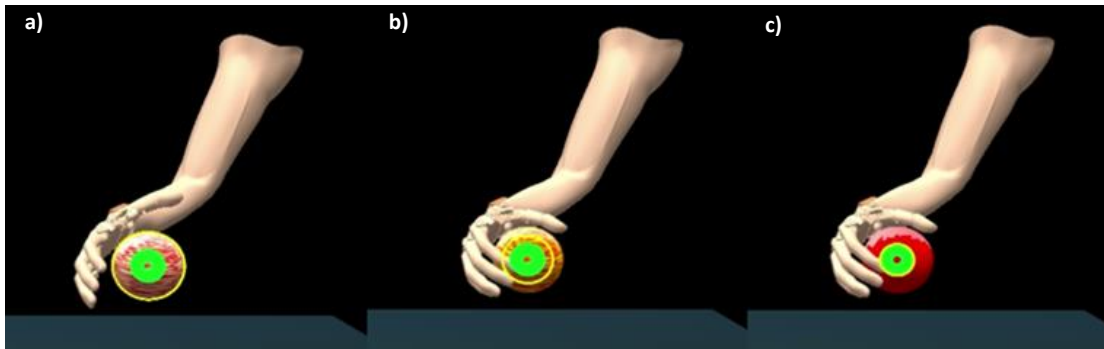


Figure 62: Three different phases of grasping: a) hand open – the measured force is zero and consequently the yellow circle is at the target object's border), b) object grasped, but the measured force did not reach the target, c) target hit – the measured force, the yellow circle, overlaps the force target – the green range.

Three distinct scenarios for the relative positions of the virtual prosthesis and the object are presented in Figure 62. On the left, the hand is completely open and there is no contact with the target object. The yellow circle, centered over the object, represents the measured force, and the green range, the force target. In the middle, the prosthesis grasped the object, but the developed force does not allow the subject to collect the object. On the right, the developed force further increased and hit the target; at which point the subject is allowed to move the object.

7.5. The Head-Mounted Display (HMD)



Figure 63: The head-mounted display.

The HMD (video glasses) is a device, worn on the head as part of a helmet that has a small optical display in front of each eye. The HMD is wirelessly connected to the VR host machine, allowing autonomy when performing within the tracking area. The HMD also has a marker on it, making it possible to track head movement. These elements facilitate an immersive feeling for the subjects performing within virtual reality [Figure 63].

7.6. Control Brace

The virtual prosthesis is virtually attached to the amputee's stump, but is controlled by real EMG signals sensed by real electrodes. The electrodes are integrated into a brace, specially designed for this application, wrapping the forearm as shown in Figure 64.

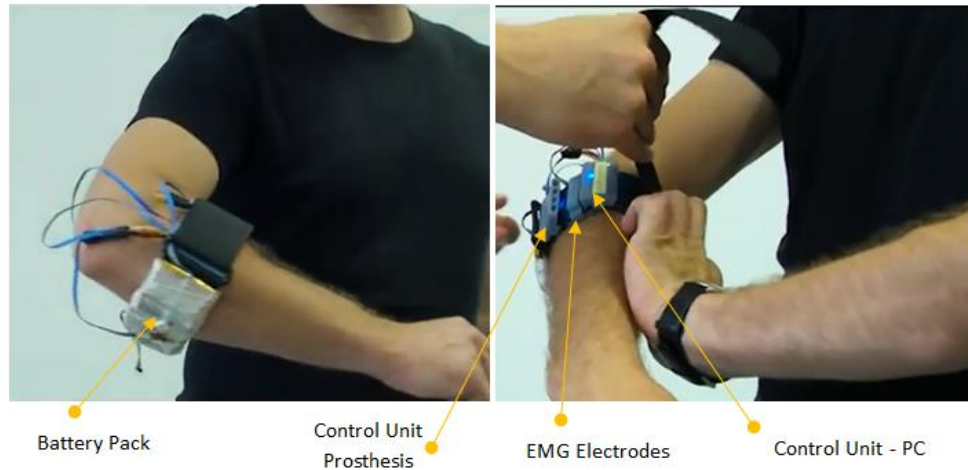


Figure 64: The Control Brace used to wirelessly control the virtual/real prosthesis, which is an autonomous system comprising a battery pack, a prosthesis control unit dedicated for EMG processing, haptic stimulation and communication with the prosthesis, EMG electrodes to sense the myo-activity in the forearm, and a PC control unit with the role to control the behavior of the virtual prosthesis based on the sensory information measured by the real prosthesis.

Up to sixteen electrodes (8inputs x 2 CU) may be used with the current set-up to sense the MYO activity of the forearm. For this application, only two electrodes were used, which were placed antagonistically on the forearm to sense the subject's intention to open and close the prosthesis. The EMG electrodes (13E200, OttoBock) are integrated with an adjustable preamplifier as well as an analogue filter to suppress the electromagnetic noise and to rectify the raw EMG. The electrodes deliver a voltage proportional to the RMS (Root Mean Square) of the sensed EMG. These analogue voltages are then forwarded to the Control Unit, where they are digitized and processed. The result - the prosthesis movement reference - then wirelessly controls the virtual or real prosthesis.

The control brace consists of two control units, with eight inputs each. When the real prosthesis has to be controlled, the electrodes are plugged into the CU-Prosthesis; otherwise, they are connected to the CU-PC to control the virtual prosthesis. The architecture of the control brace is depicted in Figure 65.

Every CU controls its corresponding prosthesis, the real or the virtual one. As a result, the prosthesis will move and interact with real or virtual objects. The movement and grasp force developed by the real/virtual prosthesis are sensed by real/virtual sensors embedded within the prosthesis and then delivered via the

AxonBus (OttoBock, Austria). AxonBus is an OttoBock communication BUS which interconnects and allows high-speed bidirectional information transfer between all partners. The physical BUS is a three-wired cable, two of them used as power supply for all communication partners, the third allowing the data transfer. The power supply is provided by a battery pack embedded in the brace, allowing autonomy when performing within the virtual environment.

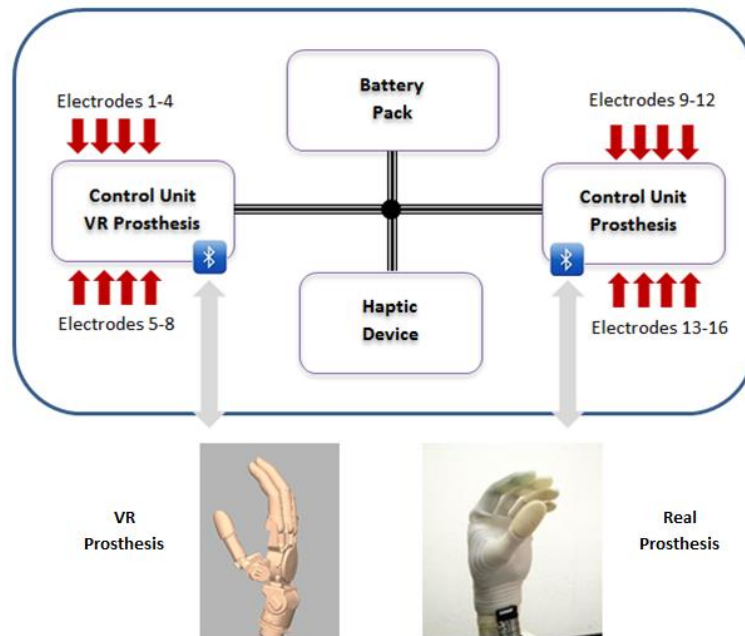


Figure 65: The architecture of the control brace allows perfect synchronization of the virtual prosthesis with the real one. Up to 16 EMG signals can be sensed by the virtual (PC) and real prosthesis control unit, which can be used to control the behavior of the virtual or real prosthesis wirelessly. Due to the AxonBUS communication system, the sensory/control information can be interchanged between all system components.

Since all components are attached to the same BUS, synchronization between the real and the virtual prosthesis is possible. The sensory information describing the movement or grasp of the real/virtual prosthesis is made available on the BUS. This allows, for example, integration of the real prosthesis into the control loop of the virtual one. For example, the real prosthesis is directly controlled by the subjects, who will grasp a physical ball mounted in the hand, but in the video glasses they will see the virtual one performing in synchrony with the real prosthesis. This feature might be very useful, e.g. when assessing the controllability of a real prosthesis within a standardized virtual environment.

Within the real environment, humans interact with various objects and sense this interaction by courtesy of proprioceptive or haptic feedback. Within the virtual environment this component is missing, and subjects rely mainly on vision to accomplish tasks. The intended goal is, however, to create a virtual environment which is both immersive and reality-faithful. Therefore, the proposed architecture allows the connection of different

haptic technologies to the AxonBUS. The prosthesis moves and interacts with various objects, and the resulting sensory information is provided via the communication BUS. Attached to the BUS, the haptic devices receive the sensory information and convert it into different modalities of haptic stimulation: electro-stimulation, vibration or steady pressure. This feature is already available in the current implementation [Figure 66] but was not exploited during this study.

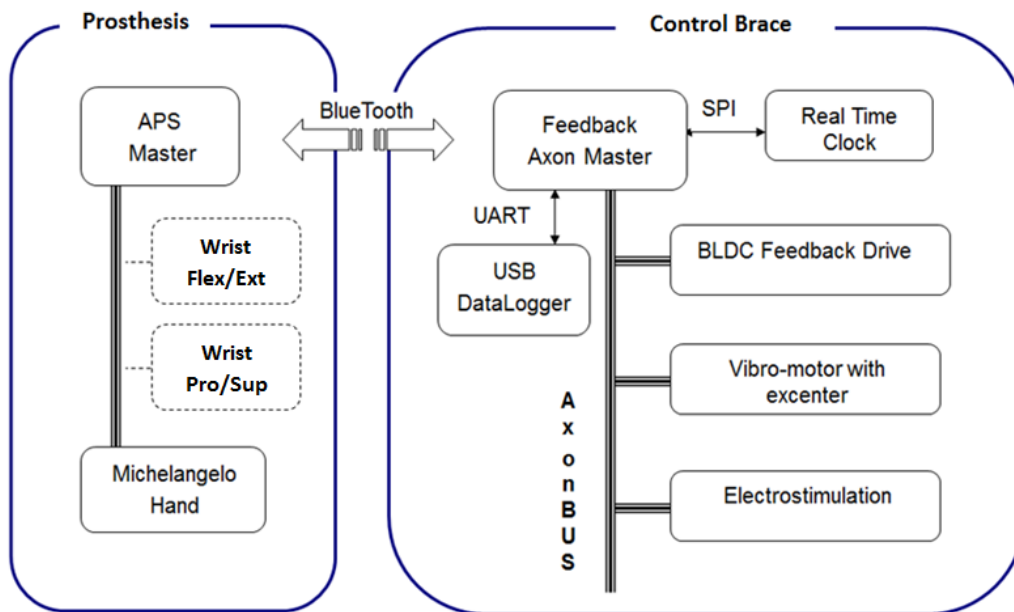


Figure 66: The control brace in its extended architecture allows multimodal cutaneous stimulation, as well as the control of all DOFs of the transradial Michelangelo hand: lateral and pinch grip of the hand, pronation/supination, and flexion/extension of the wrist.

Likewise with the prosthesis' ability to move the wrist in extension/flexion, or pronation/supination, as well as the lateral grip of the hand. The prosthesis complexity was reduced to minimum; thus, only the pinch grip was implemented. The focus was set on analyzing the factors which might facilitate more intuitive prosthesis control; less complex prostheses are less demanding and there is a higher chance of integrating them into the amputee's body schemata. However, all these extended functionalities might be exploited during upcoming studies.

8. ASSESSMENT OF EMG PROSTHESIS CONTROL

8.1. Problem Statement

Fitting an upper-limb prosthesis is a complex and multidisciplinary activity, requiring interaction between specialists from various fields; surgeons, engineers, orthopaedic technicians and occupational therapists all have to interact in an efficient way to improve the quality of life for amputees. However, the language of this interaction is currently not well defined; the surgery is considered to be successful when the amputees do not complain about other complications, the engineers are satisfied when the prosthesis works reliably, and the orthopaedic technicians are happy when the prosthesis fits the amputee well. The only people involved in this process who seem to feel the weight of responsibility for how well the amputees use the prosthetic devices in their daily lives, and how comfortable they feel wearing them, are the occupational therapists. This may explain why the most effort to find a practicable and general methodology has mostly been put forth by the occupational therapists. They have a serious need to objectively quantify the outcome of their work.

Despite the variety of methods available, there is a consensus within the rehabilitation community that the current methodologies do not entirely allow consistent and objective assessment of the controllability and effectiveness of prosthetic devices. There are various factors that have led to this situation and, in order to gain an overview of all these challenges and better understand them, the opinion of a panel of experts was included in the current study (Otto 2003).

Randall Alley, BSc, CP, FAAOP, is the head of Clinical Research and Business Development for the Hanger Prosthetics & Orthotics Upper Extremity Prosthetic Program. He is chair of the Upper-Limb Prosthetics Society of the American Academy of Orthotists and Prosthetists (AAOP) and an international lecturer and consultant.

“The problem lies in two distinct areas: the sheer scope and variety of variables surrounding and unique to each case, and the instruments used to gather the data.”

“Acceptable outcomes are elusive because many of the variables involved that are critical in determining patient acceptance of upper-extremity prosthesis, have little to do with the prosthetic device, and more to do with psychological and psychosocial adaptation to traumatic upper-limb loss, which is more common than congenital amelia or elective amputation.”

Diane Atkins, OTR, clinical assistant professor in Physical Medicine and Rehabilitation at the Baylor College of Medicine in Houston, Atkins is an occupational therapist who has specialized in amputee rehabilitation for more than 25 years, with special focus on rehabilitation of the upper-limb amputee.

“Outcomes measures for upper-extremity amputees are very difficult to define in clear objective terms. The score is prone to be very subjective - based upon (a) the experience of the evaluator - usually an occupational therapist, and (b) the knowledge of the evaluator of what is appropriate to ask the amputee to do with a prosthesis.”

John M. Miguelez, CP, FAAOP, president of Advanced Arm Dynamics, serves as a worldwide clinical consultant on issues regarding upper-extremity prosthetics and operates a Centre of Excellence in Dallas, Texas.

“Coming up with appropriate outcomes studies is difficult because not only are the practitioners' experience levels so diverse, but the outcomes are practitioner-related.”

“There are several outcomes measurement systems, but they are somewhat antiquated. They are based on a body-powered approach as the primary approach, then try to shoehorn in other prosthetic options. An appropriate outcome measurement needs to really look at all the options.”

“There are several outcome measurement tools available, but we don't have one that covers everything. If you use an existing system, you'll find that none of them have a really comprehensive approach that we can all agree upon.”

The feedback provided by the panel of specialists after their long experience in the prosthetic field, has been summarised as follows:

- The current assessment methodologies do not have a general character
- The current assessment methodologies do not address the requirements of EMG-controlled prosthesis, being only adaptations of methods used in body-powered prosthesis.
- The evaluation results are not consistent as they are tightly dependent on practitioner experience; being the result of subjective evaluation, the outcomes could not be compared between many amputees.
- The state-of-the-art methodologies do not offer a measure of cognitive and psychological health of amputees, which is an important factor role during the prosthesis fitting.

One of the most important efforts to define a standard for the assessment of EMG-controlled prostheses are considered, by the author of this manuscript, to be those made by the Upper-Limb Prosthetic Outcome Measures group – known as ULPOM (Hill et al. 2009). For this purpose, they addressed an internationally recognized standard describing health and health-related states: the *International Classification of Functioning, Disability and Health*, known as ICF (World Health Organization & others 2001). The ICF belongs to the family of international classifications developed by the World Health Organisation (WHO) for application to various aspects of health, including rehabilitation; however, ULPOM adapted and interpreted it for the special case of prosthetics.

ICF has two parts, each with two components. The first part, *Functioning and Disability*, and its components *Body Structures and Functions*, *Activity* and *Participation* describe the health and health-related states, from the perspective of the body. The second part, *Contextual Factors* and its components *Environmental Factors* and *Personal Factors* describe the external or personal influences on functioning and disability. Both parts have to be taken into consideration when completely describing the level of impairment and disability; however, proceeding step-by-step, this study is focused only on the *Functioning and Disability* part.

In order to evaluate the level of disability, ULPOM adopted the “Functioning and Disability” standards, but they changed the meaning to better fit the prosthetics requirements. According to the ICF definitions, prostheses are regarded as assistive devices, and are therefore considered an environmental factor. However, the ULPOM group considered positioning the prosthesis to be an environmental factor. The model may have limited usefulness when measuring the impact of a prosthesis on its user. Thus, the prosthesis was redefined as an extension of the amputee’s body, being a replacement of the amputated limb. Correspondingly, the three domains of ICF gained a new interpretation:

- *Body Structure and Functions* relates to performance of the prosthesis and can capture measures of grasp, release, and other abilities of the prosthesis.
- *Activity* refers to the carrying out of tasks, which relates to the assessment of function during daily life activities with prosthetic devices.
- *Participation* relates to prosthetic involvement in real life situations, which is reflected in assessment of the impact of the prosthesis function, from a user's perspective, in his/her own life situations.

The ICF is a measure of health and health-status and its components - *Body Structure and Function*, *Activity* and *Participation* - provide different measures to evaluate the capacity and performance of impaired, able-bodied subjects in controlling their natural limbs. An amputation is a total impairment and, consequently, there are no body structures or functions available; thus, no *Activity* or *Participation* is possible. The ULPOM approach considered the prosthesis to be part of the body; the prosthesis might be seen as an impaired limb which may be assessed after standard ICF rules. Consequently, the prosthesis structure and function might be considered *Body Structure and Function*, the *Activity* relates to the amputee’s capacity to perform tasks with the prosthesis, and *Participation* relates to the involvement of amputees in daily life.

This consideration has a traceable logic, very intuitive, but it does not allow for characterisation of the human-prosthesis interface, which is the most important challenge when assessing the controllability of upper-limb prosthetics.

An all-in-one score evaluates the system as a whole. Such a score might be relevant for occupational therapists, but not for engineers, orthopaedic technicians or surgeons, who require an evaluation of the individual components of the system. Worse performance is mostly generated by the interplay of many sources of instability, and an all-in-one assessment will make all these instabilities untraceable. Unlike the global

assessment, the assessment of the individual components will make it possible to identify the bottlenecks within the fitting process, in order to improve or fix them.

8.2. The Proposed Assessment Approach

In order to support and encourage new developments in the field of outcome measurements for myo-prosthetics, the ULPOM group, based on their collective experience, proposed a set of guidelines presented as follows.

Prerequisite: It is crucial that unambiguous terminology be used that allows effective and precise cross-disciplinary communication.

Measurement Properties: An important aspect of any test is its psychometric properties (i.e., scaling, reliability, validity, and sensitivity). This ensures that the test measures what it is intended to measure, that the measures are repeatable and do not depend on who conducts the test or when or where it is performed.

Essential Properties: Consensus from ULPOM working group meetings and workshops also suggested that the ultimate measurement toolkit should possess a number of features. It should:

- be easy to quantify
- be moderately easy to use
- relate to activities of daily living
- be sensitive to change in control configuration
- be sensitive to change in component design
- be usable for high-level upper-limb amputees
- be usable for bilateral upper-limb amputees
- be able to track improvement and function over time
- measure user satisfaction
- accommodate users' different tolerances to complexity of control

During this section, a new assessment approach is proposed, which should overcome the drawbacks identified in the ULPOM interpretation of the ICF. The proposed assessment methodology takes into account the ULPOM guidelines, but in contrast with the ULPOM approach, which considered the prosthesis to be part of the body, the proposed approach qualifies the prosthesis as an assistive device.

Consequently, the amputee's capacity to generate and actively use bio-signals for prosthesis control will be assessed, but not the performance in accomplishing daily tasks. This will move the focus to the interface between human and prosthetic, the improvement of which is considered to implicitly result in a better performance of the amputees during daily tasks.

Amputee and prosthesis are not merged entities anymore, but two different systems, interacting with one another. This allows for a better focus on the interface between prosthesis and amputee. The assessment of the performance is broken down into assessment of the amputee's capacity to generate control signals, to control prosthetics, and to use prosthetics in ADL activities. All three categories are interpreted in the ICF terminology as *Body Function*, *Activity* and *Performance*.

The proposed performance assessment approach isn't intended to directly evaluate what an amputee is able to do with the prosthesis, but how well the amputee controls it. The fundamental interest here is not in what tasks the amputees are able to execute in daily life, but in how well the amputees are able to coordinate their own natural movements with the prosthesis movements, which is definitively not the same goal.

Three levels of human functioning are addressed by the ICF standards when evaluating the degree of health: functioning at the levels of body or body part, the whole person, and the whole person in a social context. Therefore, the ICF standards have been interpreted as follows:

- *Body Structure* - the structure of the stump, the number of control sites (e.g. muscles) and their configuration.
- *Body Functions* - the amputee's capacity to control these muscles and to generate consistent and reproducible movement references for the control of the prosthetic devices.
- *Activity* - the amputee's capacity to control the prosthetic device.
- *Participation* - the amputee's ability to synchronise the prosthesis with body movement.

This interpretation keeps the same structure with the original ICF, but completely changes the focus of what should be assessed. It is common to assess the amputee's performance during daily life activities, but the proposed interpretation is explicitly focused on the interface between human and prosthesis. It is obvious that the ultimate goal is to improve the performance of the amputee during daily-life activities. However, it has been assumed that a better interface between amputee and prosthesis will automatically result in better performance during ADL.

The current study is not claiming to cover all the details required to make such an evaluation system effective, but it proposes an approach to qualify the amputee's level of health and their ability to control prosthetic devices. In contrast with the SOA methodologies, the proposed approach splits the system up into components, and assesses them individually.

The measured performance is like a snapshot describing the situation at a given moment. This may be useful for comparing and evaluating the differences between the conditions of many amputees. Perhaps much more important, when recorded at multiple points in time, it allows for the description of trajectories, better indicating the efficiency of one therapy, and individual factors contributing to or impeding the therapy's progress may be identified, making it not only an assessment but also a very important research tool.

For this qualification to be used in a universal manner, a procedure based on a scale provided by the ICF was proposed. This scale consists of 5 qualifiers which are presented in the table below.

Table 2: A five levels scale for the evaluation of the ICF components: body structure and functions, activity and performance.

| Score | Description | Range |
|-------|--|----------|
| xxx.0 | NO problem (none, absent, negligible,...) | 0-4 % |
| xxx.1 | MILD problem (slight, low,...) | 5-24 % |
| xxx.2 | MODERATE problem (medium, fair,...) | 25-49 % |
| xxx.3 | SEVERE problem (high, extreme, ...) | 50-95 % |
| xxx.4 | COMPLETE problem (total,...) | 96-100 % |

In the Score row, the “xxx,” may be “f” for Body Functions, “s” for Body Structures, “a” for Activities and “p” for Participation, etc. The following number 0-4 describes the level of impairment, from 0 – fully functional to 4- complete impairment. These qualifiers are defined by the “Range” which has individual meanings for the different ICF components. The qualifiers describing the ICF components, with Score, Description and Ranges from Table 2 are an example adopted from the standard ICF. However, for assessing prosthesis performance, some adaptations have to be made. Hopefully, the qualifiers will be better defined during future research.

Scoring *Body Structure* can be done only with regard to the prosthesis intended to be used. If the prosthesis has one degree of freedom and is classically controlled in voltage mode, two EMG sites are needed to fully control the hand. If more complex pattern recognition algorithms are used, it might be that the signals provided by the two EMG electrodes will result in four control signals. In this case, the two EMGs will be sufficient for a score of 100%, as the two EMGs will be able to control a prosthesis with 2 DOFs (four movement references). *Body Structure* should always be scored at 100% to allow for the evaluation of the next ICF components.

The *Body Functions* component evaluates the quality of the control signals. The quality of the EMG is evaluated with regard to the control strategy implemented by the prosthesis. If the prosthesis is controlled in position mode, the movement reference for moving the prosthesis from the start to the target positions will have an “S” profile. Otherwise, if the prosthesis is controlled in speed mode, the movement reference should have a “Bell” profile to perform the same movement [Figure 67].

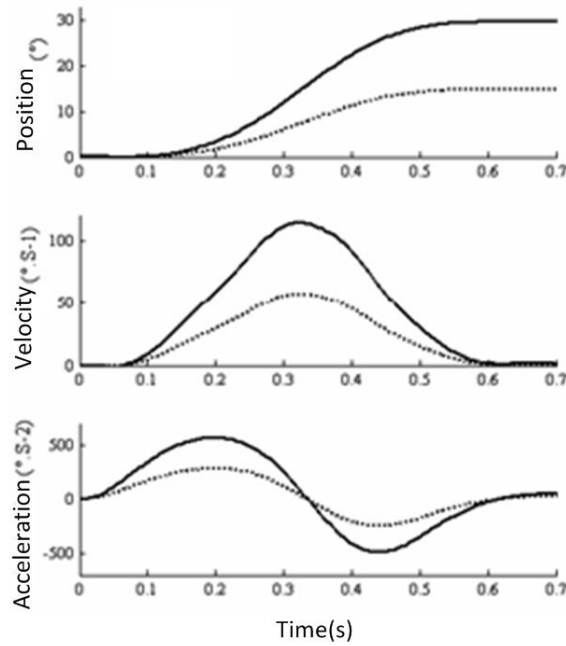


Figure 67: Various profiles used as reference for the evaluation of the ICF component – body functions.

Consequently, assessing the *Body Functions*, will assess the amputee’s capacity to generate EMGs following the the “S” or “Bell” profiles. In order to have a more general character, the assessment should be made for various gaps between start and target position. Correspondingly, the “S” or “Bell” profiles, generated by the assessment tool, will have various slopes. The subjects are instructed to follow the reference profiles, generating corresponding muscle contractions; the more precisely the profiles are followed, the higher the *Body Functions* score will be.

The *Activity* describes the amputee’s capacity to control the prosthetic devices. It is recommended that the prosthesis not be attached to the amputee’s body, as the attachment can negatively influence the EMG generation. The prosthesis should be placed, e.g. on a table in front of the amputee. The EMG electrodes will be placed on the amputee’s stump, wired/wirelessly connected with the prosthesis. To assess the level of *Activity*, the amputee has to cyclically, quickly and precisely grasp an object mounted in the hand.

The faster, more precise and consistent the grasps, the higher the score will be. The target will be defined as a percentage from the grasp range or from prosthesis aperture, and the subjects have to hit the target cyclically. The level of difficulty in reaching the target is defined by the rules describing the Fit’s law: the task difficulty will increase when the borders of the grasp target are closer or when the distance between the rest position of the hand and target objects is larger.

It may be considered that the amputees who are able to generate good individual control signals (high scored *Body Functions*) will also control the prosthesis well (high scored *Activity*). In practice this is not always the case. What might be responsible for this behaviour is the control mode implemented by the prosthesis (the

conversion between the movement reference and prosthesis movement), the cross-over between the EMGs generating movement references, the large difference between the amputee's and prosthesis' dynamics, or delays introduced by the electro-mechanical components.

Participation describes the amputee's ability to synchronise the prosthesis with the body movement. Participation will be highly scored if the amputee is able to pre-shape the hand in order to optimally grasp during approaching the target. This is an indication of how demanding prosthesis control is for the subject. If controlling the prosthesis requires special attention, the amputee will sequentially approach the target and then grasp. The more demanding the prosthesis control, the larger the gap will be between approaching the target and grasping. The *Participation* score is also an indication of the quality of the prosthesis fitting. If the *Performance* has a much lower score than *Activity*, it indicates that the drop in performance is caused by some fitting elements, e.g. socket, EMG electrode placement.

8.3. VR Scenarios

In order to implement the assessment methodology previously described, three VR scenarios have been designed. The first scenario, *Body Function*, allows for the assessment of the amputee's ability to generate movement references for prosthesis control by contracting the muscles and generating valuable EMG signals. The second one, *Activity*, facilitates the evaluation of the amputee's capacity to control prosthetic devices. The third and last is *Participation*, which comprises two tasks with different levels of difficulty and estimates the amputee's ability to synchronize the body and prosthesis movement.

8.3.1. BODY FUNCTIONS

Body Functions is mainly correlated with the capacity of the amputees to generate movement references for prosthesis control. The amputee contracts muscles or a group of muscles, generating EMG signals. These are further sensed by surface electrodes and processed by computational units, which convert them into movement references for the prosthesis. Consequently, good prosthesis control requires, as a necessary condition, the generation of differentiable and consistent EMGs. The *Body Functions* may be evaluated by qualifiers such as quality, dynamics and reproducibility. *Quality* is an indicator of how well the movement follows the reference; *dynamics*, the range of the movement able to be made (from slow to fast); and *reproducibility*, the consistency with which the movement intent is converted into movement references for prosthesis control by the amputee.

In the description of the assessment methodology, it was specified that *Body Functions* has to be evaluated with regard to the control mode implemented by the prosthesis. The different prosthesis control modes will coerce the amputee to adopt different strategies when generating EMG signals. The most common control mode implemented by the upper-limb prosthetics is a kind of hybrid; while moving, the prosthesis runs in derivative mode (velocity), and during grasping in proportional mode (force). Performing in derivative or

proportional mode, the *Body Functions* might be differently scored and will forecast whether the amputee will better control the prosthesis during movement or during grasp.

Assessment methodology in derivative mode

In order to give an example of assessment in derivative mode, three sinusoidal reference signals were presented to the subjects [Figure 68]. One period of the sinus has a “Bell” form; consequently, it will generate a trajectory determining prosthesis movement between the start and target position. The three reference signals have the frequencies of 0,26 Hz, 0,66Hz and 1,06Hz and an amplitude between 20% and 80% from the EMG range. The EMG range (0-255) was individually adjusted for every subject, so that, when they contracted the muscles at maximum strength for 5 seconds, the EMG would reach 100%. The reference signal was running on the computer screen and the subjects followed the profile, contracting the muscles and generating EMGs.

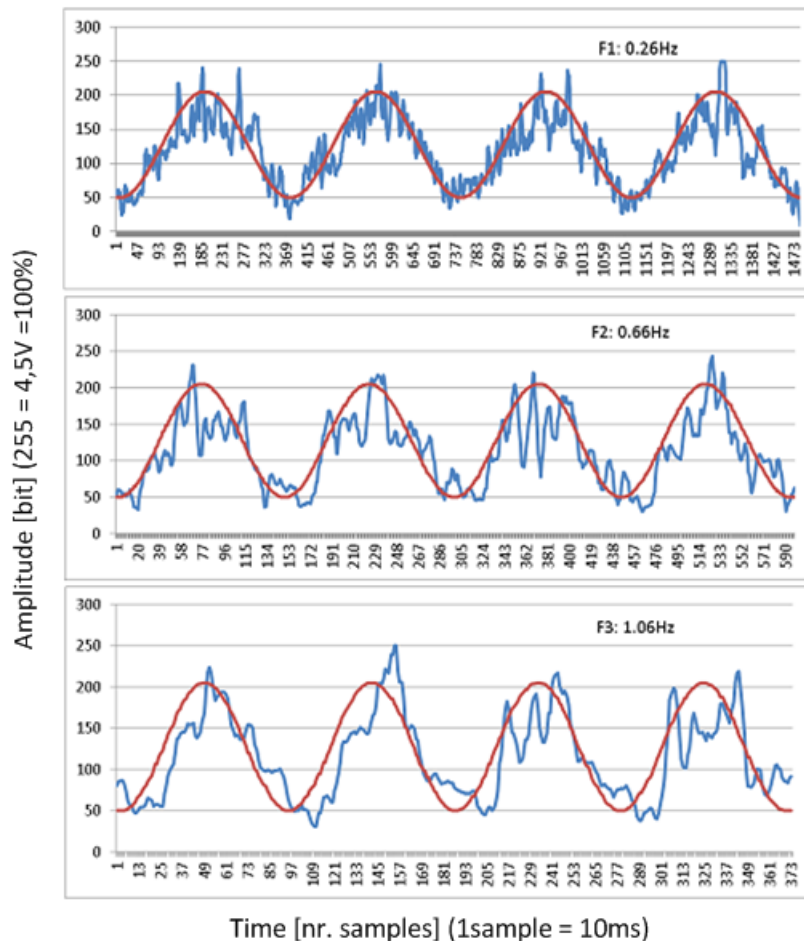


Figure 68: Three sinusoidal references (series of bell profiles), having three different frequencies, were used to evaluate the subject's capacity to generate EMG signals. The EMG signals will directly control the velocity of a prosthesis which is driven in derivative mode.

The blue signal in Figure 68 is the movement reference generated by a subject. Because the direct mode was in use, the movement reference is the same as the EMG signal. To accomplish the task, the subjects contracted the muscles and produced an EMG (blue signal), following the reference (red signal).

In the first condition, the reference signal has a frequency of 0,26 Hz, which would correspond with a very slow movement lasting for 4s, the second reference signal has a frequency of 0,66 Hz (1,5 s), and the last condition has a frequency of 1,06 Hz (0,94s). A brief analysis of the pictures above reveals that, when moving slowly, the EMG followed the reference with relative accuracy. The signal-to-noise ratio is about 20%, but, being slow, the delays introduced by filtering do not dramatically influence the outcome. For the next conditions, in which the frequencies of the references are 0,66 Hz (1,5 s) and 1,06 Hz (0,94 s) respectively, the signal reference is harder to follow. The faster the reference, the lower the precision. The signal-to-noise ratio may slightly decrease but is still very large, and delays introduced by filtering are essential when high frequency references have to be followed.

Assessment methodology in proportional mode

In proportional mode, the movement reference cannot be the same as the EMG signal, as in direct mode. The EMG is very noisy and cannot be steadily held at a level, as required by the proportional control. Moreover, muscle fatigue will strongly influence the EMG characteristics; the physiological processes of muscle contraction will continuously change the magnitude and spectrum of the sensed EMG. Consequently, the generated movement references are less consistent with the expressed movement intent. In proportional mode, the EMG cannot be directly used as movement reference, thus, the EMG was pre-processed. In the examples given in Figure 69, two antagonistic EMGs were used (blue and red signals) to generate one movement reference (green signal) to control, e.g. position of the prosthesis.

In order to exemplify the assessment methodology in proportional mode, the same sinusoidal profiles were used as references, having the frequencies of 0.26, 0.66 and 1.06 Hz. One period of a sinus has a different meaning in the derivative mode. While in derivative mode, one period of a sinus has velocity reference, moving the prosthesis from start to target ("Bell" profile). In proportional mode, a sinus consists of two "S" profiles. The first half of the sinus represents the position trajectory from the start to the target, and the second half, that from target back to start. One sinus period of the reference signal, then, corresponds to a back-and-forth movement. Consequently, the reference in proportional mode is two times faster than during velocity mode, and the movements between start and target positions will correspondingly take 2 s, 0,75 s and 0,47 s.

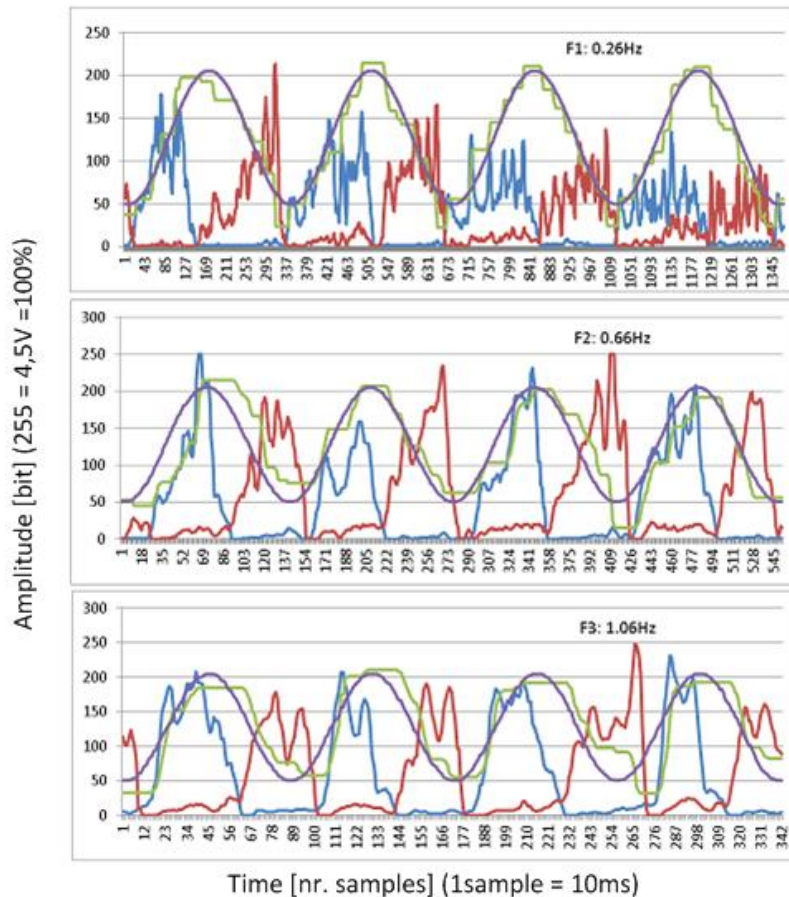


Figure 69: Three sinusoidal references (series of “s” profiles) with three different frequencies were used to evaluate the subject’s capacity to generate EMG signals. The EMG signals (red and blue) are processed and converted into a movement reference (green,) used to control a prosthesis driven in proportional mode.

From the previous measurements, performed in derivative mode, it was obvious that following the sinusoidal reference was, for the subjects, much more challenging when the frequency of the sinus was higher. With increasing frequency of the reference, delay and roughness of the EMG control signal also increased. In comparison with the derivative mode [Figure 68], the proportional control, exemplified in Figure 69 revealed good responses even during the fastest condition – F3. The sinus reference and the movement reference, after EMG processing, show closer correspondence, and delays between the signals are much lower.

However, this section does not aim to evaluate the performance of one control strategy. The two cases of proportional and derivative mode are intended as examples of how to evaluate an amputee’s capacity to generate movement references for prosthesis control – *Body Functions*. In accordance with the control mode implemented by the prosthesis - derivative or proportional - the assessment software generates a reference signal, a sequence of “Bell” or “S” profiles. The more accurately the subjects follow the reference, the better the *Body Functions* score will be.

8.3.2. ACTIVITY

Following *Body Functions*, the next assessment level is *Activity* – the ability of the amputees to control prosthetic devices. A good score in *Body Functions* indicates that the amputee can generate good control signals for the prosthesis. If the *Activity* score is lower than expected after the *Body Functions* evaluation, this could indicate the prosthesis as one factor responsible for the drop in performance: delays introduced by the prosthesis' electromechanical mechanisms or roughness of prosthesis control. Another factor which might determine a lower level for *Activity* is poor discriminability between the EMG signals for antagonist movements of the prosthesis.

For the evaluation of *Activity*, a new VR scenario was used. The subjects fitted with a virtual prosthesis had to cyclically grasp an object with a force (yellow circle) hitting the target (green range). The object is permanently attached to the hand, thus the subjects do not have to take care of reaching the object, but only of grasping it.

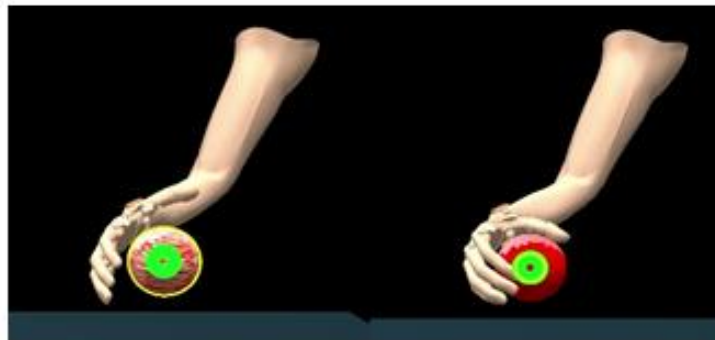


Figure 70: A virtual-reality scenario implemented to evaluate the level of activity; the object is attached to the prosthesis and the subjects concentrate only on hitting the force target.

Assessments of *Activity* were made for two conditions: during soft grasp the target force is between 10-50% of the maximum, and during hard grasp the target force is between 50-90%. Figure 70 shows the case of hard grasp: before grasping – left image; target force reached – right image.

The level of *Activity* is fully characterized by three qualifiers: the time-to-complete for successful grasps, the consistency (variance of the recorded grasp force) and the grasp precision (deviation from target centre).

8.3.1. PERFORMANCE

Performance describes the amputee's capacity to coordinate the prosthesis movement in synchronicity with the movements of his/her own body. In evaluating *Performance*, the same immersive environment was used; except that the objects were not attached to the hand, but were floating within the VR space. In order to collect the objects, the subjects had to approach and, if possible, simultaneously grasp them, reproducing the natural reach-to-grasp movement.

Reach-to-grasp is a very complex process requiring coordination between the movements of all involved joints, vision and proprioception. The more joints involved in approaching the target, the more complex are the movement synchronisation mechanisms. With complexity, the precision of reach-to-grasp movement decreases, which might mask important insights of the synchronisation between body and prosthesis movements. It is therefore worth defining two levels of *Performance*.

In the first level, *Performance_1*, only movement from the elbow is required while approaching the target; the elbow is fixed and the hand moves back and forth between the object to be grasped and the rest/release position of the arm [Figure 71].



Figure 71: A virtual-reality scenario implemented to evaluate the level of Performance_1. The subjects have to move only the elbow back and forth between the object and release position.

In the second level, *Performance_2*, the objects are uniformly distributed within the VR environment, at the same height, equidistant, and placed in circle. This placement requires the coordination of the whole body during reach-to-grasp movements. The subjects were instructed to always move forward, and the objects were always placed before them. The subjects walk from one object to the next, moving the whole arm, shoulder and elbow to approach the target, so this scenario allows the analysis of a very complex reach-to-grasp mechanism.



Figure 72: A virtual-reality scenario was used to evaluate the level of performance_2. In order to collect an object, the subjects had to make a step forward, move the shoulder and the elbow.

8.4. Control Strategies

8.4.1. GLOVE PROSTHESIS CONTROL

In order to objectively assess the performance in controlling prosthetic devices, an immersive virtual reality was proposed and developed during this study. Beside the flexibility to create new training or assessment scenarios, such a system has the advantage of offering a standardized environment which allows comparison of performance between subjects at different points in time. This would help to monitor progress through successive training sessions, or to compare performance between subjects who are geographically separated. For these tasks, the immersive VR looks to be a very promising tool. As it is driven by powerful industries, like the gaming industry, it continues to be highly dynamic in its development. However, affordable VR systems still do not allow reality-faithful interaction with objects within virtual environments. One of the most important challenges involved in this issue is the estimation of VR depth, but it is not the only issue.

Various prosthesis control strategies may be implemented in the virtual environment, but, due to current VR limitations, performance within a virtual reality cannot be directly compared with performance in real environments. Therefore, in order to have a reference for performance within VR, a VR-Glove was developed, and measurements were taken using this set-up. Healthy subjects have a VR-Glove attached to their hand and use it to control the virtual prosthesis in synchrony with the movement of their natural hand. The differences between VR-Glove measurements and grasping with a healthy hand in real environments will circumscribe the limitations of the VR technology.

The VR-Glove is able to measure the aperture and the force developed during grasping. The aperture is measured by a potentiometer placed between the thumb and index finger, while force is measured by a force transducer placed on the grasped object, mounted on the thumb [Figure 73]. This sensor placement allows a direct comparison with the performance of the prosthetic hand, which is similarly able to measure the aperture and grasp force.

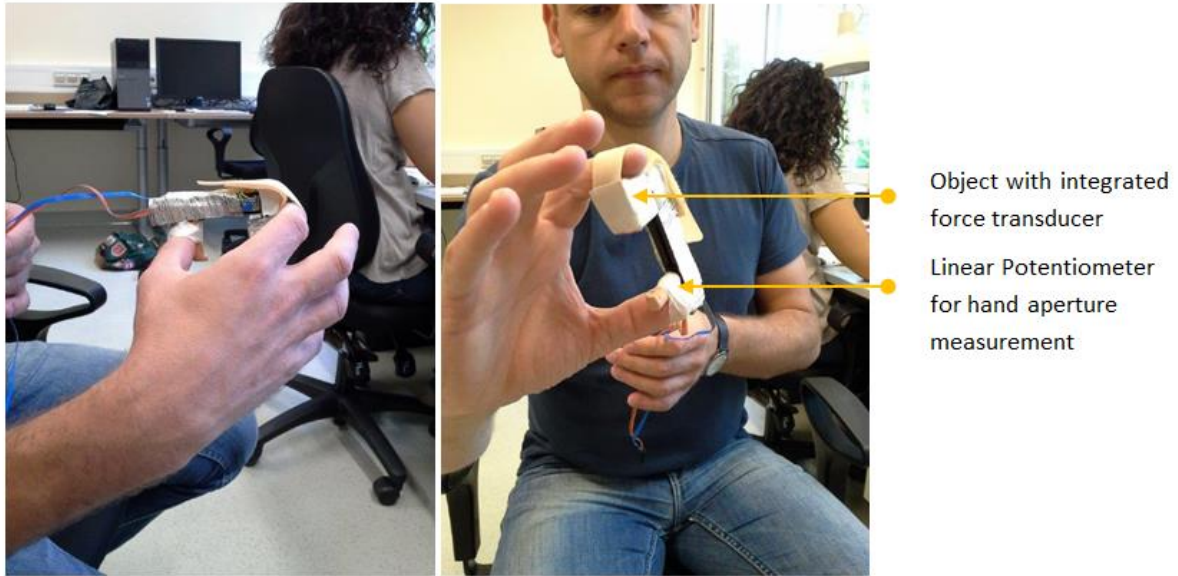


Figure 73: A benchmark measurement was performed in which able-bodied subjects collected the virtual objects with the natural hand, using a self-made “glove”. As with the prosthesis, the glove is able to measure the hand aperture and grasp force while grasping an object attached to the hand which has the same diameter as the virtual objects.

The object mounted on the hand has the same dimension as the diameter of the spheres within the VR. This strategy allows perfect congruency between the visually sensed VR grasp and the visually sensed VR-Glove grasp, but also by proprioception and tactile sensation of the hand.

The subjects performing within VR have the same target as the amputees will have: to collect the available objects within VR. However, they collect the spheres with their hand, while the amputees will do so by controlling the prosthesis. The outcomes during glove-control measurements will set the baseline for the next measurements with the prosthesis. By comparing prosthesis control relative to the glove control, it will be possible to clearly describe the characteristics of every control strategy, as distinct from the limitations of the VR itself.

8.4.2. PROSTHESIS IN THE CONTROL LOOP

A VR environment is a very powerful tool which allows flexibility in designing prosthetic devices with various kinematics and dynamics, or in implementing/testing various prosthesis control modes. It can be claimed however, that the virtual prosthesis may never faithfully replicate real prosthetics. The behaviour of physical devices is strongly influenced by tolerances and many other factors which cannot be entirely taken into account by the VR prosthesis. This is an important drawback, and could be the most important point of criticism when considering the immersive VR technology for such prosthetics applications.

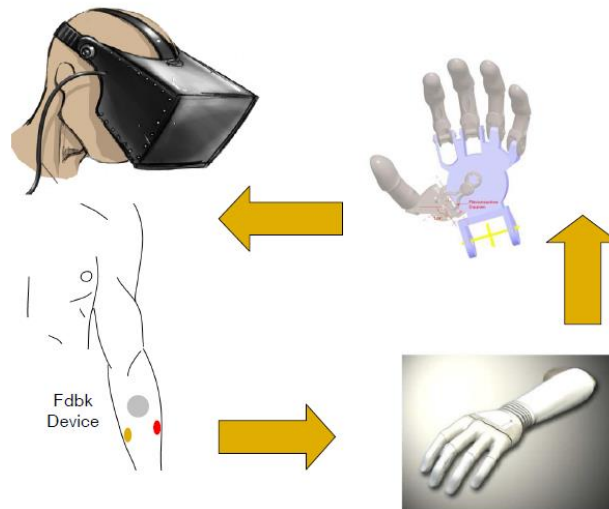


Figure 74: The virtual prosthesis might faithfully replicate the behavior of the real prosthesis, as the real prosthesis was included in the control-loop of the virtual prosthesis. The subjects wirelessly control a real prosthesis mounted on a table. The prosthesis' integrated sensory system measures the hand aperture and grip force which will control the virtual prosthesis "attached" to the subjects' forearm and visible in the video glasses.

In order to overcome this drawback, and to allow for a more realistic behaviour of the virtual prosthesis, the real prosthesis has been included in the control loop of the virtual one [Figure 74]. A control brace around the forearm of the subjects wirelessly controls the real prosthesis. Consequently, the prosthesis will move and grasp, and the sensors embedded in the real prosthesis will measure the aperture and the prosthesis grip force. This sensory information is then wirelessly forwarded to the VR environment, controlling the aperture and the grasp of the virtual prosthesis. As a result, the virtual prosthesis will move and grasp in synchronicity with the real one.

8.4.3. VR PROSTHESIS CONTROL

Performing within virtual environments has some drawbacks, as previously discussed. These drawbacks were minimized by, e.g. having a shadow of the target object attached to the hand or including the real prosthesis in the control loop of the virtual one. However, working with real prostheses is not always beneficial for research purposes when e.g. new control approaches, new prosthesis kinematics or new dynamics are intended to be evaluated. Research requires high degrees of flexibility, but physical devices have on one hand constructive limitations, on the other hand the behavior of the prosthesis is hard-encoded in the embedded software. These limitations of using real devices cannot be overcome, but the fast-developing virtual technology is a promising alternative. In order to exemplify how VR might be used as research tool, three control strategies were implemented:

- a derivative strategy in which the prosthesis will uniformly and continuously change its status (position and/or grasp force) for a constant value of the control signal
- a proportional strategy in which position and/or grasp force changes proportionally to the magnitude of the control input
- a hybrid strategy emulating real prosthesis behavior, in which prosthesis position continuously changes when the control input is kept constant, while the force is proportional with the control input.

8.5. Assessment and Comparison of Prosthesis Control Strategies

8.5.1. CONDITIONS

In order to evaluate the implemented control strategies, two grasping scenarios were considered: the first one with a force target between 10-50% of the maximum measurable force, and the second with a force between 50-90%. These scenarios are shown in Figure 75. The green range represents the target force, while the yellow circle shows the measured force. In both the low- and high-force cases, the virtual prosthesis has no contact with the object, so the measured force is zero. However, when the object is grasped, the diameter of the yellow circle will decrease with increasing grasp force. At 100% grasp force, the yellow circle will appear as one point in the center of the object. The maximum measurable force was set to 20 N.

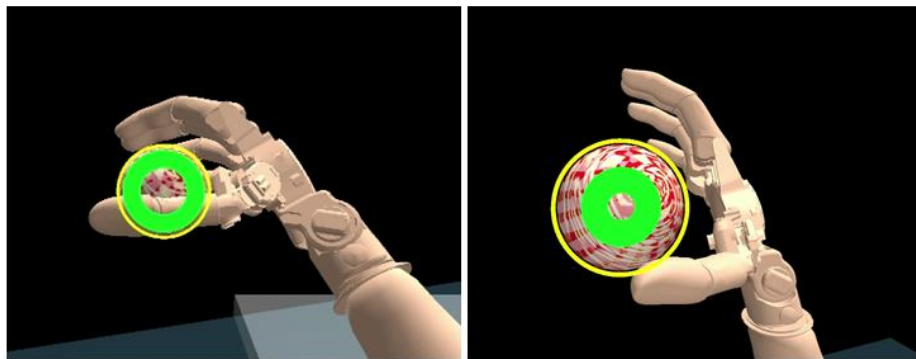


Figure 75: Two types of objects were used during this study, light (left) and hard (right). In order to collect light objects a grasp force within 10-50% of the maximum measurable force was required and for hard objects the grasp force was within 50-90%.

The evaluation of performance was done by comparing the time-to-complete (TC) required for successful grasps in all conditions. The TC is the time, measured in milliseconds, between the initiation of the hand grasp and the moment at which the target force is successfully reached.

8.5.2. GLOVE PROSTHESIS CONTROL

The subjects immersed in the virtual environment collected objects with the virtual prosthesis, the virtual prosthesis being controlled by the natural hand and the VR-Glove. The level of *Activity*, as well as the level of *Participation_1* and *Participation_2* was evaluated. During *Activity* evaluation, the objects were attached to the hand, and the subjects paid attention only to grasping, while during *Participation_1* and *Participation_2* the grasp was preceded by reach-to-grasp movements. The outcomes presented in Figure 76 describe only the grasp for all 3x2 conditions (*Activity*, *Participation_1* and *Participation_2*, for low and high targets). The “Grasp Time” is measured, for all 3x2 conditions, as the time elapsed between the moment in which the prosthesis started to grasp until the moment in which the target force was reached; the same approach to measuring the TC would allow for a direct comparison of all considered scenarios 1-3. The reach-to-grasp movement for *Participation_1* and *Participation_2* is analyzed in the following section.

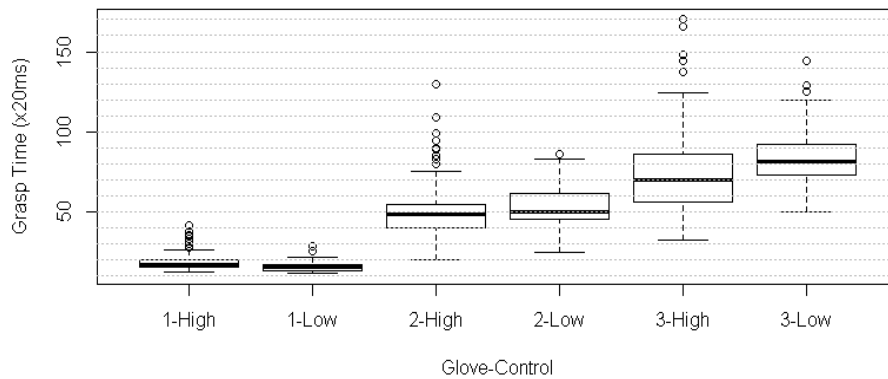


Figure 76: Glove-Control - the level of activity, performance_1 and performance_2, for high as well as for low force target, were evaluated from the direct comparison of the measured “grasp time.”

Because the VR-Glove is controlled by a healthy hand, the level of *Activity* should allow for the evaluation of all delays introduced by the system, e.g. by the wireless communication or rendering of the virtual scenes. The results obtained for this condition, depicted in Figure 76, show a TC for the 1-High and for 1-Low of around 300 ms (1-High corresponds to *Activity* for high target and 1-Low to *Activity* for low target). The TC shows minimal delays introduced by the system, which indicates that grasping within VR can faithfully replicate grasping performed with the natural hand within real environments.

One characteristic of the data is the similarity between Low and High within each of the three conditions. This is mainly explained by the large width of the target, 10-50% for Low, and 50-90% for High. The large width of the force target - 40%, was chosen to reduce the degree of difficulty of the performed tasks. Being successful in accomplishing their targets, the subjects were motivated to further perform and increase their ability in

controlling the prosthesis. However, future studies should better define the right compromises which will need to be made in order to define the optimal target width. This will better describe the level of difficulty of the task, while guaranteeing a motivating success rate for the subjects. This is no trivial task, as the function describing the correspondence between precision of control (target width) and success rate is individual, non-linear and continuously changes with training, experience and other factors.

A very interesting outcome was the large difference between the Grasp Time recorded for *Activity* (1-High/Low) and *Performance_1* (2-High/Low). During *Activity*, the objects stick to the hand and the subjects only concentrate on grasping, while during *Performance_1* the subjects should also hold the hand over the object during grasping. This requires a high level of attention, making the grasp more demanding and explaining the increase of the Grasp Time from 400 ms to 1s for accomplishing the same task.

Another reason for this increase may be a lack of precision when estimating the VR depth. Holding the prosthesis over the object, while grasping within virtual reality, is mainly supported by visual feedback and proprioception. To try to minimize the bias introduced by proprioception and poor estimation of 3D depth within VR, the *Performance_1* task was designed to minimize the movement chain involved for accomplishing the task: the subjects were required only to move the elbow, and to swing the forearm between two known positions. Nevertheless, the gap between the *Activity* and *Performance_1* was still large.

In order to evaluate to what extent the proprioception is influencing the grasp process, a second *Performance_2* task was considered: *Performance_1* involves only the movement of the elbow joint, while, for *Performance_2*, the subjects made a step toward the target and moved the shoulder and the elbow. Reaching during *Performance_2* involves a much more complex chain of movements, and the expectation was that the TC would increase. This supposition was confirmed by the results in Figure 76, but the difference between *Performance_1* and *Performance_2* was lower than expected.

Larger movement chains decrease the precision when holding the prosthesis over the target object and preparing the grasp. However, the influence of biased proprioception does not explain the large gap between *Activity* and *Performance_1*. This is mainly determined by the lack of tactile feedback at first contact with the target. During natural grasping, the human approaches the target and, at contact with the object, close the fingers to optimally grasp. Grasping is an automatism triggered by the first contact (tactile sensation) with the object, and is therefore fast.

The lack of tactile feedback is characteristic not only for the virtual prosthesis, but also for grasping with a real prosthesis within real environments. The first contact with light objects, which is mostly the case during ADL tasks, is detected only visually. If the objects are heavy, the contact will be detected also at the stump as reaction force. Grasping with the prosthesis should be easier within real than within virtual environments. However, the differences between *Activity* and *Performance_1* within VR better emphasize the importance of the first contact when the target object is approached.

Aiming at better embodiment of a prosthesis by an amputee requires decreasing the cognitive effort to control the prosthesis. It has been assumed, and partially proven by various studies, that haptic feedback for grasp force can facilitate a more intuitive prosthesis control. Nevertheless, the current outcomes indicate that the tactile feedback for first contact with the object is, by far, more important, but only when it triggers the grasp as an automatism.

This mechanism would better replicate the natural grasp. While approaching the target, the hand is pre-shaping, preparing it for an optimal grasp. When close enough, the fingers are expecting contact with the target. When the contact is acknowledged, based on tactile information and on hand proprioception, the fingers optimally grasp the target subconsciously, as an automatism reconfigures them.

8.5.3. HYBRID PROSTHESIS CONTROL

During the previous condition, the VR prosthesis was controlled by the hand itself; a VR-Glove, accommodating position and force sensors, measured the hand performance, and the resulting signals synchronously controlled the virtual prosthesis. The gap between *Activity* and *Performance* evaluation emphasized the importance of the grasp mechanisms triggered by the first contact. In the virtual reality, the interaction between the hand prosthesis and the target objects is perceived only visually, which makes the grasping tedious, generating the gap previously observed.

Similar to a VR prosthesis, real prosthetic devices lack the first-contact mechanisms, making the transition between reaching and grasping a mirror of the interaction within VR. When grasping with real prostheses in real environments, the amputees have to carefully position the prosthesis over objects and slowly grasp in order to avoid damaging the target. This process, very demanding, is considered to be an important drawback when attempting to grasp harmoniously with prosthetic devices.

In the case of EMG control of prosthetics, this might be even worse. While approaching the target, amputees have to generate EMGs to close the prosthesis, preparing it for grasp, so they have to distribute their attention between holding/moving the arm and generating EMG for control, making grasping a very tedious cognitive effort. Therefore, it has been supposed that EMG prosthesis control might influence the movement fluency when grasping.

The previous measurements were repeated, this time with the VR prosthesis being controlled by EMG rather than by the glove [Figure 77]. The prosthesis was controlled in hybrid (voltage) mode, emulating the behavior of a real prosthesis, so that the EMG was proportional to the velocity when moving, and to force when grasping.

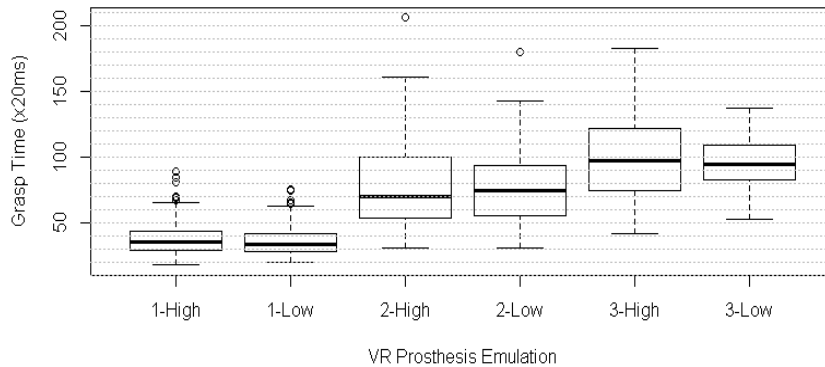


Figure 77: Hybrid Control - the level of activity, performance_1 and performance_2, for high as well as for low force target, were evaluated from the direct comparison of the measured “grasp time.”

As with the glove, the outcomes show no significant differences between the low and high target conditions, during *Activity* or *Performance*. However, the EMG controlled prosthesis required 700 ms for a grasp, compared to 300 ms during the glove control. When simulated in software, the prosthesis has no constructive limitation, thus has ideal dynamics. Nevertheless, the difference between glove and EMG control is significant, determined only by the delays introduced by the EMG processing.

Comparing the outcomes during VR-Glove Control and VR Prosthesis Emulation, the same trends can be observed in both the *Activity* and *Performance* conditions, but the grasp time was shifted 500 ms upward during the VR Prosthesis Emulation condition. Also, the gap between the *Activity* and *Performance_1* conditions is comparable to that obtained during the glove measurements. This indicates that the lack of first-contact recognition has the same influence on the flow of the reach-to-grasp movement for EMG control as it does for VR-Glove control.

The outcomes also reveal that the cognitive effort required during muscle contraction does not dramatically influence the TC. Nevertheless, there is evidence that there is some difference, and this topic should be more precisely addressed during further research. The influence of the larger cognitive effort required by EMG generation is narrow when compared directly to the delays introduced by the lack of first contact. These outcomes emphasize, once more, the importance of first contact for movement flow.

8.5.4. COMPARISON OF PROSTHESIS CONTROL STRATEGIES

As previously discussed, several control strategies were implemented: the glove-control, proportional, derivative or hybrid (voltage) control. Moreover, the real prosthesis was also integrated into the loop of VR prosthesis control. In order to identify weaknesses and strengths of the implemented control strategies, a direct comparison was made. The same TC was used as a qualifier for comparison: the amount of time that elapsed between starting to close the hand and when the target force was reached.

The strength of a control strategy should be visible when evaluating the level of *Performance*. However, evaluating *Performance* implies the interplay of many factors which will reduce the accuracy in identification of the individual characteristics of each control strategy. Therefore, the level of *Activity* was used for a more direct comparison. The electrodes were placed on the forearm and correspondingly adjusted. The same set-up was then used by the subjects to control the prosthesis in all five implemented control strategies. This allowed for a much more transparent comparison of the strengths and weaknesses of each control strategy [Figure 78]. The reach-to-grasp movements were considered to be disturbing for the specific evaluation of performance for every control strategy. Thus, the objects were attached to the hand, to allow the subjects to fully concentrate only on grasping.

The first condition was the glove measurement (1-High/Low), followed by the second condition, in which the real prosthesis was integrated into the VR control loop (2-High/Low). The third condition tested the performance of the VR prosthesis in hybrid (voltage) mode, which is the emulation of a real prosthesis (3-High/Low). The fourth condition used the derivative mode (4-High/Low), in which the speed and yank (force derivative) are directly controlled by EMG. The fifth condition (5-High/Low) tested proportional control, in which position and force are directly controlled by a movement reference resulting from the EMG processing.

For the last three control modes - hybrid (voltage), derivative and proportional - the prosthesis behavior was entirely simulated; no constructive constraints were considered, so its behavior was ideal. The task to be completed was the same for all strategies: to cyclically grasp objects with predefined force targets High (50-90% of max.) and Low (10-50% of max.).

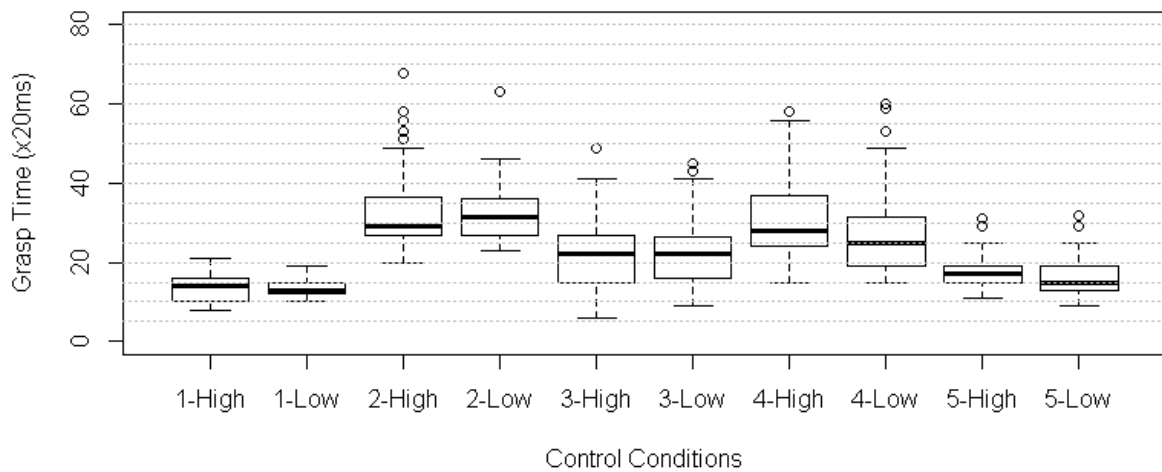


Figure 78: Comparison of the prosthesis control strategies. 1- glove control, 2 - real prosthesis integrated into the control loop of the virtual prosthesis, 3 – hybrid control, 4 – derivative control, 5- proportional control.

As expected, the direct comparison between all implemented control strategies reveals that the best TC was obtained during VR-Glove control. The prosthesis was controlled in synchrony with the healthy hand moving the glove, and the objects were attached to the hand. This set-up allows performance very similar to natural grasping, and it was regarded as a reference for comparisons with the other strategies. At the other extreme were the results obtained during the second condition. The subjects performed the same task, immersed within the VR, but the visible virtual prosthesis was the shadow of the real one, which was wirelessly controlled by the subjects.

In addition to the delays introduced by the EMG processing, the constructive limitations of the physical prosthesis also counted against the final result, explaining the largest TC among all conditions. The first two control strategies defined the borders of the TC range: the VR-Glove control similar to the natural behavior, and the real prosthesis with all its limitations. The third strategy (hybrid) simulated the real prosthesis: the EMG controls the prosthesis velocity previous to grasping, and force after grasping. It doesn't include the delays introduced by electro-mechanical components of the prosthesis, so it requires a lower TC for grasping. The delay introduced by the prosthesis was evaluated at around 300ms. Approximately the same gap was measured between the simulation of the real prosthesis, and the VR-Glove control (300 ms).

The next two control strategies have a characteristic which differentiates them from the hybrid control. In hybrid mode, the prosthesis has a derivative response when moving, and a proportional one during grasping. This might be demanding for the amputees, as they have to readjust their behavior when generating EMGs, in

accordance with the status of the prosthesis. Therefore, for comparison, a pure derivative strategy was adopted during the condition 4-High/Low and a pure proportional strategy during the condition 5-High/Low.

The derivative (4-High/Low) and the proportional prosthesis control (5-High/Low) are considered to be less demanding than the hybrid mode (3-High/Low) because the same EMG contraction similarly controls the movement and the grasp. Though derivative control better copes with the noisy EMG signals, it does have the drawback of being slower. Proportional control, on the other hand, is the fastest among the EMG control strategies. During movement, as well as during grasping, the preprocessed EMG signals set up the position and the force of the prosthesis. Compared with all implemented strategies, the performance of the position control is closest to the glove-control.

8.6. Prosthesis-Limb Coordination

Coordinating the movement of the natural limb with the movement of the prosthesis is the ultimate goal when the aim is embodiment of a prosthesis by an amputee. The degree of simultaneity is a very important qualifier, revealing how confident the amputee is in using the prosthesis, and how large the required cognitive effort in controlling it. Large delays between reaching and grasping show that the amputee has to dedicate special attention to control the prosthesis. Decreasing this gap is an indication that they are more and more able to distribute their attention in accomplishing parallel tasks, which is closer to natural behavior. Distributed attention when controlling multitask systems, however, requires a high degree of consistency when controlling the prosthesis. The amputee has to generate goal-oriented commands and the prosthesis should consistently execute the movements. If the prosthesis behavior is not consistent enough with the amputee's intention to move, he/she is forced to continuously assist and correct the prosthesis trajectory, which seriously affects the intuitiveness of the control.

In order to analyze the degree of simultaneity between body and prosthesis movement and, consequently, the intuitiveness of prosthesis control, two scenarios were used. In the first scenario, able-bodied subjects controlled a glove with their natural hand. The signals measured by the glove - hand aperture and grasp force - drove the VR prosthesis. During the second scenario, the virtual prosthesis implemented the EMG prosthesis control common in commercial systems: the hybrid/voltage mode. For these measurements, the virtual prosthesis was used instead of the real one because of a concern that the delays introduced by the physical prosthesis would strongly influence the synchronicity of the body and prosthesis movement. The goal was to identify to what extent the subjects were able to generate EMGs for prosthesis control, while at the same time moving their bodies. Therefore, the subjects controlled a virtual prosthesis, which has an ideal behavior.

8.6.1. GLOVE PROSTHESIS CONTROL

During this task, the virtual prosthesis was a shadow of the natural hand. Able-bodied subjects wore a glove that was able to measure the hand aperture and the grasp force. These signals directly drove the virtual

prosthesis. The virtual prosthesis had a behavior very close to that of the real hand, considered a reference for the following measurements.

The task to be accomplished by the subjects was to grasp a low-force target, while swinging the arm from elbow between target and home positions. The elbow movements between these positions are shown by the blue plot in the figure below. The green plot represents the hand aperture between open and grasped states (normalized between 0-100%), and the red plot is the grasp force [Figure 79].

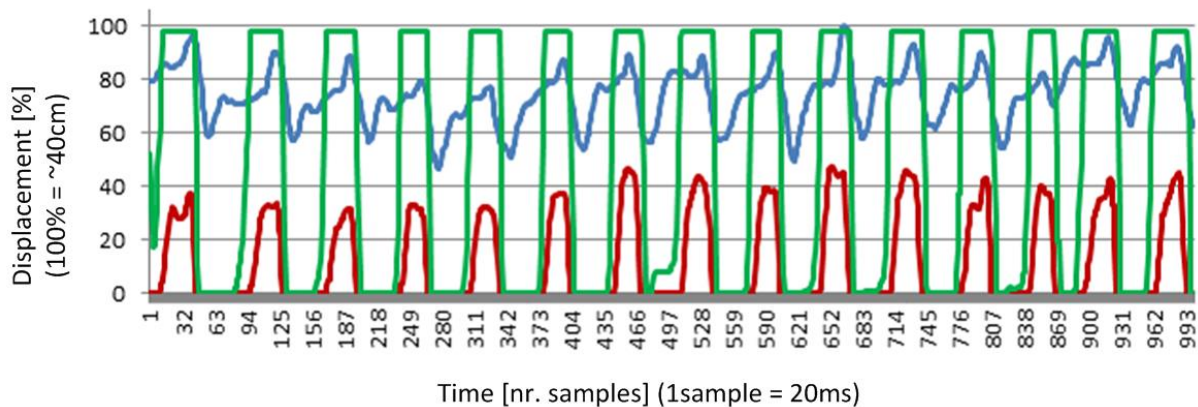


Figure 79: Glove performance_1 – the coordination between hand aperture and hand movement while approaching the target (reach-to-grasp task).

Within a window of 1000 samples (20 seconds) it was possible to perform 15 grasps, indicating an average of 1,3 grasps/second. This time includes grasping and releasing, as well as the hold time during which the hand was steadily open or closed. The time to complete is an important qualifier describing the level of confidence of the amputees during grasping, but not the primary qualifier, which is the degree of synchronicity between grasp and movement of the elbow.

Analyzing Figure 79, it is visible that the objects were grasped while the hand was continuously moving. Almost no stops preceded grasping, and the zig-zag profile of the hand showed a very good symmetry when grasping and releasing. However, before grasping there was always a small nose identifiable in the blue plot. This may be explained by a small hesitation just before grasping.

The second Performance evaluation examines the capacity of the subjects to synchronize the grasp with the movement of the whole body. While grasping, the subjects make a more complex movement, a step forward, movement of the elbow and the shoulder. This increase in the complexity of the movement chain resulted in a deterioration of performance. Movement of the elbow and the grasp of the hand are two distinct phases which do not overlap. The blue profile lost the uniformity during grasping and releasing; releasing was fast, while grasping became slow [Figure 80]. The delay, just before grasping, clearly indicates that the subjects required

time to readjust the hand position to successfully pick up the objects. Because the chain of the body movement is larger, the error in positioning is larger.

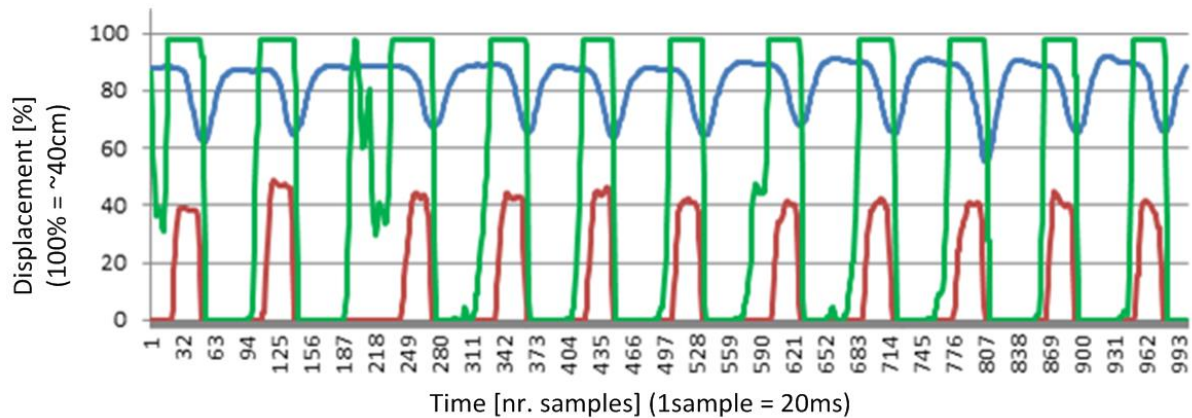


Figure 80: *Glove performance_2 – the coordination between hand aperture and hand movement while approaching the target (reach-to-grasp task).*

The glove prosthesis control offered conditions similar to the control of the natural hand during grasping. Therefore, the lack of fluency during movement may not be explained by lack of prosthesis controllability, but by lack of feedback. During natural grasping the hand is subconsciously looking for contact with the target, and only after contact is the grasp executed. Natural grasping is however preceded also by hand pre-shaping, which makes the transition between look-for-contact and grasping phase almost invisible.

8.6.2. HYBRID PROSTHESIS CONTROL

The previously described glove prosthesis control revealed the importance of the feedback regarding contact with the target object just before grasping. The virtual prosthesis was controlled by a glove with the subject's natural hand. It would be of interest for real prosthetics to evaluate if, and to what extent, EMG control influences the coordination between body movement and grasp. Prosthesis control by EMG requires an additional cognitive effort from amputees, resulting in additional time taken to complete a grasp. This was confirmed by measurements performed during the evaluations of *Performance_1* [Figure 81], and *Performance_2* [Figure 82].

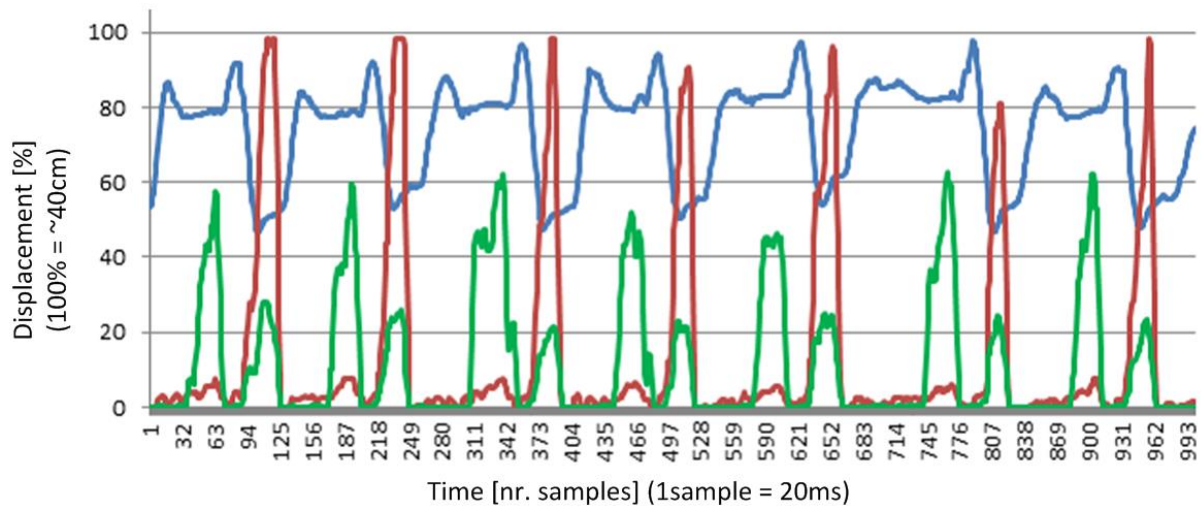


Figure 81: Hybrid performance_1 – the coordination between hand aperture and hand movement while approaching the target (reach-to-grasp task).

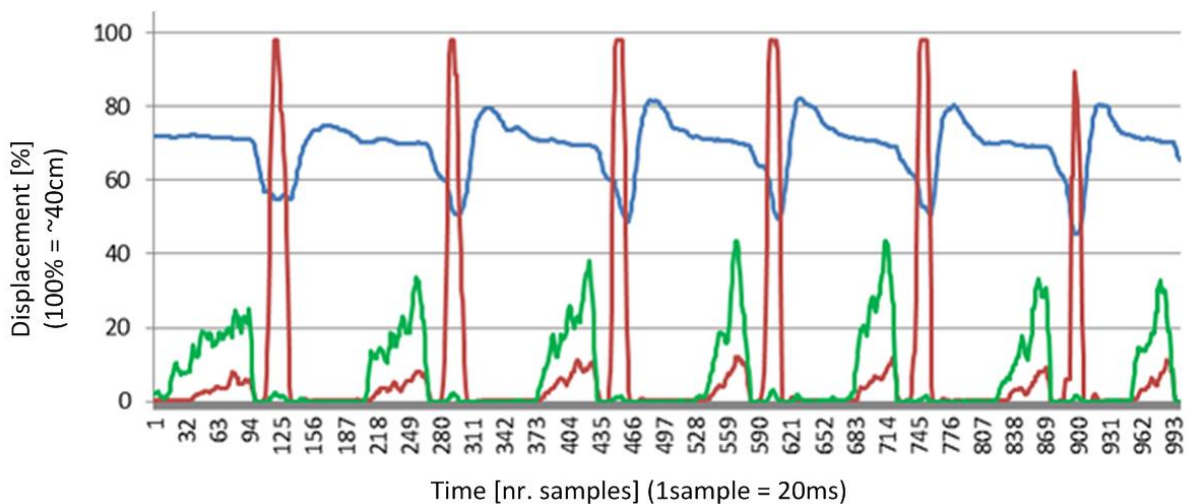


Figure 82: Hybrid performance_2 – the coordination between hand aperture and hand movement while approaching the target (reach-to-grasp task).

A direct comparison between EMG and glove prosthesis control revealed a general trend: in *Performance_1* as well as in *Performance_2*, the EMG controlled prosthesis is less well-coordinated with the natural movements, and the frequency of grasps also decreased substantially. In *Performance_1*, the number of grasps decreased from 15 during glove measurement to 7 during EMG control, and in *Performance_2*, from 11 to 7, respectively. The grasp task with the glove was more dynamic than that with EMG control; therefore the increase in difficulty from *Performance_1* to *Performance_2* was more evident, described by the decrease of the number

of successful grasps. The EMG control was, however, slow and the frequency of the grasps during *Performance_1* and *Performance_2* has been shown to be the same.

The longer the chain of the natural movement, the less precise the reach-to-grasp movement is, but the delay introduced by the EMG processing completely masked these differences. This indicates that the reaction time required by EMG processing while the hand is approaching the target makes it almost impossible to pre-shape the hand to prepare the grasp. These measurements were performed with the virtual prosthesis which is able to instantaneously react to the movement references generated after EMG signal processing. The conclusion: the delays introduced by the EMG processing were solely responsible for the dramatic decrease in system performance. The consequence is that, when using a real prosthesis, it is almost impossible to synchronize the prosthesis with the body movements, and the goal of integrating the prosthetic device into the amputee's body image remains a matter for future research.

9. DISCUSSION

The current work was initially inspired by the opportunity offered by the phantom limb phenomenon to better integrate prosthetic devices into the amputee's body image. Providing haptic feedback in congruence with movement intent, was expected to produce results similar to mirror therapy. If haptic feedback is present and integrated into the socket at all times, rather than only during therapy sessions, it will allow for conditions more conducive to long-term alleviation of phantom pain. The results obtained from mirror therapy are not merely a matter of feedback; the mirrored hand feels (visual feedback) and behaves as if it were the natural hand, congruent to and in accordance with the movement intent.

While the topic of phantom pain alleviation is very broad, the current work tried to be more focused, and mainly addressed the prosthesis embodiment process. Prosthesis embodiment targets better integration of a prosthetic device into an amputee's body image, and is considered a necessary condition to assist in alleviation of phantom limb pain.

A well-embodied prosthesis, it is obvious, will move, look and feel like a natural limb. However, replicating the natural limb, its kinematics, dynamics and interface with the central nervous system (CNS) is a very challenging task. A high-degree-of-freedom prosthetic device, moving with similar consistency and dynamics as the natural limb, is the ultimate goal, but high dimensionality is extremely challenging, requiring good interfacing of technology with the human entity's CNS. The current technologies are not entirely able to cope with the complexity of the neural information which encodes the amputee's movement intent. The higher the dimensionality of the interface, the lower the quality of the individual control channels. Thus, in order to maximize the quality of the control signals, the dimensionality was reduced to the case of a prosthesis with a single degree of freedom; the only capability of the prosthesis was grasping. Additionally, closed-loop prosthesis control was targeted by providing haptic feedback to the amputees. Intensive bidirectional informational transfer between amputee and prosthesis in a closed-loop paradigm was considered to allow the best conditions for achieving intuitiveness of prosthesis control and prosthesis embodiment. The level of intuitiveness was quantified as the subject's capacity to simultaneously control the prosthesis with the movement of the body. Only when this level of confidence is achieved, can the increase of the interface dimensionality be addressed.

While prosthesis controllability has been extensively addressed in the past, this study was more focused on closing the prosthesis control loop by providing haptic feedback to the amputees. In the incipient phase of the study, a literature review was conducted, in order to identify the available wearable SOA stimulation technologies. Results indicated that the rotary vibro-motor, in the form of a DC motor spinning an eccentric mass around its rotating axis, was one of the most widely implemented approaches. This technology is accessible, low cost, simple, practical, and energy efficient, and is therefore routinely embedded in such consumer electronics products as pagers, mobile phones and game controllers.

As indicated in various studies, this type of motor may be used to close the upper-limb prosthesis control loop, by providing vibro-tactile feedback to the amputees, informing them about the current grasp force developed by the prosthesis. In order to reproduce the results reported in the literature, the same set-up was implemented; the grasp force was measured by the OB Sensor-Hand prosthesis and encoded with vibro-tactile feedback generated by a vibration motor. The measured force proportionally controlled the voltage driving the vibration motor. Consequently, higher forces were encoded by vibrations having higher amplitude and frequency, and lower forces by vibrations having lower amplitude and frequency.

The vibration motor was integrated into the socket fitted on the forearm of an amputee, and a preliminary evaluation was made. This system has proven to be able to encode few force levels (5 or 6) with discriminable vibrations, and the results from the literature were confirmed: the haptic feedback regarding grasp force determined that amputees will typically grasp the same objects with less force with feedback than without it. On the other hand, grasping required more time and more attention from the amputees, which made the prosthesis control demanding and non-intuitive. It could be claimed that a longer accommodation period with this system would help the amputees to better understand the perceived feedback and consequently to perform faster, but the subject reported that the stimulation was annoying and rejected the idea of having such a system for daily use.

One explanation for this rejection was the discomfort generated by continuous vibration during grasping. Secondly, the stimulation itself was reported as being non-intuitive and very disturbing, which led to the idea that the stimulation parameters used to encode force did not physiologically match the tactile receptors embedded in the skin, i.e. the frequency and amplitude of the vibration did not cover the range allowing comfortable and intuitive perception of the stimulation.

During the next trials, a derivative of force, instead of force itself, was encoded with vibrations. During steady-state grasp, no vibrations were generated, but the changes of the grasp force were encoded with vibrations, and the magnitude of the delivered vibration bursts was proportional with the magnitude of the force derivative. This is a much more physiologically based mapping between the measured force and vibro-tactile feedback, better reproducing the natural interaction. Grasping with the natural hand generates vibrations at contact with an object or when dynamically grasping. This encoding is closer to how humans perceive interaction with the environment, but can be implemented only by technologies able to react quickly and deliver stimulation with higher resolution. The classical vibration motor is slow, and the resolution and diversity of the stimulation are low, characteristics which do not recommend it for this kind of application.

Another advantage of encoding the derivative, and not the absolute measured force, is the strong emphasis on the first contact when grasping. At first contact, the force derivative results in a strong spike signal which may be simply and effectively encoded by the haptic feedback. As known from the literature, and as also indicated in the performed studies, first contact is essential, being a kind of trigger for grasping. During approaching movement, the hand is pre-shaped, preparing the grasp; but grasping will only be initiated after the contact

signal is perceived. The contact can be perceived with fingers or palm, then the fingers will simultaneously close, optimally grasping the target. This process of natural grasping is subconsciously performed, based on hand proprioception, and allowed by the flexibility with which the natural hand is able to grasp. The prosthesis doesn't allow this flexibility and the embedded sensorial system is very limited. However, the mechanisms triggered by first contact, inspired from the natural behavior of the hand, may provide good recommendations to develop semi-automatizations, increasing intuitiveness of prosthesis control.

Further, in order to be able to close the prosthesis control-loop, various haptic technologies have been investigated. The goal was to identify the one most suitable for conveying the sensory information measured by prosthetics into haptic feedback. These technologies were characterized by various advantages and disadvantages. Mechanical stimulators naturally address the mechano-receptors in the skin, providing consistent and reliable stimulation, but the amount of discriminable stimulation is narrow. On the other hand, electro-stimulation is able to generate much more complex patterns by simultaneously controlling the amplitude and frequency of the stimulation. However, the electrical currents delivered at the surface of the skin stimulate the afferent nerves innervating the mechanoreceptors globally, but not the mechano-receptors directly, resulting in a diffuse sensation. The most important drawback of the electro-stimulation was the practicability in prosthetics of daily use. Acceptable stimulation requires self-adhesive electrodes placed on the surface of the skin, which seriously impedes the practicability of this technology. All these technologies were implemented. In addition, a novel self-made vibro-tactile device was proposed. This novel methodology is able to provide vibro-tactile stimulation in the range of 10-250 Hz. In this way the skin's mechano-receptors sensitive to vibrations are optimally activated: the Merkel disk (5-15Hz) sensitive to extremely low frequencies, Meissner's corpuscles (20-50 Hz) sensitive to midrange stimuli, and Pacinian corpuscles (60-400Hz), with the lowest detection threshold at 250Hz, sensitive to high-frequency vibrations. The amplitude and frequency of the vibration can be independently adjusted, allowing for the generation of a large variety of differentiable stimulation patterns.

A pool of various haptic technologies were tested, some of them stimulating in different modalities. The next serious challenge was to find a methodology to assess the capacity of these technologies to induce tactile stimuli in humans. In comparing stimulation technologies, stimulating in the same modality, using, e.g. accelerometers, force transducers or other sensors, is a trivial matter. Nevertheless, if the stimulation is provided in different modalities, e.g. mechano-stimulation versus electro-stimulation, the comparison may be made only when performing psychophysical measurements. Psychophysical measurements evaluate how much of the provided stimulation is perceived by humans. Since the tactile sensitivity of the skin strongly varies with the body sites, these measurements are valid only with regard to the specific site of the skin on which the stimulation device was placed during measurement.

A literature review was conducted in order to identify the optimal psychophysical method for evaluating perceived haptic sensations. These methodologies were generally developed for the evaluation of acoustic or visual stimulation; however, vibro-tactile perception has some individual characteristics, which required the

adaptation of these methodologies. Therefore, a modified version of the single-interval adjustment matrix procedure (SIAM) was utilized to construct a detailed psychophysical model of the stimulation. Determining a model of the stimulation is challenging and time consuming, but this effort is rewarded by the possibility of optimally mapping the sensor signals to the stimulation. This allows an efficient transfer of information between sensors and humans, exploiting the full capacity of the stimulation device to transmit information haptically to the amputees.

The natural interaction is characterized not only by vibration, but also by steady pressure and combinations of pressure and vibration. In order to better reproduce this interaction a few new devices were developed. One of the most successful trials was the “Haptic Brace.” The haptic brace consists of a motorized brace which can be strapped around the arm. The motor driving this device pulls and releases the brace, generating a fast but light sensation of squeezing. The stimulation has proven to be easily discriminable and intuitive, stimulating the whole circumference of the arm. Importantly, the device not only stimulates the receptors embedded in the skin, but also the proprioceptors of the muscles. Remarkably, the haptic brace, using only one BLDC motor, is able to induce many types of stimulation: local AF modulated vibro-tactile stimulation patterns, steady-state circumferential pressure, and circumferential vibration obtained by pulling/releasing the brace with high frequency.

The stimulation provided by the haptic brace is highly complex, being the interplay of many individually adjustable stimulation primitives: amplitude and frequency of the local vibration, amplitude and frequency of the circumferential vibration, absolute position or velocity of the squeezing brace as well as the maximum allowed squeezing force. If all these primitives are combined, it allows for the generation of very intuitive stimulation patterns. The next challenge raised by the haptic brace was to properly combine all available primitives to create intuitive and comfortable stimulation patterns.

The mechanism for generating stimulation patterns should allow diversity in combining stimulation primitives while maintaining flexibility and remaining easily adjustable. The pattern-generation mechanisms should be regarded as a block whose inputs are the sensory information measured by the prosthesis, with the outputs individually controlling the stimulation primitives. Every output is a weighted linear combination of all inputs and the individual patterns are defined by the coefficients of this linear transformation.

The stimulation patterns should not necessarily be strong in order to be well-perceived. Ideally, the stimulation should be as “silent” as possible, but still effective, allowing the amputees to accomplish tasks that would be impossible without feedback. Designing stimulation patterns is not trivial, as the stimulation has to be comfortable and intuitive, in accordance with the described prosthesis performance. For this purpose, the potential offered by the Rubber Hand Illusion (RHI) was exploited. The RHI is achieved by convincing someone that a rubber hand is their own by putting it on a table in front of them, while stimulating it with a brush in synchronicity with their real hand. This illusion opens new perspectives in understanding how sight, touch and proprioception combine to create a convincing feeling of body ownership. In order to evaluate how intuitive

the provided patterns were, the brush stimulation was replaced by artificial stimulation and the depth of the induced illusion characterized the level of intuitiveness of the stimulation pattern.

Having developed a collection of stimulation patterns, the next step was to map them with sensory-information describing the prosthesis performance. The considered prosthesis had only one degree of freedom, so its performance was described by hand aperture/velocity and grasp force. In an augmented reality environment, different mappings between prosthesis, visual feedback and haptic feedback were tested, resulting in some interesting outcomes. Encoding the prosthesis performance, in a feed-forward fashion, is more effective and intuitive than a pure feedback approach. The grasp was more intuitive when the amputees forecasted the grasp force from prosthesis velocity than when the force feedback was transmitted to the amputees directly as feedback. Contrary to a popular opinion, it seems that the commercially available prosthetic systems do provide indirect information about the grasp strength and that grasping is therefore not completely blind as usually assumed. During movement (close), the prosthesis velocity is proportionally controlled by the EMG, and during grasp by the grasp force. Consequently, the developed grasp force is proportional with the velocity of the prosthesis just before grasping (feed-forward control). Shared control, merging both feedback and feed-forward control strategies, will better reproduce the natural mechanisms of grasping, and this will be addressed during further research.

Prosthetic devices are thought as a replacement of the natural limb; however they are connected to the CNS differently, and so are also controlled differently. When a movement intent is expressed by an able-bodied person, the hand follows it completely, the hand-control benefitting from all available neural information. However, when amputees contract residual muscles in the stump, with the intention to move the prosthesis, only a narrow amount of the neural information is available, sensed as EMGs. Commercial prostheses use the sensed surface EMGs mainly to control the velocity of movement and the grip force. During this study, some other mappings were evaluated: derivative, proportional, and voltage mode. The outcomes indicated advantages and disadvantages for all implemented mappings. The derivative mode has advantages when the EMG quality is poor, but is slow and less intuitive. On the other hand, the proportional mode is fast and intuitive, but requires feedback about grasp and good quality of controlling EMGs. Proportional or derivative mode can be a challenge to implement in a daily-life prosthesis without feedback informing the amputee about the grasp force. The voltage mode is a good compromise, allowing good control of the grasp due to the predictive approach to controlling the grip force based on the velocity just before closing, and intermediate performances between derivative and proportional modes. Voltage mode is mostly used in commercial prosthetics; however, future efforts have to be made toward developing and implementing proportional control, which is faster and more intuitive.

The goal targeted by this research was better integration of prosthetic devices into an amputee's body image. Amputees should feel that their prostheses are part of their own body, and be able to move them in harmony with body movements. Humans are able to integrate external tools with their actions, and feel at the tip of a tool - *Extended Proprioception*, the tool being perceived as an extension of the body augmenting the reachable

space. When writing with a pen, we consciously feel the contact of the pen on the paper, and less the contact forces/vibrations generated by the pen during writing. This is possible just because the interaction of the pen with the paper is continuously and consistently transmitted to the hand holding the pen by mechanical stimulation: steady-forces and vibrations. Continuity and consistency of the feedback, acknowledging the expressed movement intent, are the key features allowing the shift of the attention from the interface with the tool to what can be perceived with the tip of the tool.

Similarly, when controlling a prosthesis, amputees should not have to take conscious care of the muscle contractions generating prosthesis movement, or of the provided haptic feedback; they should only have to act in a task-oriented fashion, as in the subconscious pre-shaping of the hand while approaching a target to prepare for optimal grasp. This is possible only if the amputee's movement intent, expressed as EMG, will consistently result in prosthesis movement and the prosthesis performance will be continuously and consistently transmitted to the amputee in a comfortable and intuitive way.

A stiff tool will forward the parameters describing the interaction from the tip of the tool toward the hand holding the tool; elasticity will reduce the direct interaction with the target, and a joint will cancel it completely. A functional prosthesis requires a large number of joints, while good embodiment requires a complete lack of joints. Therefore, the approach of this study was to first consider only grasping with a single degree of freedom, and to reconstruct the natural interaction by improving control of the prosthesis and providing haptic feedback. Haptic feedback should replicate the interaction of the "tool's tip" with the environment, measured by prosthesis and transmitted to the user. Only when a degree of embodiment is reached can the complexity of the prosthesis be increased, gaining more functionality.

Directly and objectively measuring the embodiment is not trivial; embodiment and the confidence of the amputee controlling the prosthesis are tightly correlated. If the amputee is able to intuitively control the prosthesis, they will also be able to move the prosthesis in simultaneity with the body while approaching the target, preparing the prosthesis for an optimal grasp. Many methods were tested and the degree of simultaneity was recorded for each. The result was that none of the tested EMG-control strategies allowed the subjects to control the prosthesis while approaching the target. These processes were sequential, grasping always being delayed until after the body had reached a stable posture. This is an indication that EMG prosthesis control requires large cognitive effort. During natural movement, humans are conscious only of the target to be reached, and the individual body movements are subconsciously performed. However, due to the inconsistencies between the amputee's movement intent and the reaction of the prosthesis, the prosthesis performance has to be supervised continuously, which is a major challenge for future development of movement automatisms.

This study addressed four general topics. The first dealt with various approaches to sensing and interpreting neural information, available as electromyography (EMG), and converting it into prosthesis movement. Then, various haptic technologies were investigated in order to identify the one most suitable for conveying the

sensory information measured by prosthetics into haptic feedback. In order to design a harmonious system, feedback and control have to be optimally mapped, this being the third topic addressed. Finally, probably the most challenging and important, was the assessment of prosthetics controllability. Without such an objective measure, it will not be possible to identify the strengths and weaknesses of various approaches, making systematic improvements to the system challenging in the extreme, if not impossible.

In order to have a general character, the assessment of prosthetics control must be done within a standardized environment. This is a vital requirement, as the outcomes should be compared between subjects who are geographically separated, and it will allow for the quantification of performance over a larger timespan. Replicating real environments and assessment scenarios in different places or at different points in time, is quite a challenge, explaining to some extent the lack of widely accepted solutions for the assessment of prosthetics performance. Therefore, a 3D immersive virtual reality (VR) system was proposed during this study. Immersed in such an artificial environment, the amputees, having attached the virtual prosthesis to the real stump, will perform similarly to how they would in the real environments. The VR scenarios and tasks can be standardized, creating a solid basis for the objective assessment of prosthesis controllability and performance improvement between training sessions. The assessment methodology, with all its components, was inspired by an internationally recognized standard, describing health and health-related states - the "International Classification of Functioning, Disability and Health" - ICF. The ICF belongs to the family of international classifications developed by the World Health Organization (WHO) for application to various aspects of health, including rehabilitation.

Besides assessment, the VR prosthesis is also a powerful tool for engineers. The kinematics or dynamics of the prosthesis can be changed easily and the impact rapidly evaluated. In addition, various stages of prosthesis fitting could be monitored by using such a virtual environment, which is essential to identifying bottlenecks within the prosthesis fitting chain: various placements of the EMG electrodes on the stump are easily evaluated, while different socket designs and motion artifacts generated by the weight of prosthesis are all individually addressable factors.

It might be claimed that a virtual prosthesis will never be able to reproduce the behavior of a real one. Therefore, the real prosthesis was included in the VR loop. The real prosthesis was not attached to the stump, but placed nearby, and the amputees controlled it wirelessly. The prosthesis moved and grasped a real object mounted in the hand and the prosthesis sensory system measured the movement and grasp. The resulting signals were directly driving the virtual prosthesis, making it a kind of shadow of the real one. This strategy fully exploited the flexibility allowed by VR, for the assessment of performance of real prosthetic devices.

The immersive 3D virtual systems are very promising tools, financially sustained by very strong industries like the car industry (prototyping), simulators, and the gaming industry, and they therefore follow a steep development curve. Currently, the affordable state-of-the-art systems do not yet entirely replicate the real environment, e.g. there are some challenges in evaluating the depth of a 3D scene; but this is compensated by

its flexibility in creating various scenarios for assessment, development and training. In such environments, free of risks and without disturbing external factors, the amputees are able to explore their abilities to more efficiently and consistently contract their muscles and move the prosthesis.

The initial idea of this thesis was simple, to close the hand-prosthesis control-loop by providing the amputees with haptic feedback, and to develop new applications which might exploit the assumed benefit of closed-loop systems: to improve prosthesis performance, embodiment, and even to alleviate phantom limb pain. However, the complexity of this apparently simple task is far greater than initially estimated. Finding the proper stimulation technology was very challenging, as the stimulation should effectively transmit information to the amputees, but equally importantly, the stimulation should be intuitive and comfortable. Moreover, prosthesis control is currently still demanding, slow and inconsistent with regard to the amputee's movement intent; thus, improving it is a determinant of increased prosthesis functionality. The most challenging issue, when prosthesis functionality is aimed to be improved, is not necessarily the development of new approaches to control prosthetic devices, but the development of a methodology to objectively assess the prosthesis' controllability in all its complexity. Without such an objective measure, it will be hard if not impossible to identify strength and weaknesses of various approaches, allowing for systematic and real improvements of the prosthesis' performance.

10. FINAL CONCLUSIONS AND FUTURE WORK

This study addressed six general topics. The first dealt with various approaches to sensing and interpreting neural information, available as electromyography (EMG), and converting it into prosthesis movement. Then, various haptic technologies were investigated in order to identify the one most suitable for transmitting sensory information measured by the prosthetics as haptic feedback to amputees. The haptic devices stimulate the skin, but from provided stimulation, the human body will be able to perceive a narrow amount of stimuli. Psychophysical measurements were made in order to quantify the amount of information transferred through the tactile interface, from stimulator to person. The result was a map of perceived stimulation which allows for comparison between different technologies even when they are stimulating in different modalities (e.g. electro-stimulation vs. mechanical stimulation). This stimulation map is especially important when building stimulation patterns, linking elementary discriminable stimulation points (called vibels) into continuous stimulation trajectories. These continuous stimulation patterns should, however, be perceived by the amputee as non-disturbing, and should intuitively describe the sensory information measured by the prosthesis. Implemented in an upper-limb prosthesis, feedback and control should harmoniously merge together, allowing for bi-directional transfer of information between amputee and prosthesis, which should, in turn, allow for less demanding and more intuitive prosthesis control.

However, without an objective measure of prosthesis controllability, in open- or close-loop, all these efforts to merge human and prosthesis into one entity cannot be quantified, and consequently there is no guaranty of real improvement, therefore, an assessment methodology was proposed. This was implemented as various standardized scenarios in an immersive virtual reality system which was designed to give the assessment outcomes a more general character. This approach allows for individual assessment of all system components contributing to the final result, for comparison between the performance of subjects geographically separated or for evaluation of the learning curve, of individual subjects, over a larger time span. All addressed topics are enumerated and summarized as follows:

- Increasing intuitiveness of prosthesis control
- Optimal wearable technology for providing haptic feedback
- Psychophysical assessment of stimulation
- Generating intuitive, comfortable and effective feedback patterns
- Intuitively mapping feedback patterns with sensory information
- Assessment of prosthesis controllability

Aiming to increase intuitiveness of prosthesis control, many control strategies were tested and directly compared. Between them, the voltage mode, mostly implemented in upper-limb commercial prosthetics proved to be a good compromise between stability and performance, even in the absence of feedback about grip force. For the proportional mode, however, which is the fastest and most physiological, feedback is an absolute must. In order to make proportional control suitable for daily life application further research is required in increasing its stability in the presence of noisy EMG or motion artifacts, as well as closing the prosthesis control loop by providing haptic feedback to the amputees.

Haptic feedback was addressed as well during this study. A survey of the wearable stimulation devices revealed that the available technologies are able to produce only a narrow amount a tactile stimuli, thus they are not able to reproduce the natural interaction of the real hand when grasping objects. Therefore, a new technology was proposed - the Haptic Brace - able to generate vibrotactile stimulation superposed with sensation of pressure and squeezing of the stump. This multi-modal stimulation looks very promising, but requires future developments (i.e. miniaturization) in order to allow its integration into a prosthesis socket. The Haptic Brace is driven by a commercial BLDC motor, which is not optimized for this kind of application, but by modifying its electrical/magnetic properties and tuning the weight of the rotor correspondingly, an optimum can be achieved. Currently the motor is driven in *voltage mode*, but future efforts for driving the motor in *current mode* will be rewarded with a higher resolution of the stimulation. The applied stimulation on the skin cannot be entirely perceived by humans, so the amount of perceived stimulation was assessed by performing a series of psychophysical measurements. After evaluating classical psychophysical methodologies (e.g. 2AFC/2IFC) it seemed that the estimated JND was strongly biased by the delay between the stimuli presentations, and consequently not suitable for this kind of application. Therefore, a Yes/No approach, SIAM, was adopted and modified in order to fit our requirements. This modified SIAM was used for the evaluation of vibrotactile stimulation showing good performance compared with the conventional methods; though it allowed the investigation of the vibrotactile sensibility in only four subjects.

Speeding up the procedure, without sacrificing precision, should be the focus of the future research, in order to allow the investigation of the haptic perception in many more subjects, giving the results a more general character. The resulting map of JNDs covering the whole AF stimulation range is an important tool for the creation of stimulation patterns. By interconnecting the stimulation points, various staircase stimulation patterns can be generated; also a strategy to generate continuous stimulation patterns was proposed. The potential offered by these approaches, to generate discriminable stimulation trajectories, was not entirely exploited during this work. Future research should address this topic more deeply and aim to decode the mechanisms which allow for the generation of intuitive and comfortable stimulation. Some preliminary trials were done in this direction by exploiting the potential offered by the RHI to study the haptic-visual sensory integration. The main idea was to substitute the complex stimulation of the hand by a brush with artificial feedback. It has been hypothesized that the stronger the induced illusion, the more intuitive the artificial feedback will be. The main limitation of this approach was the objective evaluation of the degree of the

induced illusion. We used classical approaches for this evaluation (i.e. temperature measurements, proprioceptive drift) without the targeted success, even when the induced illusion was clearly but subjectively perceived. There is however a hope that within the immersive VR environment, the induced illusion will be easily quantifiable as proprioceptive drift.

In the study about open- vs. closed-loop control, the velocity, first contact and grip force were encoded with vibrotactile feedback. The next step should be to encode redundant information with differentiable haptic patterns, e.g. velocity and position, or force and its derivative, in order to better reproduce the mechanisms of natural perception. Simultaneously encoding movement and grasp will also allow for the detection of the hardness of a grasped object; the softer the grasped object, the more overlap can be perceived between movement and grasp. With the goal of objectively assessing prosthesis controllability, an immersive virtual environment was created and a methodology based on ICF proposed. However, the main drawback of the system is its portability. A set of infra-red video cameras were used to track head and arm movements, which required complex equipment. But this field of virtual reality is sustained by very strong industries, and therefore is developing rapidly; new wearable technologies are emerging on the market, e.g. sensorized suits developed by STMMicroelectronics, or video glasses with integrated position/orientation sensors, e.g. the Oculus Rift VR headset.

The work done during this study tried to identify and address the most important aspects required for a better integration of prosthetics and amputees. The conclusions were not in all cases based on relevant statistics, but aimed to generate hypotheses for future, more elaborated research. The proposed methodologies, e.g. VR and psychophysical assessment, still lack a general character and were not defined in detail. To do so will require much more experience with real amputees to validate the procedure. However, this research did succeed in identifying new avenues of inquiry which, if addressed by future research, will indeed have an impact in improving the quality of life for amputees wearing prosthetic devices.

BIBLIOGRAPHY

- Argall, B.D. & Billard, A.G., 2010. A survey of Tactile Human–Robot Interactions. *Robotics and Autonomous Systems*, 58(10), pp.1159–1176.
- Armbrüster, C. & Spijkers, W., 2006. Movement planning in prehension: do intended actions influence the initial reach and grasp movement? *Motor Control*, 10(4), pp.311–329.
- Ayres, A.J., Robbins, J. & McAtee, S., 2005. *Sensory integration and the child: Understanding hidden sensory challenges*, Western Psychological Servi.
- Barsalou, L.W., 1999. Perceptual symbol systems. *Behavioral and Brain Sciences*, 22(4), pp.577–609; discussion 610–660.
- Benali-khoudja, M., Hafez, M. & Alexandre, J., 2004. Tactile interfaces : a state-of-the-art survey. *Symposium A Quarterly Journal In Modern Foreign Literatures*, 04(2), pp.23–26.
- Biggs, J. & Srinivasan, M.A., 2002. *Tangential versus normal displacements of skin: relative effectiveness for producing tactile sensations*, IEEE Comput. Soc.
- Blank, A., Okamura, A.M. & Kuchenbecker, K.J., 2010. Identifying the role of proprioception in upper-limb prosthesis control. *ACM Transactions on Applied Perception*, 7(3), pp.1–23.
- Bolanowski, S.J. et al., 1988. Four channels mediate the mechanical aspects of touch. *Journal of the Acoustical Society of America*, 84(5), pp.1680–1694.
- Botvinick, M. & Cohen, J., 1998. Rubber hands “feel” touch that eyes see. *Nature*, 391(6669), p.756.
- Caldwell, D.G., Lawther, S. & Wardle, A., 1996. *Multi-modal cutaneous tactile feedback*, IEEE.
- Camurri, A. et al., 2000. Eyesweb: Toward gesture and affect recognition in interactive dance and music. *Computer Music*.
- Chatterjee, A., Chaubey, P., Martin, J. & Thakor, N. V., 2008. Quantifying Prosthesis Control Improvements Using a Vibrotactile Representation of Grip Force. In *2008 IEEE Region 5 Conference*. IEEE, pp. 1–5.
- Chatterjee, A., Chaubey, P., Martin, J. & Thakor, N., 2008. Testing a Prosthetic Haptic Feedback Simulator With an Interactive Force Matching Task. *JPO Journal of Prosthetics and Orthotics*, 20(2), pp.27–34.
- Childress, D.S., 1980. Closed-loop control in prosthetic systems: Historical perspective. *Annals of Biomedical Engineering*, 8(4-6), pp.293–303.
- Choi, S. & Kuchenbecker, K.J., 2012. Vibrotactile Display: Perception, Technology, and Applications. *Proceedings of the IEEE*, pp.1–12.

- Cipriani, C. et al., 2008. On the Shared Control of an EMG-Controlled Prosthetic Hand: Analysis of User–Prosthesis Interaction. *IEEE Transactions on Robotics*, 24(1), pp.170–184.
- Cipriani, C., D’Alonzo, M. & Carrozza, M.C., 2012. A miniature vibrotactile sensory substitution device for multifingered hand prosthetics. *IEEE Transactions on Biomedical Engineering*, 59(2), pp.400–8.
- Dargahi, J. & Najarian, S., 2004. Human tactile perception as a standard for artificial tactile sensing--a review. *The international journal of medical robotics computer assisted surgery MRCAS*, 1(1), pp.23–35.
- Dhillon, G.S. & Horch, K.W., 2005. *Direct neural sensory feedback and control of a prosthetic arm*.
- Ergenzinger, E.R. & Pons, T.P., 2001. Cortical Plasticity: Use-dependent Remodelling. *Encyclopedia of Life Sciences*, pp.1–6.
- Ewert, S.D. & Dau, T., 2004. External and internal limitations in amplitude-modulation processing. *Journal of the Acoustical Society of America*, 116(1), pp.478–490.
- Farina, D. et al., 2010. Decoding the neural drive to muscles from the surface electromyogram. *Clinical Neurophysiology*, 121(10), pp.1616–1623.
- Farina, D., 2006. Interpretation of the surface electromyogram in dynamic contractions. *Exercise and Sport Sciences Reviews*, 34(3), pp.121–127.
- Farina, D. et al., 2008. Multichannel thin-film electrode for intramuscular electromyographic recordings. *Journal of Applied Physiology*, 104(3), pp.821–827.
- Farina, D. & Enoka, R.M., 2011. Surface EMG decomposition requires an appropriate validation. *Journal of Neurophysiology*, 105(2), pp.981–982; author reply 983–984.
- Farina, D., Fosci, M. & Merletti, R., 2002. *Motor unit recruitment strategies investigated by surface EMG variables.*, Am Physiological Soc.
- Farina, D., Merletti, R. & Enoka, R.M., 2004. The extraction of neural strategies from the surface EMG. *Journal of Applied Physiology*, 96(4), pp.1486–1495.
- Farina, D., Negro, F. & Jiang, N., 2013. Identification of Common Synaptic Inputs to Motor Neurons from the Rectified Electromyogram. *The Journal of physiology*.
- Flor, H. et al., 1995. Phantom-limb pain as a perceptual correlate of cortical reorganization following arm amputation. *Nature*, 375(6531), pp.482–484.
- Flor, H., Nikolajsen, L. & Staehelin Jensen, T., 2006. Phantom limb pain: a case of maladaptive CNS plasticity? *Nature Reviews Neuroscience*, 7(11), pp.873–881.
- Gardner, E.P., 1988. Somatosensory cortical mechanisms of feature detection in tactile and kinesthetic discrimination. *Canadian Journal of Physiology and Pharmacology*, 66(4), pp.439–454.
- Gentilucci, M. et al., 1991. Influence of different types of grasping on the transport component of prehension movements. *Neuropsychologia*, 29(5), pp.361–378.

- Gescheider, G.A., 1997. *Psychophysics: The Fundamentals*, 3rd Ed.
- Giummarra, M.J. & Moseley, G.L., 2011. Phantom limb pain and bodily awareness: current concepts and future directions. *Current Opinion in Anaesthesiology*, 24(5), pp.524–531.
- Griffin, M.J., 2007. Effects of Vibration on People. In *Handbook of Noise and Vibration Control*. John Wiley & Sons, Inc., pp. 343–353.
- Gruver, W.A., Gripping force sensory feedback for a myoelectrically controlled forearm prosthesis. In *1995 IEEE International Conference on Systems, Man and Cybernetics. Intelligent Systems for the 21st Century*. IEEE, pp. 501–504.
- Heller, M.A., Rogers, G.J. & Perry, C.L., 1990. WITH THE OPTACON : TOUCH AND THE LEFT HAND. *Brain*, 28(9), pp.1003–1006.
- Higgins, T., 2010. Unity-3D Game Engine.
- Hill, W. et al., 2009. Upper limb prosthetic outcome measures (ULPOM): A working group and their findings. *JPO: Journal of Prosthetics and Orthotics*, 21(9), pp.P69–P82.
- Holobar, A. et al., 2010. Experimental Analysis of Accuracy in the Identification of Motor Unit Spike Trains From High-Density Surface EMG. *IEEE Transactions on Neural Systems and Rehabilitation Engineering*, 18(3), pp.221–229.
- Jadhav, S.P., Wolfe, J. & Feldman, D.E., 2009. Sparse temporal coding of elementary tactile features during active whisker sensation. *Nature Neuroscience*, 12(6), pp.792–800.
- Jeannerod, M., 1992. Coordination mechanisms in prehension movements. In G. E. Stelmach & J. Requin, eds. *Tutorials in Motor Behavior II*. Elsevier, pp. 265–285.
- Jiang, N. et al., 2010. Myoelectric control in neurorehabilitation. *Critical Reviews in Biomedical Engineering*, 38(4), pp.381–391.
- Johansson, R.S. et al., 2001. Eye-hand coordination in object manipulation. *The Journal of Neuroscience*, 21(17), pp.6917–6932.
- Johansson, R.S. & Westling, G., 1988. Programmed and triggered actions to rapid load changes during precision grip. *Experimental Brain Research*, 71(1), pp.72–86.
- Johansson, R.S. & Westling, G., 1987. Signals in tactile afferents from the fingers eliciting adaptive motor responses during precision grip. *Experimental Brain Research*, 66, pp.141–154.
- Johnson, K.O., 2001. The roles and functions of cutaneous mechanoreceptors. *Current opinion in neurobiology*, 11(4), pp.455–61.
- Jones, L.A. & Berris, M., 2002. *The psychophysics of temperature perception and thermal-interface design*, IEEE Comput. Soc.

- Jones, L.A. & Sarter, N.B., 2008. Tactile Displays : Guidance for Their Design and Application. *Human Factors The Journal of the Human*, 50(1), pp.90–111.
- Kaczmarek, K.A. et al., 1991. Electrotactile and vibrotactile displays for sensory substitution systems. *IEEE Transactions on Biomedical Engineering*, 38(1), pp.1–16.
- Kaernbach, C., 1990. A single interval adjustment matrix (SIAM) procedure for unbiased adaptive testing. *Journal of the Acoustical Society of America*, 88(6), pp.2645–2655.
- Kamavuako, E.N. et al., 2009. Relationship between grasping force and features of single-channel intramuscular EMG signals. *Journal of Neuroscience Methods*, 185(1), pp.143–150.
- Kamavuako, E.N. et al., 2013. Surface Versus Untargeted Intramuscular EMG Based Classification of Simultaneous and Dynamically Changing Movements. *IEEE transactions on neural systems and rehabilitation engineering a publication of the IEEE Engineering in Medicine and Biology Society*.
- Kandel, E.R., Schwartz, J.H. & Jessell, T.M., 2000. *Principles of Neural Science* E. R. Kandel, J. H. Schwartz, & T. M. Jessell, eds., McGraw-Hill.
- Kingdom, F.A.A. & Prins, N., 2009. *Psychophysics: a practical introduction*, Academic New York.
- Kuchenbecker, K.J., Gurari, N. & Okamura, A.M., 2007. *Effects of Visual and Proprioceptive Motion Feedback on Human Control of Targeted Movement*, IEEE.
- Kuiken, T.A. et al., 2009. Targeted muscle reinnervation for real-time myoelectric control of multifunction artificial arms. *Jama The Journal Of The American Medical Association*, 301(6), pp.619–628.
- Kyberd, P.J. et al., 1993. A clinical experience with a hierarchically controlled myoelectric hand prosthesis with vibro-tactile feedback. *Prosthetics and orthotics international*, 17(1), pp.56–64.
- Land, M.F., 2006. Eye movements and the control of actions in everyday life J. López, E. Benfenati, & W. Dubitzky, eds. *Progress in Retinal and Eye Research*, 25(3), pp.296–324.
- Leek, M.R., 2001. Adaptive procedures in psychophysical research. *Perception & Psychophysics*, 63(8), pp.1279–1292.
- Lewkowicz, D.J. & Ghazanfar, A.A., 2009. The emergence of multisensory systems through perceptual narrowing. *Trends in Cognitive Sciences*, 13(11), pp.470–8.
- Longo, M.R. & Sadibolova, R., 2013. Seeing the body distorts tactile size perception. *Cognition*, 126(3), pp.475–481.
- Lotze, M. et al., 2001. Phantom movements and pain. An fMRI study in upper limb amputees. *Brain: A journal of neurology*, 124(Pt 11), pp.2268–2277.
- Marasco, P.D., Schultz, A.E. & Kuiken, T.A., 2009. Sensory capacity of reinnervated skin after redirection of amputated upper limb nerves to the chest. *Brain: A journal of neurology*, 132(6), pp.1441–1448.
- Marks, L., 1974. *Sensory Processes: The new Psychophysics (Google eBook)*.

- McGeoch, P.D. & Ramachandran, V.S., 2011. The appearance of new phantom fingers post-amputation in a phocomelus. *Neurocase*, 18(2), pp.1–3.
- McGrath, B. et al., 2008. *Tactile Actuator Technology*,
- Meek, S.G., Jacobsen, S.C. & Goulding, P.P., 1989. Extended physiologic taction: design and evaluation of a proportional force feedback system. *Journal of rehabilitation research and development*, 26(3), pp.53–62.
- Merletti, R. et al., 2010. Advances in surface EMG: recent progress in detection and processing techniques. *Critical Reviews in Biomedical Engineering*, 38(4), pp.305–345.
- Merletti, R., Holobar, A. & Farina, D., 2008. Analysis of motor units with high-density surface electromyography. *Journal of Electromyography and Kinesiology*, 18(6), pp.879–890.
- Merletti, R. & Parker, P.A., 2004. *Electromyography: physiology, engineering, and noninvasive applications*. R. Merletti & P. Parker, eds., Wiley-IEEE.
- Moseley, G.L., 2006. Graded motor imagery for pathologic pain: a randomized controlled trial. *Neurology*, 67(12), pp.2129–2134.
- Moseley, G.L. & Brugger, P., 2009. Interdependence of movement and anatomy persists when amputees learn a physiologically impossible. *Direct*, 106(44), pp.18798–802.
- Mossel, A. et al., 2012. ARTIFICE-Augmented Reality Framework for Distributed Collaboration. *International Journal of Virtual Reality*.
- Munih, M. & Ichie, M., 2001. Current Status and Future Prospects for Upper and Lower Extremity Motor System Neuroprostheses. *Neuromodulation*, 4(4), pp.176–186.
- Murray, D.J., 2010. A perspective for viewing the history of psychophysics. *Behavioral and Brain Sciences*, 16(01), p.115.
- Newell, K.M. & Vaillancourt, D.E., 2001. Dimensional change in motor learning. *Hum Mov Sci*, 20(4-5), pp.695–715.
- Ninu, A. et al., 2013. A novel wearable vibro-tactile haptic device. *2013 IEEE International Conference on Consumer Electronics (ICCE)*, pp.51–52.
- Ninu, A., 2010. Device and method for generating a vibration pattern.
- Olshausen, B.A. & Field, D.J., 2004. Sparse coding of sensory inputs. *Current Opinion in Neurobiology*, 14(4), pp.481–487.
- Oskoei, M.A. & Hu, H., 2007. Myoelectric control systems—A survey. *Biomedical Signal Processing and Control*, 2(4), pp.275–294.
- Otto, J., 2003. Outcomes Measurements in Upper-Limb Prosthetics: Why So Elusive? *The O&P EDGE*, January.

- Patterson, P. & Katz, J., 1992. Design and evaluation of a sensory feedback system that provides grasping pressure in a myoelectric hand. *J Rehabil Res Dev*, 29(1), pp.1–8.
- Pintaric, T. & Kaufmann, H., 2008. A Rigid-Body Target Design Methodology for Optical Pose-Tracking Systems. *Symposium A Quarterly Journal In Modern Foreign Literatures*, pp.73–76.
- Prahm, C., Ninu, A. & Rattay, F., 2011. Can I lend You a Hand? Rubber Hand Illusion for Sensory Feedback in Amputees. In *MEi: CogSci Conference 2011, Ljubljana*.
- Pylatiuk, C., Kargov, A. & Schulz, S., 2006. Design and Evaluation of a Low-Cost Force Feedback System for Myoelectric Prosthetic Hands. *JPO Journal of Prosthetics and Orthotics*, 18(2), pp.57–61.
- Pylatiuk, C. & Mounier, S., 2004. Progress in the development of a multifunctional hand prosthesis. ... in *Medicine and ...*, 6, pp.4260–3.
- Ramachandran, V.S., Rogers-Ramachandran, D. & Cobb, S., 1995. Touching the phantom limb. *Nature*, 377(6549), pp.489–490.
- Riso, R.R., 1999. Strategies for providing upper extremity amputees with tactile and hand position feedback--moving closer to the bionic arm. *Technology and health care official journal of the European Society for Engineering and Medicine*, 7(6), pp.401–409.
- Rupert, A.H., 2000. Tactile situation awareness system: proprioceptive prostheses for sensory deficiencies. *Aviation space and environmental medicine*, 71(9 Suppl), pp.A92–A99.
- Saradjian, A., Thompson, A.R. & Datta, D., 2008. The experience of men using an upper limb prosthesis following amputation: positive coping and minimizing feeling different. *Disability and rehabilitation*, 30(11), pp.871–883.
- Saunders, I. & Vijayakumar, S., 2011. The role of feed-forward and feedback processes for closed-loop prosthesis control. *Journal of neuroengineering and rehabilitation*, 8(1), p.60.
- Schmidt, R.A. & Lee, T.D., 2005. *Motor control and learning: A behavioral emphasis* T. D. Lee, ed., Human Kinetics.
- Schmidt, R.A. & Wrisberg, C.A., 2000. *Motor Learning and Performance*, Human Kinetics.
- Shimoga, K.B., 1993. *A survey of perceptual feedback issues in dexterous telemanipulation. II. Finger touch feedback*, IEEE.
- Sotnikov, O.S., 2006. Primary sensory neurons in the central nervous system. *Neuroscience and behavioral physiology*, 36(5), pp.541–8.
- Stashuk, D., 2001. EMG signal decomposition: how can it be accomplished and used? *Journal of electromyography and kinesiology official journal of the International Society of Electrophysiological Kinesiology*, 11(3), pp.151–173.
- Stepp, C.E. & Matsuoka, Y., 2010. Relative to direct haptic feedback, remote vibrotactile feedback improves but slows object manipulation. *Conference proceedings: ... Annual International Conference of the IEEE*

- Engineering in Medicine and Biology Society. IEEE Engineering in Medicine and Biology Society. Conference, 2010, pp.2089–92.*
- T. Pintaric & Kaufmann, H., 2007. Affordable infrared-optical pose-tracking for virtual and augmented reality. In *In Proceedings of Trends and Issues in Tracking for Virtual Environments Workshop.*
- Treutwein, B., 1995. e r g a m o n Minireview Adaptive Psychophysical Procedures. *Science*, 35, pp.2503–2522.
- Van Veen, H.A.H.C. & Van Erp, J.B.F., 2001. Tactile information presentation in the cockpit S. Brewster & R. Murray-Smith, eds. *Haptic HumanComputer Interaction*, 2058, pp.174–181.
- Watanabe, J. et al., 2007. Tactile motion aftereffects produced by appropriate presentation for mechanoreceptors. *Experimental Brain Research*, 180(3), pp.577–582.
- Weeks, S.R., Anderson-Barnes, V.C. & Tsao, J.W., 2010. Phantom limb pain: theories and therapies. *The neurologist*, 16(5), pp.277–86.
- Westling, G. & Johansson, R.S., 1984. Factors influencing the force control during precision grip. *Experimental Brain Research*, 53(2), pp.277–284.
- World Health Organization & others, 2001. International classification of functioning disability and health (ICF).
- Yousif, N. & Diedrichsen, J., 2012. Structural learning in feed-forward and feedback control. *Journal of neurophysiology*, (August), pp.2373–2382.
- Zajac, F.E., 1988. Muscle and tendon: properties, models, scaling, and application to biomechanics and motor control. *Critical reviews in biomedical engineering*, 17(4), pp.359–411.
- Zhou, P. & Rymer, W.Z., 2004. MUAP number estimates in surface EMG: template-matching methods and their performance boundaries. *Ann Biomed Eng*, 32(7), pp.1007–1015.
- Zopf, R., Harris, J.A. & Williams, M.A., 2011. The influence of body-ownership cues on tactile sensitivity. *Cogn Neurosci*, 2(3-4), pp.147–154.

APPENDIX

Menu - Virtual Reality Environment

In order to customize the behavior of various components within the virtual reality, and to define correspondences between real and virtual elements, a menu was created, shown in Figure 83. The menu comprises a series of tabs, whose functionality is described below.

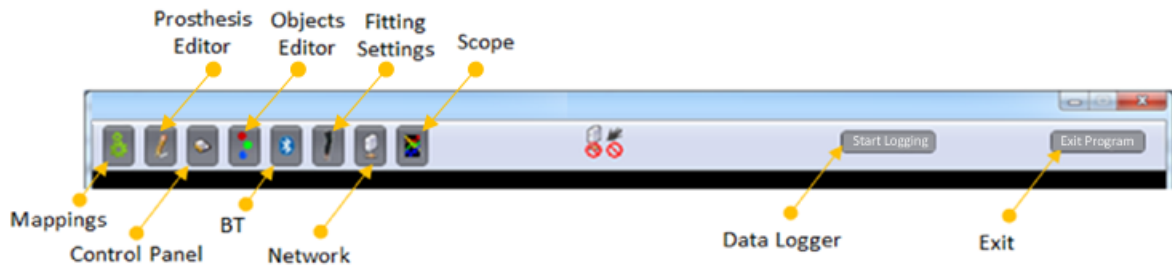


Figure 83: Menu for customization of the elements within virtual reality and of the interaction with the external physical entities.

MAPPINGS

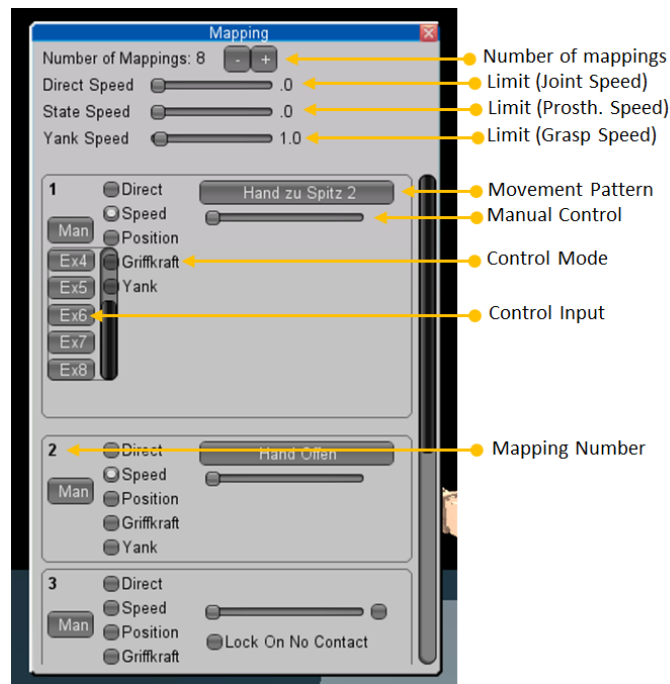


Figure 84: The mappings tab allows for defining correspondences between the control signals and prosthesis movement.

The elements contained in the “Mappings” tab [Figure 84], allow for defining correspondences between the available control signals and prosthesis movements. In the example below, eight such mappings are defined.

Every input from the eight available (Ex1-8) would control one movement of the prosthesis. A manual mode (Man) was also added, in which a slider has the same function as the control inputs (Ex1-8).

The correspondence between control input and prosthesis movement or grasp is defined by the prosthesis control modes. The available control modes are: *Direct*, *Speed*, *Position*, *Griffkraft* and *Yank*. In *Direct* mode every control signal will control an individual joint, which may be the wrist, one of the 4 fingers or 2 degrees of freedom for the thumb. In *Speed* mode, one input controls the velocity of a movement - a group of joints interconnected, moving simultaneously, e.g. hand-open or hand-close. Consequently, the *Speed* mode requires two signals to control a movement, e.g. one for *open* and the second for *close*. Such movements are editable in the "Prosthesis Editor." Another control mode is *Position*, in which a control signal is correlated with e.g. the aperture of the hand; higher magnitude input signals tell the hand to open, and lower magnitude to close. The control modes *Direct*, *Speed* and *Position* are used to set up the behavior of the prosthesis during movement.

In order to allow grasping, new mappings were defined, i.e. *Griffkraft* and *Yank*. In *Griffkraft* mode the grasp force will increase in proportion to the magnitude of the input signal (like with position control). The *Yank* mode is similar to *Speed* mode during movement; a constant input will determine the grasp force to increase linearly. The larger the input amplitude, the faster the increase in grasp.

The three sliders - *Direct Speed*, *State Speed* and *Yank Speed* - allow for defining the increase rate (the slope) of position or grasp. They are active when the prosthesis is set in one of the modes *Direct*, *Position* or *Yank*.

PROSTHESIS EDITOR

The major goal of this implementation was to build a model for the prosthetic hand (Michelangelo, OttoBock), and to study the grasp mechanisms of the EMG-controlled prosthesis. The modeled virtual prosthesis is controlled by two EMG signals, one dedicated for hand-open and the other for hand-close (similar to the real prosthesis). While the grasp patterns of the real prosthesis are constructively defined, the fingers of the virtual hand are freely moving. Their individual movement might be correlated and hard-coded in the software to simulate the movement patterns of the real prosthesis but, for the sake of flexibility, a new customizing menu was implemented - *Hand State Editor* (Figure 85).

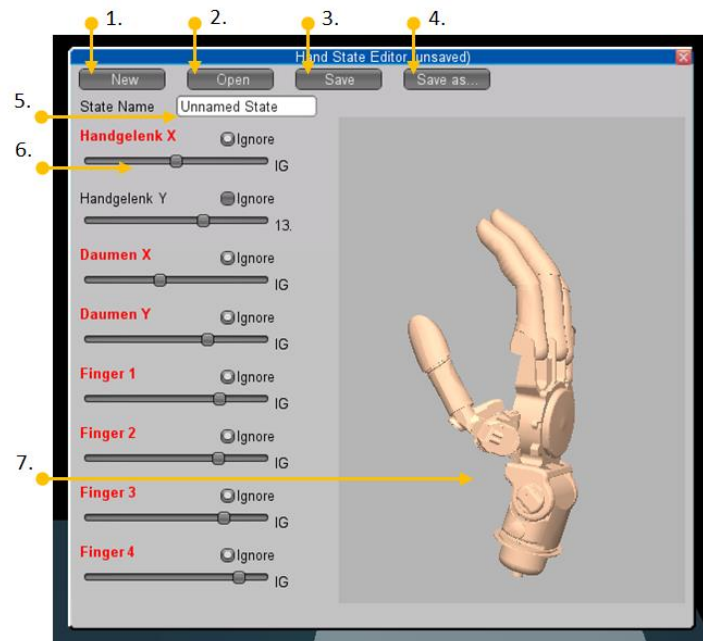


Figure 85: The hand state editor tab allows for designing of various grasp/movement patterns.

The functionality provided by this dialog might allow the engineers or clinicians to evaluate various grasp patterns before they have to implement them physically: individual control of every finger by EMG, the index finger and/or the thumb, and so on.

A movement pattern is defined by the sliders on the left side of the menu. If the *Ignore* button is active, i.e. white, the joint movement corresponding to the slider is excluded from the pattern. Otherwise, the movement pattern of the hand will include all other joints. The sliders define the absolute position of the individual joints relative to a frame, for fingers attached to the palm, and for wrist attached to the forearm.

One state defines the limit of a movement, e.g. hand-open or hand-close. For example, if the prosthesis moves in *Speed* mode, a control signal will proportionally move the prosthesis between the two hand configurations. The movement of the individual fingers, between the limit configurations, is calibrated to guarantee simultaneous movement of all joints involved in the pattern, while moving between the limit configurations.

All defined states may be saved, loaded and modified using the controls Figure 85(1-5). A preview of the hand showing the current adjusted grasp pattern, corresponding to the sliders, is also available [Figure 85(7)].

CONTROL PANEL

The virtual environment communicates wirelessly and bi-directionally with the control brace. The brace is continuously sending data about the sensed EMG activity to the virtual environment, and from the virtual environment, by means of the *Embed Commands* dialog [Figure 86] serial commands are transmitted to the control brace. The control brace has many parameters which have to be adjusted, e.g. filter gains for the EMG,

thresholds and control modes. Thus, sending serial commands to the brace was a vital requirement. All commands are defined in specific *.xml files; one command has an identifier and a certain number of parameters [Figure 86(4)]. They may be sent by pushing one button [Figure 86(3)] or by moving the slider [Figure 86(1)]. When moving a slider, only one parameter of the command is continuously changed.

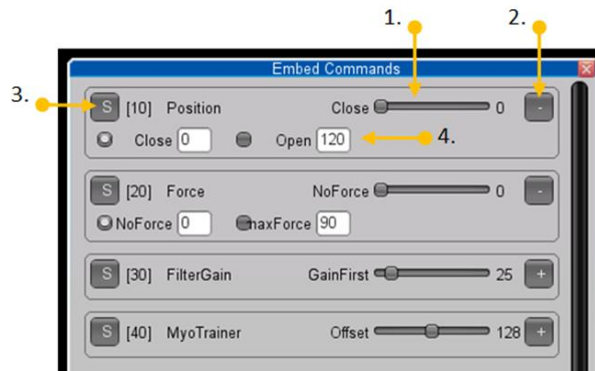


Figure 86: By using the control panel tab, serial commands might be sent from the virtual-reality environment to the control brace, which allow the customization of various parameters – e.g. Control mode, EMG gain.

OBJECTS EDITOR

The *Object Editor* dialog allows for the creation of objects within the virtual environment Figure 87. The object's type and some parameters of the interaction with the hand are adjustable in this dialog as well. All objects within the environment are spheres, whose parameters are the diameter and the target range. The diameter can be adjusted by changing the value in the box [Figure 87(8)] or by pushing the "+/-" buttons. The target range is an area defined by offset and width, which has to be reached by the measured force in order to be able to collect the virtual object. The target range is defined by the controls in [Figure 87(6)]. In order to speed-up the process of object creation, three types of objects may be generated simultaneously, e.g. heavy, normal and fragile. The first box defines the number of objects, the second box (Min), the lower threshold, and the last box (Max), the upper threshold.

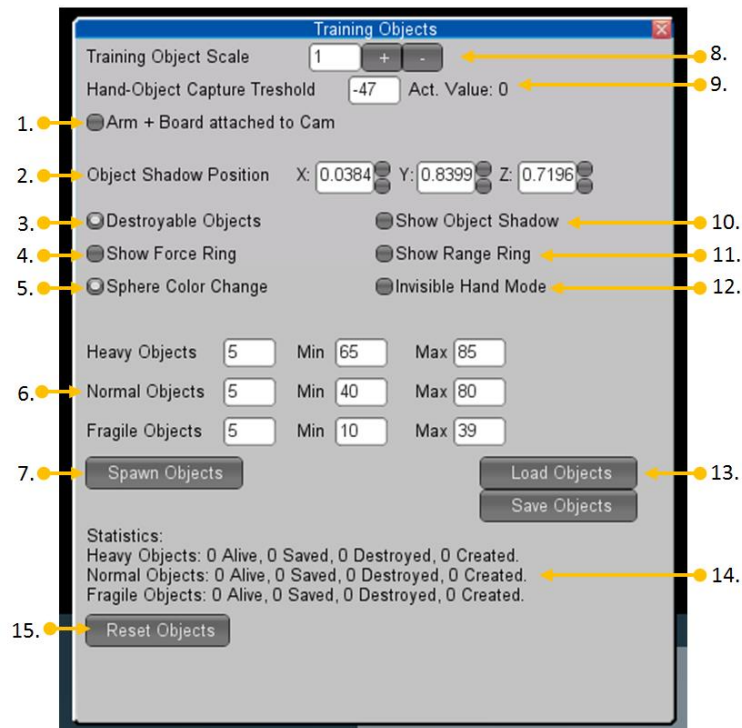


Figure 87: The object editor dialog allows for the creation of objects within the virtual environment.

The process of grasping comprises two distinct phases: the hand approaches the target, and then the grasp is initiated. The transition between the two phases is supported during grasping with the natural hand by tactile perception, proprioception and by the high flexibility of the hand. Real and virtual prostheses lack these capabilities, so the process of grasping with a prosthesis may be very challenging. While a real prosthesis provides a narrow amount of feedback (pressure at the stump) when interacting with the environment, the virtual prosthesis is completely detached. If the goal were to perfectly position the virtual prosthesis over the object preparing the grasp, this task would be almost impossible to accomplish. Therefore, some additional elements were implemented: Hand-Object Capture Threshold [Figure 87(9)], Object Shadow Position [Figure 87(2)], and Show Force Ring [Figure 87(4)].

Ideally, the object would be perfectly centered within the hand before initiating the grasp. Based only on visual feedback, accomplishing this task is very problematic. One of the aims of this project was to reproduce the degree of difficulty of grasping with real prostheses; therefore grasping within the virtual environment was designed in such a way as to allow some flexibility. The objects should not be perfect centered within the hand, but small deviations will be permitted. This is defined by a customizable parameter - The Hand-Object Capture Threshold [Figure 87(9)].

The depth of a 3D virtual environment might be hard to evaluate accurately based only on the image available in the video glasses. Therefore, a new element was introduced: The Object Shadow [Figure 88]. The Object

Shadow Position is a semi-transparent shadow of the target object, and has the same dimensions with it. The shadow is attached to the prosthesis, so that when overlapped with the target object, the optimal position for grasping with prosthesis is guaranteed. Positioning the shadow over the target object allows for a more natural flow of the movement preparing the grasp, compensating for the imprecise evaluation of the VR 3D depth.

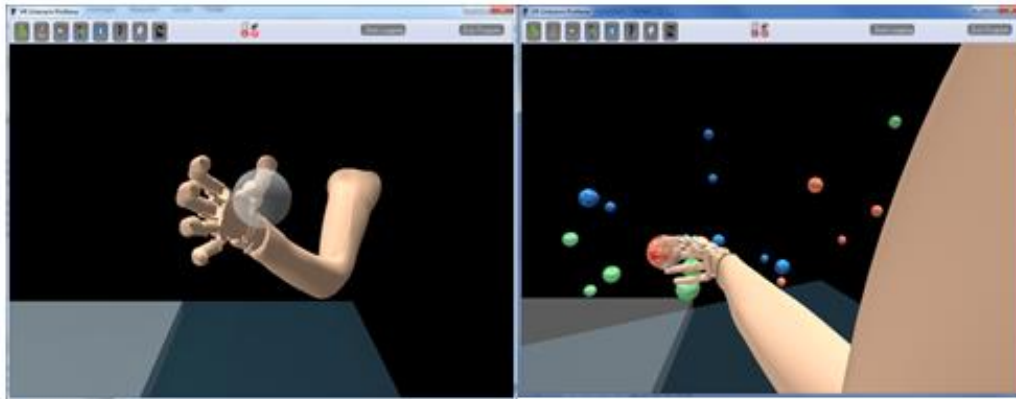


Figure 88: the object shadow, attached to the hand prosthesis, allows for a more accurate evaluation of the depth of the 3D virtual-environment.

Various grasp patterns will require different configurations for the fingers. Consequently, the shadow indicating the optimal positioning of the object-target in the hand has to be individually adjusted for every grasp pattern. Therefore, the shadow's coordinates relative to the palm were made adjustable [Figure 87(2)]. The shadow might be optionally switched ON and OFF with the control [Figure 87(10)].

The control Show Force Ring [Figure 87(4)], switches ON/OFF the visual feedback of the grasp force – the yellow circle [Figure 89]. This element has two functions: it indicates the magnitude of the grasp force, and its appearance indicates when the target and the shadow properly overlap and grasping can be initiated. If the prosthesis is far away from the target, the Show Force Ring is never visible. The same rules are also in effect for the Show Range Ring [Figure 87(11)]. This radio button switches On/Off the visual feedback of the force target range – the green circle [Figure 89].

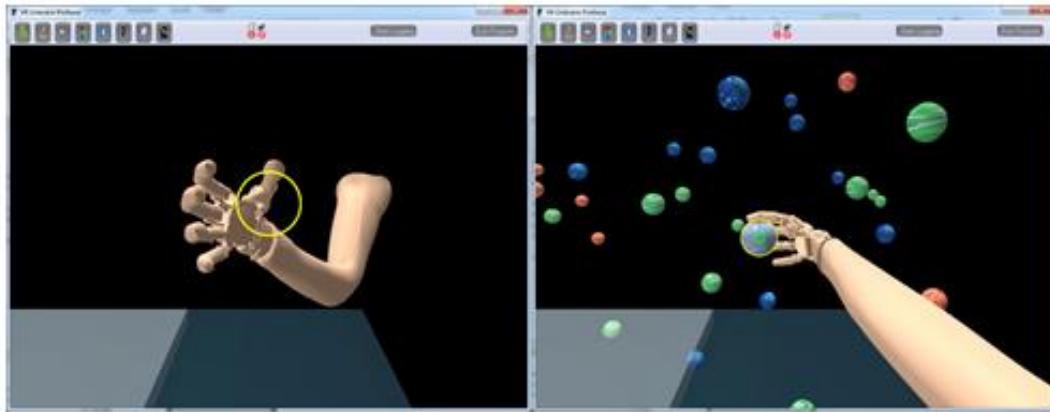


Figure 89: The force ring object (yellow circle) is a visual element which indicates the force developed by the virtual prosthesis when grasped virtual objects.

In order to augment the functionality of the virtual environment, another series of radio buttons was included. By switching on the control *Arm + Board attached to Cam* [Figure 87(1)], the destination basket, in which the successfully grasped objects are placed, is attached to the subject. Otherwise, the collection basket is placed in a corner of the tracking area. The next radio button, *Destroyable Objects* [Figure 87(3)], defines whether the objects will break or not when grasped with a force exceeding the upper border of the target. Activating *Sphere Color Change* [Figure 87(5)], causes the color of the target object to change when the applied force reaches the target force, and the object can be picked up. Pressing the button *Spawn Objects* [Figure 87(7)] causes target-objects to be generated within the environment. The coordinates of all generated objects can be set in a hidden *.xml configuration file. For various studies, e.g. providing haptic instead of visual feedback, there is also an option to hide the virtual prosthesis - *Invisible Hand Mode* [Figure 87(12)]. In this mode, the subjects do not have visual feedback about hand aperture, but can still grasp because the target object is attached to the prosthesis overlapping the shadow. The button *Load Objects* [Figure 87(13)] updates the configuration of the target objects, their type and coordinates, as predefined in an *.xml configuration file. “Statistics” [Figure 87(14)] allows for the evaluation of the performed tasks, and “Reset Objects” [Figure 87(15)] clears the virtual environment of target objects.

BLUETOOTH CONNECTION (BT)

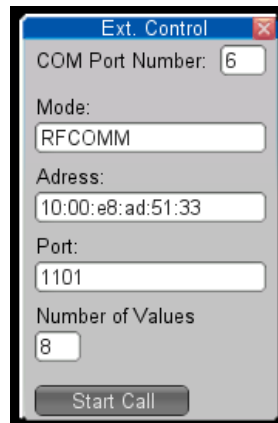


Figure 90: Bluetooth communication setup

The virtual environment communicates wirelessly with the control brace. This “Bluetooth Connection” has to be set-up to allow the virtual environment to communicate with a specific Bluetooth device which, in our case, is embedded within the control brace. This is done by adjusting the port number of the serial communication, the BT mode, address and BT port, as well as the length of the transmitted package [Figure 90].

FITTING SETTINGS

The subjects, while immersed in the virtual environment, wear a virtual prosthesis and try to accomplish tasks with it. The virtual prosthesis should be naturally attached to the subject’s body in order to induce the feeling that the virtual prosthesis is a replacement of the natural arm.

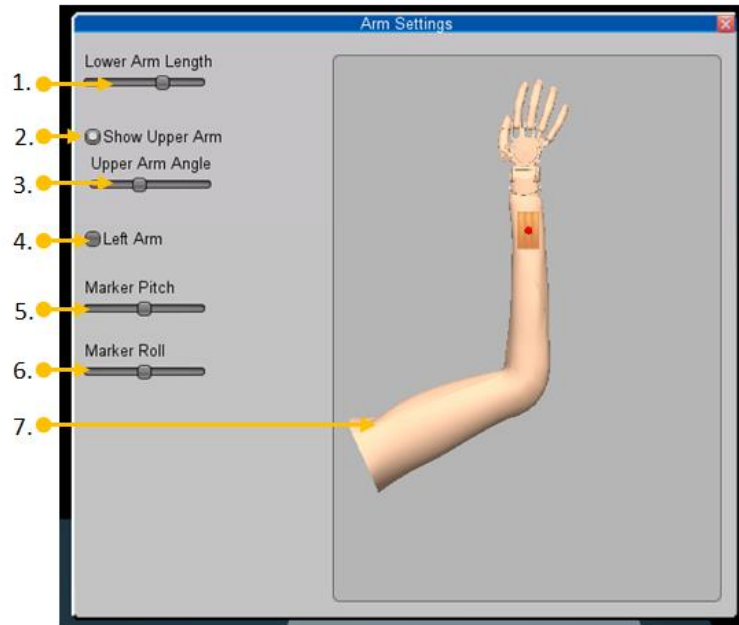


Figure 91: Fitting settings tab adjustments allow a naturally fitting of the virtual-reality prosthesis on the forearm.

Since the limbs of human subjects are very different, a new dialog was created to allow various adjustments of the limb configuration: change arm length [Figure 91(1)], make visible only the forearm [Figure 91(2)], adjust elbow angle [Figure 91(3)], mirror the virtual hand from left to right side [Figure 91(4)] and adjust the pitch [Figure 91(5)] and roll [Figure 91(6)] angles of the marker (the square on the forearm, centered by a red ball). The dialog also includes a preview of the customized arm [Figure 91(7)].

NETWORK CONNECTION (TCP/IP)

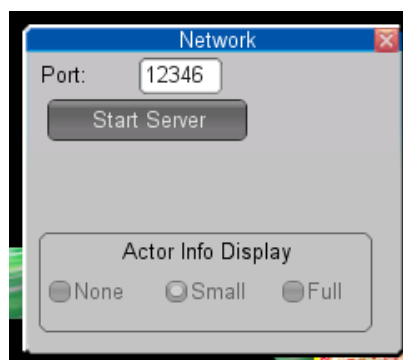


Figure 92: The TCP/IP communication partners are defined by opening a common communication port.

The software package implementing the virtual prosthesis and the software implementing the tracking algorithms run on different machines, let's call them tracking and VR host machines, but communicate with each another through a TCP/IP network connection. The tracking machine delivers information about the markers' coordination within the network (head and forearm). Connected to this network, the VR host machine will receive the tracking data, convert it into movements of the virtual prosthesis and control the viewpoint of the scene visible in the video glasses. In order to define the communication partners, the port have to be defined [Figure 92].

SCOPE

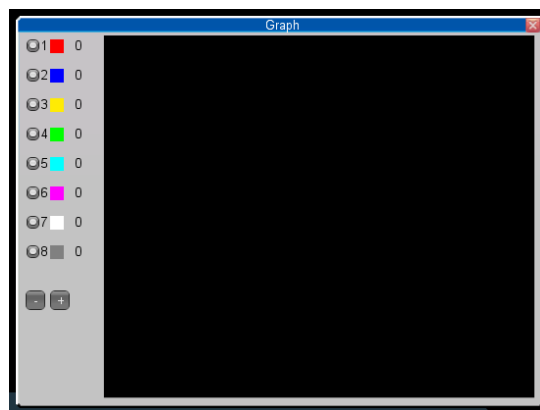


Figure 93: The scope is monitoring the on-line data continuously transmitted by the control brace to the virtual-reality environment.

The VR host machine, wirelessly receives information from the control brace, for the control of the virtual prosthesis. For debugging reasons, a scope [Figure 93] was implemented which allows visualization of the received signals transmitted by the control brace.

CURRICULUM VITAE

Andrei Ninu

| | | |
|--|---|---|
| CONTACT INFORMATION | Vienna University of Technology I. f. Analysis & Scientific Computing Operngasse 11 1040 Vienna, Austria | Phone: +43 676 7740053 E-mail: ninu_andrei@yahoo.com |
| CITIZENSHIP | Austria | |
| DAY OF BIRTH | July 28, 1973 | |
| PROFESSIONAL EXPERIENCE RESEARCH | <ul style="list-style-type: none">• 11.2012 - present: Marie-Curie Fellow / Research scientist – Department of Neurorehabilitation Engineering, University Medical Center – Göttingen, Germany• 11.2011 - present: Research scientist – Department “Strategic Technology Management,” Otto Bock Healthcare Products GmbH – Vienna, Austria• 05.2005 – 11.2011: Research engineer, Otto Bock Healthcare Products GmbH – Vienna, Austria• 07.2001 – 11.2001: Research Associate, Intelligent Handlings and Robotics – Vienna University of Technology, Austria• 11.1999 – 05.2000: Research Associate, Faculty of Automatic Control and Computer Engineering, Chair Robotics - TU Iasi, Romania | |
| PROFESSIONAL EXPERIENCE DEVELOPMENT AND TEACHING | <ul style="list-style-type: none">• 05.2002 – 05.2005: Software engineer, Otto Bock Healthcare Products GmbH – Vienna, Austria• 2010/2011 – Lector – FH Technikum Vienna, Austria / Lecture: „EMG in Myoprosthetics“• 2001/2002 – Tutor, Intelligent Handlings and Robotics – Vienna University of Technology / ANSI C, VB6, Excel Courses• 1998/2000: Seminar leader, Faculty of Automatic Control and Computer Engineering, Chair Robotics - TU Iasi, Lecture: „Kinematics and Dynamics of Industrial Robots“ | |
| PUBLICATIONS | <ul style="list-style-type: none">• A.Ninu, C.Prahn, S.Dosen, F.Rattay, H. Dietl, D.Farina (2013), A novel approach to induce haptic sensations for closing the control-loop in prosthetic devices, Submitted• A.Ninu, S.Dosen, S.Muceli, F.Rattay, H.Dietl, D.Farina (2013), Closed-loop control of hand prostheses: influence of feedback modality and variables, Submitted• C. Prahn, A. Ninu, F.Rattay (2011) Can I lend You a Hand? Rubber Hand Illusion for Sensory Feedback in Amputees, CogSci Conference, Ljubljana – Slovenia• A. Ninu, K. Kevin, HW van Vliet, F.Rattay, Feedback Integration into the Control Loop of Prosthetic Devices, 13. ISPO World Congress 2010, Leipzig – Germany• A. Ninu (2010), Device and method for generating a vibration pattern, 2010 Patent Application• Andrea G. Cutti, Angelo Davalli, Valeria Gazzotti, Andrei Ninu, (2005) Performance Evaluation of the new OttoBock “DynamicArm” by means of Biomechanical Modelling, MEC Conference, Brunswick - Canada | |
| EDUCATION | <ul style="list-style-type: none">• 2012 - “R for Statistics,” Vienna University, Austria• 2011 - Assessment of Capacity for Myoelectric Control, Fredericton - Canada• 2009 - PhD Student, Institute for Analysis und Scientific Computing, TU Vienna, Austria „Prosthesis Embodiment – Feedback integration into Control Loop of Prosthesis“• 2007 - Certification IEC 62304 – Software for Medical Product• 2003 - Anatomy Course – AMPUTATIONS for lower limbs• 2002 - Seminar – Law on Medical Devices• 2000 - Socrates Scholarship at Vienna University of Technology, Austria• 1992-1997 - University degree at the Iasi University of Technology, Romania Master thesis: „Coordination of industrial robots based on an artificial vision system“ | |
| LANGUAGES | <ul style="list-style-type: none">• English (fluent)• German (fluent)• Romanian (native) | |